AD NUMBER

AD860050

LIMITATION CHANGES

TO:

Approved for public release; distribution is unlimited.

FROM:

Distribution authorized to U.S. Gov't. agencies only; Proprietary Information; 05 SEP 1969. Other requests shall be referred to Space and Missile Systems Organization, Attn: SMSDI-STINFO, Los Angeles, CA 90045.

AUTHORITY

SAMSO ltr, 16 Aug 1973

LIQUID ROCKET DIVISION

PROGRAM TITAN IIIM

STANDARD SPACE LAUNCH VEHICLE
COMPONENT DEVELOPMENT REPORT

FOR THE

TITAN IIIM STAGE I COMBUSTION CHAMBER

9180-941-DR-3 5 September 1969

AEROJET GENERAL TIRE GENERAL

AEROJET-GENERAL CORPORATION

SACRAMENTO, CALIFORNIA

TITAN IIIM

STANDARD SPACE LAUNCH VEHICLE

DEVELOPMENT REPORT

For the

TITAN IIIM STAGE I COMBUSTION CHAMBER

Report 9180-941-DR-3

Prepared by:

Aerojet-General Corporation
Liquid Rocket Operations
Sacramento, California
95809

Contract AF 04(695)-941

Prepared by:

W. J. Nord
Titan IIIM Program Office

Approved by:

T. M. Jenkins, Manager
Titan Engineering

Approved by:

D. A. Fairchild
Supervisor, TCA Engineering

Approved by:

D. E. Robison, Manager
Titan IIIM Program

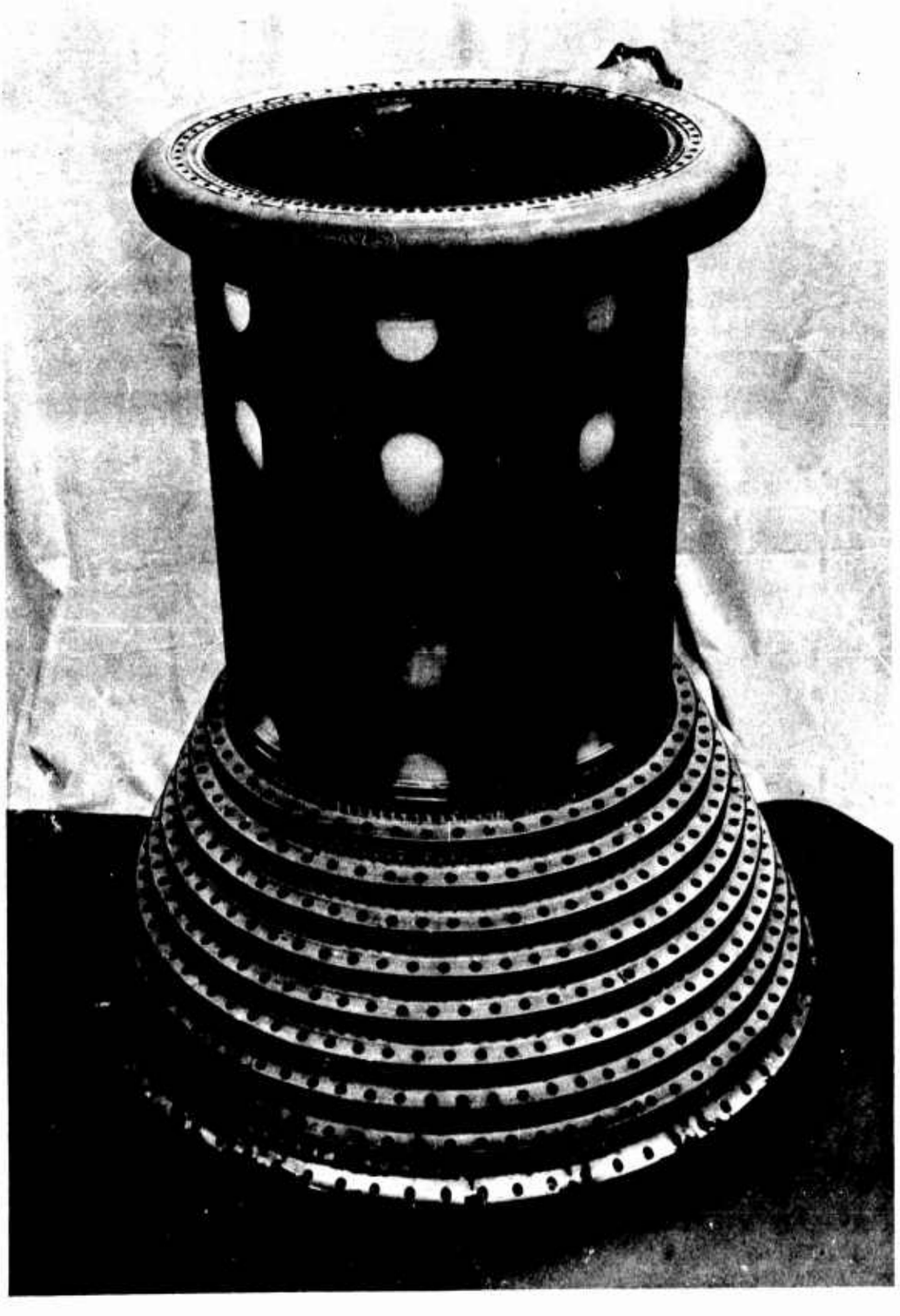

Figure 1 -- Titan IIIM Stage I Combustion Chamber

FOREWORD

This report is submitted in partial fulfillment of Line Item 29, Technical Reports, Contract Data Requirements List (CDRL), dated 2 October 1967, of Contract AF 04(695)-941, Program Titan IIIM, Standard Space Launch Vehicle, and as specified in First Stage Engine Approved CDR Minutes.

This document is one in a series of development reports covering the Titan IIIM Stage I components. Its subject is the design, fabrication, and testing of the Titan IIIM Stage I combustion chamber.

CONTENTS

REFERENCES

A Report M-13, Structural Analysis of the Titan IIM Stage I Combustion Chamber, 13 January 1967, Revised 22 October 1967, Structural Analysis Department 9632 Internal Report.

B Report TCER 9648-003, Heat Transfer Characteristics of AeroZINE 50 at High Velocities and High Subcoolings, November 1966.

C Van Huff, N.E. and Rousar, D.C. Ultimate Heat Flux Limits of Storable Propellants, paper presented at the 8th CPIA Liquid Propulsion Symposium, Cleveland, Ohio, November 1966.

TABLES

ILLUSTRATIONS

ILLUSTRATIONS (cont.)

1. INTRODUCTION AND SUMMARY

The increased thrust, higher engine performance, and greater reliability requirements of the Titan IIIM engines for application to the Manned Orbital Laboratory Program necessitated extensive redesign of the thrust chamber assembly as well as other major components for the Stage I engine. This report encompasses the design and development of the combustion chamber.

The underlying goal of the design was to provide a safe thermal margin while operating with low film cooling percentages and at the same time a safe structural margin while operating attached to an ablative nozzle extension. The thermal margin was obtained by redesigning the coolant tubes so as to provide optimum local and total heat transfer features, yet operate at minimum pressure loss. Support for the ablative skirt was provided by attaching a connecting flange and reinforcing the throat section of the chamber to withstand the added loads.

1.1 STATEMENT OF WORK

The applicable portion of the Statement of Work is as follows:

"The contractor shall assure compatibility of newly designed Thrust Chamber Assembly components with the overall assembly and shall perform the necessary thrust chamber assembly testing to assure performance objectives. The Contractor shall design a new Stage I regeneratively cooled combustion chamber, with an expansion area ratio of 6 to 1, contoured to the optimum 15 to 1 area ratio contour. The design shall reflect the requirement to operate at an R_{BO} of 0.82 or less, when calculated with the most adverse flight suction conditions to propellant inlet temperature of 90^{o} and total suction pressures of P_{ost} equal to 123 psia and P_{fst} equal to 26 psia. Reduction of the fuel film coolant weight flow requirement to 10 percent shall be a design goal. Operational and dimensional compatibility between the 624A Stage I injector, P/N 281087 and the combustion chamber developed on this program shall be demonstrated.

1.1, Statement of Work (cont.)

> Provision for the attachment of the Stage I ablative skirt being developed on this program shall be made. Reduction of combustion chamber hydraulic flow resistance shall be a design goal in order to maintain present component operating levels. The chamber structural design shall reflect the philosophy and safety factors set forth in Titan IIIM System Performance/Design Requirements General Specification when subjected to the critical set of flight and gimbal accelerations in addition to operating pressures and thrust forces."

1.2 BACKGROUND AND REQUIREMENTS

The Titan IIIM booster requires a Stage I engine thrust of 437,000 pounds at sea level and 520,000 pounds in vacuum. Compared with the Titan III system this represents an increase in thrust of 7,000 pounds at sea level and approximately 40,000 pounds at altitude. To meet this requirement without sacrificing engine performance, several major changes had to be made to the thrust chamber assembly (TCA).

The sea level thrust was increased by raising the nominal chamber pressure from 760 to approximately 808 psia. The altitude thrust was obtained by increasing the expansion ratio from 8:1 to 15:1, by attaching a 15:1 ablative nozzle extension (skirt) to the chamber. The best point to attach the skirt was determined to be where the area ratio is 6:1 which thereby became the area ratio of the combustion chamber, that is, the regeneratively cooled part of the thrust chamber assembly. The chamber was also intended for use with other ablative skirt designs, but maximum performance for altitude applications was of prime importance at the time, and the divergence angle and contour were therefore optimized for the 15:1 skirt. The double-pass semiregeneratively cooled configuration of the Titan III design was retained, but the number of tubes and the tube cross-sections had to be modified substantially to absorb greater sea level start loads and much higher heat fluxes.

1.2, Background and Requirements (cont.)

Combustion chamber design requirements include:

(a) dimensional and operational compatibility with the 624A Stage I baseline injector,

(b) capability to operate with a maximum tube burnout ratio (R_{BO}) of 0.82, with propellant inlet temperatures (engine interface) of 90^{o} (max), and with oxidizer and fuel total suction pressures equal to 123 and 26 psia, respectively,

(c) capability to operate with a reduction of fuel film coolant flow, from the injector, to approximately 10 percent,

(d) reduction of the fuel system hydraulic resistance of the 624A baseline chamber,

(e) maintaining chamber fuel volume equivalent to that of the 8:1 area ratio 624A baseline chamber in order to retain existing oxidizer lead characteristics during the engine start transient,

(f) incorporation of a mounting flange for attachment of the ablative nozzle extension,

(g) provision for structural reinforcement to reduce stresses in the throat area, and

(h) where applicable the design safety factor considered is as discussed in SSD Exhibit 62-127 (factors of 1.32 on yield and 1.80 on ultimate).

1.3 DESIGN APPROACH

Redesign of the combustion chamber centered basically on resizing the tubes so as to accommodate a 15:1 ablative nozzle extension, while at the same time increasing the heat transfer burnout margin without loosing performance. This required the use of tapered tube walls to reduce the local heat

1.3, Design Approach (cont.)

flux, and optimization of the local coolant velocity (or tube cross-sectional area) so as to minimize the pressure drop. The redesign was based upon analytical techniques and empirical data gained from Titan II, Titan III, and Gemini chamber experience. Improved heat-transfer and hydraulic calculation methods permitted nearly optimum sizing of the chamber tubes in the initial layout, but additional data from heated tube tests were necessary to refine the local heat flux calculations prior to finalizing the design. Flight data from Titan III and consideration of Titan IIIM requirements established the strength requirements for bending loads.

Construction of the new chamber is similar to the Titan II chamber. Apart from the contour, the major differences are a 6:1 area ratio at the aft flange, which is modified to provide for mounting the ablative skirt; fewer tubes, with thicker walls to restrict the heat flow to the coolant; and a stronger forward flange to reduce distortion of the chamber-injection seal glands. The internal contour was optimized for minimum expansion loss. The flow distribution was equalized to the coolant tubes and inlet hydraulic flow losses were reduced by tapering the fuel torus (collector ring) inlet and by inserting deflector vanes. A reinforcing shell enclosed the chamber from the torus to the first reinforcing band around the tubes in order to relieve the stresses in the tubes at the throat (the weakest section in bending) imposed by the higher nozzle thrust and side loads developed by the 15:1 area ratio ablative skirt.

1.4 DEVELOPMENT SUMMARY

The chamber design was initiated in the latter part of 1965, and drawings were released for fabrication in January 1966. The first unit was completed early in May 1966. During June a revised design was released which incorporated minor changes based on experience from fabricating the first unit. Major development mileposts are shown in Figure 2.

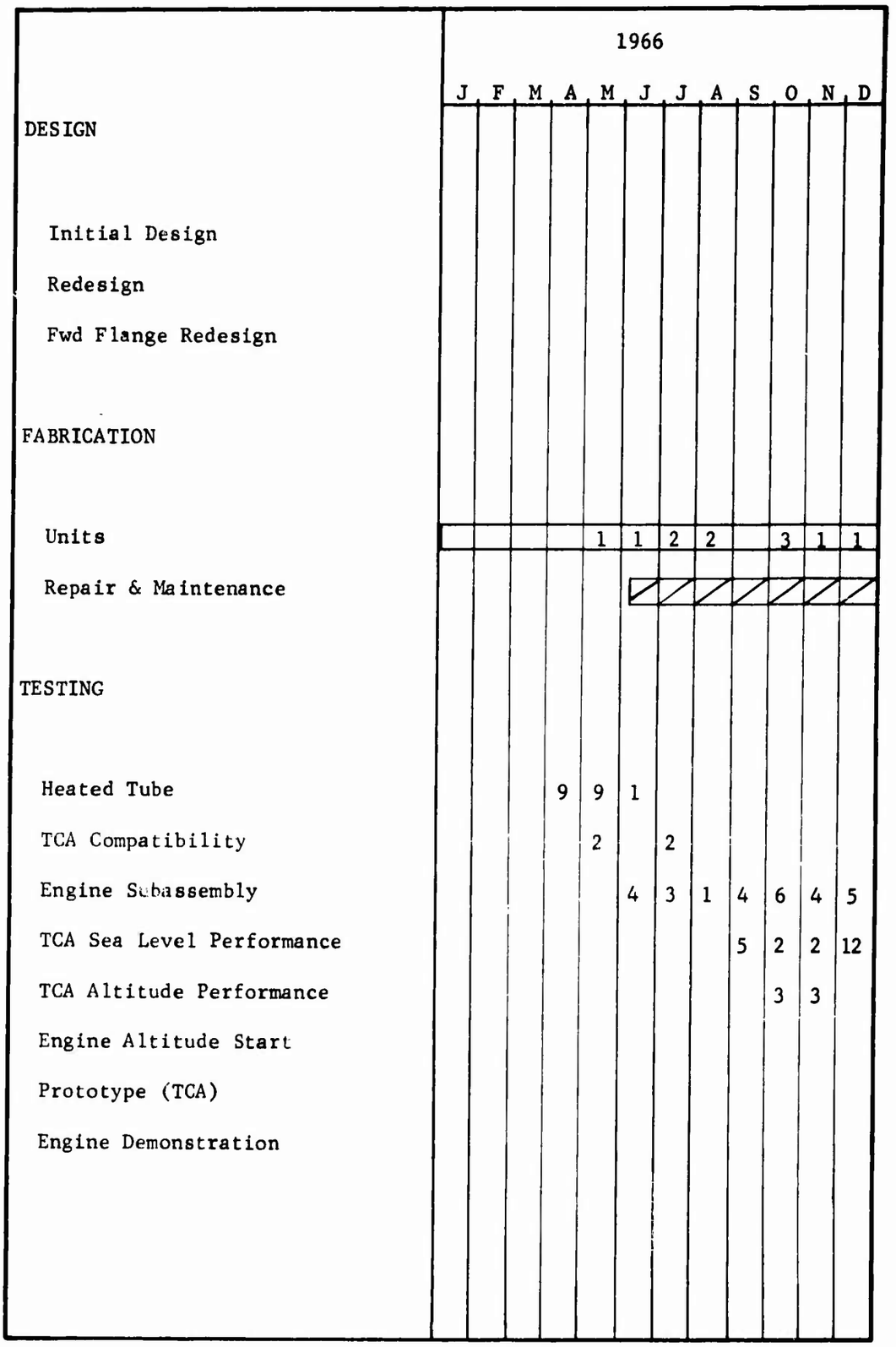

Figure 2 -- Combustion Chamber Development Schedule

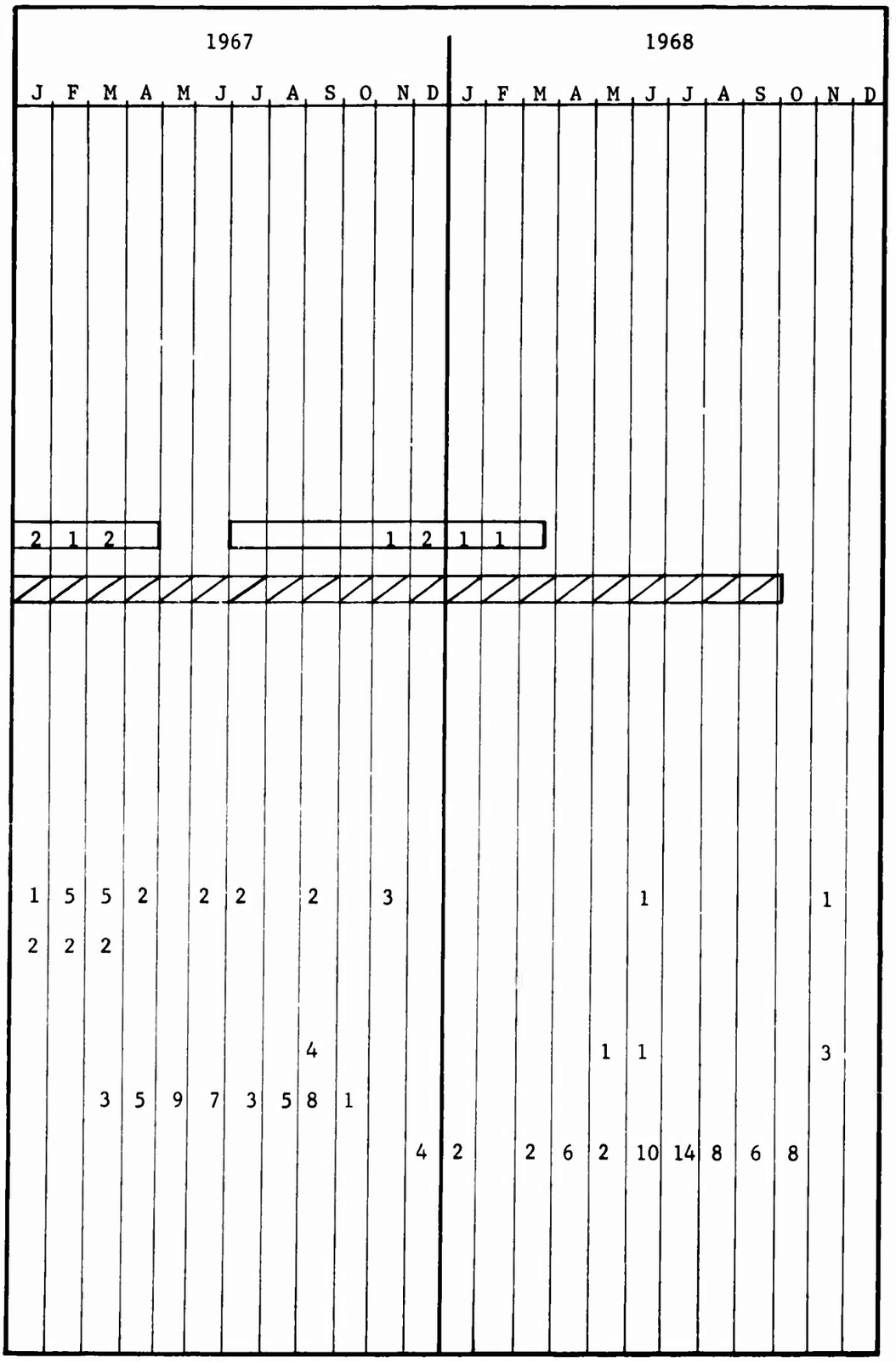

Figure 2 -- Combustion Chamber Development Schedule

1.4, Development Summary (cont.)

Laboratory testing was initiated to obtain additional heat transfer data at the higher tube velocities of the Titan IIIM design. Hydraulic testing was performed to demonstrate adequate flow distribution. A structural load test was performed on the combustion chamber together with the other thrust chamber components in December 1966. The test showed an adequate margin of safety.

Additional instrumentation was provided for development hot firings. Strain patches were mounted on the chamber during engine gimballing and sea level starting tests to determine the magnitude of side loads and the amount of chamber deflection. Brazing alloys with different melting temperatures were applied in small patches at representative locations on the chamber tubes. Examination of the condition of the braze after firing gave an indication of the gas wall temperature.

A series of three TCA tests in May and July 1966 demonstrated that the new combustion chamber was compatible with the 2 BIE-38 (Titan III) injector when operated at Titan III film cooling rates. This was confirmed by seven engine tests.

From September 1966 through March 1967, three test series totalling 42 firings were conducted in conjunction with development tests of the Titan IIIM baffled injector. Heat transfer excursions were conducted at mixture ratios ranging from 1.8 to slightly over 2.1.

No serious damage to the combustion chamber was experienced on any of the tests. Slight tube erosion was noted on one test and minor flange erosion on two others. The problem was traced to maldistribution of film cooling by the injector, which was corrected without increasing the total film cooling flow.

Table 1 -- Titan IIIM Combustion Chamber Test Summary

Serial No.	Engine		TCA		Total Time
	Tests	Time	Tests	Time	
001	0	0	3	102.4	102.4
002	6	679.0	18	802.7	1481.7
003	2	257.2	0	0	257.2
004	2	58.5	8	476.6	535.1
005	6	528.6	3	84.6	613.2
006	3	322.7	0	0	322.7
007	3	384.2	0	0	384.2
008	5	167.3	0	0	167.3
009	9	1034.5	0	0	1034.5
011	2	321.2	8	487.6	808.8
012	12	1030.7	0	0	1030.7
013	1	60.6	5	287.3	347.9
014	0	0	16	878.6	878.6
015	6	235.2	20	1047.6	1282.8
016	0	0	1	6.8	6.8
017	12	1425.5	0	0	1425.5
019	8	981.4	0	0	981.4
020	3	421.2	0	0	421.2
021	15	2133.7	0	0	2133.7
022	15	2133.7	0	0	2133.7
092	7	865.3	0	0	865.3
158	2	522.0	4	242.7	764.7
159	6	811.1	0	0	811.1

1.4, Development Summary (cont.)

Fifty engine tests utilizing Titan IIIM combustion chambers were conducted from June 1966 through September 1967. Only one incident of tube erosion was recorded. Investigation was unable to ascertain the exact cause, and after repair the damaged area sustained no further erosion during numerous development tests. Other chamber damage was limited to V-Band and shell tack weld failure during operation with 1000-cps, 100-psi-amplitude oscillations in the combustion chamber and fuel system. These oscillations were eliminated through changes to the injector, and no further cases of structural damage were experienced.

A series of 41 TCA verification tests was conducted from March through October 1967. Slight erosion of the injector-to-chamber mating flange was experienced twice with combustion chamber S/N 014 and three times with chamber S/N 015. The erosion was traced to improper distribution of chamber film cooling by the injector. The injector pattern was corrected, the flanges repaired, and there was no recurrence of the problem. A pinhole leak was experienced with chamber S/N 014 on one occasion and a slight hot gas leak in chamber S/N 011 was noted once. One split tube was found in chamber S/N 013 as the result of a test to determine the mixture ratio at which burnout would occur. These were minor random failures for which corrective action was not necessary beyond weld repair. Chamber S/N 016 was destroyed by a test stand malfunction the only time it was fired. In summarizing the development testing it should be noted that there were no failures traceable to inadequate design of the combustion chamber.

A summary of the testing is given in Table 1. The detailed test log is contained in Appendix A.

The development testing was evaluated during the Critical Design Review of the Stage I engine. The design approach was judged to be adequate and acceptable in light of program requirements.

1.4, Development Summary (cont.)

Six combustion chambers of prototype configuration were tested with the Demonstration Engine for a total of 60 separate test firings. Two of these chambers completed the full cycle of 15 tests. Aside from the normal deterioration ensuing from usage there was one incident of failure of the wire wrap and one incident of cracking of the forward flange. Both discrepancies were traced to fabrication defects. The fabrication procedures have since been corrected to avoid such incidents occuring again.

1.5 SPECIFICATIONS AND DOCUMENTATION

The basic specification for the Titan IIIM combustion chamber is Engineering Critical Component Specification, EC-43471A, Thrust Chamber Assembly, YLR87-AJ-11; the combustion chamber is one component of the Thrust Chamber Assembly. The combustion chamber was included in the Critical Design Review of the Stage I engine conducted 30 and 31 August 1967.

Further documentation of the combustion chamber is contained in Proposals LR666000 and LR666000A submitted 18 March 1966 and 30 September 1966, in the Engineering and System Test Implementation Plans, SSD-CR-65-8180-120 and -140 respectively, and in the Titan IIIM Program Progress Reports 8180-126-MR-1 through MR-6 and 9180-941-MR-1 through MR-35.

1.6 CONCLUSIONS

The Titan IIIM combustion chamber has met all contractual requirements.

1. Compatibility with engine design and performance: Demonstrated by 31 full-engine, 62 engine subassembly, and 86 component tests.*
2. Compatibility with the Titan III baseline injector: Demonstrated by three component and seven engine tests.
3. Capability to operate below the maximum tube burnout heat flux ratio (R_{BO}) of 0.82 utilizing propellants at 90°F inlet temperature and worst flight inlet conditions: Demonstrated with three different chambers during seven total tests.
4. Capability to operate with reduction of film coolant flow to approximately 10 percent: Demonstrated by the 179 engine and component tests noted above.
5. Reduction of the fuel system resistance from that of the 624A baseline chamber: Demonstrated by water flow tests and confirmed by test firing data.
6. Maintaining the chamber fuel volume equivalent to the 8:1 baseline chamber: This requirement is met by the chamber design.
7. Incorporation of a mounting flange for the ablative skirt: This is incorporated in the drawing and was tested by hot firings and structural loading tests.
8. Provision for structural reinforcement of the throat: The provision is on the drawing, and the design passed a structural loading test.
9. Design safety factors in SSD Exhibit 62-127, System Design Specification: The safety factors have been confirmed by stress analysis and by the structural test series.

*See Appendix A. The test series are: 3051-D01-1C, -D04-1J, -D01-1M, -D01-0X, -D02-1M, -D06-1J, and 3269-D01-1M (component); 3051-D01-1A, -D02-1A, -D03-1A, -D04-1A, -D07-1A, and 3269-D01-1A and -A01-1A, (engine subassembly) and 3051-D07-1A and 3269-D04-1A (complete engine).

Report 9180-941-DR-3

Section 2 Design

2. DESIGN

2.1 PRINCIPAL DESIGN FEATURES

The Titan IIIM Stage I combustion chamber is similar in concept to that employed by the Titan III and Gemini engines. The most important new features are: (a) a 6:1 area ratio exit cone with (b) a redesigned aft flange for supporting the ablative skirt, (c) greater thermal load capacity, and (d) increased structural strength. The skirt increases the area ratio to 15:1 to provide additional thrust at altitude. The 6:1 area ratio enables a shorter chamber length, which makes it easier to cool.

Some of the other features are:

optimum contour, tubular construction,

fewer and stronger tubes, with circular cross-section,

tapered tube wall thickness,

reshaped toroidal fuel manifold with tapered inlet and flow splitters for uniform flow distribution,

stronger aft end flange with streamlined collector ring and cross-over gates,

stronger forward flange with improved braze design.

Because of the increased side loads imposed by the larger expansion ratio, the chamber was enclosed from the torus to the first reinforcing V-Band by a stainless steel reinforcing shell to minimize the stresses at the throat. The chamber is shown pictorially in Figure 3. It weighs 341.1 lbs.

2.2 PRELIMINARY DESIGN

Gas dynamics studies were initiated to compute the baseline performance parameters for the TCA with chamber exit areas of 6:1, 8:1, 9:1, 10:1,

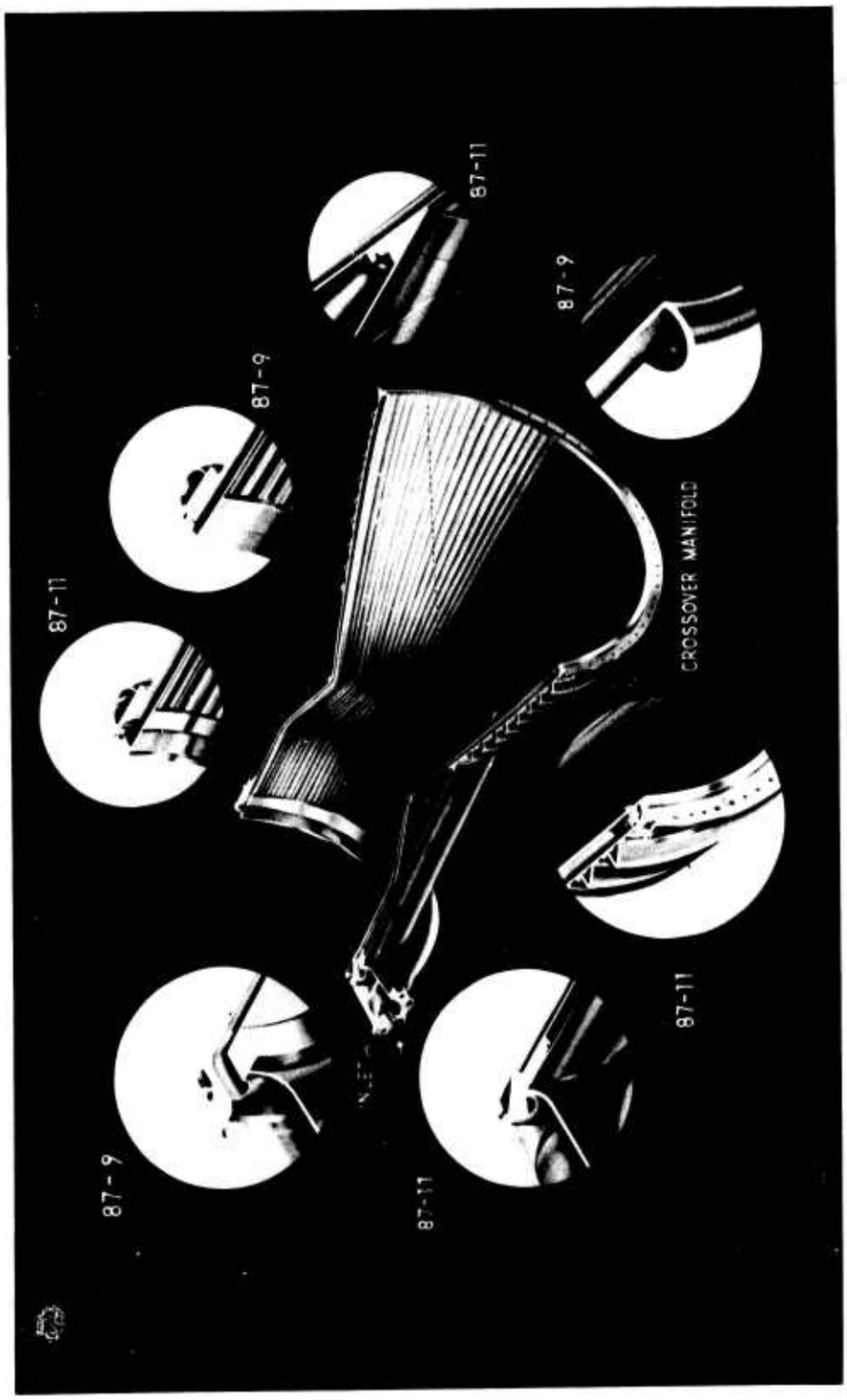

Figure 3 -- Titan IIIM Stage I Combustion Chamber (Sectional View)

2.2, Preliminary Design (cont.)

and 10.45:1, with and without ablative skirts. The assumptions were: throat area, A_t = 182.7, mixture ratio, MR = 1.91 and propellant inlet temperature TCI - 60°F.

Preliminary heat transfer studies indicated that 128 round tubes with 0.024-inch thick walls at the throat were optimum. The wall thickness in the aft end of the tubes was increased later at the exit end of the tubes where the thermal margins were the greatest in order to reduce the total heat input to the coolant.

A stress analysis showed that a throat support was necessary to absorb the sea level start loads. The throat reinforcement consists of a two-piece welded cylindrical steel shell attached by welding at the forward end to the fuel torus and at the aft end to a reinforced aft wirelock band. The shell is made from rolled CRES 347 sheet stock 0.109 in. (No. 12 guage) thick. (Originally the gauge thickness was 0.063 in. (No. 16), but because of an increase in the expected side loads it was made thicker.) The shell contains 24 lightening holes, which also serve as inspection holes to permit observation of the wire wrap during leak checks. The preliminary and final designs are shown in Figures 4 and 1, respectively.

2.3 PROTOTYPE DESIGN

Fabrication of the first two combustion chambers was completed in May 1966. Four TCA tests and three engine subassembly tests were conducted that month, utilizing the new hardware. Preliminary test experience (Section 5) combined with experience gained in fabrication of the first article (Section 3) and the results of special studies (Section 4) were used in the prototype design. The prototype drawings released are given in Table 2. Design changes resulting from special analyses are discussed in Section 2.5. Problem areas which developed in the course of fabrication and testing are discussed in Section 2.6 together with the recommended corrective action. The results of these studies were

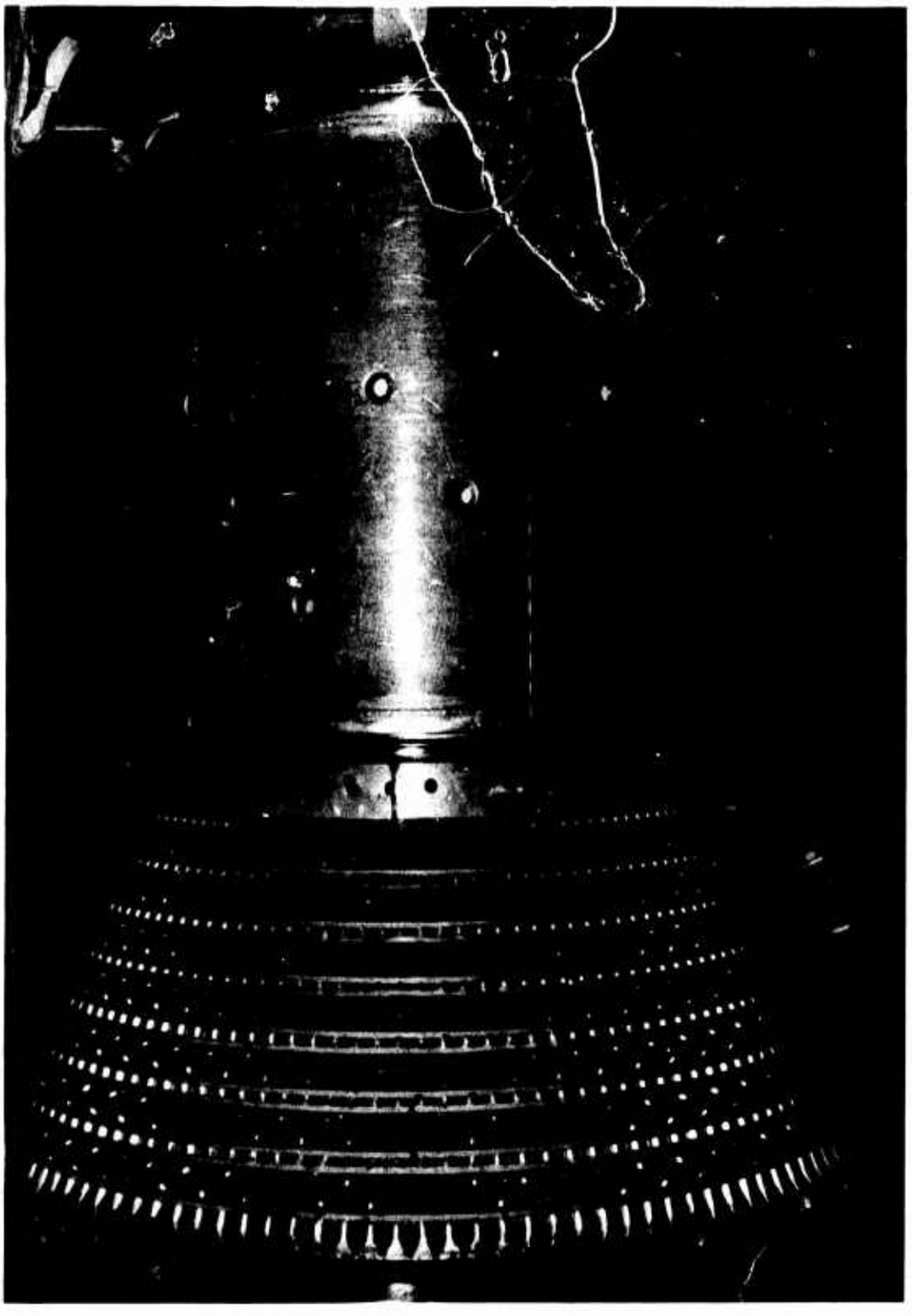

Figure 4 -- Combustion Chamber S/N 002, Showing Reinforcement

Figure 4 (cont.) -- Shell Details

Table 2 -- Design Release

Description	Original P/N	New P/N
Combustion Chamber	1121170-9	1133311-29
Torus and Injector Mounting Flange	1121169-19	1129950-29
Torus Assy	1121166-9	1129941-19
Torus Half, Fuel	1121168-1	1129942-3
Vane, Torus	1121165-1	1129944-3
Injector Mounting Flange	1121167-3	1154236-3
Forging, Injector Mounting Flange	1121167-1	1154236-1
Com'l Forging	None	C/C964000440
Flange, Inlet 4"	250331-1	1130105-1
Band, Closing - Injector Mounting	1122759-1	1154237-1
Ring, Shell Attaching Forward	1121163-1	1129949-3
Forging, Shell Attaching	None	1129949-1
Com'l Forging	None	C/C964000441
Ring, Shell Attaching Aft	1121161-1	1169923-3
Forging, Shell Attaching	None	1129923-1
Com'l Forging	None	C/C964000442
Ring, Reinforcing C/C	1121160-1 thru 1121160-15	Same
Ring, Reinforcing, C/C	1121160-17	1121160-21
Flange, C/C Aft	1121159-3	1130069-19
Forging, C/C Aft	1121159-1	1130069-1
Adapter	None	1130177-1
Tube, C/C	1121164-1	1130896-5
Tube, C/C	1121164-3	1130896-7
Shell Assy	1121811-9	Deleted
Shell	1121811-1	1130228-7
Gusset	1121881-3	Deleted
Adapter	250484-1	Same
Retaining Band, Throat	1121162-1	Same
Adapter	257554-1	Deleted
Ring, Reinforcing C/C	1123164-1	N/A
Flange Retainer	1123169-19	Deleted

2.3, Prototype Design, (cont.)

incorporated by change orders in the final prototype design as described by the Controlled Engineering Parts List for the Demonstration Engine.

2.4 HASTELLOY-X TUBE SAMPLE DESIGN

Drawings for the Stage I combustion chamber design, incorporating six Hastelloy-X tubes, were released in November 1966. The design was a basic 1130174-49 Titan III Stage I combustion chamber with six Hastelloy-X tubes replacing a corresponding quantity of CRES 347 tubes.

Three adjacent Hastelloy-X tubes (two return and one down) were located in the same quandrant as the injector mounting flange tooling hole, with one return Hastelloy-X tube located in each of the remaining three quandrants.

The location and number of the Hastelloy-X tubes were selected so as to expose the material to non-uniform combustion conditions while using the least number of tubes. This permitted evaluation of heat transfer characteristics of Hastelloy-X against 347 stainless steel under actual chamber temperature and pressure conditions.

2.5 SPECIAL DESIGN ANALYSIS

Special analyses of stress, heat transfer, hydraulics, materials, and fabrication processes were conducted to support the design in those areas where the adequacy of the preliminary design was not immediately evident.

2.5.1 Stress Analysis

Analysis of Titan II captive and flight tests applied to Titan IIIM components indicated that the maximum side load to which the Titan IIIM engine would be subjected was 64,000 lb. This was greater than could be resisted by the chamber throat if unsupported, and a reinforcement was recommended.

2.5, Special Design Analysis (cont.)

Strain-guage data from engine tests were analyzed in order to assess the loads and deflections of the chamber.

An analysis was performed to determine the instrumentation points and load vectors for the structural test. The chamber passed the test requirements with only minor yielding under the maximum combined loads.

Detailed analyses were made of the aft reinforcing ring, forward flange and throat support; composite loading conditions; plastic analysis of the tubular structure; revisions based on higher wall temperature; and of the forward flange distortion.

Analyses were conducted as part of the wire wrap and chamber tube failure analyses discussed in Sections 2.6.1 and 2.6.2.

2.5.2 Heat Transfer

On the basis of established heat transfer correlations for AeroZINE 50, analyses were made for the initial design of the combustion chamber tubes in order to determine the number of tubes, wall thickness and minimum velocity for the propellant. The analyses included calculations of:

(a) the local burnout heat flux ratio (R_{BO}) for all component and engine development tests. (See Table 12 Section 4.2),

(b) the local heat flux conditions for "worst flight" conditions,

(c) a special two-dimensional stress analysis of the forward and aft chamber flanges,

(d) a correlation for burnout with AeroZINE 50 at high velocities using heated tube test data. (See Section 5.1.2).

2.5, Special Design Analyses (cont.)

Braze patch data were analyzed for all the tests where the above-mentioned techniques were applied in order to refine the estimate of gas-side wall temperature.

Techniques for mounting thermocouple junctions on the gas side of combustion chamber tubes were also analyzed, and a satisfactory mounting technique was developed; but it was not employed because of test schedule constraints.

2.5.3 Hydraulics

Hydraulic analyses were performed for the fuel inlet and torus, chamber tube resistance flow splitter, and chamber aft flange prior to completing the preliminary design of the chamber. These analyses were confirmed by subsequent measurements of the distribution of flow through the combustion chamber tubes.

2.5.4 Materials and Processes

Investigation of tube leakage at the joint with the forward flange revealed inadequate braze coverage. A design recommendation was made to correct the problem.

The occurrence of cracks in the cover band weld in the forward flange was analyzed. A new method for preparing the weld was recommended.

A study of alloys and procedures for brazing on Hastelloy-X was made in conjunction with the fabrication of chamber S/N 013. New braze materials and brazing procedures were adopted as a result of the study.

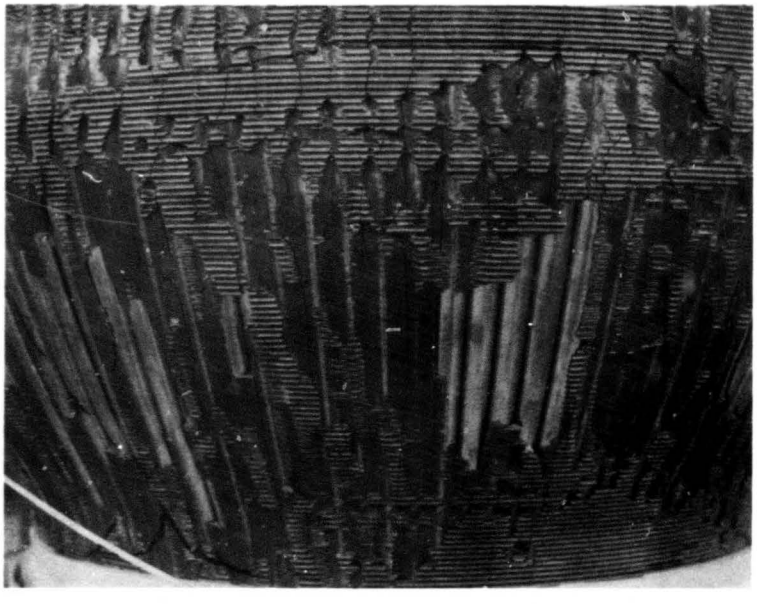

Figure 5 -- Combustion Chamber S/N 001, Showing Failure of Wire Wrapping

2, Design (cont.)

2.6 PROBLEM AREAS AND CORRECTIVE ACTION

2.6.1 Wirewrap Problem

Postfire examination of combustion chamber S/N 001 after Test No. 3051-D01-1C-002 revealed that the wirewrap was dislodged from about 3 inches below the torus to approximately 1 inch above the throat. Bulging was apparent in the tubular contour in the unwrapped portion of the chamber, most prominently midway down the convergent section as shown in Figure 5.

Failure analysis of the wirewrap separation produced the following information:

(a) Posttest inspection revealed an unwrapped condition from approximately 3 in. below the torus to approximately 1 in. above the throat. These tubes were bulged approximately 1/2 in. in the convergent section, and the tubes appeared to be elliptical in this area.

(b) Material evaluation indicated there was an insufficient thickness of Epon over large portions of the wirewrapped area. It was apparent by visual inspection that the Epon was not flush with the high point of the wire. Samples of Epon were visually examined and found to be acceptable in respect to material properties.

(c) Structural evaluation of the tension on the wirewrap and of the design of the tube bundle indicated acceptable strength loads. The technique of fabrication was reviewed, including preloads on the wire and associated manufacturing processes.

(d) Stability evaluation of high frequency data from injector manifold pressures (Pfj's and Poj's), indicated no acoustic mode of combustion instability nor any coupled oscillations in either the oxidizer or fuel circuits during steady state operation for Test Nos -001 and -002. However,

2.6, Problem Areas and Corrective Action (cont.)

during shutdown there were high-amplitude perturbations that are typical for Titan TCA tests.

After the first test of Demonstration Engine S/N 14 (Demo 14) the wirewrap on the divergent section of chamber S/N 020 was loose (see Figure 6). The loose strands started about 1 inch aft of the throat plane and extended over 2 inches of the nozzle length. Two additional tests were conducted with the loose wire. For the second of these tests the wire was taped in place to hold the wire in position during the start transient. The wire was removed after this test, but it was never replaced because the chamber was withdrawn from the test program.

During initial fabrication, the chamber had been wirewrapped twice in the forward section (forward of the throat plane), the second time because the wire was loose after completion of final proof-and-leak testing. The wire in the aft section did not appear loose and was not similarly replaced. No specific cause for the loose wire in the forward section was ascertained, but it was noted that the surface of the wire was not clean. Little effort was necessary to strip the wire from the chamber, and no adhesive forces were apparent between the wire and the Epon bed. When the aft wirewrap was removed after loosening, the wire was also found to be dirty.

The looseness of the wire is not fully explainable, but it can be attributed to the same elements that caused the forward section of wirewrap to loosen during proof testing. The cleanliness of the wire and the depth of Epon during wrapping are believed to be important in maintaining wire location and tension through adhesion of the Epon bed to the wire. The corrective action calls for stripping both wire sections if either loosens during fabrication and for cleaning the wire to a degreased condition prior to and during wirewrap.

The corrective action was limited to adding cleaning operations to the wirewrap procedure and requiring that both wirewrap sections be stripped

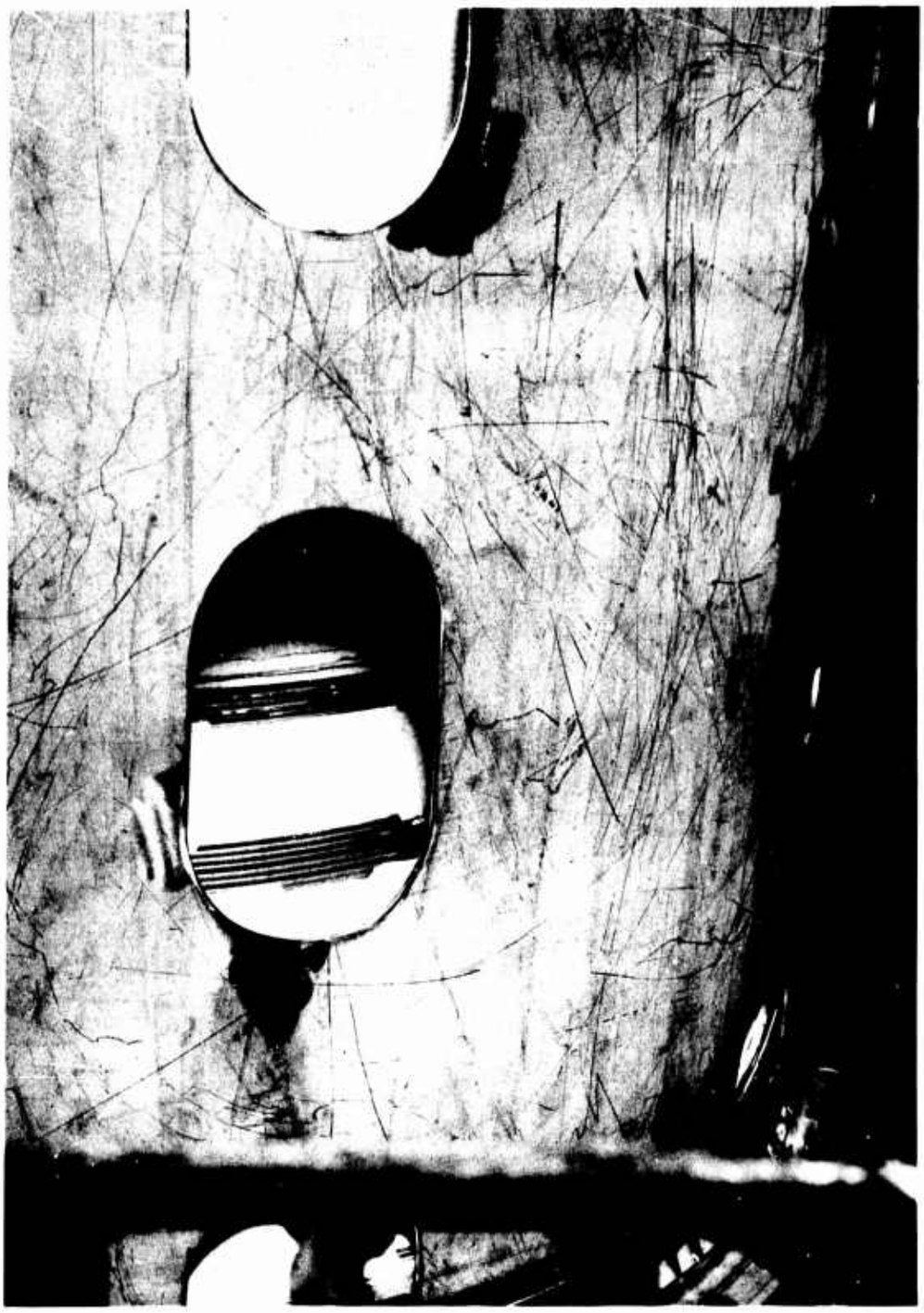

Figure 6 -- Loose Wire Wrap -- Chamber S/N 020 after Test No. 3051-D07-1A-201 (1 of 3)

Figure 6 -- Loose Wire Wrap -- Chamber S/N 020 after Test No. 3051-D07-1A-201 (2 of 3)

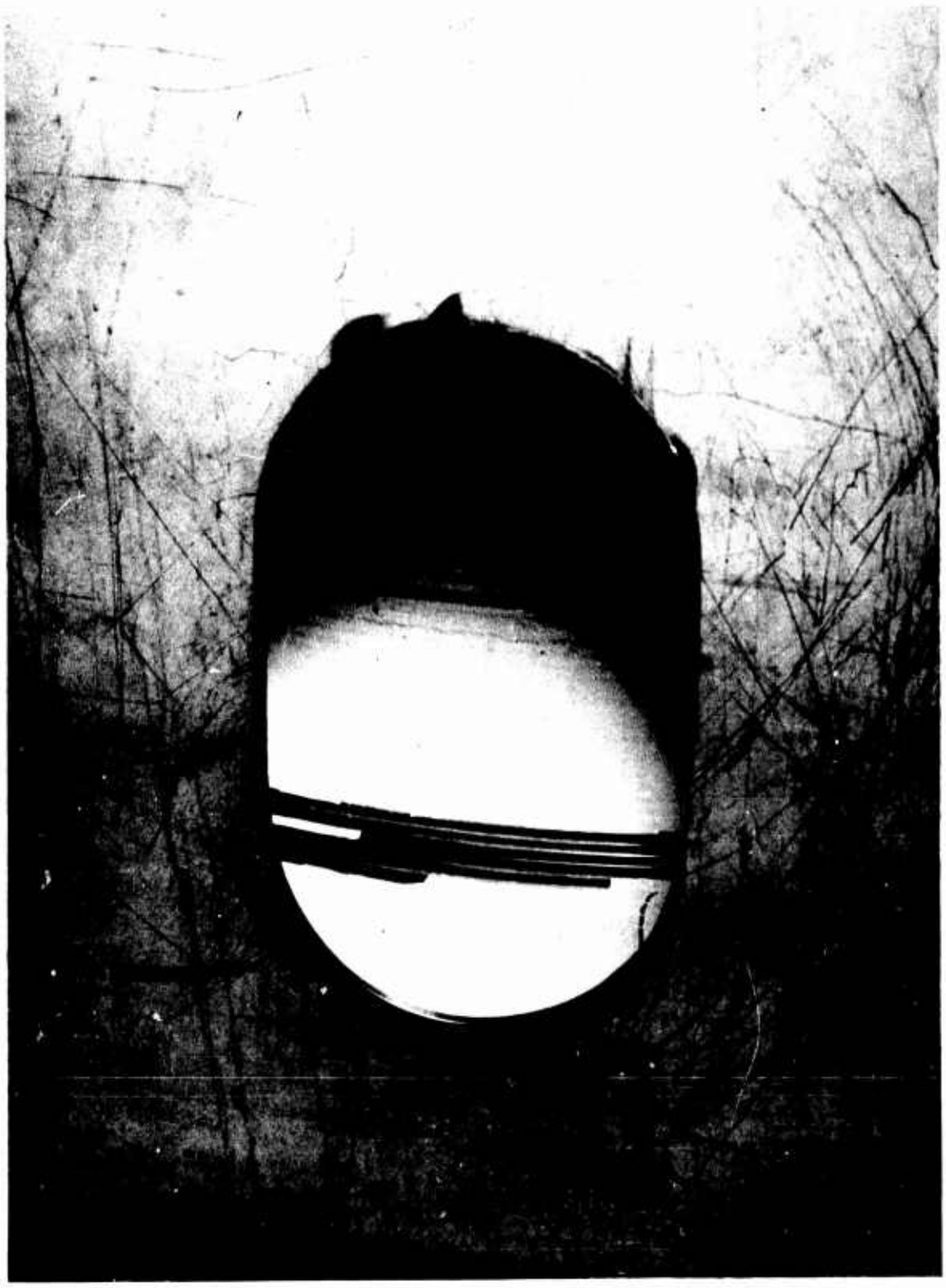

Figure 6 -- Loose Wire Wrap -- Chamber S/N 020 after Test No. 3051-D07-1A-201 (3 of 3)

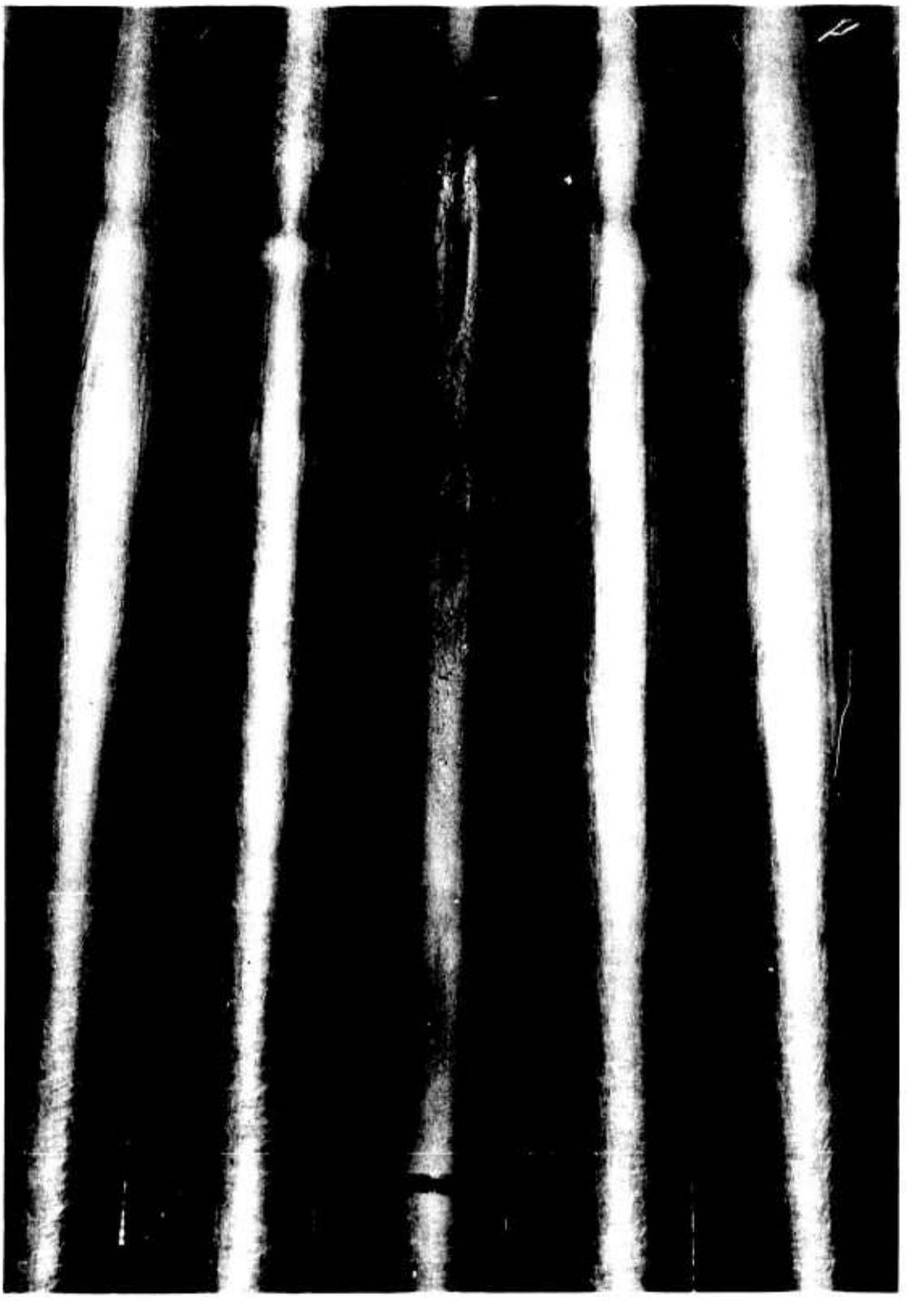

Figure 7 -- Tube Failure

2.6, Problem Areas and Corrective Action (cont.)

and replaced if either must be replaced. The cleaning consists of vapor-degreasing of the spool of wire in a hot atmosphere and, as the wire is wrapped, cleaning it with a cold degreasing agent applied to felt wipers on the wirewrapping machine. The wrapping procedure specifies the requirements for maintaining the felt pads at adequate effectiveness.

The final measure of the acceptability of a wirewrap is the prefire proof and leak test and the acceptance test. If the wirewrap appears loose after either of these tests, it can be readily replaced by proven procedures.

2.6.2 Tube Erosion and Leakage

Minor tube damage occurred on a few development tests and was repaired as required. The damage occurred during the following tests:

Test No. 3051-D04-1J-010 - S/N 002. Rough tubes in throat.

Test No. 3051-D04-1J-015 - S/N 002. Rough tubes in throat. (There may have been no change since Test No. -010).

Test No. 3051-D02-1M-018 - S/N 014. Pinhole leak.

Test No. 3051-D01-1A-008 - S/N 003. Minor repairable damage to injector and chamber.

During Test No. 3051-D01-1A-004 and -005, a down tube in combustion chamber S/N 002 ruptured in two places and the tube showed heat marking below the first failure (See Figure 7). Metallographic and heat transfer analyses agreed in placing the failure at a relatively low temperature (circa 1150°F) which could only be accounted for by a temporary flow decrease of approximately 30%. Hydraulic analysis showed that such a decrease could not be attributed to differences in flow rate between tubes, and moreover a change of such magnitude could not occur during a test except for some external cause. This would indicate that a foreign object was lodged in the tube and was expelled subsequent to burnout.

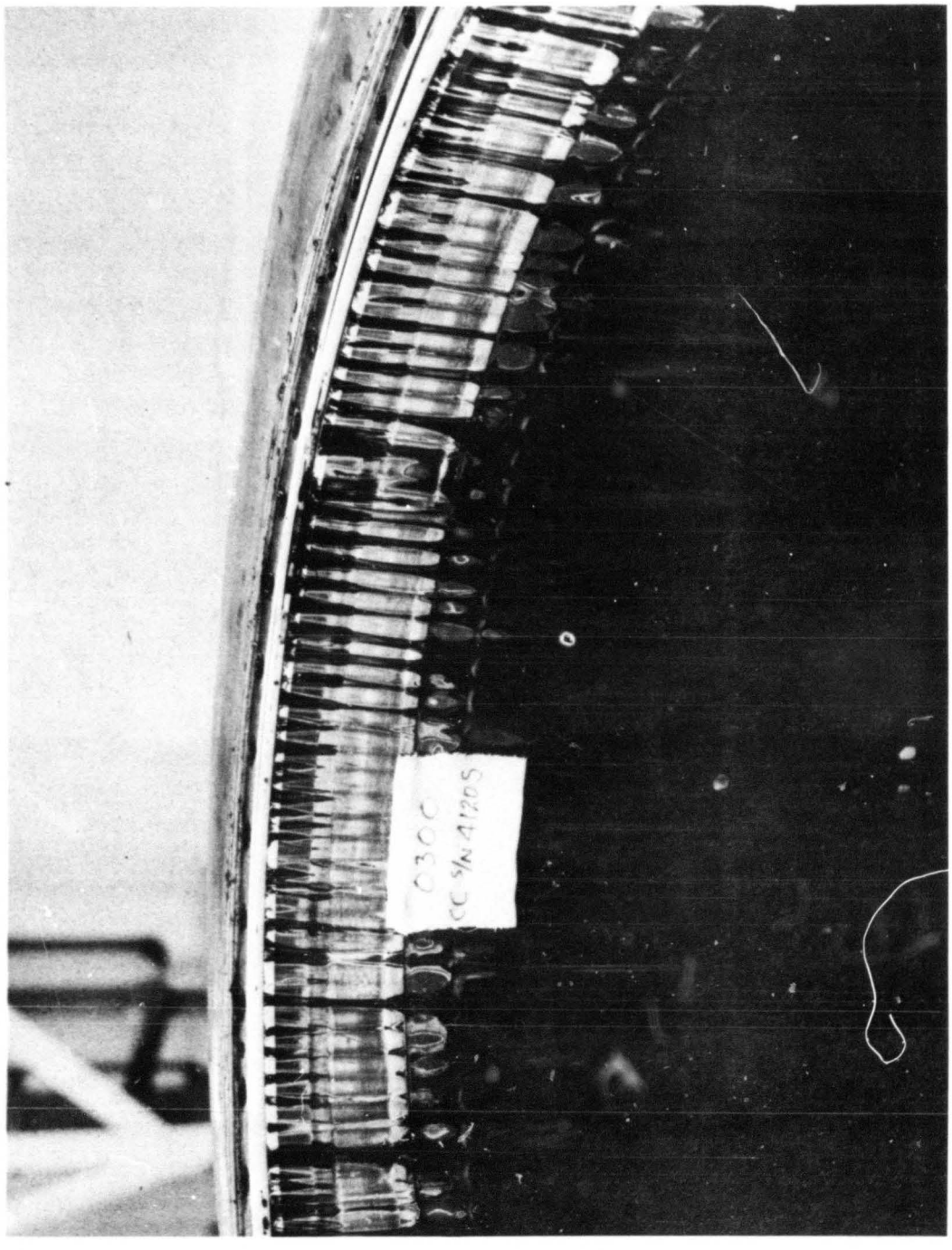

Figure 8 -- Forward Flange -- Chamber S/N 003 after Test No. 3051-D01-1A-008

2.6, Problem Areas and Corrective Action (cont.)

Chamber S/N 016 was destroyed during Test No. 3051-D02-1M-005 as the direct result of a test stand malfunction. The tubes were badly eroded and split because of an extremely high mixture ratio arising from the malfunction.

Four tube leaks were detected during Engine Demonstration. Following Test No. -207 with engine S/N 14, Tube No. 28 in chamber S/N 019 was found leaking at a rate of one drop per second. The leak was located four inches above the chamber throat and was not repaired prior to the following test. No investigation was conducted since the chamber was disqualified for other reasons and removed from the program after Test No. -208.

During the leak check of engine S/N 15 following Test No. -315, external tube leakage was detected through Tube No. 123 on chamber S/N 022. The leakage was located at a tack weld attaching the No. 1 V-band to the chamber tubes. The leak was repaired on the engine prior to the last test of the program. No investigation was conducted. See Figures 56 and 57.

Two of the chambers developed cracks in the crowns of a coolant tube in the cylindrical section of the combustion chamber. Both cracks were found to be caused by the deposition of molten, metallic particles on the surface of the tubes. The particles evolved from slight erosions in the forward flanges directly in line with the cracked tube. The molten particles on the tube surface caused a momentarily excessive heat load, and carburization of the based metal was initiated. Local film boiling may have taken place, but the film could not develop fully in such a restricted area. The molten particles also subjected the tube wall to excessive thermal stresses, and the cracks ensued.

2.6.3 Forward Flange Erosion

During the development and early verification testing there were instances of heat marking and erosion on the forward flange such as shown in Figure 8. This was attributable to inadequate dispersion of the fuel film cooling from the baffle injector. The film cooling pattern of the injector was modified as shown in Figure 9. Thereafter such minor instances of erosion as occurred were all within acceptable limits as given by the specification.

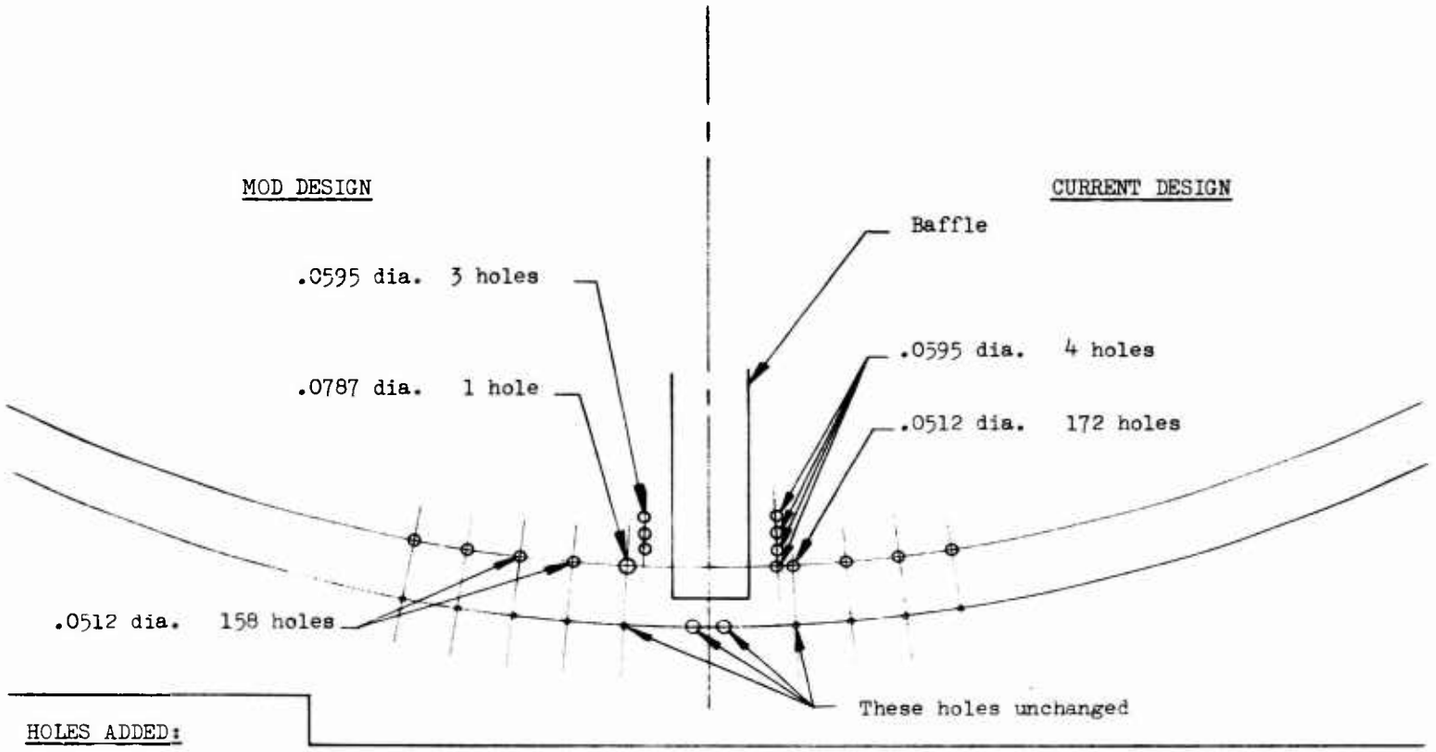

Figure 9 -- Film Cooling Modification

2.6, Problem Areas and Corrective Action (cont.)

2.6.4 Braze Joint Leaks at Forward Flange

Leakage was detected in chamber S/N 008 in the braze joining the coolant tubes to the forward flange. The chamber was submitted to metallographic analysis. It was determined that the brazing was quite porous and that it did not coat the whole of the tube within the joint.

The imperfect brazed joints resulted both from the inadequate physical preparation of the coolant tubes, such that the tubes fit too tightly into the flange holes, and from a braze cycle that maintained the temperature of the chamber too long above the liquidus point of the braze alloy. The coolant tubes were inserted directly into the forward flange without supplemental swaging, and the total diametric clearance varied from 0.001 inch to metal-to-metal contact. This clearance is too small to effect a proper brazed joint with CM 62 "B" alloy. These chambers were also brazed at a time when the total temperature range throughout the chamber was required to be less than 20°F. This was achieved by using a slow temperature rise rate above 1850°F up to a target of about 1950°F, and the result was that the chamber would be at temperatures above braze liquidus for periods of 25-30 minutes. During this extensive period, braze runoff would be excessive, and some "higher melt" constituents would form and fail to flow at all. Therefore, the forward flange was joined to the chamber tubes with a lean, nonuniform brazed joint that failed prematurely under repeated pressure and temperature cycling.

As a result of the brazing study, the following specific changes were made to the brazing procedures:

(a) Swage the forward end of the coolant tubes to guarantee that a positive clearance of up to 0.004 inches exists between the tube and the insertion holes in the flange;

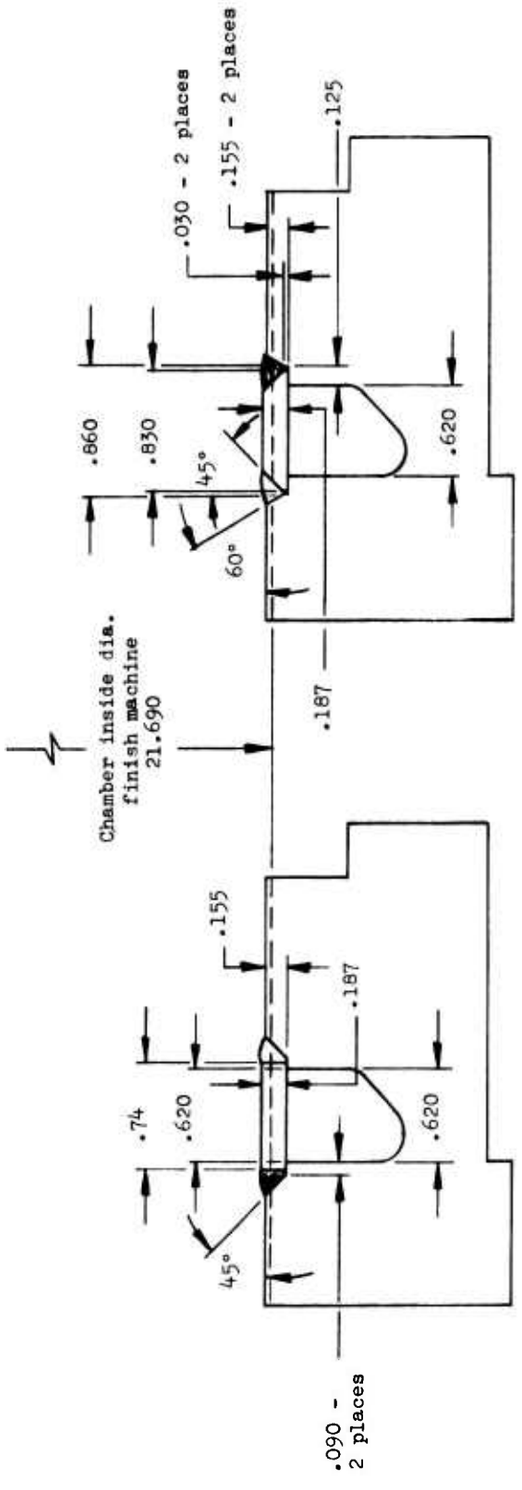

Figure 10 -- Redesign of Cover Band Joint

2.6, Problem Areas and Corrective Action (cont.)

(b) Reduce the brazing time (time above braze liquidus) to less than 10 minutes;

(c) Bright-anneal the chambers prior to brazing to clean up the surfaces that are to be brazed; and

(d) Perform the brazing at lower temperatures than had previously been used with CM 62 "B" alloy. Temperatures of 1920-1940°F are satisfactory to achieve good wetting yet retard runoff.

Leaks developed in the interior of three of the chambers during the demonstration testing. The leaks were all isolated to the forward flange-to-tube brazed joint and were the result of normal wear on chambers that were brazed prior to the advent of tighter controls on the brazing procedures to improve the chamber structure and brazed joints.

2.6.5 Cracks in Mounting Flange

Inspection of Chamber S/N 011 following Test No. 3051-D06-1M-017 revealed a crack approximately 1/2 inch long in the lower weld of the cover band to the forward flange. In addition two pinhole leaks were discovered in the weld.

The chamber was submitted to metallographic analysis to determine the cause of the crack. The conclusion drawn from the analysis was that there was insufficient penetration in making the weld. The design of the coverband and of the manifold region in the forward flange was modified as shown in Figure 10. The chamfer on the cover band in addition to the chamfer on the flange provides increased accessibility for welding. The matching shoulders on the cover band and the flange provides accurate positioning of the band prior to welding.

2.6, Problem Areas and Corrective Action (cont.)

Inspection of combustion chamber S/N 020 following Demonstration Test No. -203 disclosed two small cracks in the forward flange. The cracks were about one-half inch long and ran longitudinally through the wall at the crown of the up-tube feed holes. The forward end of the cracks was located at the aft weld joint of the closure band, and the cracks extended aft to nearly the up-tube brazed area.

These cracks were a direct result of a weld repair operation that was performed during chamber fabrication. Prior to brazing, the chamber had been assembled with a forward flange that had defective closure band welds similar to those in chamber S/N 011. The defect was not discovered until after chamber S/N 020 had been brazed, and a repair procedure was prescribed to remove the weld defect. The procedure called for grinding out the existing fore and aft weld areas with a V-shaped groove and rewelding using standard GTAW methods. However, the aft V-groove inadvertently cut into each up-tube passage, and residual braze within the passages contaminated the weld repair at the two crack locations. This residual braze material was identified and confirmed by X-ray.

The cracks are ascribed to the braze contamination of the weld because the X-rays show braze material only in the areas of the cracks. Cracking due to such contamination is commonly understood to result from the formation of intermetallic, brittle compounds during welding, and these compounds crack during thermal transients. The exact constituency of the brittle compounds is not known without metallurgical analysis or a theoretical study of the chemistry, but the manganese in the braze is presumed to be primarily involved.

No corrective action was applied because the primary weld procedure had been changed.

2.6, Problem Areas and Corrective Action (cont.)

2.6.6 Combustion Chamber Shell Cracks

No failures connected with the reinforcing shell were detected during development. Two incidents of cracking were noted during Engine Demonstration.

A failure analysis was conducted to determine the cause for a crack in the weld joint at the shell, P/N 1130228 and the aft attaching ring, P/N 1129923, on combustion chamber S/N 092. This chamber was removed from Demonstration Engine S/N 14 after Test No. -215 following 7 cycles and 865.06 seconds operation. Additionally, cracks were discovered in the weld joint at the shell to aft wire lock ring on Engine S/N 15 following Test No. -315. Five cracks had occurred on the shell lands on Subassembly 1 and on one land on Subassembly 2. Combustion chamber S/N 021 (Subassembly 1) had experienced a total hot firing time of 1912.25 seconds over 14 cycles; combustion chamber S/N 022 (Subassembly 2) performed 15 cycles for 1914.82 seconds. These cracks were repaired prior to Test No. -316.

A section of the shell was removed, including the cracked area of the weld, for analysis of mode-of-fracture. The replicated surface of the fracture was examined in the electron microscope. Ripple marks characteristic of fatigue caused by cyclic load were observed starting from the edge and extending down the fractured areas. The main fracture surface was indicative of cleavage and stress rupture (tensile). There were no dimples present, indicating a lack of ductility.

It was concluded that the fracture initiated in fatigue and rapid rupture followed as a result of cleavage and tension. It was concluded further that improved welding practice will minimize the probability of crack recurrence at this location.

2.6, Problem Areas and Corrective Action (cont.)

While the design of the J-groove is satisfactory, a provision has since been made for a "wrap-around" weld, starting on the side of the shell slot 90° from the shell land, which reduces the stress concentration point at the corner of the slot by permitting a smooth, continuous weld bead at the corner. The loading also has been changed on the weld head terminal from tension to shear, which is advantageous in this application. This technique has proved successful in similar welding applications subjected to high cycle vibration.

2.6.7 Injector/Chamber Gap Problem

The maximum permissible gap at the injector-to-chamber interface is 0.020 inch as specified by Engine Test Directive No. 21.1-2.6, which is applicable to all Titan family thrust chamber assemblies. Gaps in excess of that figure were observed during design verification testing. A gap of 0.040 in. was measured during prefire inspection of injector S/N 661 and chamber S/N 012 (Test 3051-D02-1A-110). A gap of 0.035 in. was measured during prefire inspection of injector S/N 664M and chamber S/N 015 (Test No. 3051-D02-1M-108). There was no noticeable effect on TCA performance as a result of these reported gaps. Postfire inspection of the seals revealed no change in seal condition as compared to seals used with low-gap chamber and injector combinations.

A summary of the measured gaps on tests conducted to this point revealed that of the nine chambers tested, S/N 012 and S/N 015 were the only units that exceeded 0.020 in. The chambers measured and maximum gaps observed are as follows:

2.6, Problem Areas and Corrective Action (cont.)

Table 3 -- Injector-to-Chamber Flange Gap

S/N	Max. Gap (in.)	Test Totals (sec)
006	.015	322
007	.020	384
008	.010	168
009	.015	1006
012	.040	1007
013	.020	302
014	.020	360
011	.025	320
015	.030	480

Combustion chamber S/N 012 was subjected to a dimensional inspection after the conclusion of its testing. Combustion chamber S/N 009, which did not have an excessive gap condition, was also inspected for comparative purposes. Both combustion chambers had been subjected to identical test series. The results of these inspections are presented in Figure 11. The baffle numbers refer to the injector baffles and are included to provide circumferential reference points. The mid points between the baffles are also shown. The inspection results illustrate that the flange was distorted similarly in both chambers. It is of interest to note that chamber S/N 009 did not exhibit a gap problem during testing, while chamber S/N 012 did. After this disclosure, a flatness check of injector S/N 661 was made. The mounting flange of the injector was found to be flat within 0.003 in.

The flange of the chamber becomes distorted as a result of testing. Surface No. 1 and Surface No. 2 (from Figure 11) are obtained in a single machining operation. This would produce surface differences (dimension "A") of approximately $\pm$ 0.001 in. in an unfired chamber. Combustion chamber S/N 015 was inspected before testing and the "A" dimensions recorded varied from +0.003 to -0.001 inches.

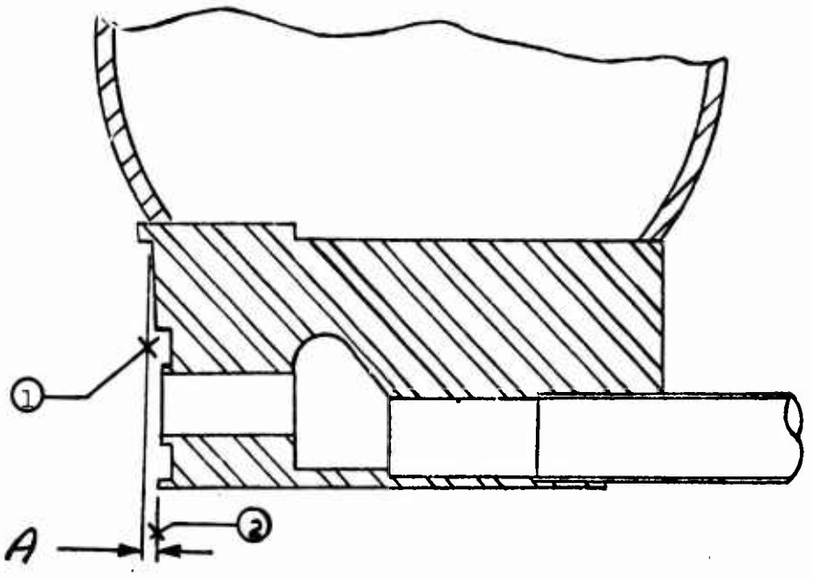

A DIM.

Baffle No.	S/N 009	S/N 012	S/N 015
1	.013	.015	.018
-	.013	.012	.012
2	.015	.022	.023
-	.007	.008	.014
3	.007	.015	.018
-	.010	.010	.010
4	.011	.024	.021
-	.013	.015	.014
5	.014	.016	.020
-	.016	.015	.010
6	.024	.018	.016
-	.016	.010	.013
7	.022	.024	.030

Figure 11 -- Combustion Chamber Flange Distortions

2.6, Problem Areas and Corrective Action (cont.)

The results of the dimensional inspection of chamber S/N 012 and injector S/N 66i indicate that the gap reported may have been the result of an inaccurate measurement. The flat injector flange and the chamber distortion of 0.024 in. should have produced a gap of approximately 0.024 in. and when the components were reassembled, that is the maximum gap reported.

2.6.8 Raco Seal Damage

During the TCA verification testing, instances of damage to the inner Raco seal (Figure 12) at the injector to chamber interface occurred. The damage consisted of charring and cracking of the Teflon portion of the seal. The cracks provided a leak path for the fuel directly to the combustion zone rather than through the injector, resulting in inefficient utilization of the propellant. Such a leak path is shown in Figure 13 and a damaged seal in Figure 14.

During TCA Test No. 3051-D02-1M-011 this seal leaked sufficiently to cause a loss of 1.60 second in specific impulse. A downward shift in injector fuel circuit resistance (RFJC) accompanied the performance loss. The performance loss was verified by reassembling the TCA and repeating the test with a new seal.

The Titan IIIM TCA may subject the seal to a more severe environment than other Titan family systems. The injector operates with 10.5% chamber fuel film coolant, as compared to 16.1% with the 87-9 design. Therefore, surface temperatures on the chamber flange are 1500°F on Titan IIIM, and only 1000°F on the production flange.

A record of seal damage similar to that of the Titan IIIM was also encountered on the Titan B and C and the Titan II programs, although the thermal environment of those chambers is less severe than the Titan IIIM. Disassembly of a SLAP (Service Life Analysis Program) engine revealed the Raco seal also to be in a condition similar to that of the Titan IIIM seal. The SLAP engine had been subjected to two acceptance tests (20 seconds and 165 seconds) prior to its delivery.

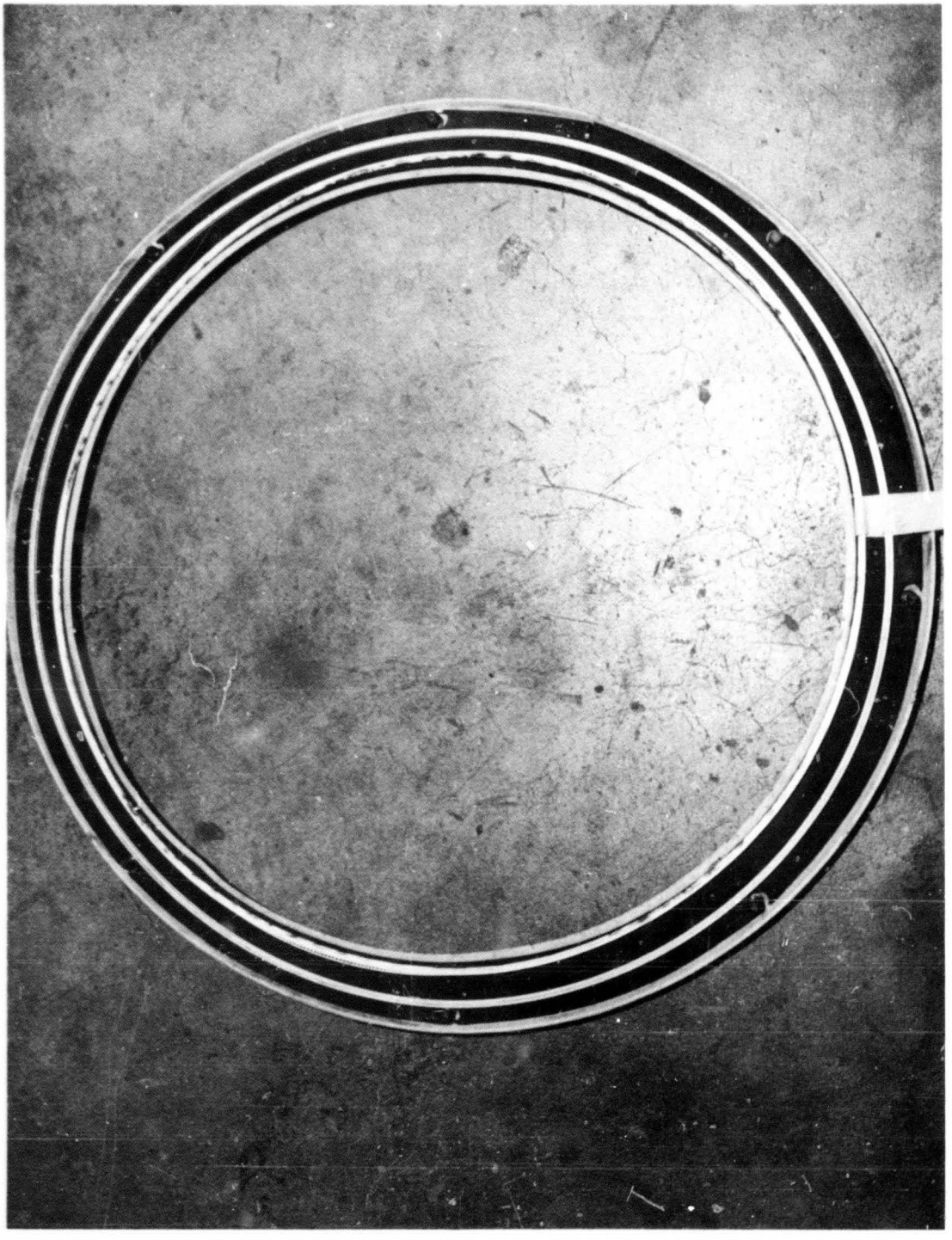

Figure 12 -- Raco Seals

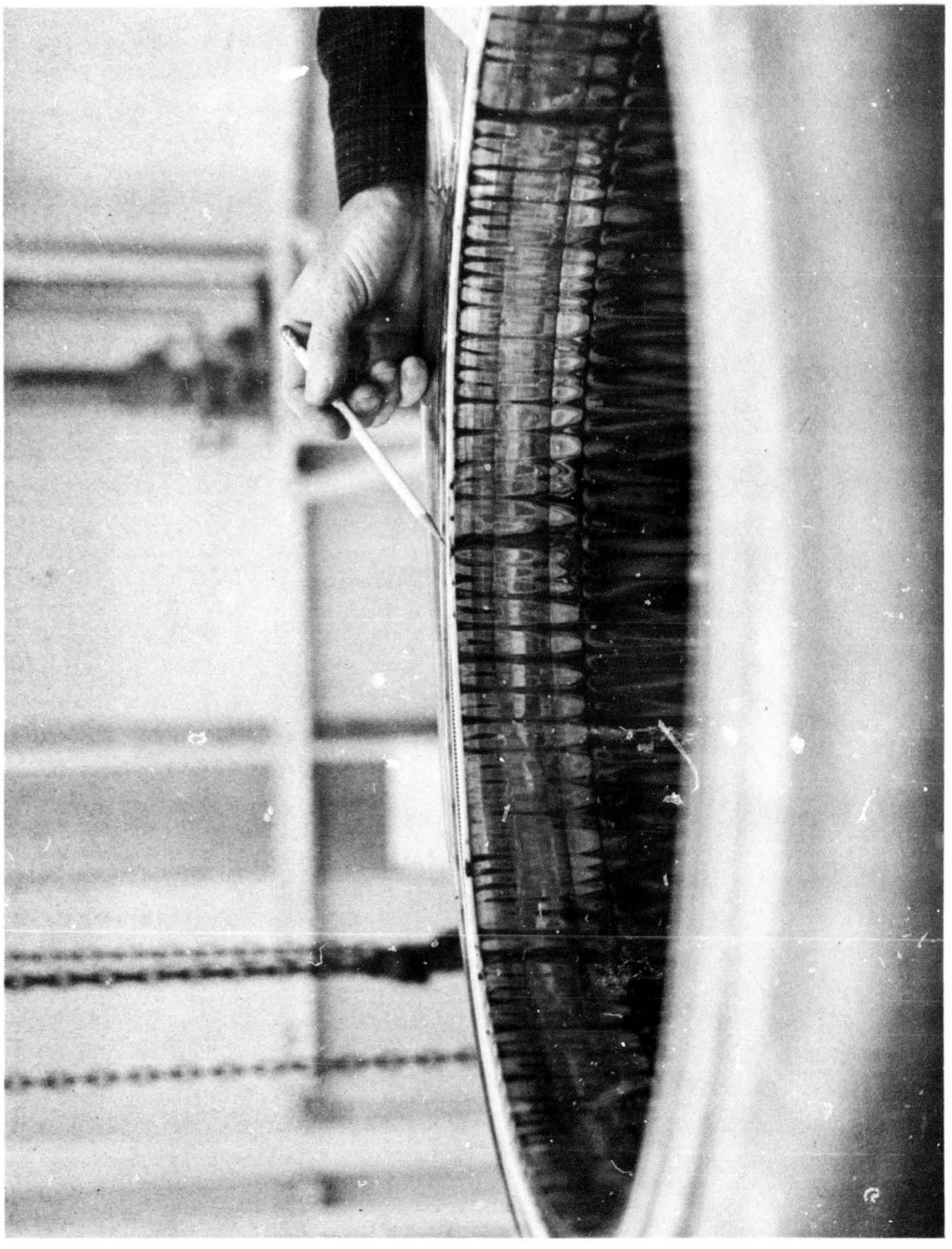

Figure 13 -- Raco Seal Leak

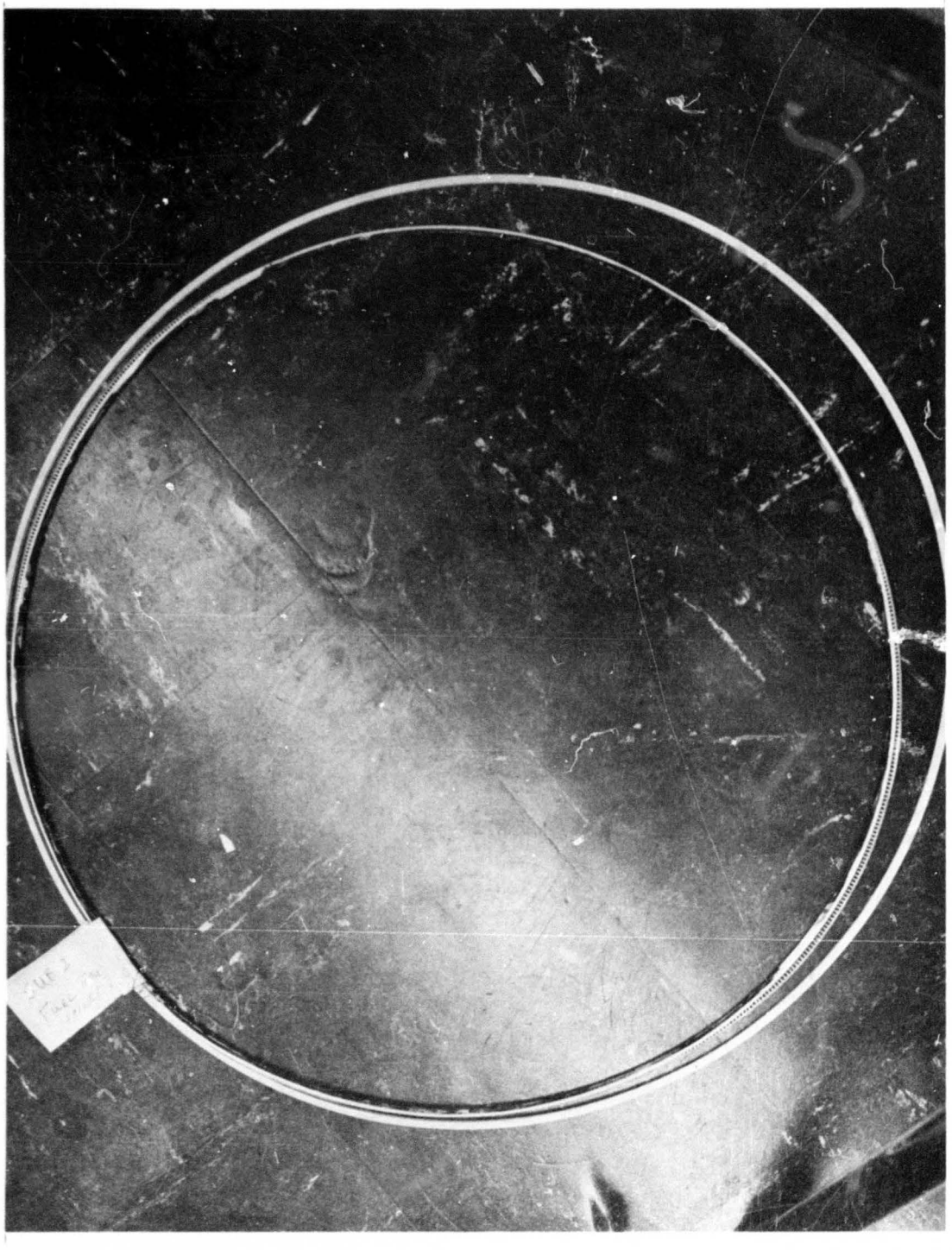

Figure 14 -- Damaged Raco Seal (1 of 2)

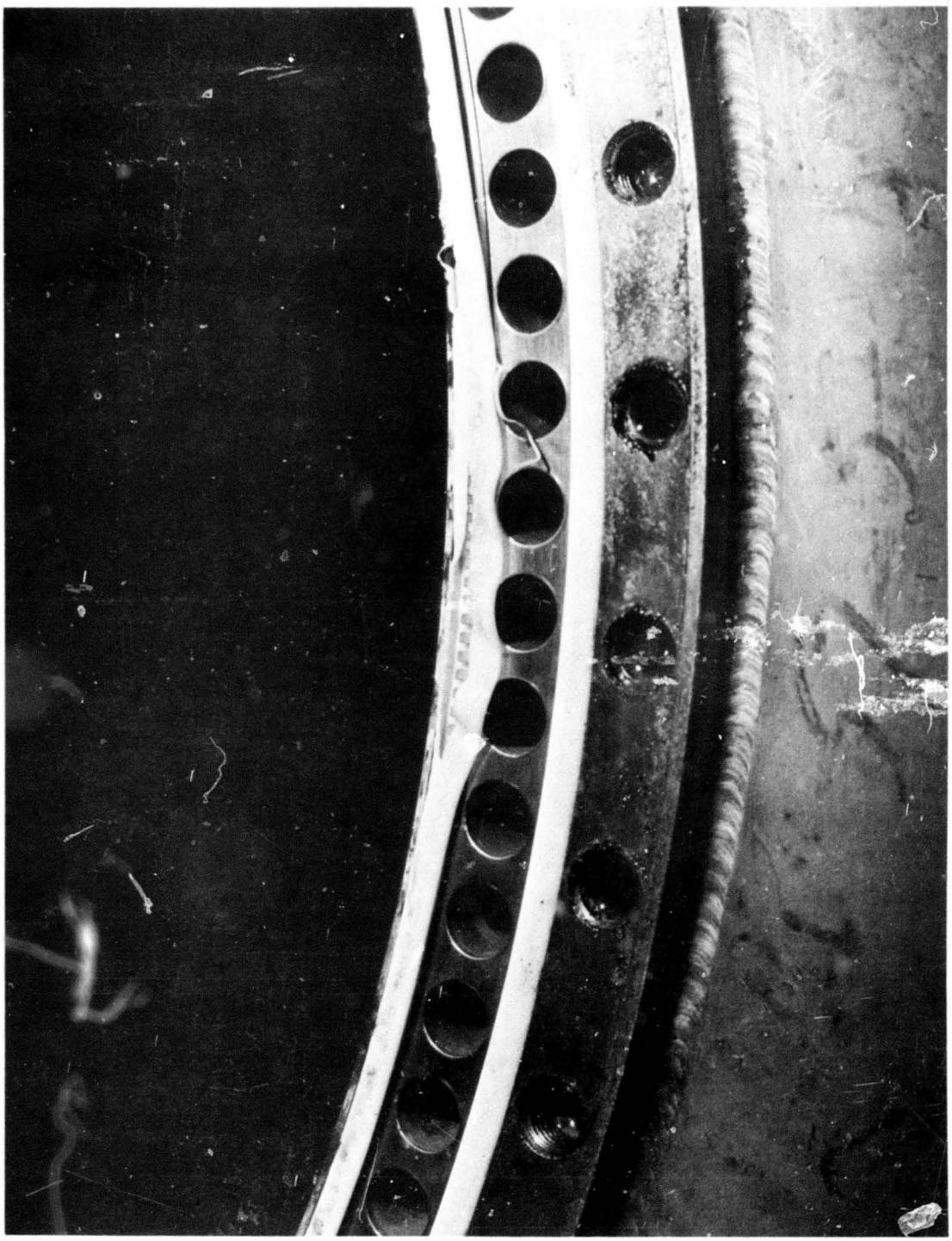

Figure 14 -- Damaged Raco Seal (2 of 2)

2.6, Problem Areas and Corrective Action (cont.)

The inner Raco seal was changed prior to each subsequent Titan IIIM TCA verification test. This was required to obtain valid injector performance data. The seals which had been used during tests were collected for observation.

An investigation for a possible replacement seal was initiated and a metal seal produced by Raco Engineering appeared to be promising. The proposed seal operated on the same principle as the current Raco seal, but had higher temperature capabilities because of its all metal construction. Preliminary negotiations with Raco Engineering resulted in Raco Engineering agreeing to furnish such a seal, but fabrication of the design proved to be impractical, since the required flatness and orientation of the seal could not be maintained.

Test No. 3051-D02-0M-110 was conducted with a "solid spring Raco" in place of the conventional Raco (injector to chamber) seal. This seal was identical to the standard seal, except the inner spring was solid rather than serrated. The postfire inspection of the seal revealed that a positive seal was effected throughout the run. The solid inner spring is stiffer than a standard unit, and it does not leak if the Teflon lining is damaged.

2.7 FINAL PROTOTYPE CONFIGURATION

The combustion chambers used during the demonstration test program incurred only normal wear with little damage. The normal appearance of the chambers included blackened coolant tubes, minor fuel leakage at the forward flanges (at the tube joints), slightly distorted forward flanges that resulted in chamber-to-injector gaps up to 0.035 inch, cracks in the shell-to-chamber welds at the lower attachment, cracks and flaking of the epoxy coating, minor erosion on the forward flanges, and general discoloration. Damages other than normal that were noted, consisted of one instance of loose wirewrap, one instance of forward flange cracking and two instances of tube cracking.

2.7, Final Prototype Configuration, (cont.)

The loose wire wrap was attributed to an improper application and use of unclean wire both above and below the throat sections. The wire wrap above the throat was replaced and remained intact during test, but the aft section loosened.

Cracking in the forward flange was attributed to an in-process rework operation that had contaminated the weld joint between the closing band (P/N 1154237) and the flange (P/N 1154236) with braze alloy. The contamination induced brittleness of the material which produced cracking under thermal stress conditions.

Both tube cracks were precipitated by the deposition of molten metal from erosions in the forward flanges. Although the exact mechanism of damage is not known, the deposition of the metal on the tubes probably induced high local wall temperatures which led to metallurgical or chemical erosion and extensive carburization of the tube wall.

Section 3 Fabrication

3. FABRICATION

3.1 FABRICATION SUMMARY

The combustion chamber was released for fabrication in January 1966. Items requiring the longest lead time had been pre-released.

The first sample Titan IIIM combustion chamber tube was received in February from the vendor and indicated that the tapered wall concept in this configuration was feasible. A shipment of the "up" and "down" tubes (150 each) arrived early in March.

The torus with the flow splitters was received and welded to the injector mounting flange; assembly difficulty and weld distortion were minimum.

Assembly of the first Titan IIIM combustion chamber was started on 19 March. (Views of the tube layup mandrel and wire wrap machine are presented in Figure 15). The only significant setback was a deficiency in the aft flange as received from the supplier. The outside diameter was undersized by 0.046 in., which caused a mismatch of the aft flange and tubes. A machine-cut to the aft tube corrected the mismatch. The chamber prior to wirewrap is shown in Figure 16.

During April, assembly of the first and second Titan IIIM combustion chambers (S/N 001 and 002) continued, but because of numerous fabrication and design difficulties, the first unit (S/N 001) was not completed until May 1966. This chamber, shown in Figure 16 before wire-wrapping, did not have a reinforcing shell.

Chambers S/N 003 through 022 were completed as scheduled (see Figure 17).

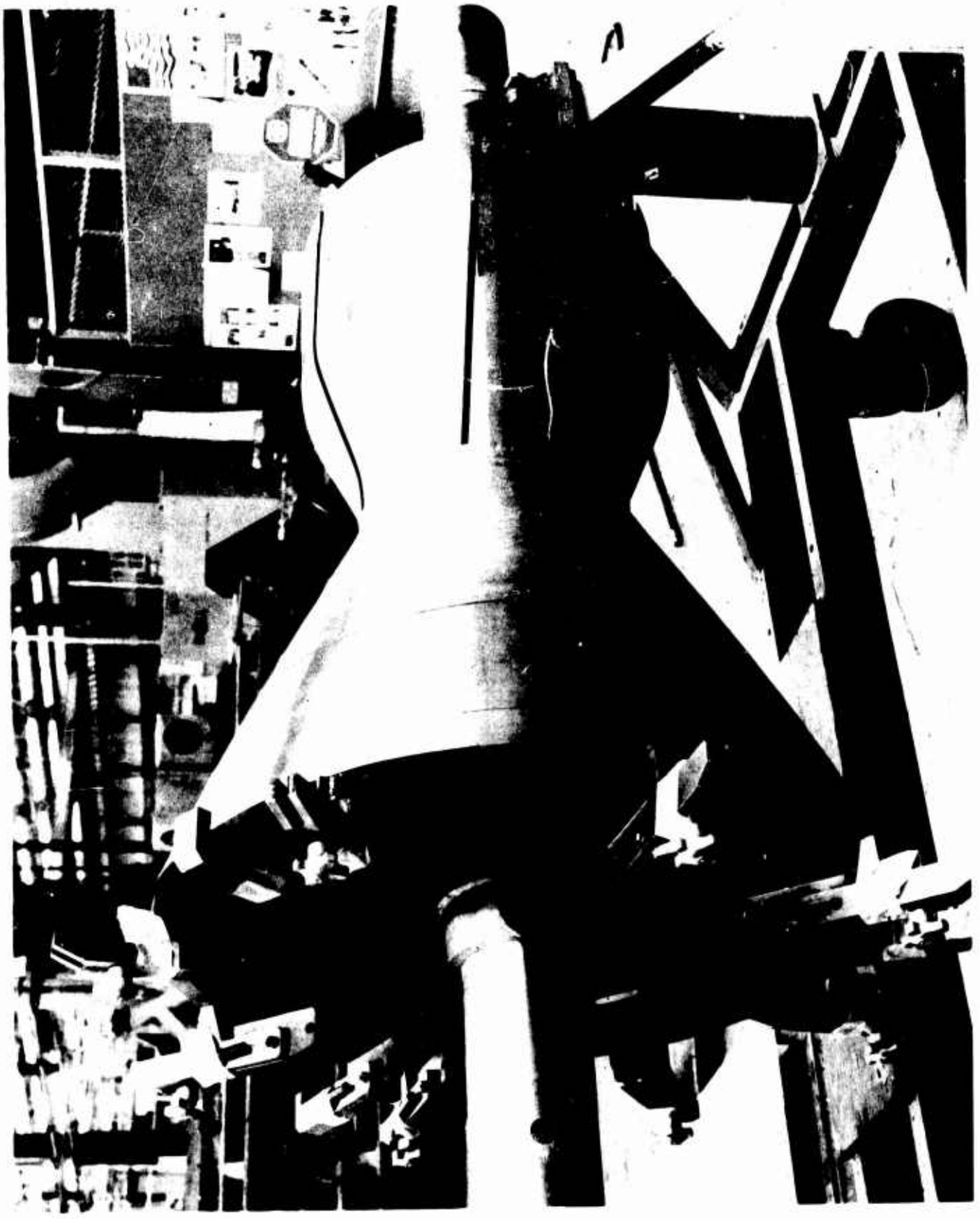

Figure 15 -- Tube Assembly Mandrel

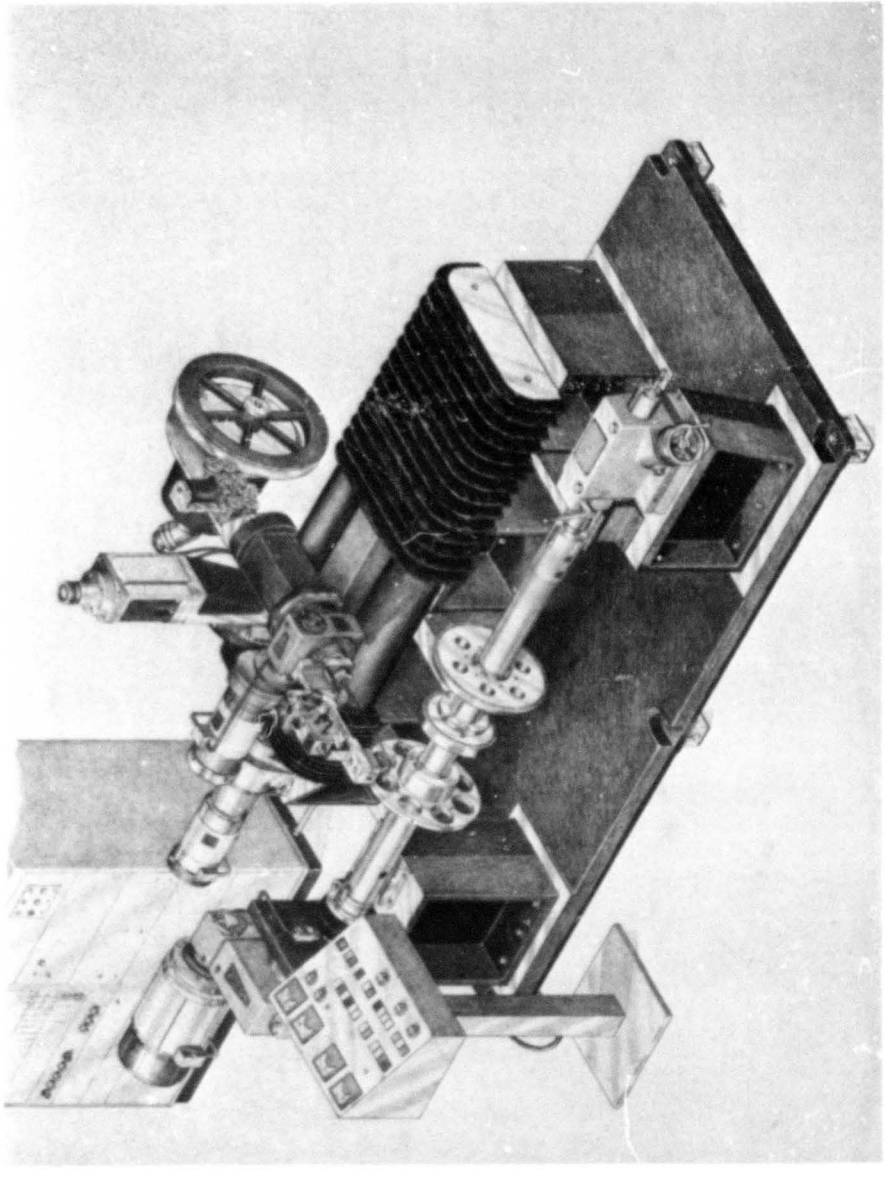

Figure 15 (cont.) -- Wire Wrap Machine

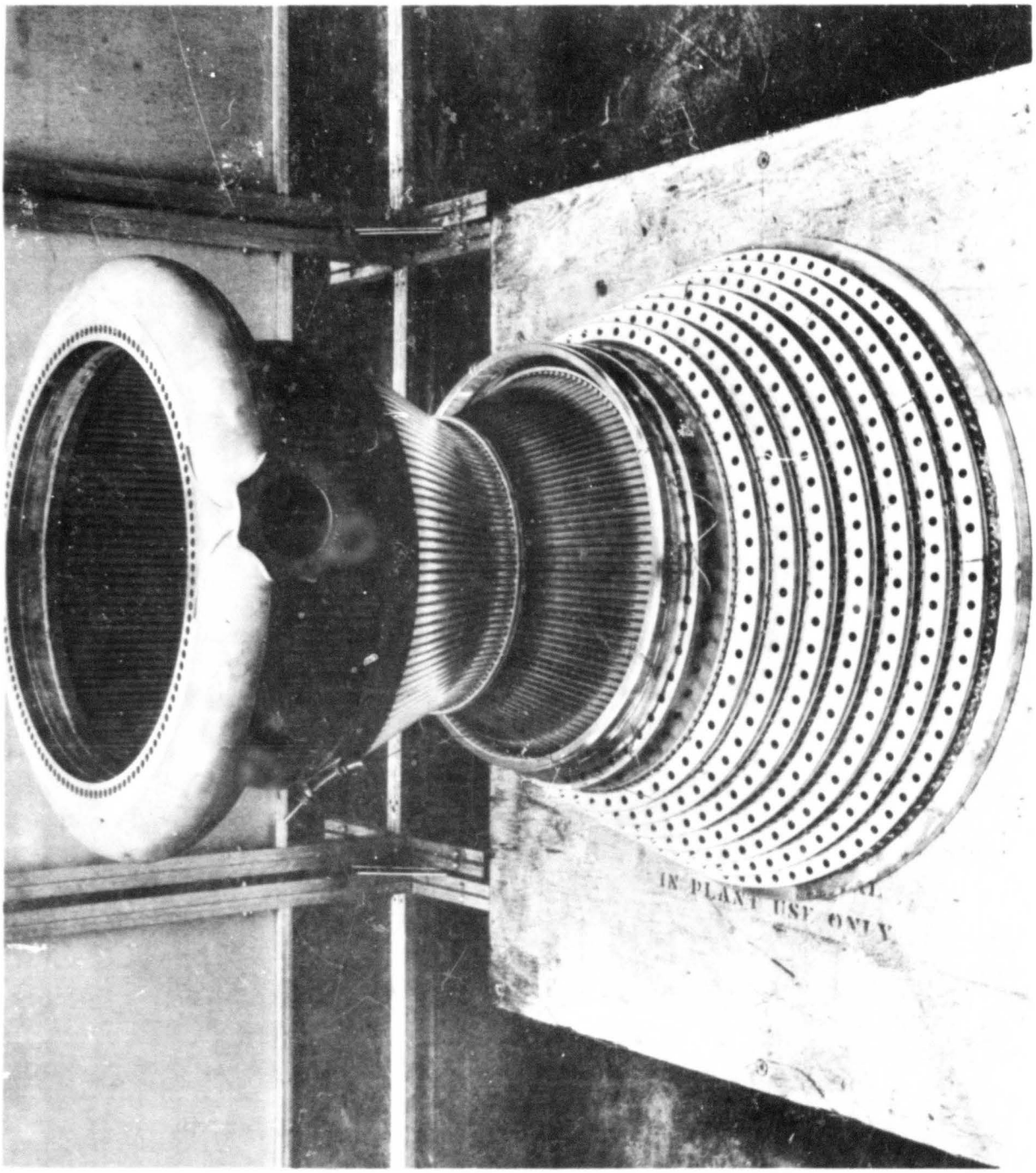

Figure 16 -- Combustion Chambe before Wire Wrapping

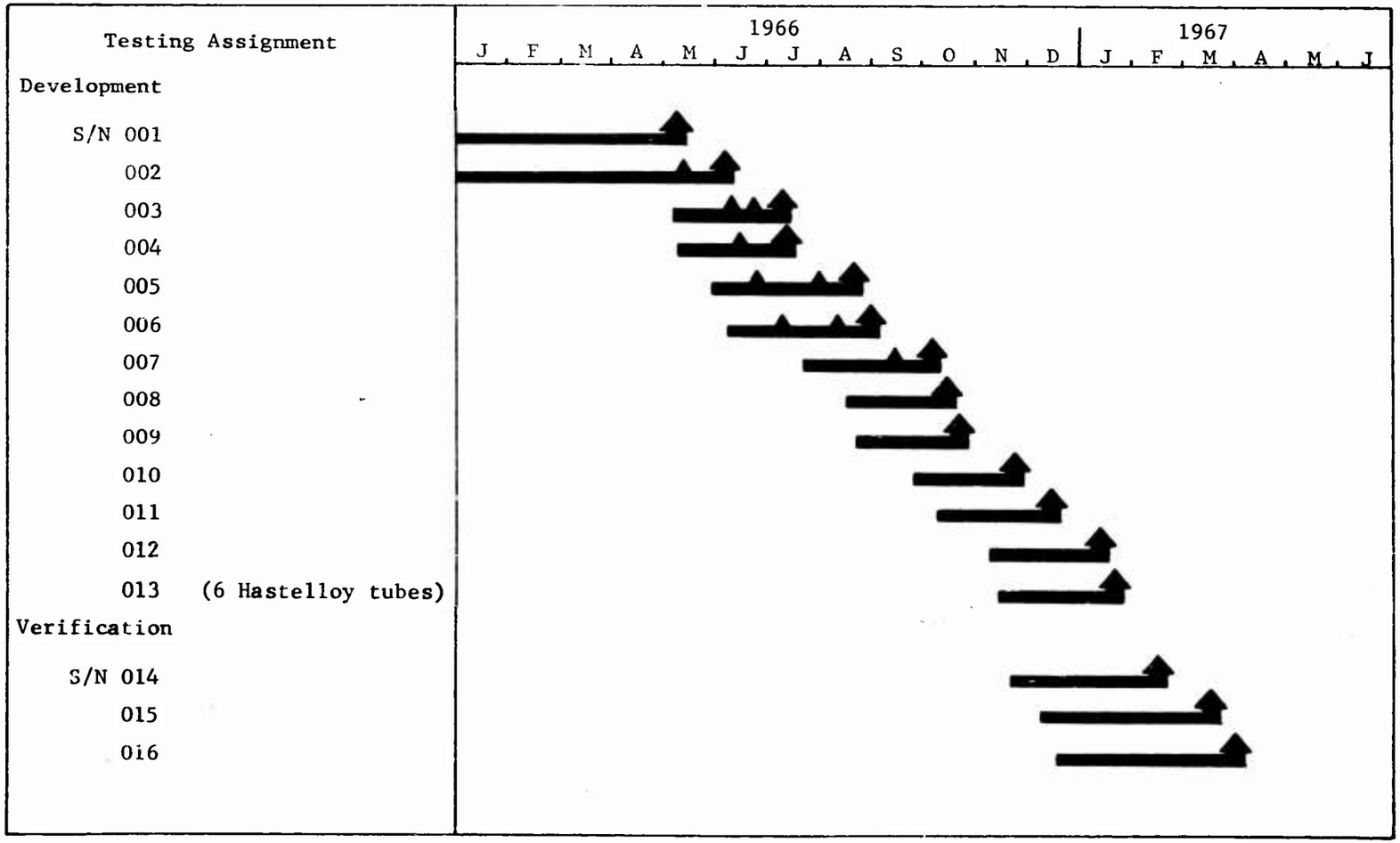

Figure 17 -- Combustion Chamber Fabrication Schedule

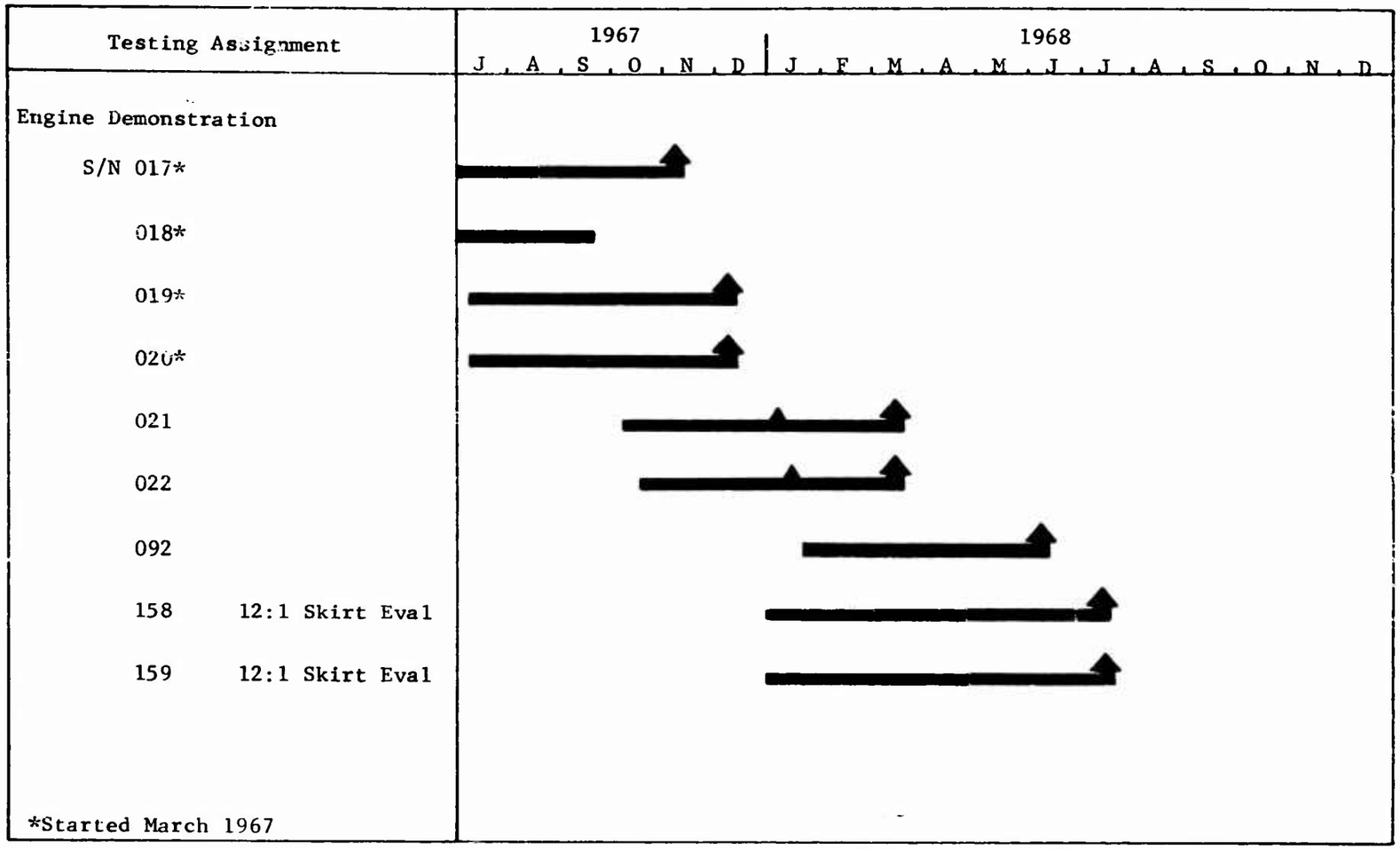

Figure 17 -- Combustion Chamber Fabrication Schedule

3.1, Fabrication Summary (cont.)

Problems associated with their fabrication are discussed in Section 3.2. Chambers S/N 002, S/N 003, and S/N 010 were equipped with strain gages for measuring side loads and for structural testing as described more fully in Section 4.1. Chambers S/N 005, S/N 006, S/N 007, S/N 008, and S/N 009 had braze patches installed as described in Section 4.2.

Combustion chambers S/N 011 and S/N 012 were equipped with shells instrumented with strain gauges in order to obtain data concerning side loads from altitude testing. Combustion chamber S/N 013 (using six Hastelloy tubes) was also equipped with braze patches.

Chambers S/N 014, S/N 015 and S/N 016 intended for verification testing were completed in March 1967. Chamber S/N 016 was equipped with the braze patch pattern illustrated in Figure 18. This pattern is designed to develop a circumferential profile of tube wall temperatures. Previous braze patterns had concentrated on longitudinal rather than circumferential temperature variations, but temperature data from previous tests indicated that tubes adjacent to baffles are hotter than the tubes between baffles. In addition the braze patches were useful to provide flange surface temperatures for comparison with those utilized in the structural analysis.

Tube layup of the first chamber for the Demonstration Engines was initiated in May 1967. During this period the Aerojet brazing furnace was being repaired; therefore chambers S/N 017 and S/N 018 were sent to Pyromet for two braze cycles using AGC-44080 "B" alloy. Upon receipt at Aerojet it was noted from the report that these chambers were brazed without monitoring the dew point of the hydrogen atmosphere and of the temperature of the combustion chamber as detailed in Specification AGC-46865. In addition, chamber S/N 017 also had a 7-in. long leak between tubes 52 and 53 extending from the throat band to under the aft wire lock band. Since the leak was reparable with Premabraze 250, and the braze appearance was similar to other Titan

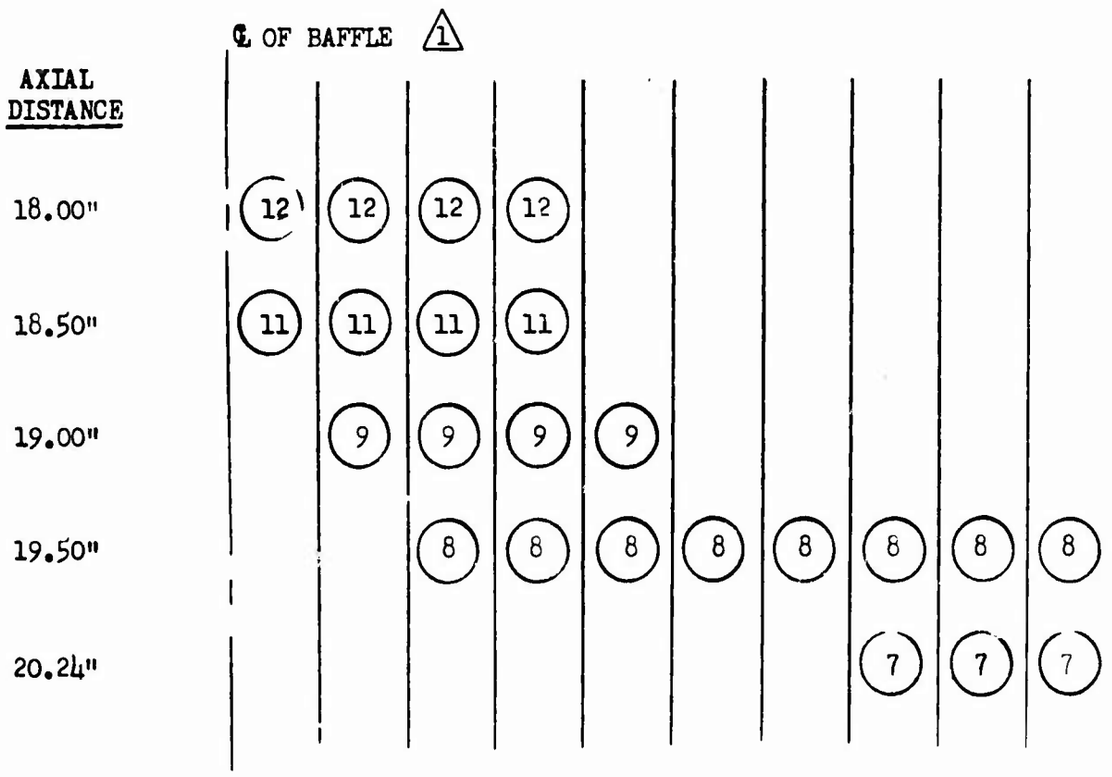

AXIAL DISTANCE	ALLOY NUMBER	BRAZE ALLOY	COMPOSITION	SOLIDUS TEMP, °F	LIQUIDUS TEMP, °F
18.00	12	CRONIRO	72Au-22Ni-6Cr	1785	1835
18.50	11	NIORO	82Au-18Ni	1742	- -
19.00	9	NICORO 80	82Au-16Cu-2Ni	1670	1697
19.50	8	T.E. SPECIAL	5Ag-52Cu-37Zn	1575	1600
20.24 (THROAT)	7	N.E.	25Ag-53Cu-22Zn	1500	1575

1 THIS BRAZE PATCH LAYOUT IS TYPICAL AT BAFFLES #3, #6 & #7

Figure 18 -- Braze Patch Pattern -- Chamber S/N 016

3.1, Fabrication Summary (cont.)

chambers that were brazed to Specification AGC-46865, with the "B" alloy, the chambers were accepted for demonstration usage.

On the basis of schedule and testing requirements, Chambers S/N 019 through S/N 022 were assigned to Engine Demonstration. Chamber S/N 017 was held in reserve and eventually replaced chamber S/N 020 after Test No. 3051-D01-1A-203. Chamber S/N 018 became unsuitable for Demonstration use because of an accident during hydrotest and was assigned to experimental use.

3.2 FABRICATION PROBLEMS

3.2.1 First Article Problems

As is frequently the case with the first units of a new design, minor difficulties were experienced in controlling dimensions and in executing the assembly of chambers S/N 001 and S/N 002. The problems fell within the following general categories:

Physical Interference During Assembly

The most notable instances of such interference were between the torus weld head and the injector mounting flange and the shell retaining ring and the torus. Small dimensional changes corrected both problems. The original configuration with the high weld is shown in Figure 19a, (chamber S/N 003); the revision is shown in Figure 19b (chamber S/N 007).

Dimensional Changes Resulting from Welding

This problem occurred in the concentricity between the holes and centerbores in the forward flange where the holes were milled prior to welding the closure ring and torus while the counterbores were made after welding. The problem was corrected by performing both operations after welding.

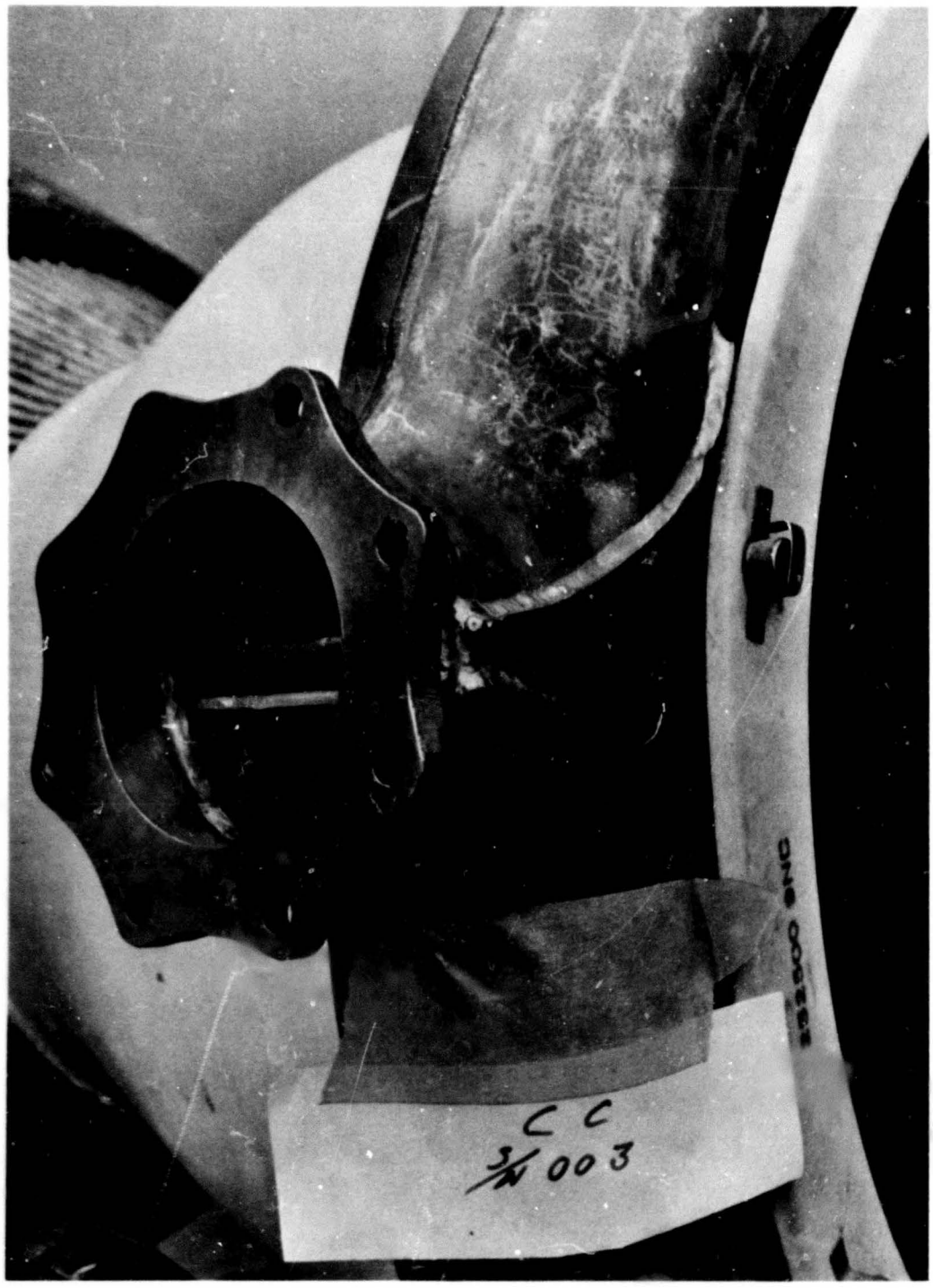

Figure 19 -- Mounting Flange and Torus Changes -- Chamber S/N 003

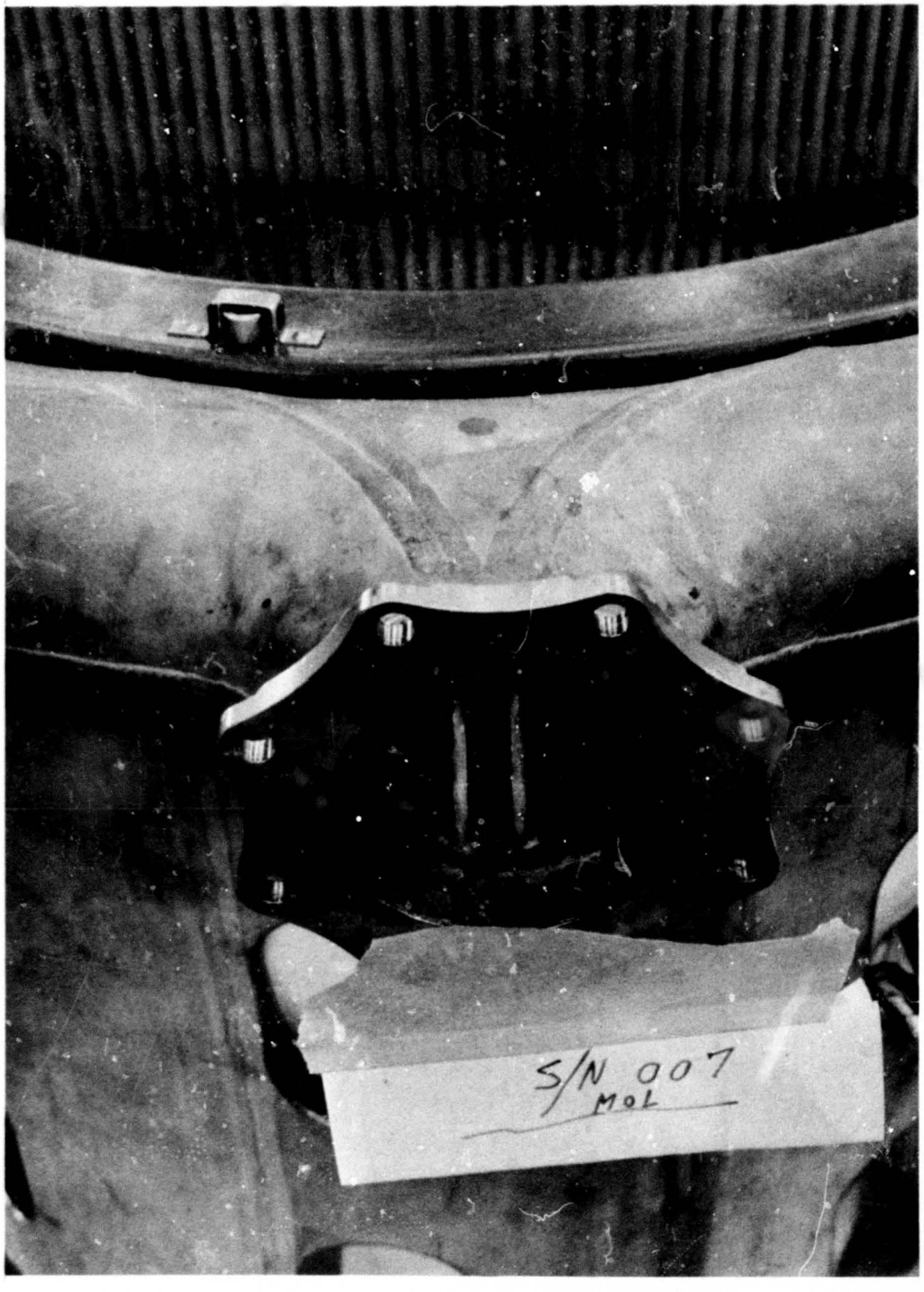

Figure 19 -- Mounting Flange and Torus Changes -- Chamber S/N 007

3.2, Fabrication Problems (cont.)

Indexing and Tolerances

In some cases polar coordinates were given in the prints. It was necessary to convert to rectilineal coordinates where tape-controlled machines were used. Mislocatio. of the fuel inlet flange resulted from a tolerance buildup, which was corrected. In another place the tolerance was eased in order to facilitate machining. A misfit between the torus and the mounting flange was corrected by redimensioning the respective parts to move the line of contact to where it was more easily controlled. A similar correction was applied to the locating of the V-bands.

The reinforcing shell is installed after hydrotest in order to keep the area clear for the inspection for leaks. After hydrotest the orientation of the first V-band, where the shell is attached, is displaced slightly. The problem was corrected by machining the locating dimension after hydrotest.

Complex Assembly Procedure

The only instance of this problem occurred at the aft end of the shell which is also where the end of the wire wrapping is secured by a lock band. The lock band and the clamp securing the shell were redesigned to facilitate assembly.

Tooling Problems

The tool finishing the conical feed holes in the forward flange leading to the down tubes tended to bind and there was also entrapment of lubricating oil. A relief was furnished for the tool and a drain hole provided for the escape of the oil.

In one instance the chamber could not be freed from the mandrel after wirewrap. Closer control of the wire tension eliminated a repetition.

3.2, Fabrication Problems (cont.)

3.2.2 Forward Flange Closure Band

The internal surface of the forward flange is finished-machined after welding of the closure ring. In the original design the excess material on the closure band was not removed for fear of leaving the ring too thin afterward. This left a discontinuity on the flange surface that prevented the even spread of the film coolant from the injector with the possibility of overheating and erosion. The closure band was made shorter and thicker to permit cleanup during the finishing operation and also to make up for shrinkage resulting from welding the closure band to the flange. The contour of the collector ring (manifold) was also reshaped to maintain a smooth flow.

3.2.3 Cooling Tube Tolerances

Difficulties experienced by the vendor in controlling the cooling tube circumferences to the tolerances specified led to re-examination of the heat transfer calculations and of the operations performed for the assembly of tubes. It was found that the tolerances could be relaxed and the drawings were changed to the new tolerance.

3.2.4 Brazing and Wire Wrap Procedures

A characteristic of all Titan combustion chambers is their thin-walled tubular construction, which has the advantages of efficient cooling and light weight. However, in order to seal the chamber walls against the escape of combustion gases, the tubes are caulked with a brazing compound and to prevent fuel leakage braze is also applied where the tubes are joined to the mounting flanges. In order to retain the pressure of the combustion gases it is necessary to wrap the tubes on the ouside with wire, like a spool of thread, which is held in place with epoxy resin. The wire must be installed prior to high pressure leak tests but removed, if leaks are discovered, in order to make repairs.

3.2, Fabrication Problems (cont.)

Brazing and wirewrapping procedures, originally defined for Titan I, have been extended and elaborated for Titan II, Gemini, and Titan III. Critical points in the processes are: cleaning and degreasing, braze preparation, wire-tension during wrapping, and the application of epoxy. Titan IIIM procedures are further refinements of Titan III practice.

A new brazing technique was to swage the ends of the tubes before brazing them to the mounting flanges. Metallurgical inspection of chambers that had developed leakage disclosed that the braze covering was inadequate on the surfaces where the tubes actually contacted the flange. The swaging makes certain that the braze penetrates to an adequate depth around the entire tube circumference. To make sure the tubes were centered in the holes they were tack-welded in place before brazing. Better joints were made also by reducing the braze temperature and shortening the "dwell" time, which assured liquefaction of the braze while reducing the runoff.

The tubes for chamber S/N 021 were stacked prior to brazing, but the stack was unsatisfactory because of a slight tube twist and uneven tube ends. Because of this difficulty the tube layup operation was changed so as to tack weld the aft ends of the tubes together prior to strapping the tubes down. In this way the slack is taken up throughout the length including the forward end, rather than at the aft end, where the tube fit is so critical.

Wirewrapping procedures were modified to make certain the wire is clean and to assure closer control of wire tension. The procedures for applying the epoxy bed and covering were tightened to ensure against cold joints. The cleaning procedures were also modified to prevent water from getting into the stripping tank when the wire wrap must be removed after leaks are located during hydrotest. Also provision was made to make certain all stripping caustic has been removed before braze repair.

3.2, Fabrication Problems (cont.)

3.2.5 Hydrotest Procedure

Hydrotest procedures also have evolved along with the other Titan fabrication procedures. They provide for a low pressure gas leak check after brazing and before wirewrap and a high pressure proof-and-leak check after wirewrap, using water. During a period of intensive rework, the separate requirements for braze preparation, wirewrapping, cleaning, and hydrotest made the rework cycle quite complex and lengthy, with occasional procedural errors resulting from the complications. The hydrotest procedures were investigated in view of possible simplification. The test pressures were also examined to determine whether they were realistic.

On the basis of this study it was concluded that the test pressure requirements were correct and both tests were necessary. However, it was decided to conduct the high pressure leak test of the liquid (fuel) circuit prior to wire wrap so that any leaks could be repaired without removing the wire. This also subjects all brazed joints to proof pressure so that incipient leaks between tubes can be detected before the wire is applied.

3.2.6 Flange Distortion

Distortion of the forward flange similar to that shown in Figure 20 occurred on both chambers S/N 019 and S/N 020 after the cover band weld repair. The injector feed holes which are drilled on a 22.730-in. diameter were on a diameter of 22.516-in. after the weld repair. This contraction caused an interference between the feed holes and the outer diameter of the inner seal groove. The alternatives then were: (1) to machine the seal grooves per blueprint and let the groove outer diameter break into the feed holes as occurred on S/N 017, or (2) to machine the inner seal inside diameter to blueprint and adjust the outside diameter to provide the minimum width groove required for correct Raco seal installation and operation.

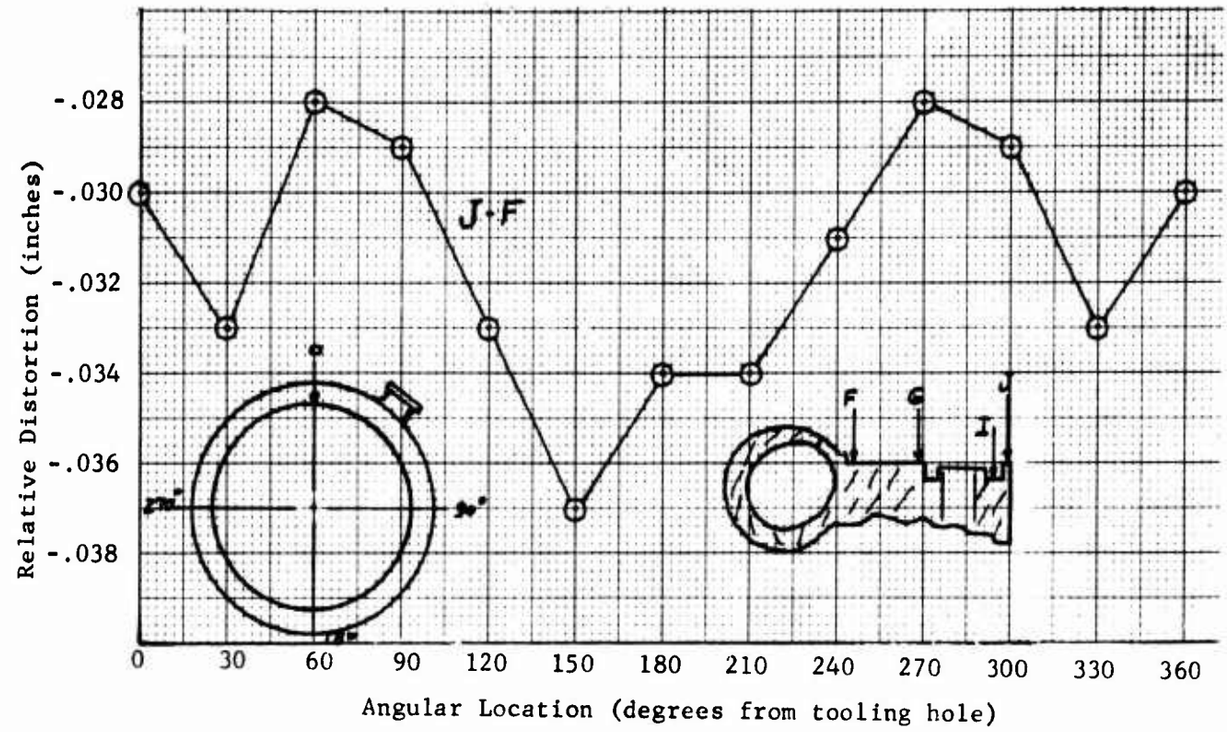

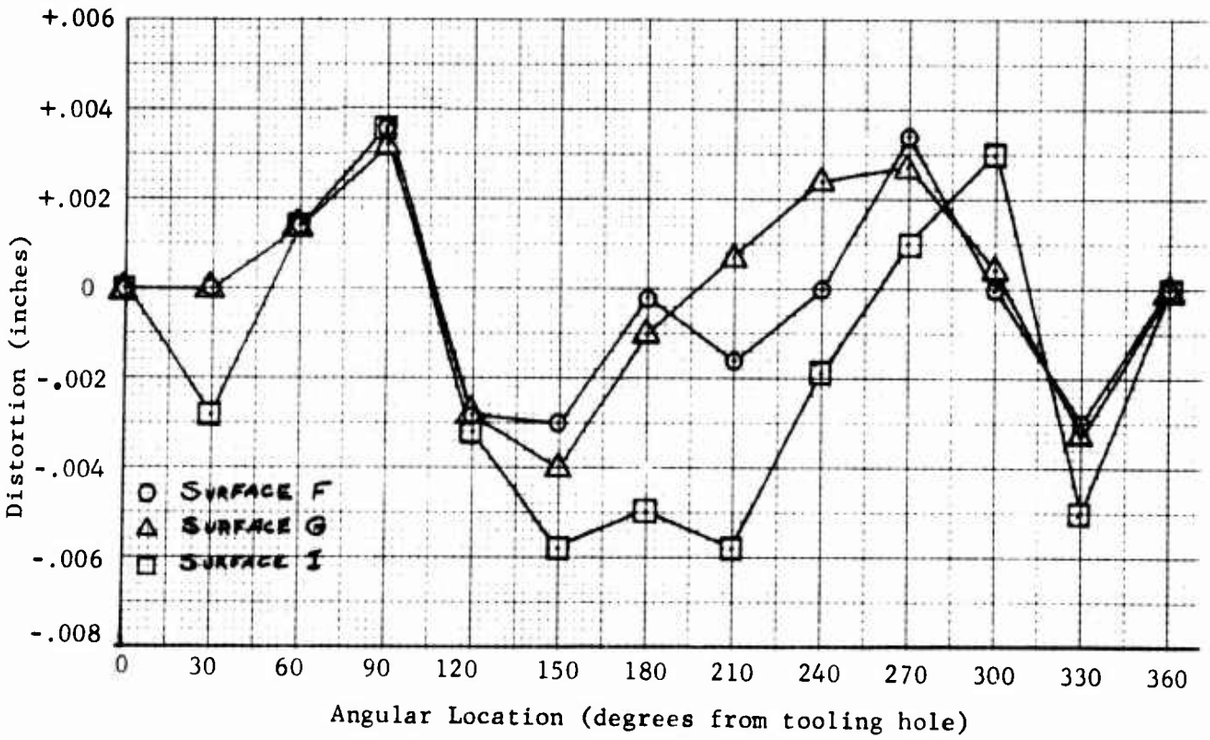

Figure 20 -- Forward Flange Map--
Combustion Chamber S/N 018

3.2, Fabrication (cont.)

Alternative (2) was therefore selected as the more satisfactory means for correcting the problem in chambers S/N 019 and S/N 020. Drawing No. 701773 (AEIP seal utilized for Titan IIIM at the inner seal) requires a minimum seal groove width of 0.195 while the chamber flange per B/P 1130174 is designed for a minimum groove width of 0.214 in. The chambers were machined as shown on Figure 21. All dimensions are to be to blueprint with the exception of the 22.167 in. dia, which normally is 22.250 $\pm$ 0.010 in. dia.

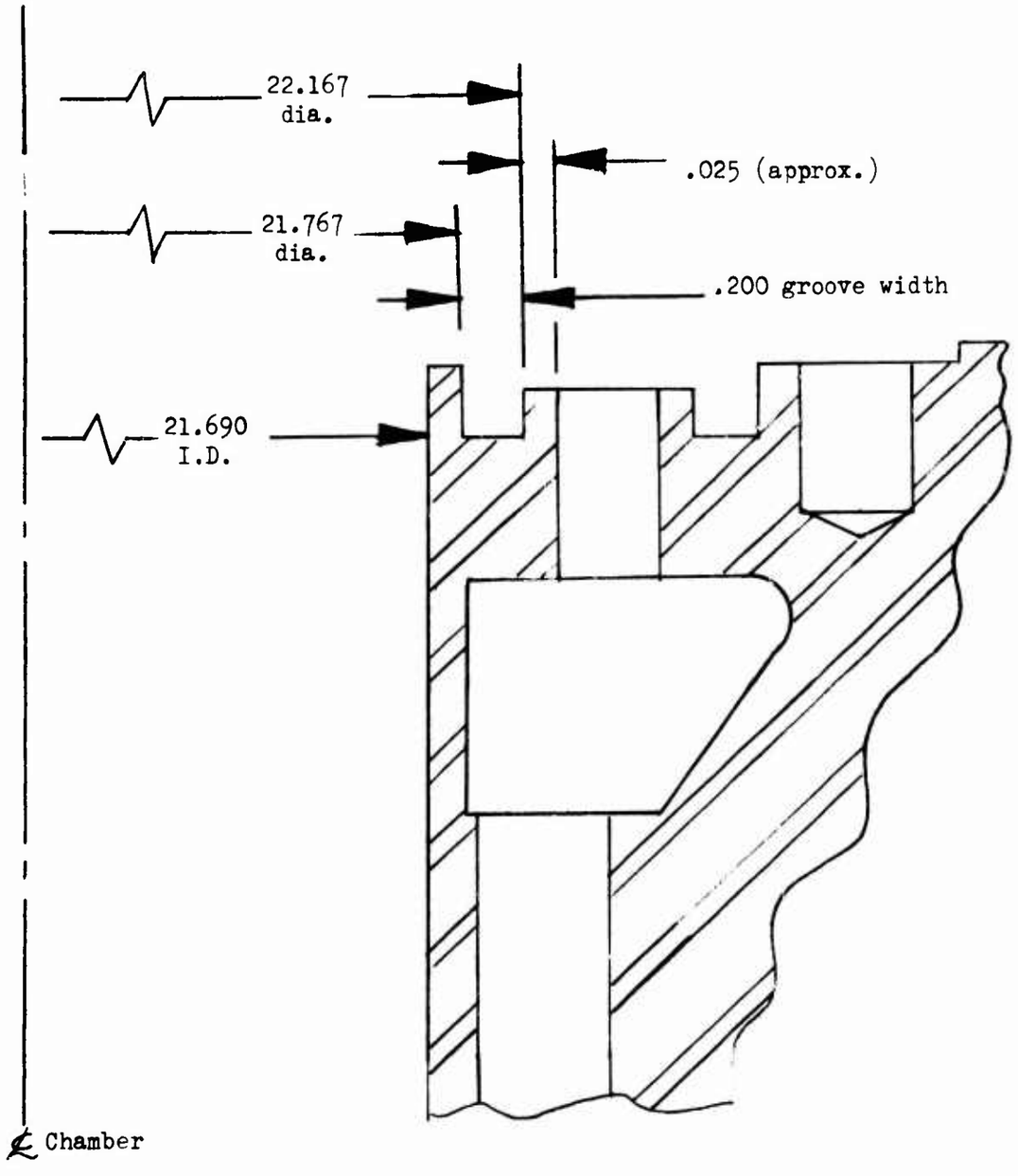

Figure 21 -- Combustion Chamber Flange -- S/N 019

Section 4 Analytical Programs

4. ANALYTICAL PROGRAMS

Special analytical studies were undertaken in the areas of stress, heat transfer, hydraulics, and materials and processes to support the design effort and to interpret the results from test data.

4.1 STRESS ANALYSIS

A thorough analysis of combustion chamber stresses under all anticipated conditions was made and published*. Essential to this analysis were:

(a) Determination of the side loads that might be imposed on the chamber by asymmetric flow during sea level starts and by altitude starting and maneuvering,

(b) development of instrumentation to acquire the side load information during captive tests,

(c) checking of stress calculations by static load testing, and

(d) revising the computer program used for stress calculations to add the capability to handle these additional data.

A summary of the activities and findings in these areas follows.

---

* AGC Report M-18, Structural Analysis of the Titan III M Stage I Combustion Chamber, 13 January 1967, Revised 22 October 1967, Structural Analysis Dept. 9632. (Reference A)

4.1, Stress Analysis (cont.)

4.1.1 Analysis of Side Loads

The sea level start requirement for the YLR87-AJ-11 engine necessitates the definition of the asymmetric flow separation that results from overexpansion in the ablative skirt during sea level operation. This permits establishment of design values for the bending moment on the chamber.

Tests in which actuator loads of up to 22,000 lbs were applied to a composite structure of the dome, injector and combustion chamber were completed in May 1966. The test set-up used at that time is shown in Figures 22 and 23. The actuator load tests were made at the actuator-to-vertical angles of 10 degrees and 23 degrees. The 10 degree angle is the normal vehicle configuration and the 23 degree angle is an AGC test stand configuration. The tests included tension, compression and combined tension-compression loading.

An analysis determined that flow separation at sea level occurred at approximately 11:1 area ratio. The resulting maximum side forces, predicted are as shown below:

Table 4 -- Side Loads, 12:1 and 15:1 Exit Area

P_c	=	27	30	50	100	150	176
F	=	10,600	10,600	10,500	9,700	8,500	7,700
X	=	30.0	30.0	30.7	35.5	39.4	41.0
$M_{gimbal\ (6:1)}$	=	24,200	24,200	24,100	23,700	19,900	17,100
$M_{gimbal\ (12:1)}$	=	65,700	65,700	65,700	65,300	60,200	56,500
$M_{gimbal\ (15:1)}$	=	81,000	81,600	81,500	82,300	78,000	77,100

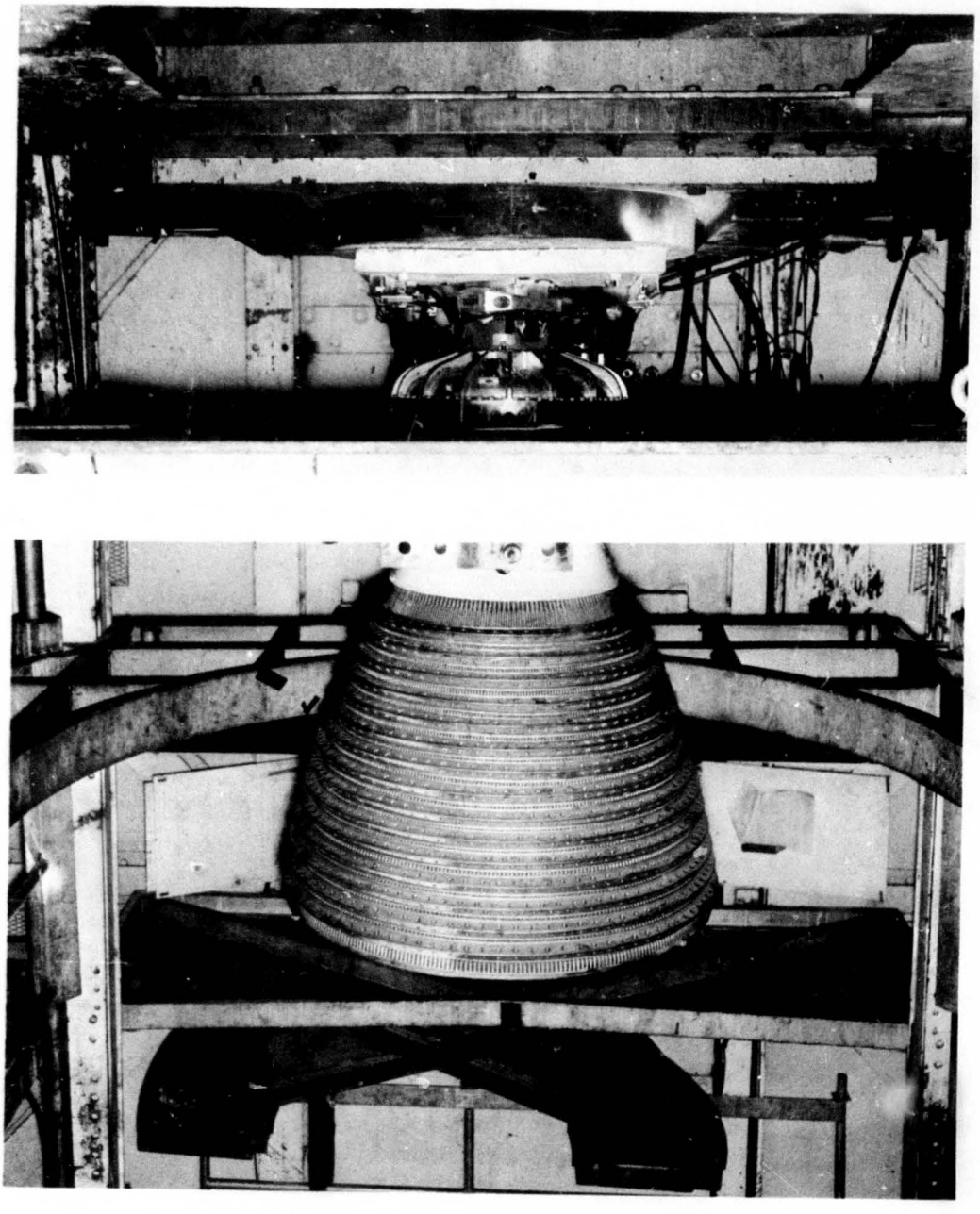

Figure 22 -- Test Setup to Measure Actuator Loads

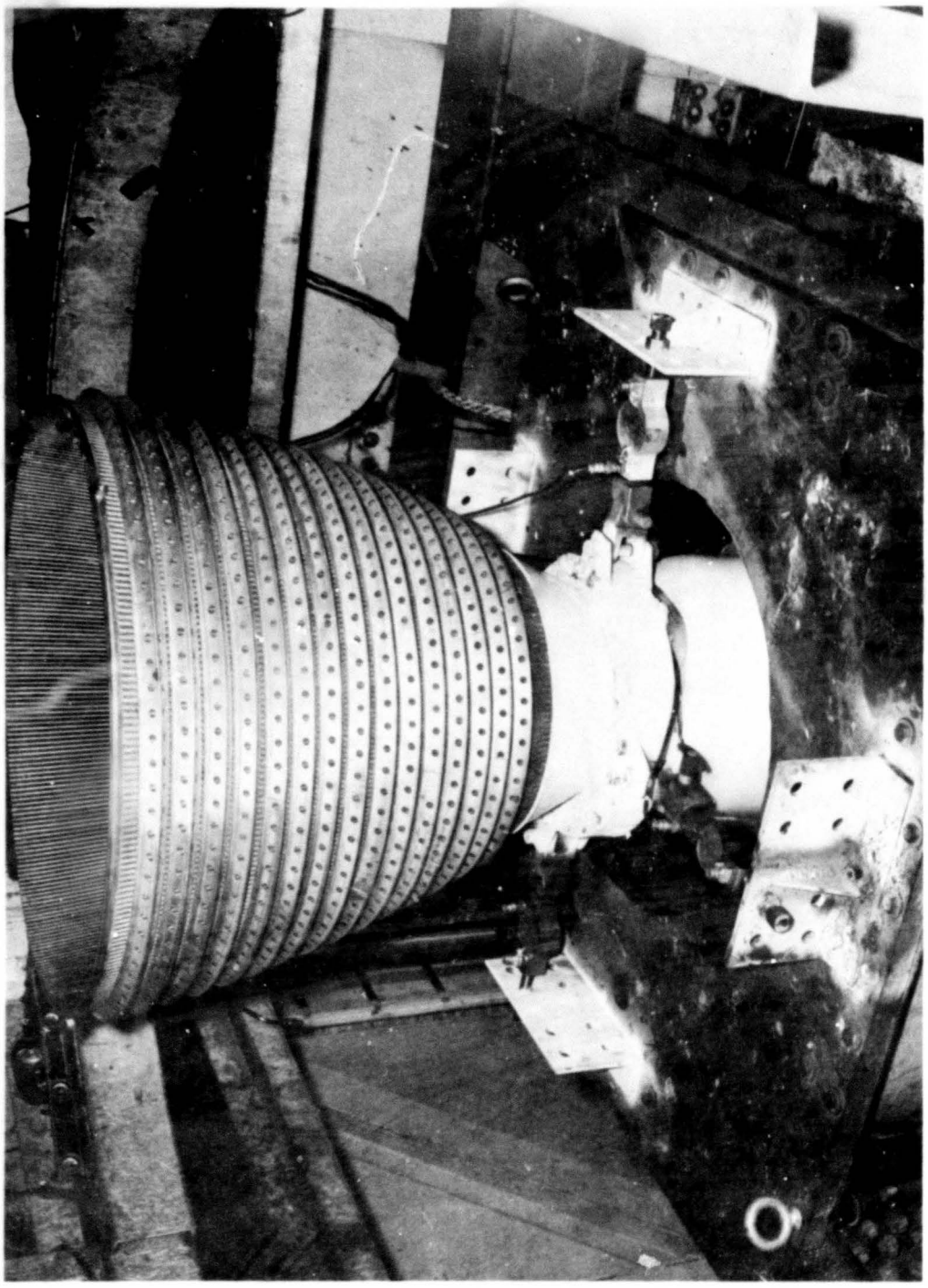

Figure 23 -- Test Setup Showing Load Cells

4.1, Stress Analysis (cont.)

Side forces were measured during the altitude test series (Section 5.4.4). The recorded side loads were all less than the analysis predicted.

A detailed discussion of the analysis and the findings resulting from it is contained in Reference A.

4.1.2 Strain Patch Data

To improve the data for static side loads by actual test, strain gages were installed on chamber S/N 002 prior to its use for engine firings. Figure 24 shows the chamber instrumented.

Data obtained from engine test Nos. 3051-D01-1A-002 and -003 are tabulated below:

Table 5 -- Combustion Chamber Strain Patch Data

	Strain, in./in. x 10^6			
	Test		Analysis	
Time Period	0°	180°	0°	180°
Start	-187	+321	-901	+365
Steady State	-587	-325	-470	-311
Shutdown	-1320	+456	-11	+631

The 15-second and 200-second hot firing strain gage data were compared to the analysis. The start transient condition indicated that the loads used in the analysis were slightly high. The nominal flight condition showed very good correlation between test and analysis.

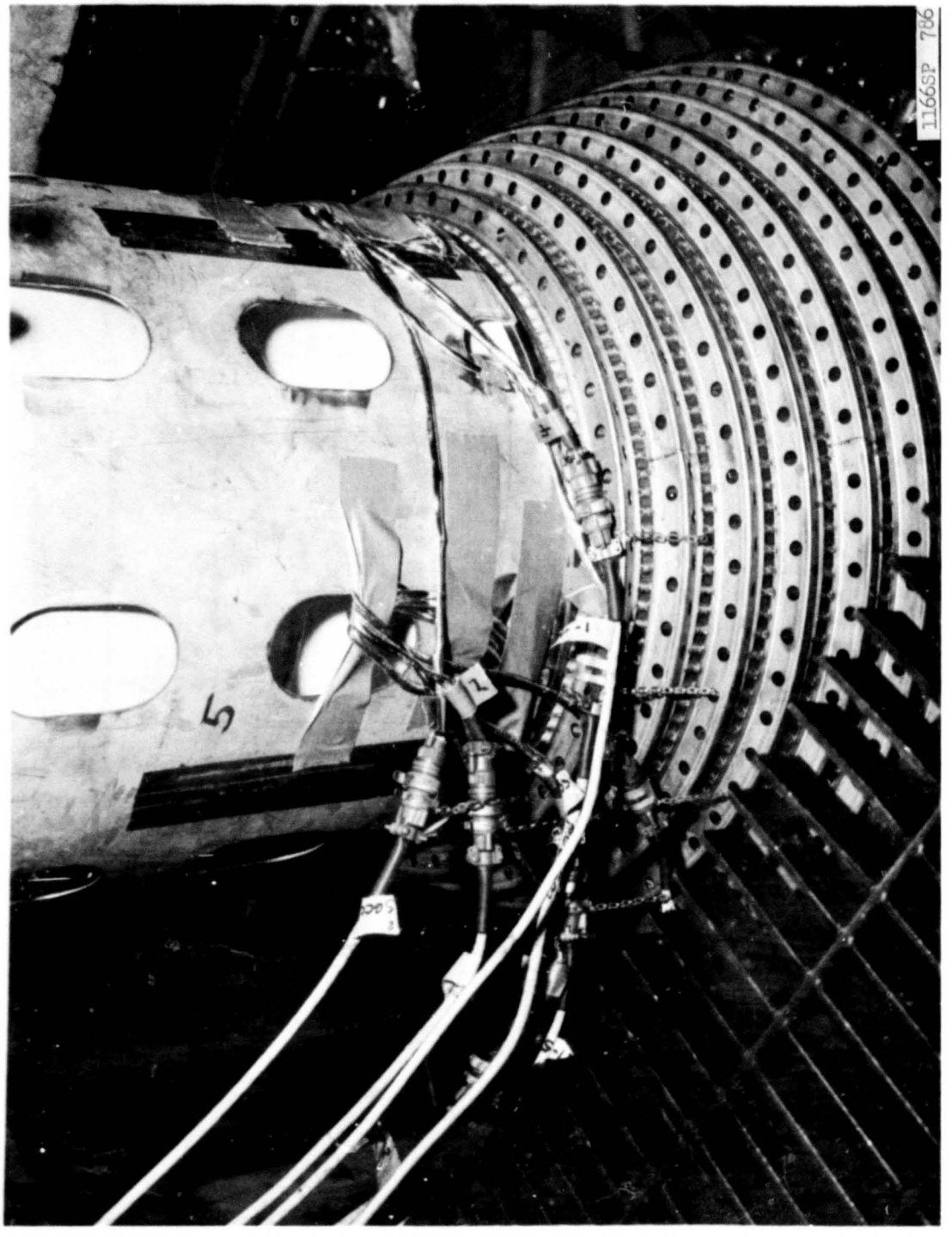

Figure 24 -- Strain Patch Instrumentation

4.1, Stress Analysis (cont.)

4.1.3 Structural Testing

A series of tests was performed during December 196 in the Structures Laboratory to determine the structural properties of the Titan III M Stage I combustion chamber. In preparation a study was made to determine required thrust, side loads, and chamber and tube pressures necessary to simulate different design load conditions for the static testing. The test conditions are given in Table 6.

Table 6 -- Structural Test Summary

Test	Chamber Pressure psi	Coolant Tube Pressure psi	Side Load lb	Thrust Load lb
A	817.0	1,105	3,720	89,000
B	14.7	1,100	19,800	21,300
C	14.7	1,705	3,720	180,000
D	14.7	1,705	8,800	180,000

Test A subjected the chamber to design limit loads at steady state conditions. No yielding or permanent deformation to the chamber occurred during this test.

Test B simulated the design limit loads incurred during a sea level start with a 15:1 expansion nozzle. No permanent deformation occurred.

Test C loaded the chamber to the design ultimate thrust load while maintaining a design limit side load derived from gimballing. These loads caused a small permanent set.

Test D loaded the chamber to design ultimate thrust; then the side load was increased in increments to failure. Approximately 2-1/2 degrees of permanent

4.1, Stress Analysis (cont.)

deformation occurred. The failure occurred between the shell attachment point and the first V-band. A close-up of the area in which maximum deformation occurred (Figure 35) is enclosed.

The static load test as conducted differed from a technically exact simulation in two particulars: (1) the chamber was not tested under the normal operating thermal environment, and (2) the thrust was applied at a single location aft of the chamber exit flange. However, the loads actually applied to the chamber and the induced stresses were more severe than those required by exact simulation.

The conditions examined during the test include (1) a sea level start transient condition providing maximum side forces (flow separation and start dynamics), (2) an altitude start transient providing maximum thrust loads. In both these cases the loads were at least 25 percent greater than those that would exist at operating (steady state) temperatures.

Because of the manner in which the axial load was applied, all sections below the throat were subjected to thrust loads in excess of the 1.8 safety factor as shown by the following tabulation:

Table 7 -- Comparison of Actual and Required Stresses

Location	Nominal	1.25 + 3%	Ultimate Required	Test
Throat	76,000	100,000	180,000	180,000
Shell-to-Nozzle Intersection	58,000	76,000	137,000	180,000
6:1 Flange	49,600	64,000	115,000	180,000
Aft of 6:1			115,000	180,000

4.1, Stress Analysis (cont.)

During firing the chamber sections above the throat would be relieved by internal pressure in the plenum. Because chamber pressure was not simulated during the test, the area above the throat was also subjected to the full 180,000 lbs load. The degredation in tube strength caused by temperature during firing is 12 percent aft of the reinforcing shell and 15 percent at the throat. This was more than offset by the increased static load during the structural test.

4.1.4 Stress Analyses

The complete detailed stress analysis of the combustion chamber is contained in Reference A. The analysis shows that the combustion chamber design meets all structural requirements as specified by contract. Besides the general analysis, special studies were made as design and test results uncovered potential problems.

Areas of original concern included the region at the juncture of the cooling jacket to the forward flange, the aft end of the reinforcing shell where the load is transmitted through the support ring, and the aft flange where the loads from the ablative skirt are imposed. The analysis of the forward flange indicated yielding and therefore a plastic analysis was made also. Included in the analysis was the effect of thermal stresses imposed on the tubes. It was recommended that the forward flange be strengthened in the region where the tubes are joined.

An evaluation was made of chamber stress for a condition of 1650^{o}F gas side wall temperature at the throat as against the 1523^{o}F design value. The study showed there was still a 0.1 positive margin of safety at this extreme condition.

4.1, Stress Analysis (cont.)

A plastic analysis was made of the chamber to evaluate local stresses resulting from yielding caused by chamber pressure, tube pressure, thermal gradients from tube-to-tube contact, and wire wrap interference. The results showed that the maximum stress was approximately 40,500 lbs and that there was a positive ultimate margin of safety throughout the chamber, based on a 1.8 safety factor on mechanical stresses and 1.0 safety factor on thermal stresses.

An analysis of the divergent section of the nozzle showed that the number of V-bands could be reduced from eight to four and still furnish adequate reinforcement. (This was not done, however.)

A special analysis was made of the fuel inlet and torus. The torus inlet was described by a quarter section with appropriate boundary conditions at the sections of symmetry. The inlet area was evaluated at 1185 psia (maximum engine operating pressure). The calculation considered that the inlet flange was fixed against deflection and rotation and included the effect of vanes. Yielding was assumed to occur in shear. The calculated margin of safety at yield was +0.25. No ultimate stress evaluation was run, but ratioing the limit stresses by a safety factor of 1.8 and comparing the result with the maximum allowable stress provides a margin of safety (ult) of 0.60.

The torus was evaluated by a finite element analysis using a computer program. The maximum stress in the torus was found to be meridional bending located at the point where the torus attaches to the forward part of the flange. The minimum margin of safety for the nominal operating condition is +0.27.

The computer model of the chamber was updated as additional data

4.1, Stress Analysis (cont.)

were obtained from testing. These tests include the sea level engine tests using chambers instrumented with strain gages, the altitude tests conducted with engine S/N RD-12, the vibrational test of the engine, and the engine demonstration tests. Except for the first series, loads were obtained from strain gages mounted on the gimbal actuators instead of the stiff links.

Detailed analyses were conducted when failures were recorded after the following test firings:

Test No. 3051-D01-1C, wire-wrap failure. It was found that the elongation of the tubes produced by a hard shutdown would permit the wire loops to slip over each other.

Test No. 3051-D01-1A-005, tube failure. The analysis showed a positive ultimate margin of safety in the failed region if the thrust chamber performance was within the design condition. Failure would occur if the gas side wall temperature reached 1650^{o}F.

Test Series 3051-D02-1M (Verification), injector-to-chamber flange gap and closure band cracking. Examination of the flange indicated yielding and set induced by thermal growth of approximately 0.010 in. per test cycle. This exposes the chamber-to-injector (Raco) seal to hot chamber gases and permits fuel to leak into the chamber, by-passing the injector.

As shown in Figure 10 there is a small dihedral angle between the flanges of the chamber and of the injector. When the flange bolts are tightened to the requisite torque, the surfaces are brought into contact. This force causes the surfaces of the flanges to yield in compression, starting from the inner diameter. During firing the set is stabilized. Following cooldown the yielded regions revert to tension, thus opening a

4.1, Stress Analysis (cont.)

gap between the flanges. Repeated firings aggravate the problem, though the increase in the gap is slower after the first set.

Calculations showed that one-half the specified bolt torque was sufficient to cause yielding of the flange and that a nominal gap of 0.012 in. would occur following the first firing. The calculations agree with experimental data taken from chambers and injectors whose flanges were flat before testing. Successive firings conceivably could cause the gap to grow to 0.020 in. the maximum allowable as given by the specification. Gaps greater than 0.020 in. are attributable to warping of either the injector or chamber flange prior to testing. However, it has since been shown that a gap as great as 0.030 in. is not detrimental to performance or to the integrity of the seal, and the specification has since been changed to reflect this fact.

The fuel closure band with attaching welds was analyzed as a flat plate under thermal stress and hydraulic pressure. Consideration was taken of the effects of the film cooling pattern. Tensile stresses were shown to arise in the cooler portion of the streak pattern on the closure band but not of sufficient intensity to cause cracking in the weld area, presuming that the welds were made properly. Inspection of several sections cut from chambers showed, however, that the welds were not to blueprint requirements, the result of inadequate access for full penetration.

Recommendations were made for recontouring the fuel manifold (collector ring) in the flange for added strength, and for modification of the weld groove for the closure band to assure adequate penetration. The latter modification was made and solved the cracking in the closure band weld. There were no excessive flange gaps subsequent to this modification, so further redesign of the flange was unnecessary.

4.1, Stress Analysis (cont.)

4.1.5 Structural Analysis Summary

A complete structural analysis is contained in Reference A, Aerojet Internal Report M-18. The findings were presented at the Critical Design Review.

The objective of the analysis was to evaluate the structural integrity of the redesigned (6:1 area ratio) thrust chamber. Secondary objectives were to analyze the forward flange as influenced by the injector, to apply a new approach for analyzing the torus, to determine the effect of the revised pressure schedule, to evaluate the axial load on the tubes and reinforcing shell assuming both that the shell carried the total load and that the load was distributed, and to evaluate the results of the static load test.

The analysis considered five different design conditions: sea level start transient, altitude start transient, sea level shutdown transient, nominal flight, and proof pressure loads. The loading conditions are given in Table 8.

Design Criteria

The design criteria pertaining to thrust, actuator control force, gimballing rates and acceleration, combustion dynamics, fluid dynamics, structural dynamics, heat transfer, flow separation, chamber tube pressures, engine dynamics, and temperature profiles were taken from IFS 12001. Analytical criteria pertaining to factors of safety were derived from SSD Exhibit 62-127. An exception was taken by agreement between Aerojet and Aerospace Corporation making the 1.32 safety factor for limit loads not applicable to areas of the component subject to hot gases. This exception

4.1, Stress Analysis (cont.)

was proposed because local yielding is not detrimental in regions where the load is transferred easily to adjacent members and because the reduction of nonfiring mechanical stresses due to thicker tube walls is offset by increased thermal stresses when firing. With this exception, the design safety factors were 1.32 yield and 1.80 ultimate.

Table 8 -- Design Loading Conditions

Loading Case	Pc	P_{Tubes}	Thrust	Moment about Gimbal	Angular Accel.	Vehicle Accel.
1. Proof	1132 psi	1773 psi	-	-	-	-
2. Nominal* Flight	858 psi	1200 psi	278,000 lb		25 rad/sec^2	Ax = 3 g
3. Sea Level Start	590 psi	830 psi	222,000 lb	87,500 ft-lb	-	-
4. Sea Level Shutdown	25 psi	35 psi	-	65,000 ft-lb	-	-
5. Altitude Start	1012 psi	1400 psi	328,750 lb	-	-	-

*Maximum steady state

The maximum moment about the gimbal is based upon pressure separation in the nozzle and engine dynamics during sea level operation with an ablative nozzle extension.

Nominal flight pressures are from the engine system design pressure schedule.

Sea level start and shutdown pressures are from analyses of test data.

4.1, Stress Analysis (cont.)

Acceleration requirements are per the IFS 12001M document.

Design Loads

The design loads were obtained from the engine operating parameters as given by IFS 12001 and supplemented by pertinent design data supplied by the appropriate departments. These produced the loading conditions of Table 8. The loads were recalculated following the issuance of a revised pressure schedule. The new schedule led to a slight increase in margins of safety but otherwise did not affect the analysis.

The lateral loads imposed by gimballing were determined by calculating the moments at discrete stations marked out along the chamber contour. Formulae based on the chamber geometry were established for calculating elemental masses between stations from the enclosed volumes and material densities. Other formulae expressed the local angular acceleration at each station. Equal stresses on both sides of each station were then obtained by iteration.

Method of Calculation

The analysis was conducted utilizing three computer programs: Program No. 14063, "Digital Computer Program for the Finite Element Analysis of Solids with Linear or Nonlinear Material Properties", Program No. 14064, "Shells of Revolution Subjected to Nonsymmetrical Loads"; Program No. 1040, (AVCO), "Linear Shell Program".

Programs 14063 and 14064 are developments of the finite element analytical approach. In these programs a continuous body is replaced by a system of elements of arbitrary shape and material properties.

4.1, Stress Analysis (cont.)

Program 14064 utilizes a layered shell approach capable of analyzing nonaxisymmetric pressure loads. It cannot be utilized for inelastic strains or temperatures.

The analytical capability of Program 14063 includes consideration of all axisymmetric loads (pressures and temperatures) for both elastic and inelastic stress/strains. This program utilizes a finite element method to determine the displacements and stresses within plane or axisymmetric solids with linear or nonlinear material properties. The continuous body is replaced by a system of elements with triangular or quadrilateral cross section. As the stress output is an average value for each element, it is necessary to utilize a fine mesh in areas where stress is changing rapidly.

A method of successive approximations is used to solve structures with non-linear material properties. The successive approximations are repeated until a converged solution is found. The stresses and displacements are printed by the program after each approximation. The number of iterations required will depend on the specific problem and must be specified as computer input.

Computer Program 1040 provides a means of analyzing axisymmetric shells of revolution with multi-layered construction composed of isotropic materials with linear properties. The program permits a shell configuration consisting of up to 25 regions and 24 junctions. Each region can consist of from 1 to 12 layers. There can be at most 7 free ends. Each free end must have 2 boundary conditions specified. At each region, input data such as pressures, temperatures, thicknesses and material properties can be specified at an arbitrarily chosen number of stations along the region.

4.1, Stress Analysis (cont.)

The program uses a 2 by 2 matrix in a step iteration procedure to solve the finite difference equations. After the integration is completed for each region, the regions are "connected" together and the junction and boundary conditions are satisfied. The machine then prints out deflection, strain, load and stress data for each specified interval.

The nonsymmetrical capability of Program No. 14064 was utilized in constructing a model for the complete chamber to obtain stresses, rotations and deflections for both symmetric and nonsymmetric loads at various chamber sections. The construction of two models was necessary as the nonsymmetrical load program does not have the nonlinear solution capabilities, and similarly the nonlinear solution program does not have the capability to analyze nonsymmetrical loads.

The detailed use of Program No. 14064 was as follows. The tube bundle was represented by an equivalent shell whose thickness and elastic moduli in the hoop and meridional directions were calculated to provide hoop and meridional stiffnesses equivalent to the tubes. The wirewrap layer was represented by a constant thickness shell with the elastic modulus in the chamber longitudinal direction reduced to represent the discontinuous nature of the wirewrap in the meridional direction. The external jacket was represented as a continuous shell attached at the appropriate locations.

To this completed chamber model was applied the design limit loads of internal pressure along the chamber wall and inertial side loads due to gimballing. The thrust reaction produced by the skirt was applied at the skirt-chamber flange.

Approximate stress levels were calculated by application of simple stress formulas to provide a check upon the resonableness of the computer solutions.

4.1, Stress Analysis (cont.)

Fuel Torus and Inlet

The torus and inlet were analyzed using Program No. 1040 (Linear Shell). Details of input and plots of the stresses generated are given in Reference A. The following assumptions were made:

a. Maximum torus stresses occur at the largest torus radii.
b. The temperature distribution is uniform.
c. The ends of the torus are fixed in respect to each other.
d. The torus is axisymmetric.
e. Rotation and deflection of the forward flange can be used for end conditions.

The results for the torus were:

Maximum Stress (axial)	29,000 psi*
Maximum Stress (bending)	10,000 psi*
Factor of Safety	1.8
Bending Modulus	1.3
Ultimate Material Stress (tensile)	80,000 psi (Room Temp)
Margins of Safety	+1.37

The results for the inlet flange were:

Maximum Stress (axial) (pressurized)	42,500 psi
Maximum Stress (bending) (pressurized)	12,500 psi
Factor of Safety	1.8

*With pressure in the torus

4.1, Stress Analysis (cont.)

Bending Modulus	1.3
Ultimate Material Stress (tensile)	80,000
Margin of Safety	+0.54

Forward Flange

A plastic analysis of the forward flange was made utilizing Program No. 14063. The analysis examined 22 contiguous elements from which contour stress maps, contained in Reference A, were prepared. Assumptions made in relation to the input were:

a. Hoop stiffness is zero in areas with holes.

b. Yield strength and coefficient of thermal expansion are the same in the equivalent sections as in the original material.

c. The centerlines of the holes are the same above and below the cover band.

d. The inlet from the torus is cylindrical and perpendicular to the axis of the flange.

e. The number of holes above and below the closure band are the same.

Because the heat transfer analysis had not been completed for the 6:1 area ratio chamber, temperature data were obtained from the analysis for the Stage II chamber. On the basis of preliminary study it was concluded that the Stage II data were similar and would be on the conservative side.

4.1, Stress Analysis (cont.)

The results of the analysis of the forward flange were:

At Room Temperature

Maximum Stress	54,000 psi
Ultimate Material Stress (tensile)	80,000 psi
Factor of Safety	1.8
Margin of Safety	+0.48

At 1300°F

Maximum Stress	30,000 psi
Ultimate Material Stress (tensile)	40,000 psi
Factor of Safety	1.8
Margin of Safety	+0.33

Chamber Tubes

A study was made to determine tube stresses in a plane transverse to the tube axis. Loads considered were those due to chamber pressure, tube pressure, tube-to-tube contact, thermal gradients and wire wrap interference. Points investigated were the forward flange intersection, shell attachment point, throat section and aft flange intersection.

As thermal gradients in the tube wall are high in the transverse plane, Program No. 14063 was utilized. This computor program has the capabilities for determining stresses in the plastic or non-linear range by an iterative approach.

A plot of a typical tube cross-section in the neighborhood of the forward flange which shows the matrix that defines the discrete elements

4.1, Stress Analysis (cont.)

is contained in Reference A. By utilizing the skew boundary option of the program the model nodal points defined by the chamber diameters were forced to slide along boundaries forming an angle of $360^{\circ}/2n$ where n is the number of tubes making up the chamber. In this way hoop forces were generated which should closely match those actually occurring.

As this model utilizes the plane stress option of the program, no meridional stress output is generated.

The stresses and margins of safety for the chamber horizontal sections do not reflect the effect of meridional forces in this hoop plane.

The effect of the axial forces is to further the plastic yielding occurring due to temperatures. As the portion of the tube not subject to hot gas is not under nigh stresses, this extension of plasticity should be minimal.

The pressure differential across the hot tube wall would not result in any significant lowering of the safety margins in this area because of its already plastic state and the meridional forces being reacted by the cooler portions of the tube.

Lessening of tube axial stiffness would cause a shift of load to the shell and therefore the shell-to-tube structure acts as a self balancing system. It has been shown that all the meridional forces could be reacted by the shell, therefore giving credence to the integrity of the composite structure even if the tubes axial loads were completely transferred to the shell.

4.1, Stress Analysis (cont.)

The margins of safety as determined by the plastic tube analysis were:

Forward Flange Intersection	+0.78
Throat Section	+0.38
Attachment Point for Shell	+1.27
Aft Flange	+1.16

Aft Flange

A similar plastic analysis was conducted for the aft flange, using the finite element technique with a very fine mesh. Loading from the skirt was simulated by an equivalent cylinder. An equivalent cone reacted the load into the tube bundle. The following parameter data were used:

Tube Pressure	2160 psia, ultimate
Chamber Pressure	54 psia, ultimate
Skirt Thrust	68,800 lbs
Temperature, Hot Side	727°F
Temperature, Cold Side	120°F

The following results were obtained:

Hot Side, T = 727°F

Ultimate Stress	53,000 psi
Ultimate Material Stress	65,000 psi
Margin of Safety	+0.23

4.1, Stress Analysis (cont.)

Cold Side, T = 120°F

Ultimate Stress	63,000 psi
Ultimate Material Stress	87,000 psi
Margin of Safety	+0.38

Reinforcing Shell

A manual calculation was made to determine the axial stress in the shell, assuming that none of the load was carried by the tubes. The calculated stress was 29,000 psi.

The calculation was also made using Computer Program No. 14064 which yielded utlimate stress values of 31,800 psi (tension) and 13,900 psi (bending). This calculation was also conservative in that all the bending moment was reacted by the shell.

The material properties are 80,000 psi ult (tension) and 95,000 psi ult (bending). This yields a margin of safety of 0.02. That this margin is quite conservative is evidenced by the results of structural load test where the recorded strains were much lower than predicted.

V-Bands

The maximum strain level occurs in hoop tension in the third V-band. The calculated strain, assuming that holes of the size employed do not lead to significant stress concentrations, is 1200 micro in./in. This corresponds to a stress of 34,000 psi. Allowing for the holes, the stress becomes 38,000 psi. The actual stress level is somewhat higher, but no greater than 40,000 psi, which corresponds to a strain of

4.1, Stress Analysis (cont.)

6000 micro in./in. Taking the material properties at 80,000 psi (tension) and a factor of safety of 1.8, the margin of safety is

$$MS = \frac{80,000}{1.8 \times 40,000} - 1 = +0.10$$

Throat Buckling

An investigation was made into the possibility of a throat buckling problem such as has recently been found to occur on the Titan III Stage II chambers when subjected to a combination of thrust and transverse loading. A lateral instability mode of failure was reached in Stage II when a hoop load of 19,000 lb/in. compression at the throat or 12,000 lb/in. compression 0.75 inches aft of the throat was reached.

The major difference between the Stage I Titan IIIM and Stage II Titan chambers is the addition of the shell on the Stage I chamber. The shell, which is rigidly attached to the chamber forward flange and to the tubes aft of the wire-wrapped region, is significantly more rigid longitudinaly than the tube bundle and consequently carries the greater portion of the longitudinal loads. In the Stage II chamber, prior to redesign under Titan IIIM, no redundant load path is provided and therefore all of the applied thrust, shear and bending moment must be carried by the tube bundle.

A review of the output from Computer Program No. 14064 using the complete chamber model indicated that the maximum hoop compression was 1099(1.8) = 1980 lb/in. and occurred on the compression side of the chamber when subjected to sea level shutdown loading conditions. This load is much less than the critical buckling load of 8200 lb/in. for the throat area.

4.1, Stress Analysis (cont.)

That throat buckling is not a problem with the Titan IIIM Stage I chamber was proven by test when a load to failure test resulted in tube collapse aft of the shell with no tube damage in the throat region.

Conclusions

From the foregoing discussions, which are summarized in Table 9, it will be noted that a positive margin of safety exists at all the critical locations in the combustion chamber. Except for the areas exposed to hot gases, these safety margins also include a 1.8 safety factor. In many cases the results are exceptionally conservative as witnessed by the structural load test. It may therefore be concluded that the Titan IIIM Stage I 6:1 area ratio combustion chamber is structurally sound, and meets the required margins of safety.

4.1, Stress Analysis (cont.)

Table 9 -- Minimum Margins of Safety*

Component	Region	Load Condition	Margin of Safety	Remarks	Ref. Page	
Tube Bundle	Just aft of jacket	Sea level start	+.17	Local circumferential stress	90	98
Fwd Flange	See References	Steady State	+.33		103	110
Aft Flange	Hot side near tube joint	Steady State	+.23		131	137
Jacket	Near Fwd end	Sea level start	+.02	Conservative	138	144
Wire Wrap	6" Aft of Fwd end	Altitude	+.27		73	84
Fuel Torus	Fixed Edge at large dia	Ultimate Pressure	+1.37	See Reference A	97	104
Fuel Torus Inlet	At Inlet Flange	Ultimate Pressure	+.54	See Reference A	101	108
"V" Bands	Third band aft of throat	Ultimate sea level stress	+.10	Conservative	149	155
Tube Bundle	Throat	Ultimate sea level start	+.10	See Text	152	159
Tube Bundle	Throat Plane Stress	Steady State Temp-Press.	+.38	Does not include meridioral effects	128	134

*Reference: Aerojet Internal Report M-31, Structural Analysis of the Titan IIIM Stage I Combustion Chamber.

4, Analytical Programs (cont.)

4.2 HEAT TRANSFER

The heat transfer effort consisted of testing to obtain necessary data concerning the properties of AeroZINE 50 at higher velocities than previously studied, determining the heat transfer characteristics of the combustion chamber from the development test data, and predicting the burnout heat flux ratio at nominal and "worst flight" conditions.

4.2.1 Heated Tube Test Evaluation

Previous investigations into the burnout heat flux characteristics of AeroZINE 50 had covered the pressure and bulk temperature range of Titan IIIM operation but not the high velocities in the cooling tubes as required by the new 6:1 chamber design. Experience had shown the advisability of using data obtained at the actual range of operation rather than extrapolating from lower values of the parameters. A short laboratory test program utilizing electrical heated tubes was therefore conducted to get the required data.

The program consisted of 18 burnout tests and one extended duration test covering the velocity range of 90 to 180 ft/sec, the pressure range of 1000 to 1200 psia, and the bulk temperature range of 100 to 200^{o}F. Besides the necessary information for designing the combustion chamber and analyzing test data an improved correlation equation was obtained for the burnout head flux with AeroZINE 50 and valuable observations were made of nucleate boiling and the formation of carbon deposits prior to burnout.

From the heat flux and resulting inside tube wall temperatures it appears that, in general, the heat transfer characteristics of AeroZINE 50 at subcritical pressures are similar to those which have been observed for many

Table 10 -- AeroZINE 50 Burnout Test Results

Burnout Site Conditions										
V ft/sec	T_{B_o} °F	P psia	ϕ_{Bo} Btu/in.^{2}sec	ΔT_{sub} °F	$V\Delta T_{sub} \times 10^{-3}$ ft °F/sec	X_{Bo} in.	X_B in °F	T_B out °F	Energy Balance, %	Test No.
8.9	140.0	1117	3.96	426	3.79	0.5	73.8	147.0	+5.3	HT-5-121
93.7	106.6	1125	13.14	460	43.10	0.25	79.4	109.4	+5.4	-111
89.1	134.9	1050	11.70	422	37.60	1.1	89.7	145.0	-0.4	-102
90.9	146.6	1131	12.08	421	38.27	0.25	87.3	149.7	+0.9	-112
98.4	69.0	1166	15.67	503	49.50	0.5	46.3	76.6	+4.9	-126B
121.9	103.8	1130	17.36	464	56.56	0.5	77.6	109.0	-4.7	-113
123.9	151.4	1132	19.32	417	51.67	0.45	72.7	158.4	+3.8	-104
123.1	200.7	1150	16.88	370	45.55	0.25	124.0	203.6	+5.2	-107
153.5	171.6	844	22.82	355	54.49	0.1	97.5	173.1	+1.3	-117
(3)145.5	63.6	1213	22.37	515	74.93	2.35	61.4	98.0	+1.3	-116
149.1	158.6	1127	20.35	408	60.83	0.1	91.8	160.1	+2.8	-105
147.0	209.4	1129	21.11	359	52.77	0.1	117.6	211.3	+3.1	-109
152.6	158.0	1475	23.60	450	68.67	0.4	89.5	163.9	+4.7	-118
161.0	110.5	1136	26.54	459	74.36	0.1	71.8	111.9	+0.7	-114
182.9	202.3	874	25.19	330	60.36	0.1	114.3	203.8	+6.1	-122
179.6	107.2	1137	28.19	462	82.98	0.1	70.4	108.7	+1.4	-115
179.0	163.8	1163	24.38	408	73.03	0.1	95.5	165.2	+4.1	-106
174.5	199.1	1148	24.54	371	64.74	0.25	110.7	202.9	+5.5	-110

(1) X_{Bo} = Distance Between Burnout Site and Downstream End of Test Section

(2) Energy Balance = (Qin - Qout)/Qin

$Q_{in} = .948 \times 10^{-3} \Delta E\ I \qquad Q_{out} = \dot{W}\ \bar{C}p\ (T_{B\ out} - T_{B\ in} - \Delta To)$

(3) Burnout occurred near the test section inlet

4.2, Heat Transfer (cont.)

other fluids at pressures below critical. A summary of the results is presented in Table10 and plotted in Figure 25together with previously published results obtained at Aerojet, Rocketdyne, and JPL. Most of the data indicates local boiling at wall temperatures somewhat below the saturation temperature, particularly at the higher heat fluxes. Possible explanations are instrumentation error or error in the published data concerning saturation temperature.

Correlation of Data

A number of correlations have been developed for the burnout heat flux of flowing subcooled fluids. In most of these, the burnout heat flux is expressed in terms of velocity and subcooling ($T_{Bulk} - T_{Sat}$) as in the correlation for relatively low velocity water developed by Gunther:

$$\phi_{BO} = 0.0135\ V^{0.5}\ \Delta T_{sub}$$

Variations of Gunther's correlation have been used extensively in which the exponents employed on the velocity and subcooling terms have been adjusted to correlate specific sets of data.

For AeroZINE 50, however, it was found that the correlation was linear with the product of velocity and subcooling. The data from the test program are plotted in Figure Y together with previous published data. The best correlation obtained for the range $V\ \Delta T_{sub} > 8000$ ft/sec^{o}F was

$$\phi_{BO} = 4.4 + 0.00275\ V\ \Delta T_{sub} \qquad \text{Eq. 1}$$

$$V\ \Delta T_{sub} \geq 8000 \text{ ft } ^{o}\text{F/sec}$$

($V\ \Delta T_{sub} = 8000$ ft ^{o}F/sec at 1000 psia pressure, 150^{o}F bulk temperature, and 20 ft/sec velocity)

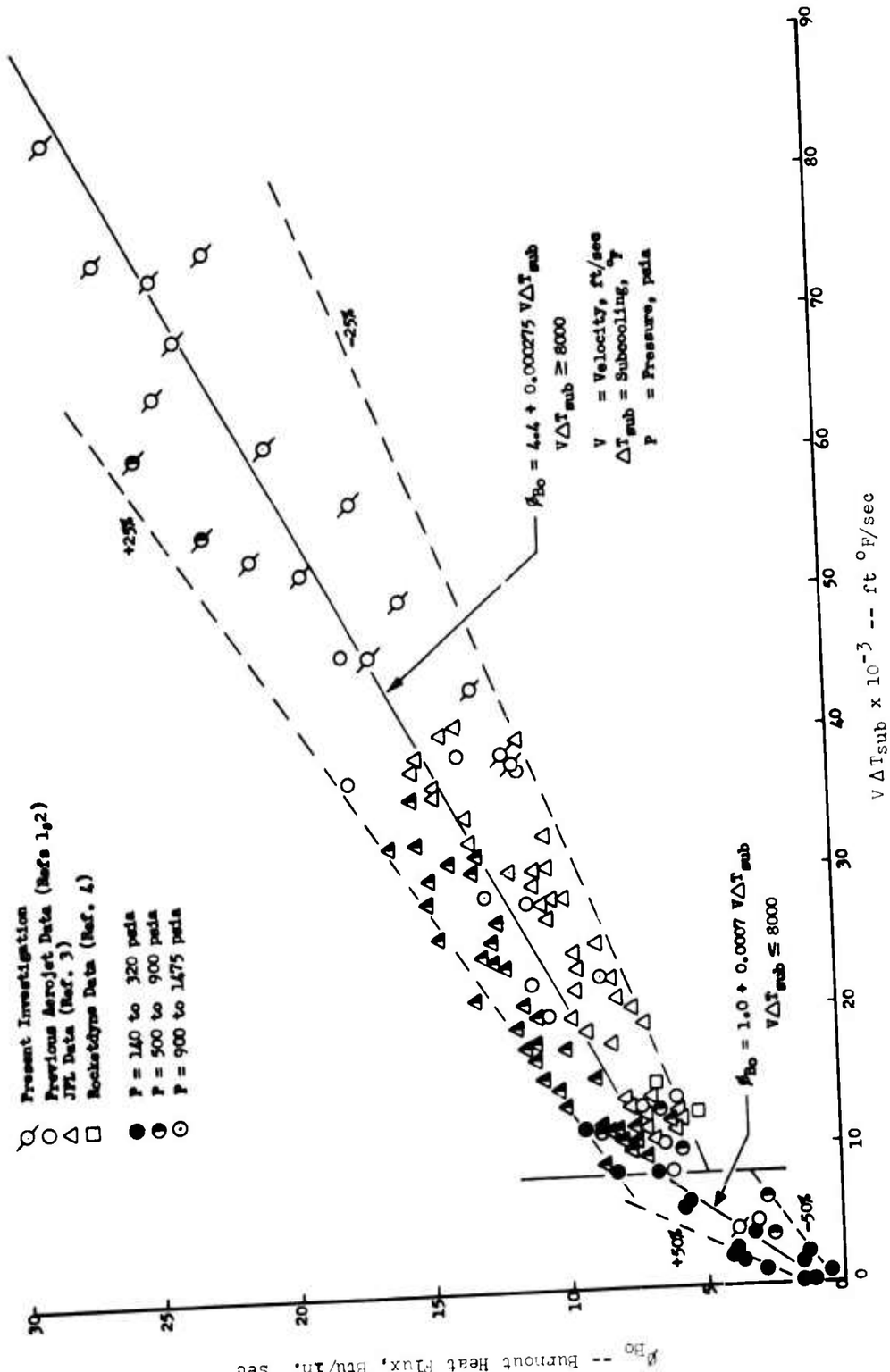

Figure 25 -- Recommended AeroZINE 50 Burnout Heat Flux Correlations

4.2, Heat Transfer (cont.)

Equation 1 predicts 95% of the data within ± 25% and 99% of the data within ± 30%. The ranges of conditions existing in the data from which Equation 1 was derived are:

Velocity:	27.0 to 182.9 ft/sec
Bulk Temperature:	63.6 to 431 ^{o}F
Pressure:	252 to 1475 psia
$V \Delta T_{sub}$:	8000 to 83,000 ft ^{o}F/sec
Burnout Heat Flux:	5.2 to 28.19 Btu/in^{2} sec

The burnout heat fluxes at relatively low values of $V \Delta T_{sub}$ ($V \Delta T_{sub}$ 8000 ft ^{o}F/sec) do not correlate in the same manner as the higher $V \Delta T_{sub}$ data and are generally somewhat less than predicted by Equation 1. In addition, the data scatter is more pronounced in this low $V \Delta T_{sub}$ region.

A relatively simple correlation was obtained for the range $V \Delta T_{sub} <$ 8000 ft/sec^{o}F:

$$\phi_{BO} = 1.0 + 0.0007 \quad V \Delta T_{sub} \qquad \text{Eq. 2}$$

$$V \Delta T_{sub} \leq 8000 \text{ ft } ^{o}\text{F/sec}$$

Equation 2 yields a ± 50% prediction of the low $V \Delta T_{sub}$ data. In addition, Equation 2 provides a logical transition to the high $V \Delta T_{sub}$ correlation, Equation 1, since both relationships yield the same value of ϕ_{BO} at $V \Delta T_{sub}$ = 8000 ft ^{o}F/sec.

Equation 2 is based on data for the following ranges of conditions:

Velocity	8.3 to 36.0 ft/sec
Bulk Temperature:	140 to 416 ^{o}F
Pressure:	142 to 1117 psia
$V \Delta T_{sub}$:	73 to 6020 ft ^{o}F/sec
Burnout Heat Flux:	0.5 to 5.8 Btu/in^{2}sec

4.2, Heat Transfer (cont.)

Pressure Effects

Examination of the data shown in Figure 25 reveals a slight effect of pressure on the burnout heat flux. This effect is particularly noticeable in the region of high $V\Delta T_{sub}$, where the data obtained at pressures between 500 and 900 psi exhibit higher values of burnout heat flux than the corresponding values at 900 to 1475 psia.

While a complete evaluation of this pressure effect is difficult because of the shortage of data at pressures below 500 psia and above 1200 psia, three general trends are indicated.

(1) At pressures below 500 to 600 psia the experimental burnout flux data are from 10 to 30 percent greater than predicted by equation 1.

(2) In the range from 500 psia to 900 psia the deviation between experimental and predicted burnout tends to decrease with increasing pressure.

(3) At pressures greater than 900 psia there is substantial agreement with Equation 1 and the dispersion is small.

These apparent effects of pressure on the burnout heat flux of AeroZINE-50 may actually be mixture effects resulting from the disparate critical pressure of UDMH and N_2H_4, assuming that these two constituents do not combine chemically. By this assumption vigorous nucleate boiling and mixing of both constituents occurs at low pressures (500 to 600 psia). As the critical pressure of UDMH is approached (between 785 psia and 880 psia as given by the literature) the contribution of this constituent to nucleate boiling and resulting mixing is reduced, though not to the full extent of its proportion in the mixture. This degredation of the boiling process tends to yield a lower burnout heat flux. Boiling of the N_2H_4 constituent would be unaffected until its critical pressure (2131 psia) was approached.

4.2, Heat Transfer (cont.)

Attempts to include a pressure term in Equation 1 did not decrease the scatter of the data significantly. The added complexity of a pressure correction factor does not therefore appear to be warranted.

Bulk Temperature Effects

Two tests indicate that the burnout heat flux of AeroZINE 50 at low bulk temperatures may be less than predicted by Equation 1. The local temperature at the point of burnout ranged from 64 to 69°F. It is significant that in one of these tests the burnout occurred at the inlet end of the test section. Until additional low temperature data become available, it is recommended that Equation 1 be used with caution for bulk temperatures below 60°F.

Coking

Five of the test sections used in the burnout studies were sectioned longitudinally and examined. The test section employed at 9 ft/sec velocity (Test HT-5-121) was found to contain black deposits, apparently carbonaceous, in the immediate area of the burnout. The thickness of these deposits was estimated to range from 0.001 to 0.010 inches.

Two test sections used in 90 ft/sec tests (Tests HT-5-102 and HT-5-112) also contained black deposits in the immediate vicinity of the burnout point. The deposits in these test sections were much thinner (approximately 0.001 to 0.002 inches thick) and covered a much smaller area than the deposits contained in the 9 ft/sec velocity test section.

There was a thin layer of a dark deposit found in the entire length of the test section used for the extended duration test. The fluid velocity was 155 ft/sec. The composition of the deposit was not determined.

4.2, Heat Transfer (cont.)

Two of the test sections in which burnout occurred at 180 ft/sec velocity were also examined. No deposits were found in the Test HT-5-106 test section. The Test HT-5-115 test section contained a very thin layer of black deposit right at the severance point.

It appears that coking, i.e., the formation of a carbonaceous deposit, can be expected to occur when the burnout heat flux of AeroZINE 50 is approached. High velocities tend to retard the formation of this deposit. No chemical analyses of the deposits were made to determine their chemical composition or the mechanism by which they were formed.

Extended Duration

Cooling with AeroZINE 50 for an extended duration in a 347 stainless steel tube was investigated in one test which was conducted for a total duration of 8 minutes. The objective of this test was to determine if the burnout heat flux limits at extended durations were significantly different from those for relatively short durations. In a previous test program with 98% H_2O_2, a significant effect of duration was found to exist. In the AeroZINE 50 extended duration test, two heat flux levels (corresponding to 68% and 79% of the burnout heat flux predicted by Equation 1) were maintained for a period of approximately 4 minutes each. The conditions of this test (outlet of the test section) are tabulated below:

Duration (sec)	V ft/sec	T_B ^oF	Heat Flux Btu/in.^{2} sec	P psia	T_{sub} ^oF	V T_{sub} x 10^{-3} ft^oF/sec
260	155.3	152-155	14.9-15.0	1130	409-412	64.0
220	155.3-157.0	163-164	17.0-17.1	1120	399-401	62.5

4.2, Heat Transfer (cont.)

Burnout did not occur during the AeroZINE 50 extended duration test and apparently normal steady-state heat transfer was achieved at both heat flux levels. However, analysis of the wall temperature data revealed that a slowly increasing inside tube wall temperature was indicated. This increase in wall temperature is particularly noticeable at the lower heat flux level which was maintained during the first 4 minutes of the test. Wall temperature from 500 to 550°F are indicated during this period.

Posttest examination of the test section revealed that a thin layer of a dark deposit had formed along the entire length of the test section. The coloration of this deposit ranged from grey-yellow at the test section inlet to black at the outlet. No detailed material analysis of the deposited layer was conducted.

The indicated increase in inside tube wall temperature could be caused by the deposition of a thin carbon layer on the tube wall. The inside surface temperature probably did not actually increase. However, the additional thermal resistance of a carbon layer would yield a higher outside tube wall temperature which would, in turn, yield higher calculated values of inside tube wall temperature since the thermal resistance of the carbon layer was not considered in the inside wall temperature calculation.

Conclusions

1. The burnout heat flux data for AeroZINE 50 at high velocities and high subcoolings are adequately correlated with the equation:

$$\phi_{BO} = 4.4 + 0.000275\ V\,\Delta T_{sub} \qquad \text{Eq. 1}$$

$$V\,\Delta T_{sub} \geq 8000\ \text{ft}^{\circ}\text{F/sec}$$

Equation 1 predicts 95% of the burnout data within ± 25% and 99% of the data within ± 30%.

4.2, Heat Transfer (cont.)

2. Equation 1 is recommended as a best estimate correlation for AeroZINE 50 burnout heat flux at high $V\Delta T_{sub}$ conditions. It is further recommended that the data scatter be considered when design conditions are established using Equation 1.

3. An entirely satisfactory correlation for AeroZINE 50 burnout heat flux at low velocities and subcoolings has not been established; however, a fair representation of the data is obtained with the equation:

$$\phi_{BO} = 1.0 + 0.0070\ V\Delta T_{sub} \qquad \text{Eq. 2}$$

$$V\Delta T_{sub} \leq 8000\ ft^{o}F/sec$$

This expression predicts the data within $\pm$ 50%.

4. Equation 2 is recommended as a best estimate correlation for AeroZINE 50 burnout heat flux at low $V\Delta T_{sub}$ conditions. Because of the scatter in the data, it is further recommended that a heat flux 50% less than given by Equation 2 be used as a maximum design heat flux unless the particular design conditions duplicate the conditions at which a higher burnout heat flux has been measured.

5. The AeroZINE 50 forced convection data from this investigation are adequately predicted by the Hines correlation:

$$Nu_b = 0.005\ Re_b^{0.95} Pr_b^{0.4} \qquad \text{Eq. 3}$$

6. Equation 3 is recommended as a design correlation for AeroZINE 50 forced convection heat transfer coefficients.

4.2, Heat Transfer (cont.)

7. Pressure appears to exert a secondary influence on the burnout heat flux of AeroZINE 50. However, attempts to incorporate this pressure effect into the burnout heat flux correlation did not yield a substantially better prediction of the data than given by Equation 1. Additional testing at pressures less than 500 psia and greater than 1200 psia is needed to fully evaluate this pressure effect.

8. Low bulk temperatures may possibly yield unexpectedly low values of burnout heat flux. However, testing at bulk temperatures below 60°F is needed to verify this effect.

9. AeroZINE 50 does not exhibit any unusual burnout heat flux characteristics in extended duration operation with 347 stainless steel tubing.

10. Black deposits were found in the vicinity of the burnout site in some of the burned out test sections. A thin layer of deposit was also found along the entire length of the test section used in an extended duration test. The thickness of these deposits appeared to decrease with increasing fluid velocity. Further investigations into the nature of these deposits are needed.

11. Additional analysis of the nucleate boiling data is needed.

12. The following reference should be consulted for information on the effects of assymmetric heating, tube curvature, and tube flattening on burnout heat flux:
N. E. Van Huff, D. C. Rousar, Ultimate Heat Flux Limits of Storable Propellants, paper presented at the 8th CPIA Liquid Propulsion Symposium, Cleveland, Ohio, November 1966.

4.2, Heat Transfer (cont.)

4.2.2 Instrumented Tubes

Work was initiated November 1965 to establish the feasibility of instrumenting combustion chamber tubes with thermocouples to measure the gas-side wall temperatures. The method proposed located the junction in the crown of the tube with the leads carried to the outside. Methods were established for etching slots for the thermocouple wires and for chemically milling the thermocouple mounting slots in the tubes. Vapor deposition of alumina 0.0005 in. thick over the wire was perfected as means of securing the wire and establishing gas side contact.

Two specimens were furnace-brazed during May 1966. Both specimens involved only half of the groove designs for holding the thermocouple because a limited number of grooved tubes was available for evaluation. The first specimen was brazed with G.E. 8102 alloy, a nickel base braze alloy containing chromium and silicon. The second specimen was furnace-brazed with G.E. 8102 alloy, overlaid with AGC 4, a gold, nickel, and palladium braze alloy. Both specimen resulted in satisfactory brazing of the thermocouple wire in the groove; the latter specimen, with the soft, ductile overlay of AGC 4 is easier to polish down to the level of the crown of the tubes. Preparation of the tube samples with the thermocouples in the wall was made for testing and calibration with the plasma arc.

Further development of the instrumented tube was discontinued in June 1966. While all indications were that the technique was eminently feasible, there was doubt whether the chambers could be instrumented in time to keep pace with the testing schedule.

4.2, Heat Transfer (cont.)

4.2.3 Braze Patch Analysis

A quicker, though less accurate and flexible, method for obtaining gas-side wall temperature data was the application of braze and solder alloys of differing thermal coloring in patches on the chamber wall. Laboratory compatibility tests were made of sample specimen, using a plasma gun to simulate chamber conditions. Fourteen braze alloy specimen, deposited on the crown of five CRES 347 type tubes, were tested in a simulated environment of a fuel-rich combustion chamber. Each of the specimen was first melted in the plasma flame to determine stress cracking susceptibility and proper settings for the plasma equipment. The specimen were then tested for 3 minutes in the simulated environment at temperatures just below their melting points to establish their appearance for future reference. The melted specimen were then sent to the metallographic laboratory and examined to determine the possible existence of liquid-metal corrosion or cracking.

Examination of the braze alloy specimen revealed no cracking or metal corrosion of the stainless steel tubes. The testing of the specimen was limited to visual examination at high magnification and dye penetrant inspection because the specimen were intended to be kept intact for subsequent use as standards for comparison with braze deposits on fired chambers.

Chamber S/N 003 was instrumented with 129 braze patches located at three circumferential and ten axial locations. The patches were applied prior to wire-wrapping the tube bundle so that leak checks between tubes could be made in the wire wrap region.

Locations were specified for the braze alloy patches and aft flange thermocouples (for coolant bulk temperature measurements). The braze alloy patches were centered about four circumferential planes corresponding to the locations of gas-side thermocouples on both the uncooled and cooled chamber. The aft flange thermocouples were positioned in the entrance of the up-tubes nearest the four instrumented tubes so as to provide a mixed coolant bulk temperature at these locations.

4.2, Heat Transfer (cont.)

Test 3051-D01-1A-006 was made with the braze chamber S/N 003. Figure 26 shows one section of the braze patches installed. Figure 27 shows the chamber after firing. The results, in general, agreed very well with the predicted values. In the throat the braze indicated a wall temperature between 1570°F and 1670°F; the predicted was 1510°F.

The application of braze alloys to the coolant tubes was continued on chambers S/N 005 and S/N 006. Brazes used on these chambers were changed in the throat region (Table11) as a result of Test No. 3051-D01-1A-006, which indicated temperatures are higher than predicted forward of the throat and lower than predicted aft of the throat. Figure 28 shows the braze patches installed in combustion chamber S/N 005.

A third Titan IIIM chamber (S/N 006), instrumented with braze patches as shown in Figure 29, was tested on an engine subassembly (Test No. 3051-D01-1A-021) with injector S/N 653, which had 9.4 percent film cooling. The braze patch data indicated that this low film cooling flow resulted in more circumferential temperature variations than the previous two chambers (S/N 003 and 005). The hottest zones were directly under and just adjacent to the baffles where temperatures of 1740°F were noted. The region between baffles was the coolest with the maximum temperature range the same as the previous two chambers, i.e., 1575 to 1670°F. Although the tubes were ebony black above the throat, no heat marked tubes were noted.

The maximum temperatures noted at the throat were 1740°F. All braze patches located adjacent to the baffle ("A" location in Figure 30) melted from the throat to the injector end, and there were more variations and local streaking in the patch data above the throat then in the previous two chambers. The braze patches used at each location are listed in Table 11.

Figure 31 shows a correlation of braze patch data with predicted temperatures.

Figure 26 -- Chamber S/N 003 -- Braze Patch Installation

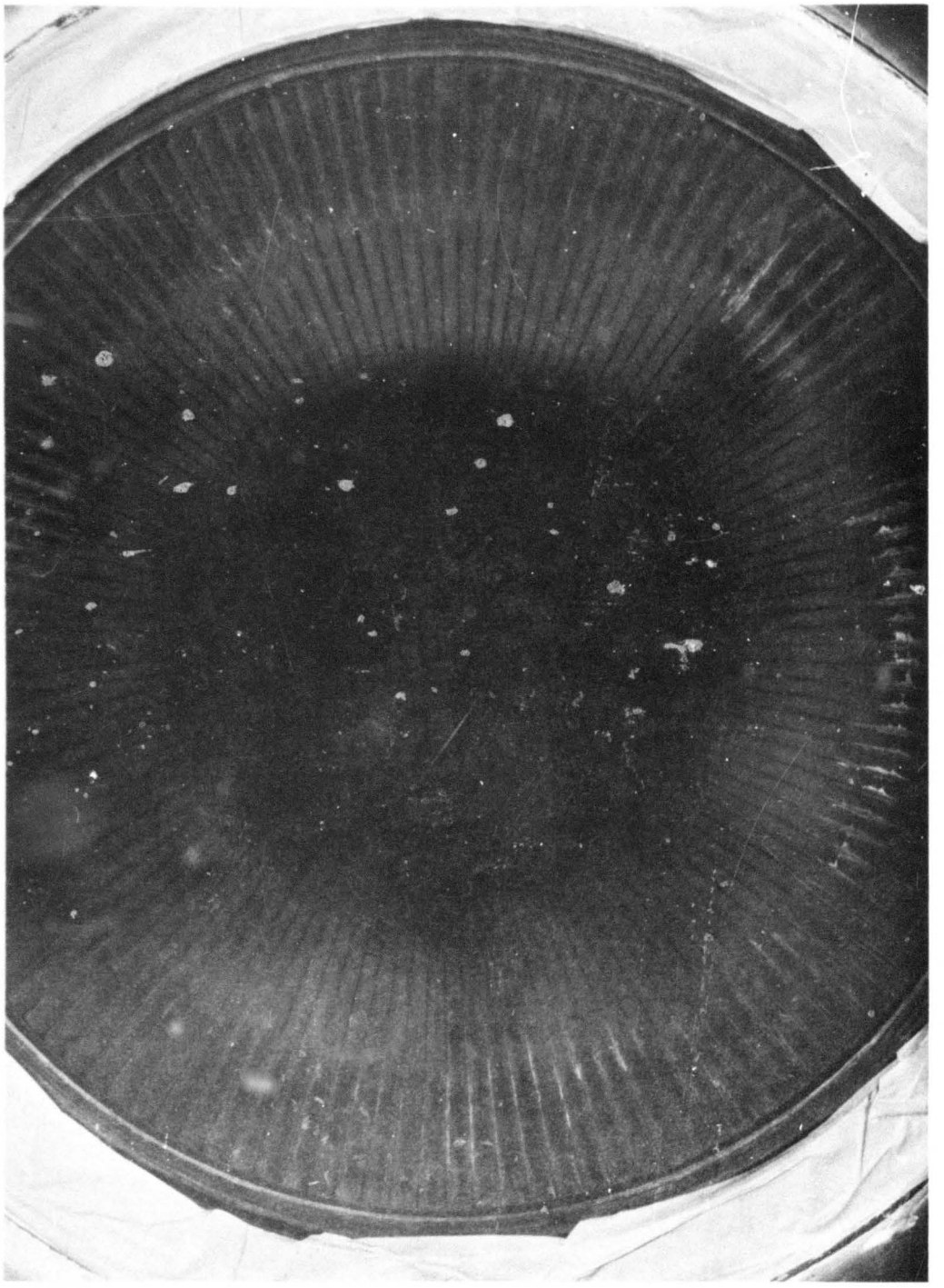

Figure 27 -- Chamber S/N 003 After Firing

4.2, Heat Transfer (cont.)

Table 11-- Braze Patch Material and Locations
Titan IIIM Stage I Chamber S/N 006

Materials

Alloy Number	Manufacturer's Name	Supplier	Composition	Solidus Temp °F	Liquidus Temp °F
1	Alloy X	AGC	Sn-Cu-Ag-Pb-Cd	850	-
2	Alloy Y	AGC	Sn-Cu-Ag-Pb-Cd	990	-
3	Easyflow 45	Handy-Harman	45Ag-15Cu-16Z-24Cd	1125	1145
4	Easy	Same	65Ag-20Cu-15Zn	1235	1310
5	Hard	Same	75Ag-22Cu-3Zn	1365	1450
6	A.T. Special	Same	20Ag-45Cu-35Zn	1430	1500
7	N.E.	Same	25Ag-53Cu-22Zn	1500	1575
8	T.E. Special	Same	5Ag-58Cu-37Zn	1575	1600
9	Nicoro 80	Wesgo	82Au-16Cu-2Ni	1670	1697
10	Eutecrod 155	Eutectic	95Sn-5Ag	710	725
11	Nioro	Wesgo	82Au-18Ni	1742	1742

Axial Plane	Tabulation Block Axial Distance (in.)	Braze Alloys
0	4.00	1,2,3,10
1	7.10	1,2,3,4
2	10.35	1,2,3,4
3	14.10	2,3,4,5
4	18.10	6,7,8,9,11
5	20.24	6,7,8,9,11
6	23.24	2,3,4,5,6
7	29.10	1,2,3,4
8	34.10	1,2,3,4
9	40.10	1,2,3,4
10	44.10	1,2,3,4

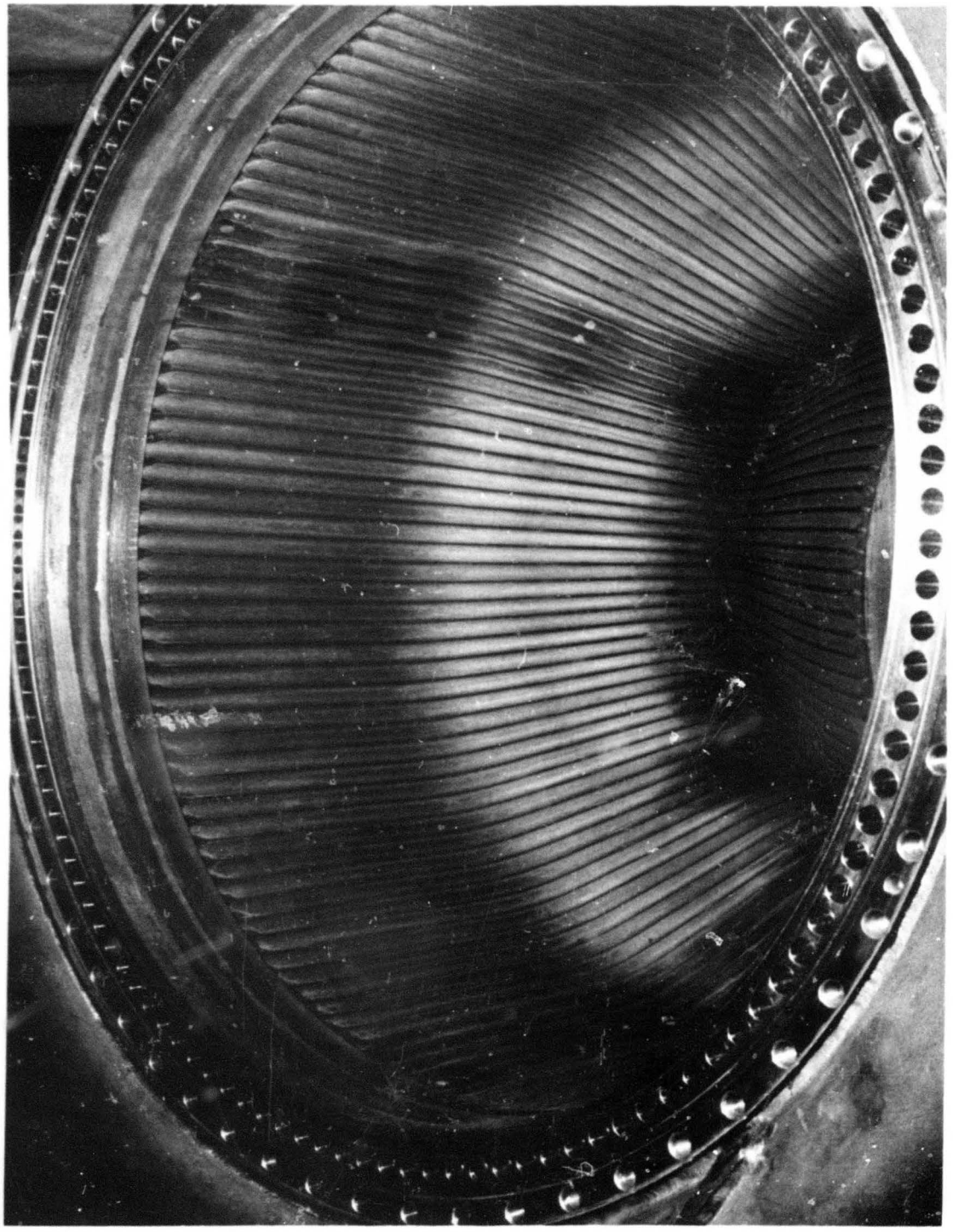

Figure 28 -- Chamber S/N 005 -- Braze Patch Installation

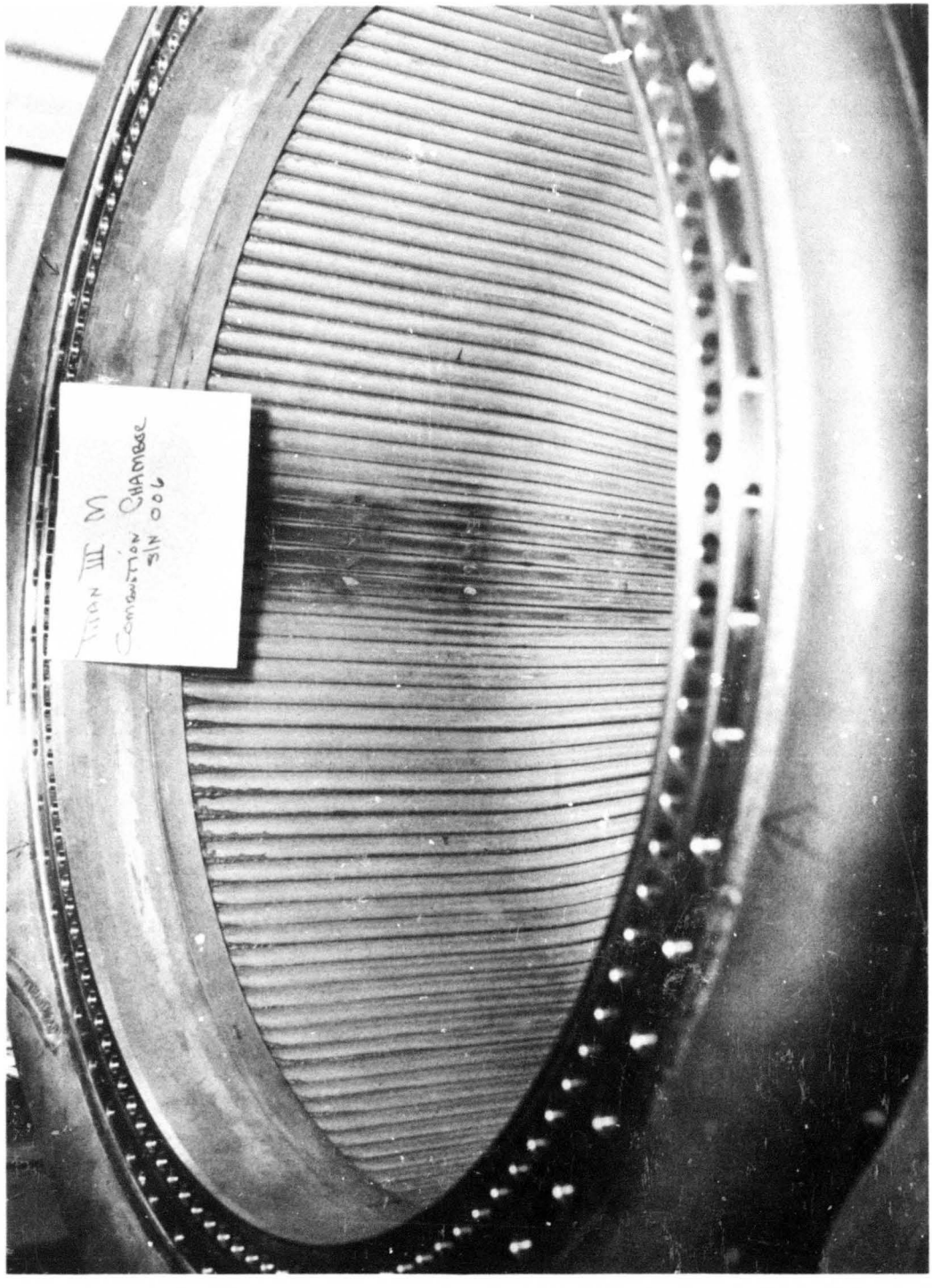

Figure 29 -- Chamber S/N 006 -- Braze Patch Installation

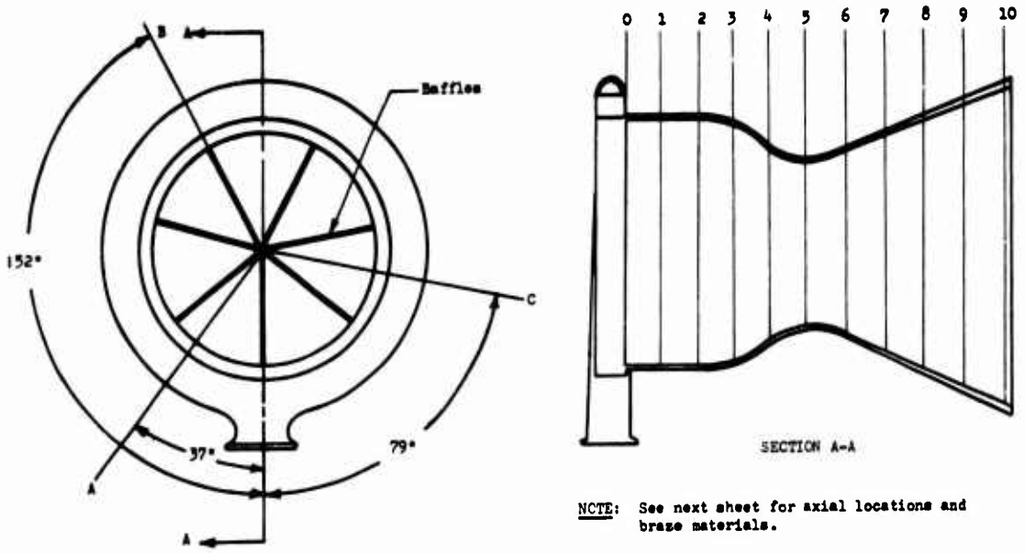

Figure 30 - -Braze Patch Locations

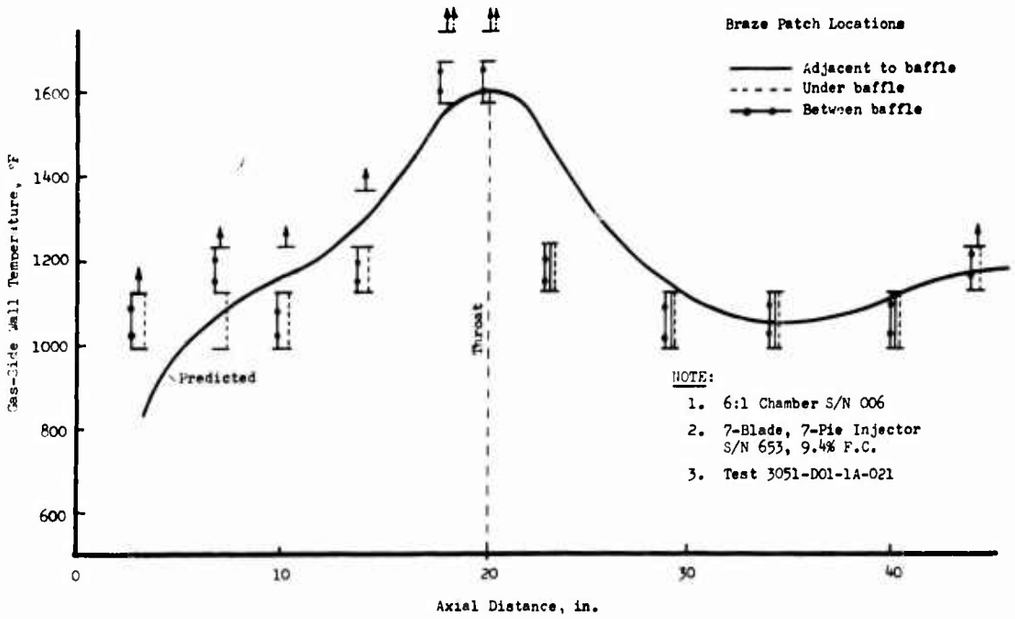

Figure 31 --Comparison of Braze Patch Data with Predicted Temperatures

4.2.4 Heat Transfer Analysis

A heat transfer analysis of the tube bundle was conducted at the "worst flight" conditions relative to tube burnout (R_{BO}). These conditions are +3 percent mixture ration and -3 percent thrust, altitude environment. Fuel film cooling was assumed to be 15 percent. The inlet conditions leading to this operational balance for the engine are:

Worst Flight Condition

Suction		TCA	
P_{ost}	= 123 psia	MR	= 2.13
P_{fst}	= 26 psia	P_c	= 794 psia
T_{os}	= 90°F	T_{ci}	= 104°F
T_{fs}	= 90°F	T_oJ	= 96°F

The values calculated for the maximum wall temperature (T_{wg}) and burnout ratio (R_{BO}) at the about worst flight condition and at nominal conditions are as follows:

Flight Condition

	Worst	Nominal
T_{wg}	1515°F	1523°F
R_{BO}	0.70	0.65

A two-dimensional nominal steady-state condition analysis of the aft flange (turn-around manifold) was also conducted and the maximum temperature indicated was 1580°F, located at the aft end on the hot-gas side.

A heat transfer analysis was later made of two tests on a 6:1 first-stage Titan IIIM regeneratively-cooled chamber. The tests were conducted at the nominal and worst flight conditions. Respectively, the analysis indicated a maximum wall temperature and R_{BO} of 1518°F and 0.65 for the first test and 1510°F and 0.71 for the second test.

4.2, Heat Transfer (cont.)

Heat transfer analysis was made from data from the Series "A" engine subassembly tests. The maximum burnout heat flux ratios, R_{BO}, and gas-side wall temperatures, T_{wg} are listed in Table 12.

4.3 HYDRAULICS

Hydraulic analyses were performed for the various TCA components -- injector, fuel inlet and torus, chamber tube resistance, flow splitter, and chamber aft (turn around) flange -- prior to completing the preliminary design of the chamber. These analyses predicted a decrease in differential pressure of 45 psi for the TCA as a whole, mostly accounted for by the combustion chamber.

Between October 1966 and February 1967 a series of water flow tests was conducted to confirm previous analyses and to verify that the distribution of flow among the individual tubes was within the range required to maintain the burnout heat flux ratio below 0.82.

Chamber hydraulic resistances were compiled from inspection flow test data. The resistance is defined by

$$R = \frac{P\ (S.G.)}{W_f{}^2}$$

The nominal pressure drop for the combustion chamber is 145 psi. Data from the water flow tests are presented in Table 13.

Table 12 -- Thrust Chamber Compatibility Summary--Engine Subassembly Tests

(Test Series 3051-D01-1A)

Run	Dur.	Data Period	C.C.	Injector	Tcc	Pc5B (a)	MR	R_{cc} Static	Q_R	R_{FTCA} Static	R_{BO}
001	30.450	2.0/29.9	002	S/N 1110 2BIE-38 16.3% FFC	80.0	824.9	1.946	15.3	23,376	38.9	0.618
002	15.447	2.0/14.9	002	S/N 1110 2BIE-38 16.3% FFC	79.5	811.8	1.936	14.7	23,047	39.0	0.624
003	200.890	2.0/200	002	S/N 1110 2BIE-38 16.3% FFC	77.2	830.3	1.983	14.8	22,558	38.5	0.628
004	30.548	2.0/30.0	002	S/N 249 2BIE-38 12.0% FFC	83.8	880.8	1.972	14.5	25,836	42.4	0.662
005	200.713	2.0/220	002	S/N 249 2BIE-38 12.0% FFC	89.0	874.0	2.105	15.5	26,308	42.6	0.649
006	196.285	2.0/196	003	S/N 214 2BIE-38 16.3% FFC	87.2	787.1	2.131	14.7	23,064	40.0	0.704
007	200.873	2.0/200	002	S/N 214 2BIE-38 16.3% FFC	95.3	796.9	2.126	14.7	25,464	40.0	0.700
008	60.985	2.0/60.5	003	S/N 657 300 Quad 12.6% FFC	73.4	807.0	1.880	Invalid	21,650	39.8	0.640
009	53.169	19.0/21.0	004	S/N 651 400 Quad 12.6% FFC	78.9	824.2	1.985	17.0	22,900	39.7	0.670
010	40.850	2.0/40.35	005	S/N 251 400 Quad 14.6% FFC	79.5	856.7	1.999	16.2	24,041	40.6	0.660
011	20.773	19.0/20.7	005	S/N 65 450 Quad 12.6% FFC	79.9	824.7	1.870	Invalid	23,938	38.7	Not Avail.

Table 12 -- Thrust Chamber Compatibility Summary--Engine Subassembly Tests

(Test Series 3051-D01-1A)

(cont.)

Run	Dur.	Data Period	C.C.	Injector	Tcc	Pc5B (a)	MR	R_{cc} Static	Q_R	R_{FTCA} Static	R_{BO}
012	186.6	2.0/186.6	005	S/N 650 450 Quad 12.6% FFC	76.6	840.1	1.859	Invalid	23,450	38.5	Not Avail.
013	200.2	2.0/200.2	005	S/N 650 450 Quad 12.6% FFC	89.4	763.0	2.18	Invalid	22,800	39.8	0.740
014	73.826	2.0/73.826	005	S/N 651 400 Quad 12.6% FFC	81.6	843.7	1.976	16.3	24,350	39.5	0.650
015	5.635	2.0/5.4	005	S/N 657 300 Quad 12.6% FFC	77.3	833.0	1.938	17.1	23,000	40.5	0.660
016	36.7	2.0/36.2	007	S/N 650 450 Quad 12.6% FFC	97.0	509.3	2.223	16.8	16,550	44.1	0.720
017	207.410	2.0/206.9	007	S/N 650 450 Quad 12.6% FFC	88.0	814.7	2.162	16.1	24,450	39.0	
018	5.367	2.0/4.8	004	S/N 657 300 Quad 12.6% FFC	82.2	833.8	2.060	16.0	24,000	39.8	0.680
019	140.149	2.0/139.7	007	S/N 650 450 Quad 12.6% FFC	73.6	826.4	1.839	16.7	22,500	40.7	N.A.
020	20.677	2.0/20.2	008	S/N 655 400 Quad 12.6% FFC	79.3	801.2	2.004	16.9	22,600	37.0	N.A.
021	200.818	2.0/200.3	006	S/N 653 450 Quad 9.4% FFC	97.0	812.3	2.169	16.3	26,400	39.1	N.A.
022	5.198	4.0/5.0	008	S/N 651 400 Quad 12.6% FFC	76.5	845.6	1.926	15.9	23,300	38.2	N.A.

Table 12 -- Thrust Chamber Compatibility Summary--Engine Subassembly Tests

(Test Series 3051-D01-1A)

(cont.)

Run	Dur.	Data Period	C.C.	Injector	Tcc	Pc5B (a)	MR	R_{cc} Static	Q_R	R_{FTCA} Static	R_{BO}
023	60.427	2.0/60.0	008	S/N 662 450 Quad 10.3% FFC	85.5	820.8	1.967	17.4	24,488	44.2	N.A.
024	60.170	2.0/61.7	006	S/N 653 450 Quad 10.3% FFC	86.0	814.9	1.956	16.9	25,017	44.1	N.A.
025	20.504	2.0/20.5	008	S/N 651 400 Quad 12.7% FFC	75.1	815.6	2.057	17.4	21.569	43.7	N.A.
026	60.764	2.0/60.2	006	S/N 661 450 Quad 10.3% FFC	Invalid	851.9	1.934	16.0	Invalid	42.9	N.A.
027	61.442	2.0/61.4	008	S/N 662 450 Quad 10.5% FFC	84.4	830.8	1.952	16.8	25,080	43.2	N.A.

4.3 Hydraulics (cont.)

Table 13 -- Chamber Resistance Summary

S/N	Hydrolab Run Date	P	R
001	5-3-66	134.3	14.8
002	5-11-66	138.0	15.2
003	6-29-66	135.0	14.9
004	7-22-66	144.0	15.9
005	8-23-66	150.7	16.3
006	9-13-66	144.0	16.0
007	10-3-66	138.5	15.3
008	10-28-66	143.0	15.8
009	11-7-66	140.4	15.5

4.4 MATERIALS AND PROCESSES

No new materials were introduced into the design of the Titan IIIM combustion chamber. Consideration was given during the preliminary design to the use of Hastelloy because of its purportedly superior thermal and non-oxidizing properties. However, it was rated as a high risk because of its high cost, fabrication difficulties and because of the lack of extensive industrial experience with Hastelloy fabrication. One stainless steel chamber which incorporated six tubes of Hastelloy-X was fabricated for experimental use. Micrographic evaluation of the metallurgical properties of the tubes after the chamber was fired showed that Hastelloy-X was less sensitive to carburization than 347 stainless steel. Nevertheless 347 stainless steel was adequate for the stage I chamber. Further studies of Hastelloy-X were performed, however, for the gas cooler redesign. Material studies were therefore limited to corrective actions and to investigation of improved processes as material problems were uncovered by testing.

4.4, Materials and Processes (cont.)

The chamber tube cleaning method was reviewed for ways of eliminating residues from the cleaning agents. Tube bundles and furnace braze samples were prepared, subjected to storage and to contaminants prevalent in the shop, and then vapor-degreased. On the basis of the investigation methylene chloride was substituted for trichlorethylene for the degreasing agent.

The principal problem areas investigated were the tube-to-forward flange leaks (chamber S/N 008) and the closure band weld cracks (chamber S/N 011).

Postfire examination of combustion chamber S/N 008 following engine test No. 3051-D01-1A-027 revealed both external and internal tube leakage. The external leak was the result of the fracture of single V-band-to-cooling tube tack weld. This leak was minor in nature and easily repairable; no further corrective action in this area was required. Seven leaks were detected in the joint of the coolant tubes to the forward flange by pressurizing the tubes to approximately 80 psig and observing with the aid of liquid soap. All of the leaks were from the "down" (first pass) tubes. As the chamber had been fired five times, including one very rough start, the question arose whether the leakage was due to inadequate brazing at the time of fabrication or resulted from the stresses arising from the rough start. A metallographic examination of the joint was directed.

As a control case, chamber S/N 003, which had been brazed in the same manner as chamber S/N 008, was examined first. Visual inspection through a 40X microscope showed no indication of cracks but considerable evidence of porosity. Microphotographs of a typical section disclosed that the tube was markedly off center with respect to the recess in the flange, that the porosity was greatest where there was the widest gap between the tube and the flange, and that the porosity extended throughout the length of the joint.

4.4, Materials and Processes (cont.)

Examination of chamber S/N 008 showed the same visual indications of porosity and in addition cracks in the braze were evident under 10X magnification. Photomicrographs of one cracked joint showed that the crack extended the length of the joint. It was concluded that the joint was originally weak and had fractured under the additional stresses imposed by the rough start.

The weak joint is attributable to insufficient coverage of the tube surface with braze material, caused by improper centering of the tube in the recess and to porosity caused by runoff of material during brazing. Recommendations were made for centering the tubes by mechanical means and for lowering the brazing temperature slightly and shortening the period of the braze cycle in order to reduce runoff.

The specific changes were:

(a) Swaging the forward end of the coolant tubes to guarantee a positive clearance of up to 0.004 inches between the tube and the insertion holes in the flange;

(b) reduction of the brazing time (time above braze liquidus) tc less than 10 minutes;

(c) bright-annealing of the chambers preparatory to brazing to ensure clean, scale-free surfaces; and

(d) brazing at temperatures of 1920 to 1940^{o}F, which had been determined from test samples to provide good "wetting" of the surfaces by the braze material and yet retard braze runoff.

Forward flange leaks did not occur on chambers where these procedures were followed.

4.4, Materials and Processes (cont.)

Postfire inspection of chamber S/N 011 after Verification Test No. -017 revealed a slight hot gas leak and a half-inch long crack in the lower weld holding the cover band to the forward flange. The cover band closes the inside of the flange after machining of the manifold. The crack was disclosed during a postfire checking for hydraulic leakage. In addition to the crack two pinhole leaks were detected in the weld. The chamber had been subjected to a total of 873 sec testing during 12 cycles.

A complete metallographic inspection was made of the cover band area. The crack was attributed to inadequate weld penetration and to improper positioning of the band. These conditions are shown in Figure 32.

Accordingly the weld for the cover band was redesigned as shown previously in Figure 10 Section 2.6. A chamfer on the cover band was provided in addition to the chamfer on the flange in order to make it more accessible for welding and thus insure a fully penetrating weld. Shoulders on the cover band were also supplied to make certain that the band was properly positioned before welding. Further cracks in the cover band welds were never a problem.

Materials evaluations were made prior to the fabrication of chamber S/N 013, which has six coolant tubes of Hastelloy-X.

Tensile data were obtained from butt-brazed sheet specimen made from actual chamber tubing. The specimen were brazed for five minutes with AGC 44080B braze alloy in a dry hydrogen atmosphere at 1950^{o}F, hand polished to remove excess braze, and tensile tested at room temperature. Six specimens were used, two with zero joint clearance, two with 0.0015 in. clearance, and two with 0.003 in. clearance. Results range from 65,000 to 80,000 psi, with the larger clearances displaying the lower strengths. This strength level is normally greater than the yield strength of the parent material. The Hastelloy-X aluminum content was 0.14%.

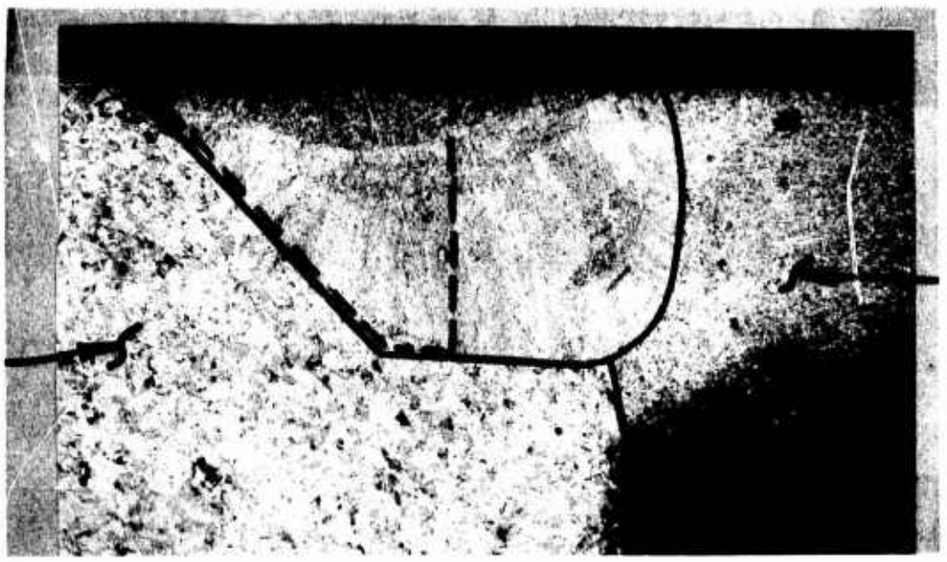

Aft Weld

NOTE: The solid line outlines the weld nugget. The dotted line represents correct position of cover band.

Figure 32 -- Chamber S/N 011 -- Section through Forward Flange

4.4, Materials and Processes (cont.)

In order to determine the effects of multiple furnace cycling upon oxide formation and thus the brazeability of the Hastelloy-X material, three 1/4-in. dia. tube specimens were exposed for five minutes to each of three normal brazing cycles of 1950°F. On the first cycle, braze alloy (AGC 44080B) was applied to Specimen No. I, on the second cycle braze alloy was applied to Specimen No. II, and on the third cycle braze alloy was applied to Specimen No. III. Examination of the joints revealed equivalent good braze joints on all three specimens. The Hastelloy-X aluminum content was 0.18%.

Brazing of combustion chamber S/N 013 was accomplished during December 1966. The chamber was brazed in two cycles using AGC 44080A braze alloy. The first cycle was performed with the aft end down, to braze the tube-to-tube joints from the throat area aft, at approximately 2010°F. The second cycle was performed with the forward flange down, to braze the combustion zone tube-to-tube joints and the tube-to-fuel torus joints, at approximately 2000°F. All tube-to-tube joints appeared sound although braze alloy progression through the joint to the "back side" on both of the Hastelloy-X-to-Hastelloy-X joints was less than that noted on the CRES 347-to-CRES 347 joints. An area of braze alloy dissolution (erosion) was noted on five of the six Hastelloy-X tubes at the point of tangency between the tube crowns and aft edge of the forward flange. The eroded condition is attributed to the excessive amount of braze alloy which had been preplaced in this area prior to the second braze cycle, coupled with the higher brazing temperature employed for the "A" revision braze alloy. The manganese-nickel binary equilibrium diagram shows a solid solution type diagram with a liquid phase occurring at 1840°F. The reaction between the liquid manganese-base braze alloy with the nickel-base tube material at the brazing temperature resulted in the tube dissolution. The sixth tube did not erode because of tack weld joining the tube crown to the flange occupied the area. The areas of dissolution were repaired by applying Nioro (82 Au-18Ni) braze alloy to the discrepant areas by the manual TIG method.

Report 9180-941-DR-3

Section 5 Testing

5. TESTING

The combustion chamber testing program consisted of laboratory tests to obtain design parametric data expeditiously, with more convenience, and less cost than hot firings; development firings to evaluate thrust heat transfer and durability; component verification firings to establish performance characteristics of the prototype design; and engine demonstration firings to verify that the production configuration met all requirements.

5.1 LABORATORY TESTS

The principal laboratory test programs were a structural load test, a heated tube test to obtain special heat transfer data pertaining to coolant tube burnout, and a hydraulics flow test to measure the distribution in flow rate among the coolant tubes.

5.1.1 Structural Load Test

A series of tests was performed during December 1966 in the Structures Laboratory to determine the structural properties of the Titan IIIM Stage I combustion chamber. The tests were performed on P/N 1130174, S/N 010, a new, unfired combustion chamber.

The chamber was instrumented with approximately 60 strain gages, Figure 33, pressurized with water to maximum specification limits, and subjected to side and axial loads. An evaluation to determine location of strain gages had been made prior to this test.

In preparation a study was made to determine required thrust and design load conditions for the static testing and a structural test plan was established for evaluating the structural characteristics of the combustion chamber at limit and ultimate loading. Chamber S/N 010, was received in the Structures Laboratory in December 1966. Installation of strain gages was completed and testing was initiated in the later part of December. Test equipment for mounting the chamber in the universal test fixture and applying

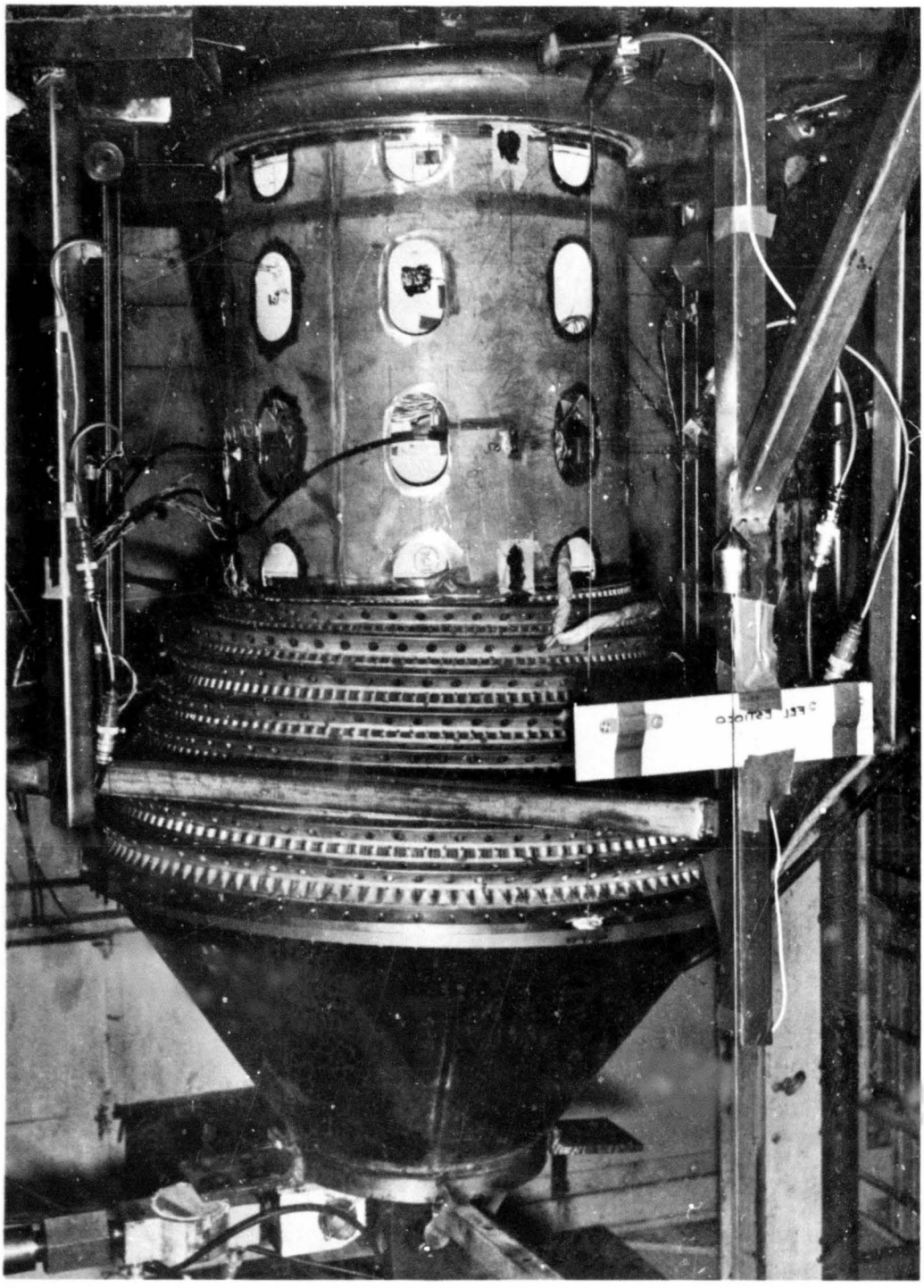

Figure 33 -- Structural Test -- Strain Gauges

5.1, Laboratory Tests (cont.)

the test loads was fabricated and delivered to the Structures Laboratory. Another piece of equipment for positioning the throat plug retainer during installation was fabricated. A photograph of the test setup is presented in Figure 34.

The test conditions are given in Table 8, Section 4.1.3. The tests simulated design limit loads for a sea level start and for steady state and maximum load while gimballing. For practical reasons no tests were run at elevated temperatures; however, the high static load representing a sea level start imposed a more severe condition than the degradation in the physical properties of the tubes during firing. The last test was conducted at design limit axial load after which side loads were increased until failure occurred between the attachment point for the reinforcing shell and the first V-band (Figure 35).

Where the chamber failed, the failed portion was subjected to 3.27 times the design limit load. Allowing for the degradation of tube strength during firing, the tubes would have failed at 2.88 times the design limit load.

The chamber, after completing the structural test, was subjected to standard proof and leak tests. No leaks were observed in the combustion zone (hot gas area) or coolant tubes. The tube braze joints below the throat were not leak checked due to the 2-1/2 degree distortion of the chamber resulting at the times of failure. The distortion prevented the required hydrotest tooling from mating to the aft flange. A dimensional check of the chamber disclosed no change in its geometry above the throat.

5.1.2 Heated Tube Test Program

Previous investigations into the burnout heat flux of AeroZINE 50 had yielded considerable data for velocity ranges below 100 ft/sec. Experience had shown, however, that extrapolating these data unsupported by tests conducted in the immediate design range is hazardous. Moreover data at the supercritical pressures applicable to Titan IIIM design were not available.

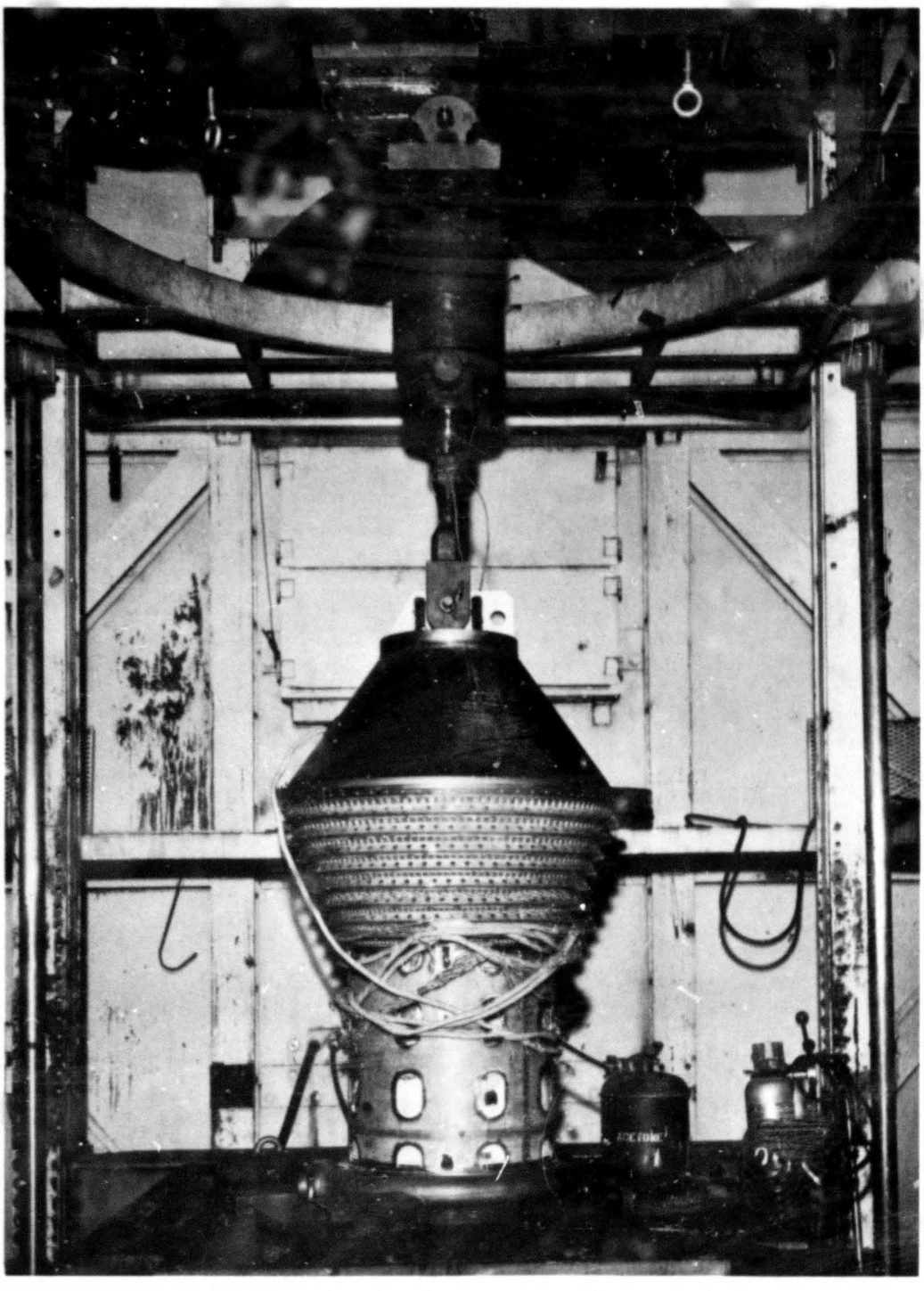

Figure 34 -- Structural Test Setup

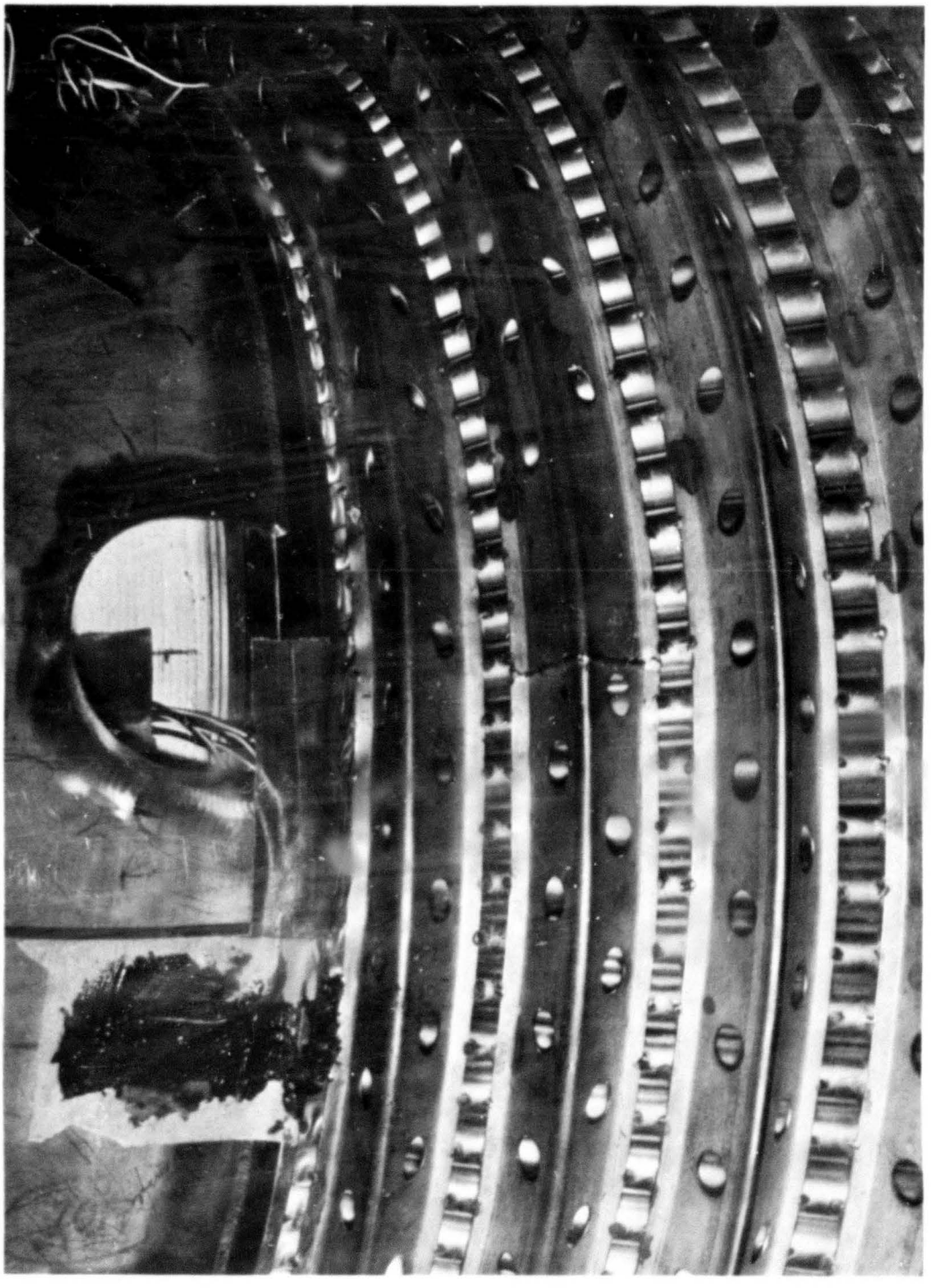

Figure 35 -- Chamber S/N 010 -- Closeup of Failure

Table 14 -- Test Section Dimensions

(Material: 347 Stainless Steel)

	Nominal Values		Measured Values		
Test	OD, in.	Wall Thickness, in.	OD, in.	ID, in.	Heated Length, in.
HT-8-102	1/4	0.016	0.251	0.221	6.00
-104	3/16	0.016	0.187	0.154	5.50
-105	3/16	0.016	0.187	0.156	5.00
-106	3/16	0.016	0.187	0.156	5.00
-107	3/16	0.016	0.187	0.156	6.00
-109	3/16	0.024	0.187	0.141	6.00
-110	3/16	0.024	0.188	0.141	6.00
-111	1/4	0.016	0.251	0.218	3.00
-112	3/16	0.012	0.188	0.163	5.00
-113	1/4	0.016	0.251	0.218	3.00
-114	3/16	0.012	0.188	0.164	2.50
-115	3/16	0.012	0.188	0.164	2.50
-116	3/16	0.012	0.188	0.164	2.50
-117	3/16	0.016	0.187	0.155	5.00
-118	3/16	0.016	0.187	0.155	5.00
-119	3/16	0.016	0.187	0.155	6.00
-121	1/2	0.028	0.500	0.443	5.00
-122	3/16	0.024	0.187	0.140	6.00
-126B	3/16	0.016	0.187	0.156	2.00

5.1, Laboratory Tests (cont.)

A short test program covering 18 tests was conducted to obtain the additional data points at velocities of 90 to 180 ft/sec, pressures of 1000 to 1200 psia, and bulk temperatures from 100°F to 200°F. A complete report of the program is included in Reference B. A brief summary of the program and findings follows.

The testing consisted of 18 burnout tests and one extended duration test. All were conducted with electrically heated test sections fabricated from CRES 347 tubes which provided uniform axial and circumferential heat flux distributions.

All tests were conducted on Aerojet's high-pressure blowdown heat transfer loop. The principal components of the loop are the pressurization system, run tank assembly, preheater-test section assembly, heat exchanger, flow control valve, and dump tank assembly. Electrical power for the preheater-test section assembly is provided by four 15-volt 50-kw dc power supplies which operate from a 440-bolt 3-phase ac line voltage.

Test sections were fabricated from AISI 347 stainless-steel tubing with wall thicknesses ranging from 0.012 to 0.028 in. and outside diameters from 3/16 to 1/2 in. The basic test section configuration is illustrated in Figure 36. Dimensions of the test sections used in each test are given in Table 14.

It should be noted that almost all of the available AeroZINE 50 burnout heat flux data were obtained in similar round, uniformly heated tubes. In actual rocket coolant tubes, the effects of asymmetric heating, tube curvature, and tube flattening should also be considered. These effects were not studied in this program and Reference C should be consulted if information on these more practical aspects is required.

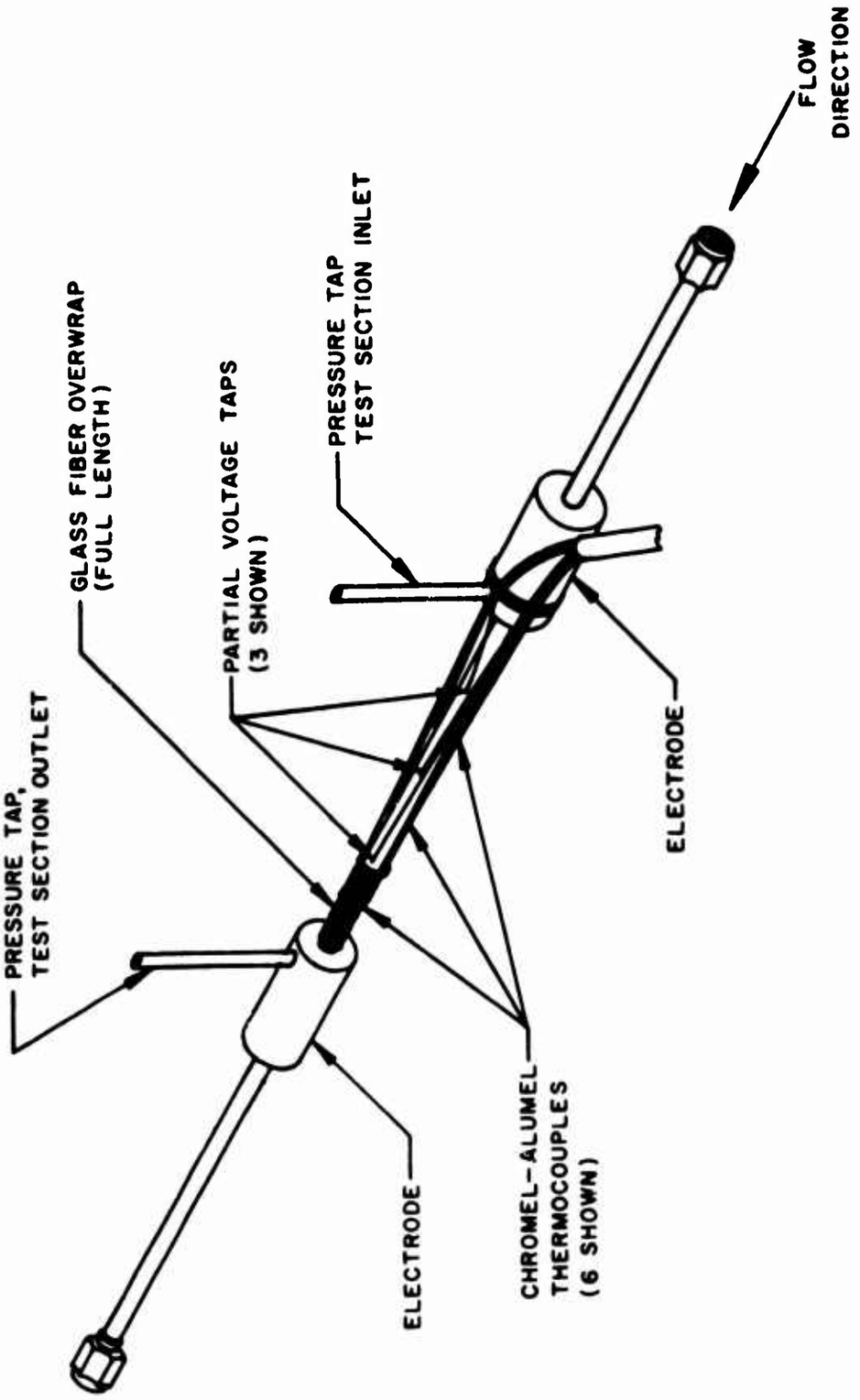

Figure 36 -- Instrumented Test Section Assembly

5.1, Laboratory Tests (cont.)

The heated lengths of the test sections were formed by silver brazing two predrilled copper cylinders onto the tubing. These copper cylinders fit into copper bus-bar clamps. Fittings for connecting the test section to the mixing sections and pressure transducer lines were incorporated and the wall-temperature and voltage tap instrumentation were then installed. A minimum unheated entrance length of 5 in. was maintained on all test sections.

The following parameters were measured in each test:

Test section outer wall temperature (at 2 to 3 axial positions)
Test section inlet and outlet bulk temperature
Flow rate
Test section inlet and outlet pressure
Test section current
Overall test section voltage drop
Voltage levels at incremental distances along the test section

The accuracy of the data was enhanced by taking redundant measurements whenever possible. Average readings of these measurements were used in evaluating the data.

Test section outer wall temperatures were measured with 40-gauge chromel-alumel thermocouples installed upon a 0.005-in. thick layer of mica and wrapped with glass roving to hold them in place. The accuracy of these measurements was evaluated by placing two thermocouples 180°F apart at each axial position where a wall temperature measurement was desired. In most of the tests conducted in this program, the thermocouples were held firmly in place by spot-welding them to a 0.010-in. diameter 304 stainless steel wire which was then twisted around the test section tubing. (The wire was installed on top of the mica layer and underneath the glass roving.) The data at a given axial position generally indicated agreement ranging from 20 to 50°F

5.1, Laboratory Tests (cont.)

at wall temperatures in the range of 500 to 1500°F. The readings from the tube wall thermocouples were adjusted using the result of previous thermocouple calibration tests which were conducted as part of the program. In the calibration tests, the thermocouple error was determined at temperatures up to 1400°F using an A-C heated tube. Readings from thermocouples spot-welded directly to the tube wall were used as standard measurements.

Inlet and outlet bulk temperatures were each measured with three copper-constantan immersion type thermocouples installed downstream of mixing baffles in the fluid mixing sections. Agreement between the readings of the three thermocouples was generally within 2°F.

Flow rate measurements were obtained from two turbine-type flowmeters connected in series upstream of the preheater. Agreement between these two meters was consistently within two percent.

Test section inlet and outlet pressures were measured with transducers connected to pressure tap fittings upstream and downstream of the test section electrical connections. Readings from these two transducers consistently agreed within two percent at the no flow data point recorded in each test after system pressurization had been achieved.

Overall test section voltage drop was measured by attaching lead wires to the test section electrodes. Incremental voltage levels were measured with voltage taps which consisted of 0.005-in. diameter wire spot-welded to the tube. Agreement between these voltage measurements was good, and a linear voltage variation was found to exist along the test section.

Test section current was measured using a 50-mv shunt arrangement. The accuracy of this measurement was good as gauged by the overall energy

5.1, Laboratory Tests (cont.)

balances, performed for each test, which were generally repeatable within ± 5 percent deviation in the energy balance, it is felt that the current measurement was accurate within about one percent.

In the burnout tests, the test section heat flux was increased stepwise until burnout occurred. Steady-state heat transfer was achieved at several heat flux levels below the burnout point so that the forced convection and nucleate boiling characteristics of AeroZINE 50 could also be observed. In the extended duration test, two levels of heat flux were applied to the test section, each for a four minute duration. One low velocity burnout test was also conducted in which the conditions at the aft end of the second-stage Titan II coolant tube were duplicated.

Activation of the heat transfer loop for the A-50 Heated Tube Test Program was initiated April 1966. Necessary facility hardware was purchased and the supporting tube design work was conducted. The test program was reduced to 18 tests to stay within the reduced budget. Test was completed in July 1966.

The test data are analyzed and discussed in Section 4.2.1.

Following burnout five tubes were sectioned longitudinally and examined. Each section was found to contain black deposits on the liquid side of tube wall, apparently carbonaceous, in the immediate area of burnout. The apparent thickness of the deposits varied from 0.001 in. to 0.010 in., the thickest deposits occurring in the tubes where the velocity of flow had been least. A similar thin deposit was found in the tube used for the extended duration test.

Increases in wall temperature immediately prior to burnout were also noted, indicating the initiation of film boiling.

The test program is discussed in greater detail in Reference B.

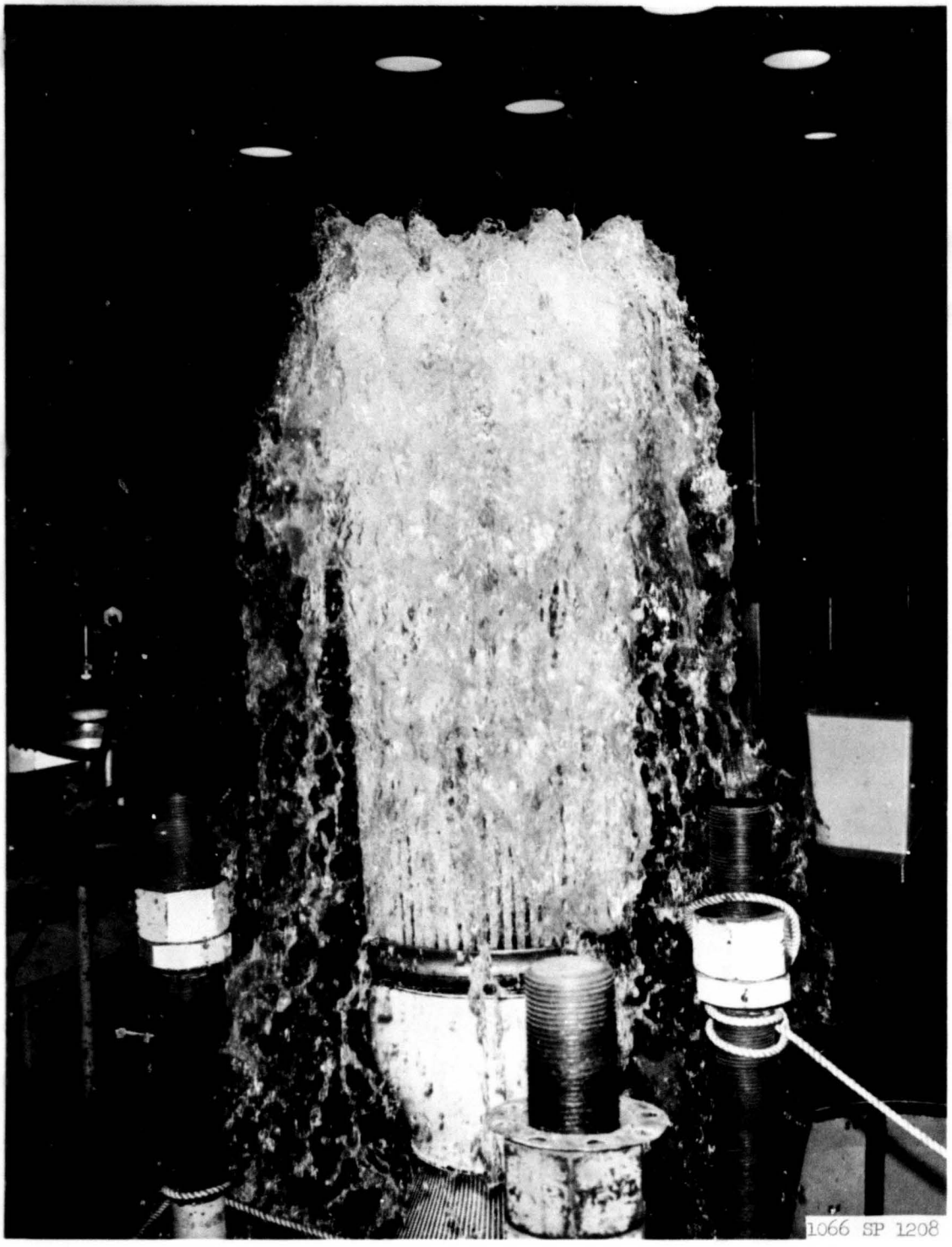

Figure 37 -- Combustion Chamber Flow Test to Atmosphere

5.1, Laboratory Tests (cont.)

5.1.3 Flow Splitter Evaluation

Water flow tests were conducted to evaluate the hydraulic effect of the flow splitter in the torus inlet. Hardware utilized for these tests included combustion chambers S/N 001 and S/N 003 and the torus assemblies for chambers S/N 003 and S/N 013.

A portion of the forward flange of the chamber was removed to allow the individual coolant tubes to flow to atmosphere rather than into the common forward manifold. The chamber was installed in the Hydraulics Laboratory in the normal upright position. The combustion chamber, with 90 lb/sec of water flowing through the tubes, was photographed (Figure 37) from various positions. An attempt was made to determine the flow rates of the individual tubes by measuring their respective water discharge heights. Examination of Figure 37 illustrates the difficulty of making an accurate measurement of the flow variations by this method, since the technique measures only static pressure at the discharge, not flow rate.

The method of determining the flow variation later utilized was similar with the exception that the discharge from each chamber tube was flowed into a time weight setup. This method worked extremely well and produced accurate, repeatable data.

The typical setup for the water flow testing is shown in Figure 38. The combustion chamber shown in the photograph is S/N 001. The water was introduced to the torus inlet at a measured flowrate. The aft flange of the combustion chamber had been removed previously, which allowed the water to travel through the first-pass ("down") tube to atmosphere, rather than into the aft flange and into the adjacent second-pass ("up") tube. The individual streams of water were diverted to a container which was placed on the scales of an electrically operated weight-vs-time recorder. The time required to collect a specified amount of water was recorded and converted to pounds per second. All flow data were reduced to percent of nominal flow. The nominal flow per tube was obtained by dividing the total measured

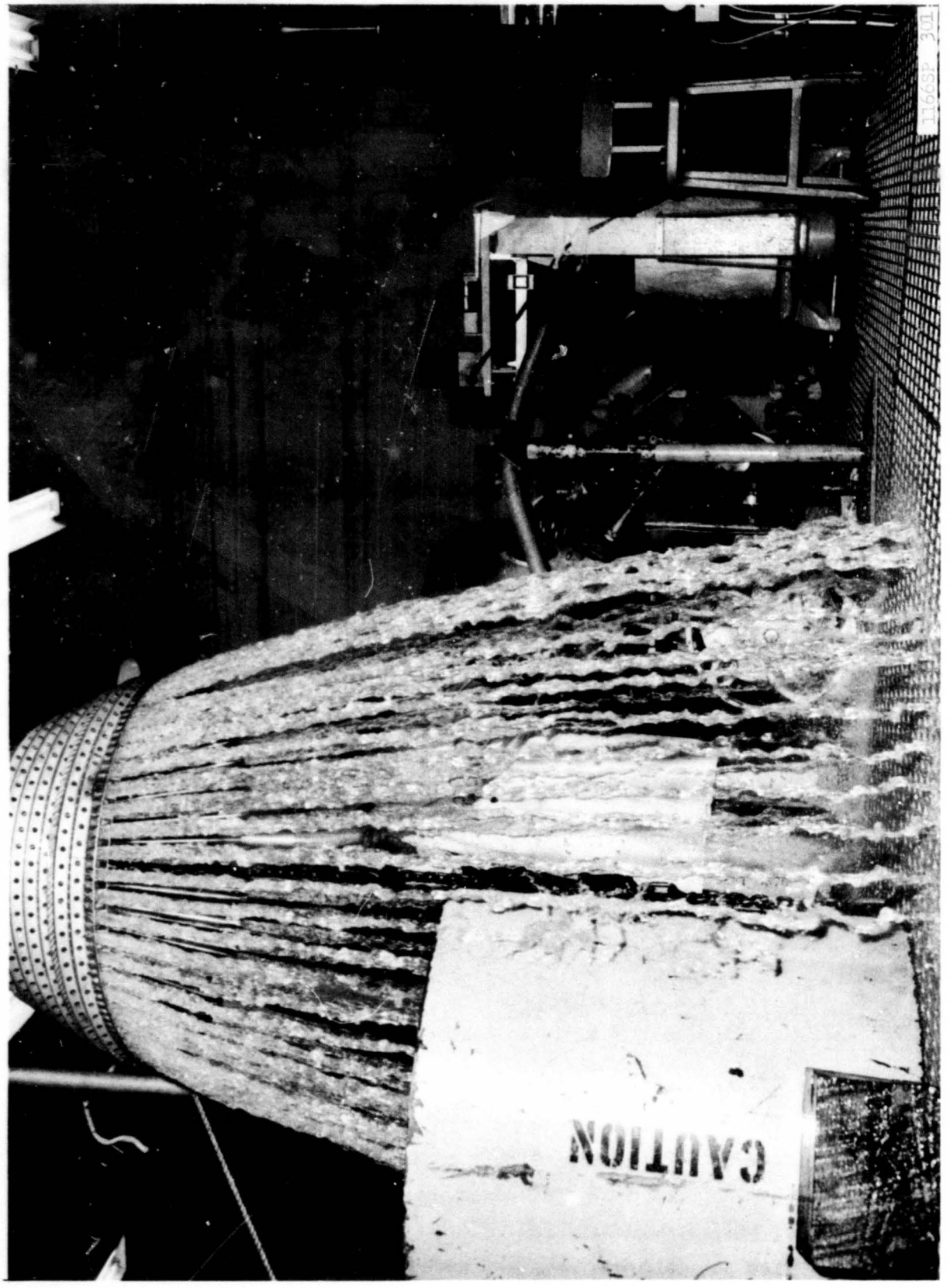

Figure 38 -- Revised Flow Splitter Test Setup

5.1, Laboratory Tests (cont.)

flow to the torus inlet by the number of first-pass tubes in the combustion chamber. The accuracy, for flow testing, of the method described is verified by comparing the total of the measured individual tubes with the measured torus inlet flow rate. In all tests, the amount of water collected was within $\pm$ 1 percent of the inlet flow rate as measured independently. The torus assemblies were tested in the same manner as the combustion chambers. Figure 39 identifies the location of the tubes by number.

Flow testing of the second-pass tubes was conducted with combustion chamber S/N 003. Prior to delivery to the Hydraulics Laboratory, the forward flange of the chamber had been modified to permit the "up" tubes to discharge to atmosphere in the same way as the "down" tubes in chamber S/N 001. The test setup remained the same except that the chamber was inverted so that the tubes drained directly into the flow collector. The water flow rate to the torus inlet was 89.1 lb/sec (27 percent of rated flow) for this test. The total amount of water collected from the individual tubes was 89.7 lb/sec. The individual tube flow rates varied from 96.4 percent of nominal (tube No. 109) to 103.9 percent of nominal (tube No. 87). This spread in flow rate in the second-pass tubes is satisfactory with respect to maintaining minimum velocity of flow for regenerative cooling.

Testing was next initiated to determine the distribution in the first-pass ("down") tubes. Testing began with chamber S/N 003, whose aft flange had been removed in order to measure the flow rates before they were equallized in the aft collector ring. The initial results showed a wide dispersion, from 51 percent to 117 percent of nominal. During a test of the torus assembly conducted separately, it was observed that some tubes slots were not flowing. Examination of the test setup disclosed that a 2-in. connection had been made at the torus inlet. This produced a high velocity jet with unequal pressure distribution in the torus. The proper 4-in. connection, corresponding to the engine plumbing, was made in the test setup and testing resumed.

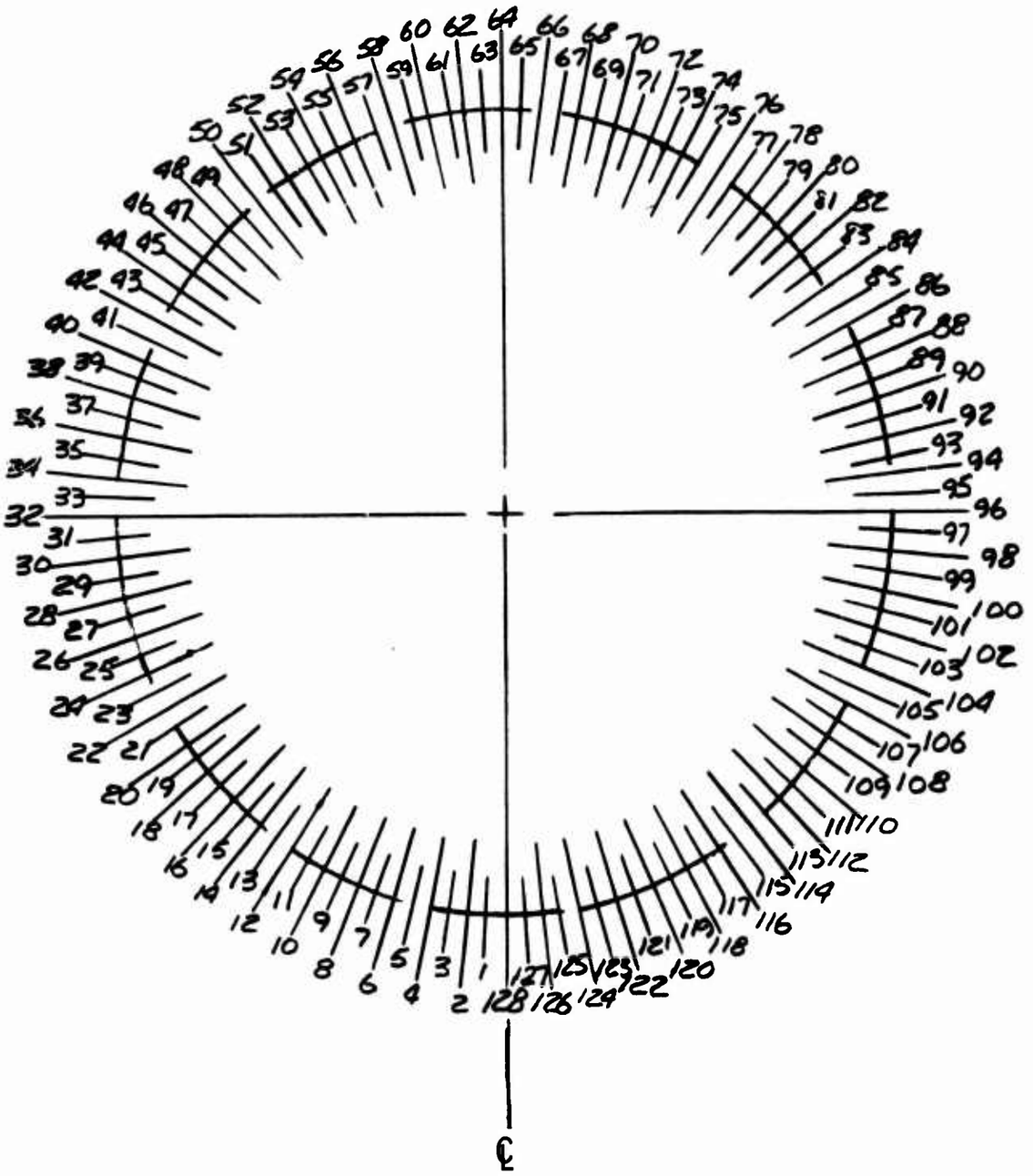

Figure 39 -- Flow Splitter Test -- Tube Locations

5.1, Laboratory Tests (cont.)

The improper inlet fitting invalidated only the data obtained for the first-pass tubes. During the tests of the second-pass tubes the maldistribution in the first-pass tubes was compensated by the aft manifold, which produced nearly equal pressures at the inlet to the second-pass tubes. The differences in pressure were therefore small with respect to the total pressure drop in the tubes.

The data for the first-pass tubes, chamber S/N 003, after the correction of the test set up, are presented in Table 15. The dispersion was from 81.5 percent minimum to 108 percent maximum. The variation among the tubes not shown in Table 15 ranged from 96 percent to 108 percent.

Table 15 -- Flow Distribution-Torus, Chamber S/N 003

Tube No.	% of Nominal Flow
2	96.8
4	89.2
6	88.5
8	83.3
10	81.5
66	103.5
120	93.9
122	91.7
124	94.5
126	96.7
128	107.0

The first-pass tubes in chamber S/N 001 were retested using the correct inlet fixture. The water flow rate to the torus inlet was 150 lb/sec. Data are presented in Table 16.

Table 16 -- Flow Distribution-Chamber, S/N 001
(Down Tubes Only)

Tube No.	% of Nominal Flow
2	93.6
4	94.0
6	94.9
8	98.2
10	101.5
118	91.4
120	94.7
122	94.0
124	97.4
126	99.5

5.1, Laboratory Tests (cont.)

The spread in the flow data varied from 91.4% of nominal (Tube No. 118) to 104.0% of nominal (Tube No. 74). The flow variation observed in this test is within acceptable limits for a down tube when fired with an injector using 10.4%, or more, chamber film cooling.

The last water flow test utilized the torus assembly from combustion chamber S/N 013. The purpose of this test was to compare the flow distribution of a production torus (S/N 013) versus a development torus (S/N 003). Data from this test disclosed only minor variations in flow distribution between the two units.

A test was conducted with chamber S/N 007 to confirm the validity of the data obtained for the second-pass tubes. Twenty tubes in the chamber were instrumented with pressure taps at each end. The combustion chamber was mated to an injector and to the two fuel elbows that connect to the torus inlet flange. Static pressure readings were recorded at each of the pressure taps with the thrust chamber assembly operating at rated flow. A throat plug was also utilized to provide a 150-psig pressure in the combustion chamber while flowing at the water equivalent of the fuel flow rate.

The results of this water flow test were unsatisfactory. The flow variations observed in this test are much greater than obtained in previous flow tests and the proportional variations were not repeatable at other flow rates with the same test setup. Inspection of the pressure taps (by splitting the tube and visually observing) revealed large burrs and weld penetration on the inside of the tubes, which caused flow disturbances that affected the static pressure readings. Moreover, an accurate mean flow could not be determined since most instrumented tubes were in the proximity of the flow splitters.

These necessary corrections were made:

5.1, Laboratory Tests (cont.)

(a) The holes were deburred and inspected by engineering personnel prior to installing the pressure taps.

(b) The fittings were brazed to the tubes rather than welded to insure against weld drop-through.

(c) A larger number of tubes was instrumented.

(d) The pressure taps were located farther from the torus and the exit manifold ends of the tubes to reduce hydraulic entrance effects. Figure 40 illustrates the location of the tubes.

When the test was repeated, the flow rates in the individual tubes varied from -8.6 percent to +4 percent of nominal, confirming the results obtained from chambers S/N 001 and S/N 003.

The most reliable data obtained during the various tests conducted disclosed a flow variation from -8.6% to +4.0% of the nominal weight flow per tube. The R_{BO} of the tube with least flow (-8.6%) was determined to be 0.765 with the engine operating at the worst chamber thermal conditions: MR = 2.15, P_c = 796 psia, T_{ci} = 98°F, chamber film coolant - 10%. The actual R_{BO} is therefore within the design limit of 0.82.*

*Complete test data as well as a more detailed analysis are contained in AGC Memorandum 9642:0552.

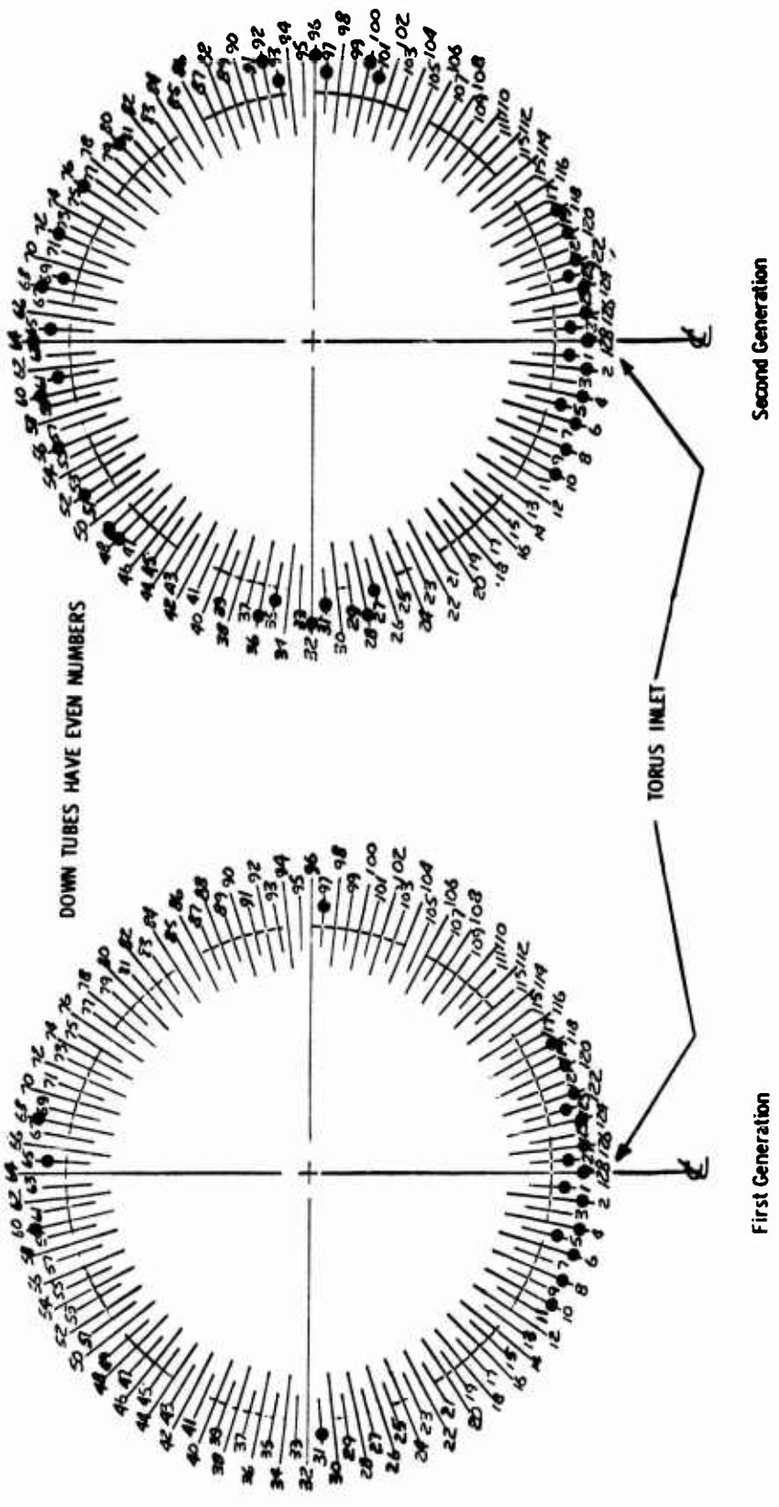

Figure 40. Pressure Tap Locations

5, Testing (cont.)

5.2 PRELIMINARY COMBUSTION CHAMBER TESTS

During the GEMSIP program Test Stand C-2 had been equipped with servo-operated flow control valves in order to obtain test data at programmed values of thrust and mixture ratio. Excellent results had been obtained with this system, which permitted acquiring data from as many as 10 test points during a single firing besides providing more uniform steady state plateau. This system, originally designed for Stage II, was modified for Stage I flow rates and improved by providing faster and more precisely operated control valves and a more versatile computer-generated program. An equivalent system was installed at Test Stand C-1. The thrust take-off and measuring system at Test Stand C-2 was also improved.

Figure 41 shows the diffuser employed at Test Stand C-2 for altitude simulation. Figure 42 is another view of the stand including the thrust take-out and metering system. Figure 43 shows the flow control system at Test Stand C-1 with the similar system on Test Stand C-2 shown in Figure 44. With this system the interacting effects of flow rate, mixture ratio, thrust, and heat transfer could be evaluated over the full range of interest during a single test.

Testing was initiated in May 1966, utilizing chamber S/N 001. The chamber was delivered to the test area without a shell in order to expedite testing because it was not scheduled to be tested in conjunction with a skirt. A prefire photograph of the TCA used in Test No. 001 is shown in Figure 45. The duration of the first test was approximately 31 sec with all parameters recording approximately the predicted values. Posttest hardware inspection indicated no heat marked tubes, no epon cracking, nor any other abnormalities.

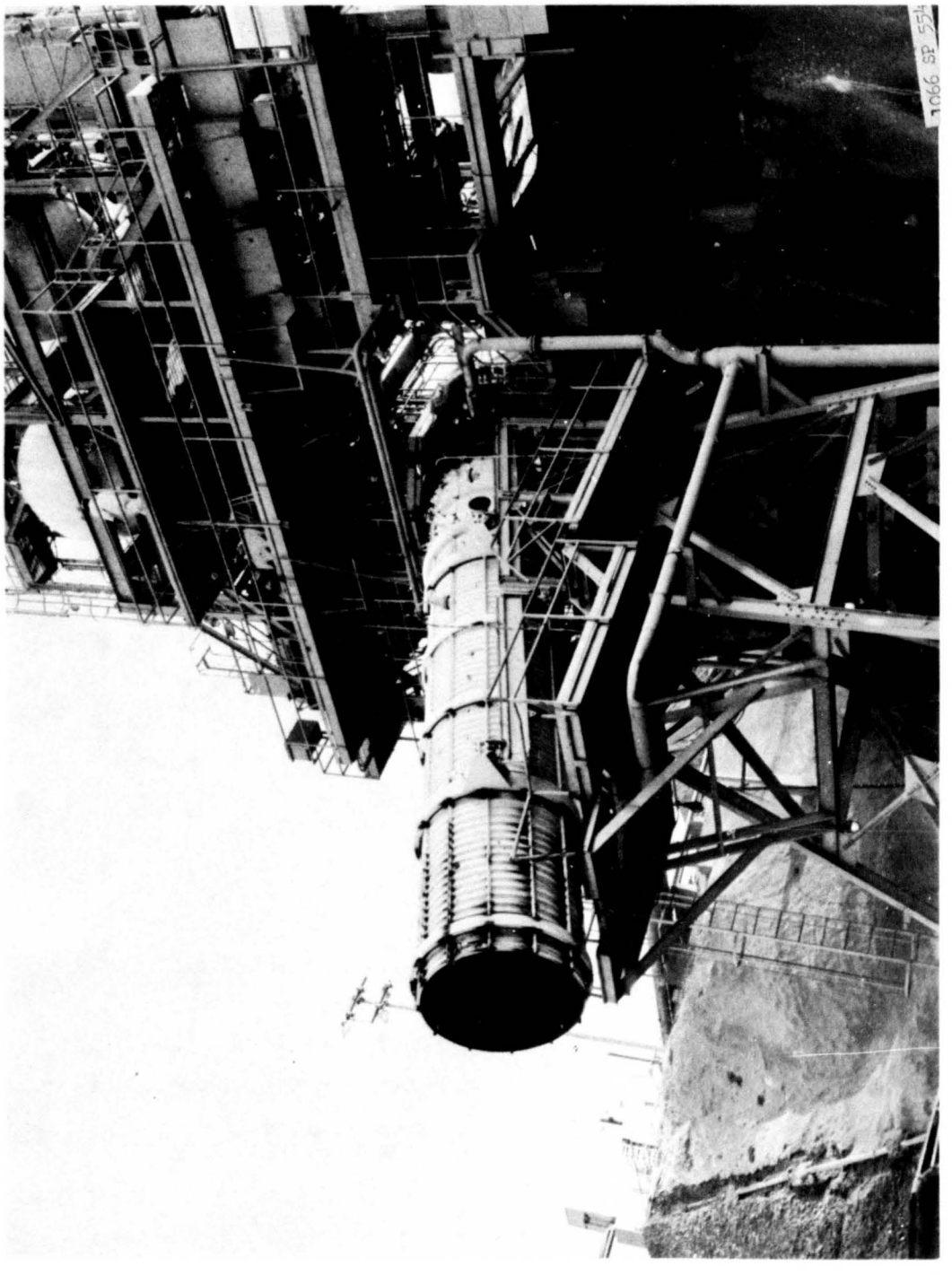

Figure 41 -- Altitude Simulation -- Test Stand C-2

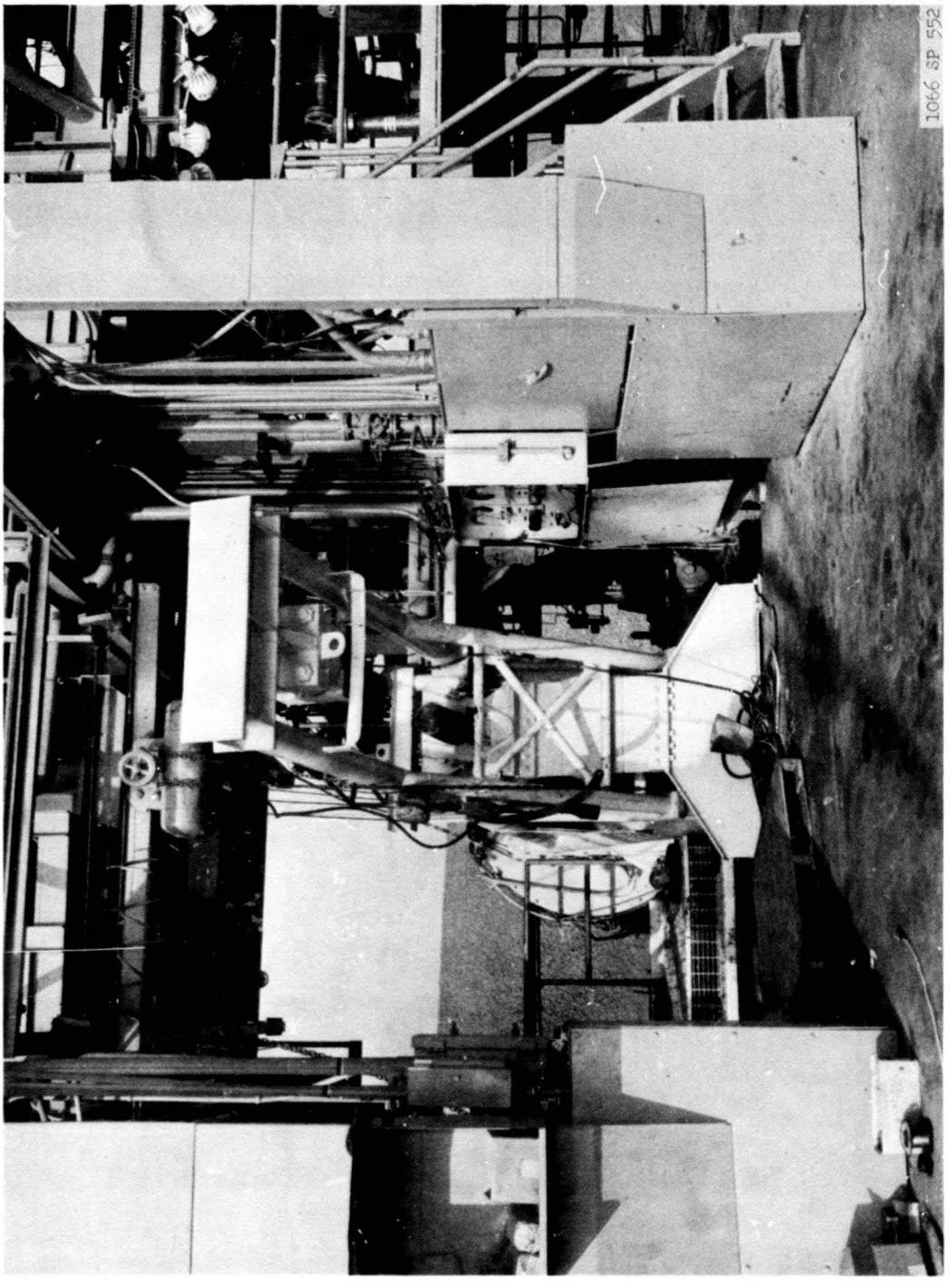

Figure 42 -- Thrust Measurement System -- Test Stand C-2

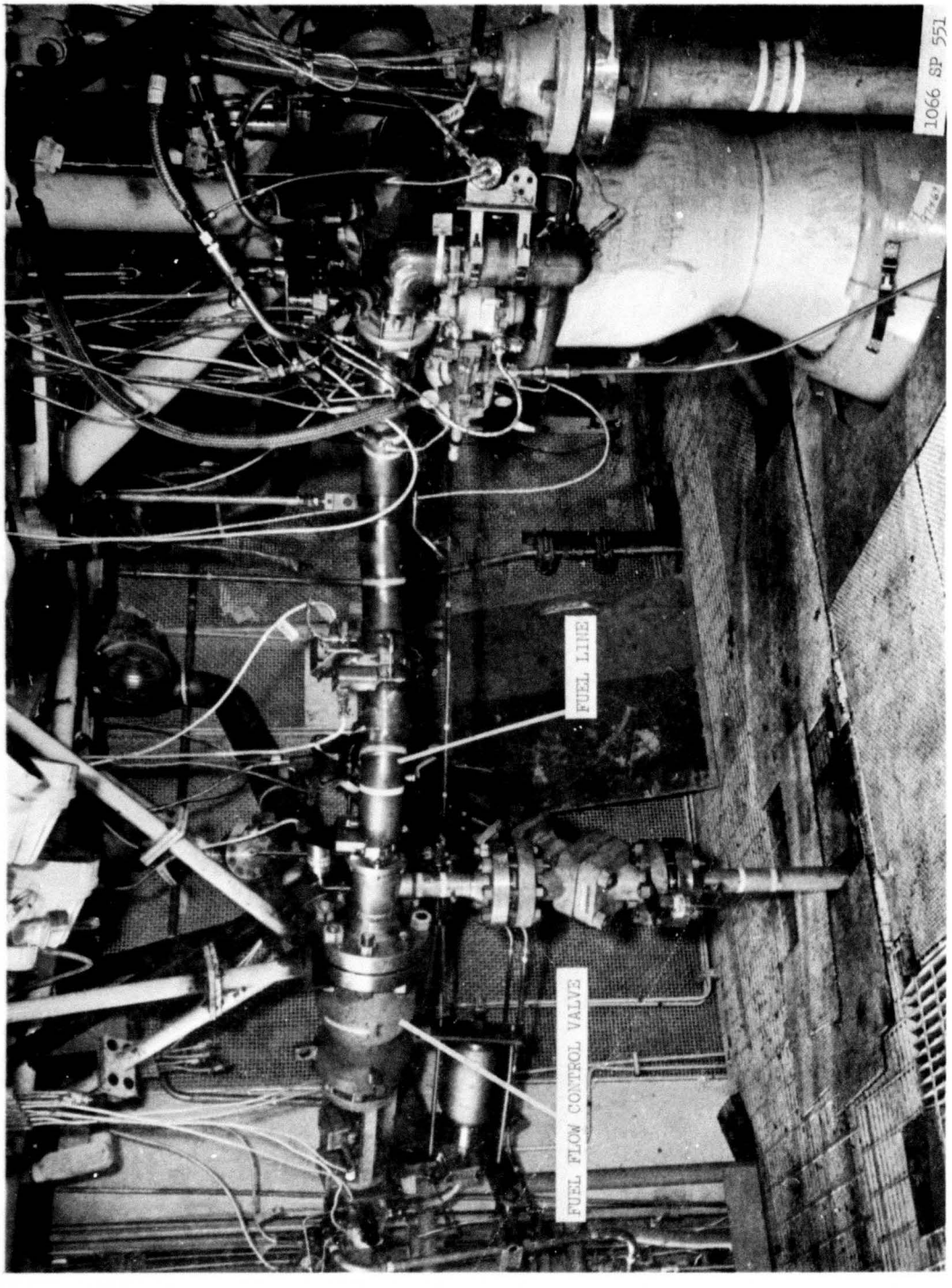

Figure 43 (1 of 2) -- Flow Control System -- Test Stand C-1 (Fuel Side)

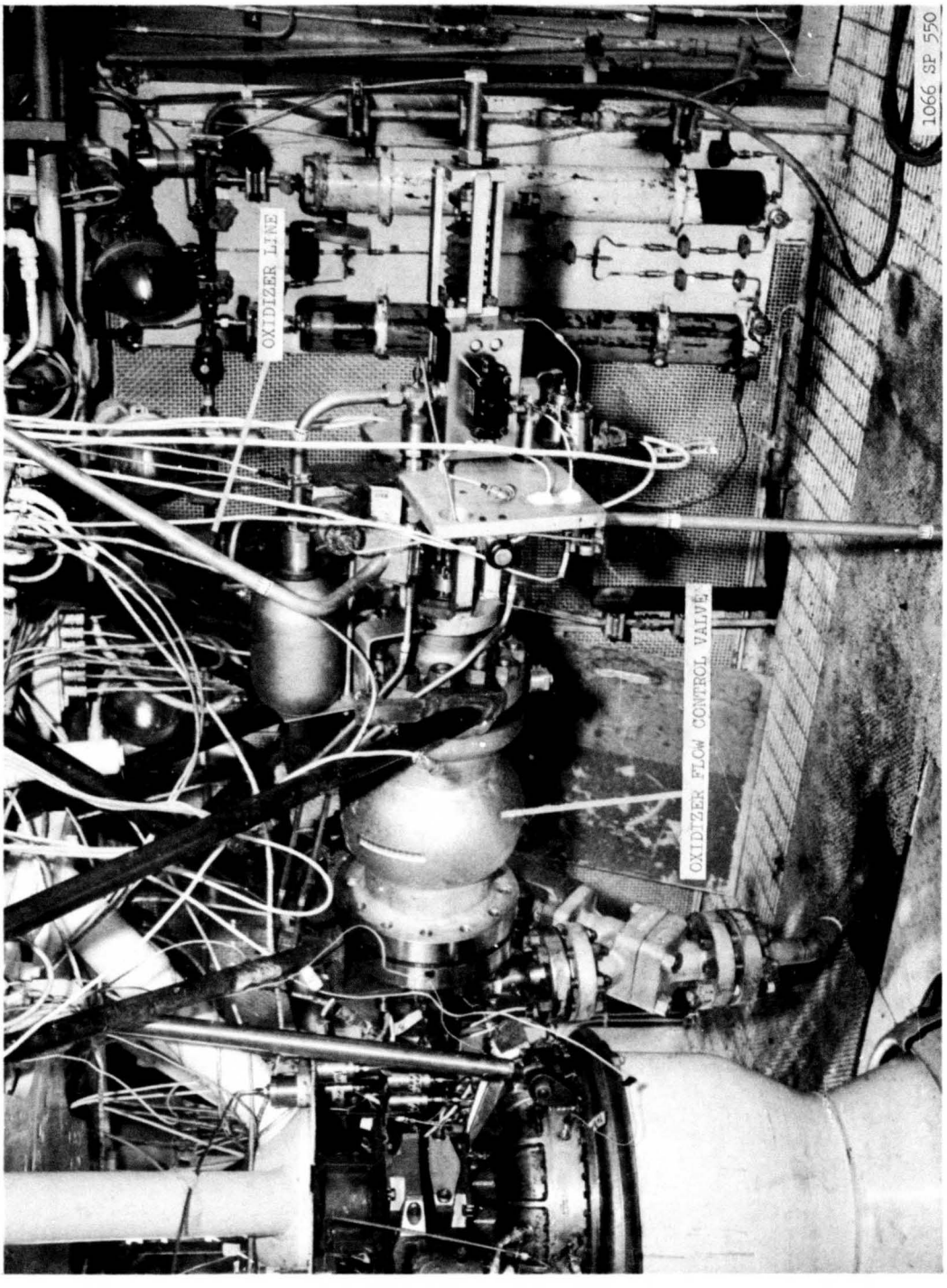

Figure 43 (2 of 2) -- Flow Control System -- Test Stand C-1 (Oxidizer Side)

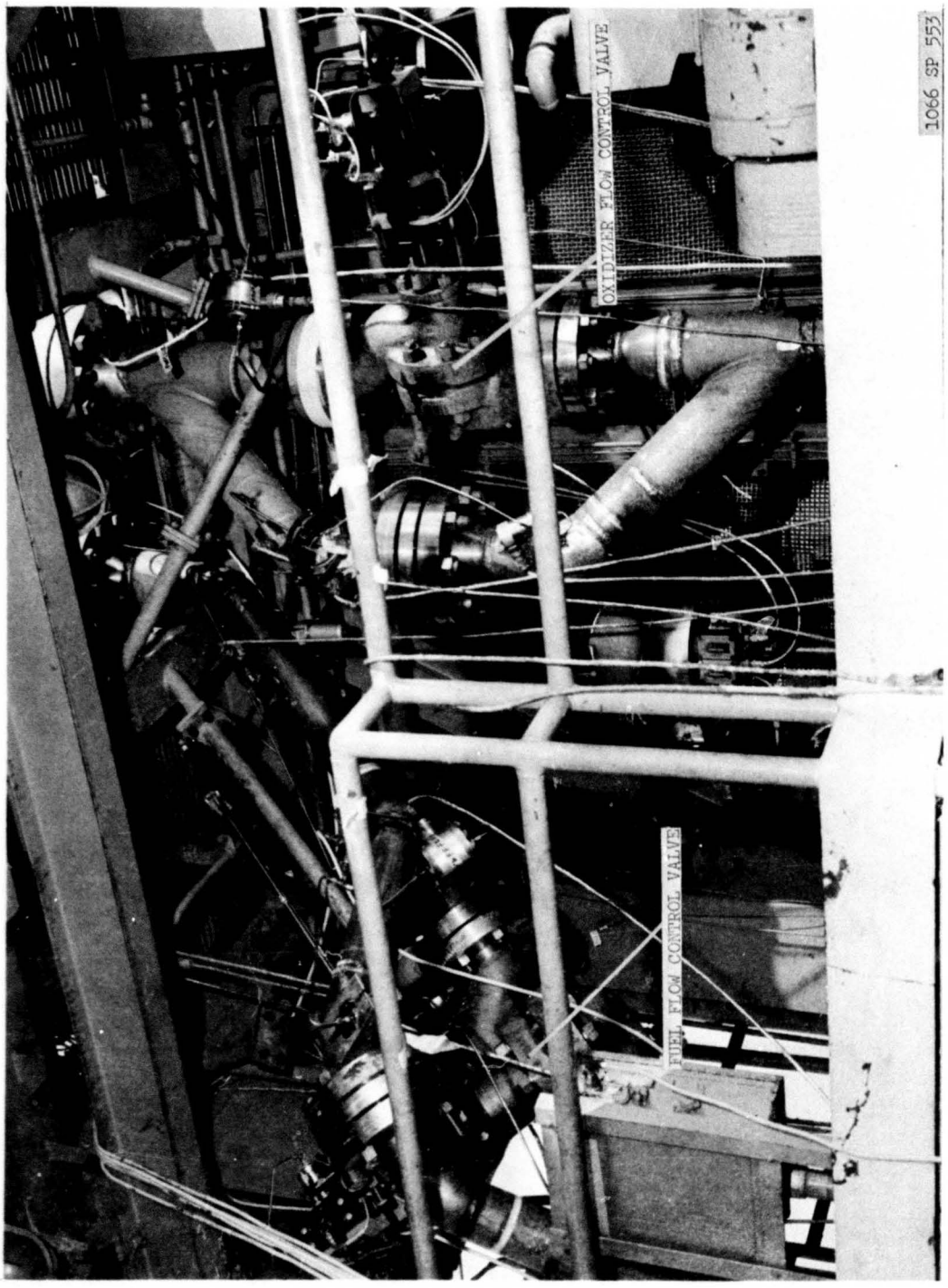

Figure 44 -- Flow Control Valves -- Test Stand C-2

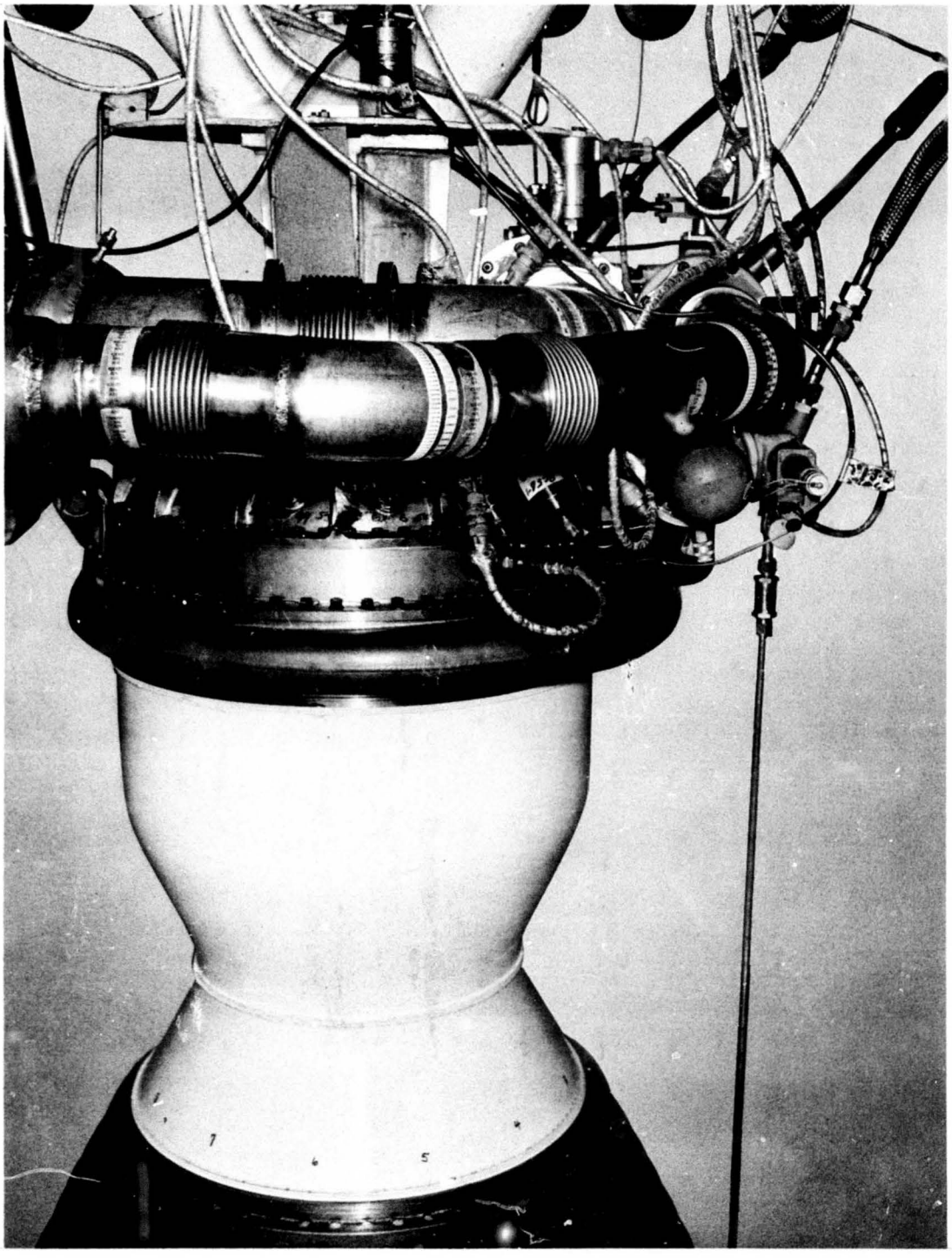

Figure 45 -- Chamber S/N 001 Prior to Test

5.2, Preliminary Combustion Chamber Tests (cont.)

The second test was conducted for 60 sec at the most severe specification requirements. All parameters were similar to Test No. -001. The posttest inspection of chamber S/N 001 revealed that the wire wrap was dislodged from about 3 in. below the torus to approximately 1 in. above the throat. The tubes in the unwrapped area were bulged approximately 0.75 in. on the diameter. The bulging was most prominent midway down the convergent section.

Investigation of the failure led to the conclusion that epon covering did not adequately surround and bond to the wrapping wire. The shutdown, while rough, was no more severe than suffered by other Titan chambers where the wire wrap installation was adequate and the manufacturing process specification had been complied with.

Stress analysis indicated that the chamber tubes yield when the wrapping tension exceeds 60 lbs. When the tension is relieved, loss of friction causes the wrapping to fall toward the chamber throat. The epoxy (Epon 901) prevents this. It was concluded that the rough shutdown combined with the incorrect application of epoxy caused the wire wrap of chamber S/N 001 to fail.

Remedial action was taken for subsequent chambers to obtain the correct application of epoxy during wire wrapping operations in order to assure adequate covering of the wire. In addition, the process specification was examined and revised to provide a more adequate description of the method of application and improved inspection procedures.

A subsequent test was conducted with chamber S/N 001 (after ironing out the bluge) in conjunction with injector S/N 248, which had a Titan III production (2BIE-38) pattern modified for 10 percent chamber film cooling. The objectives were to check out Test Stand "C-2" which had the newly installed servo flow control system and to evaluate a 10% film cooling 2BIE injector in conjunction with an 87-11 chamber.

5.2, Preliminary Combustion Chamber Tests (cont.)

The test results showed that the 2BIE-38 injector was incompatible with the 87-11 chamber. The postfire inspection of the hardware revealed approximately 50 "up" tubes and 6 "down" tubes were failed (Figure 46) to the extent that chamber pressure and other parameters started dropping at FS_1 + 4.5 seconds.

Checkout of the flow control system was attempted during the next test during which both the injector and chamber were AJ-9 configuration. An improperly sized orifice made the servo system on the flow control valves inoperative. A summary of the data from both tests is presented in Table 17.

Table 17 -- Chamber Compatibility Test Summary

Run	Date	Dur.	C.C.	Inj.	$P_{c(g)}$	M.R.	T_p (°F)	Data Time	Tcc
101	7-19	10.380	001	248 (10% 2BIE)	855	2.17	75	3.0133	105
					853	2.19	75	4.0189	110
					855	2.10	75	5.0027	112
					847	1.95	75	6.0083	116
					829	181	75	7.0139	120
					761	1.68	75	8.0409	103
					728	1.65	75	9.0033	89
					724	1.64	75	10.0089	85
102	7-23	60.705	310 (Std 8:1)	1110 Std 2BIE)	802	2.06	78	20 30	126.9

A successful checkout of the flow control system was accomplished during Test No. 3051-D01-DX-001.

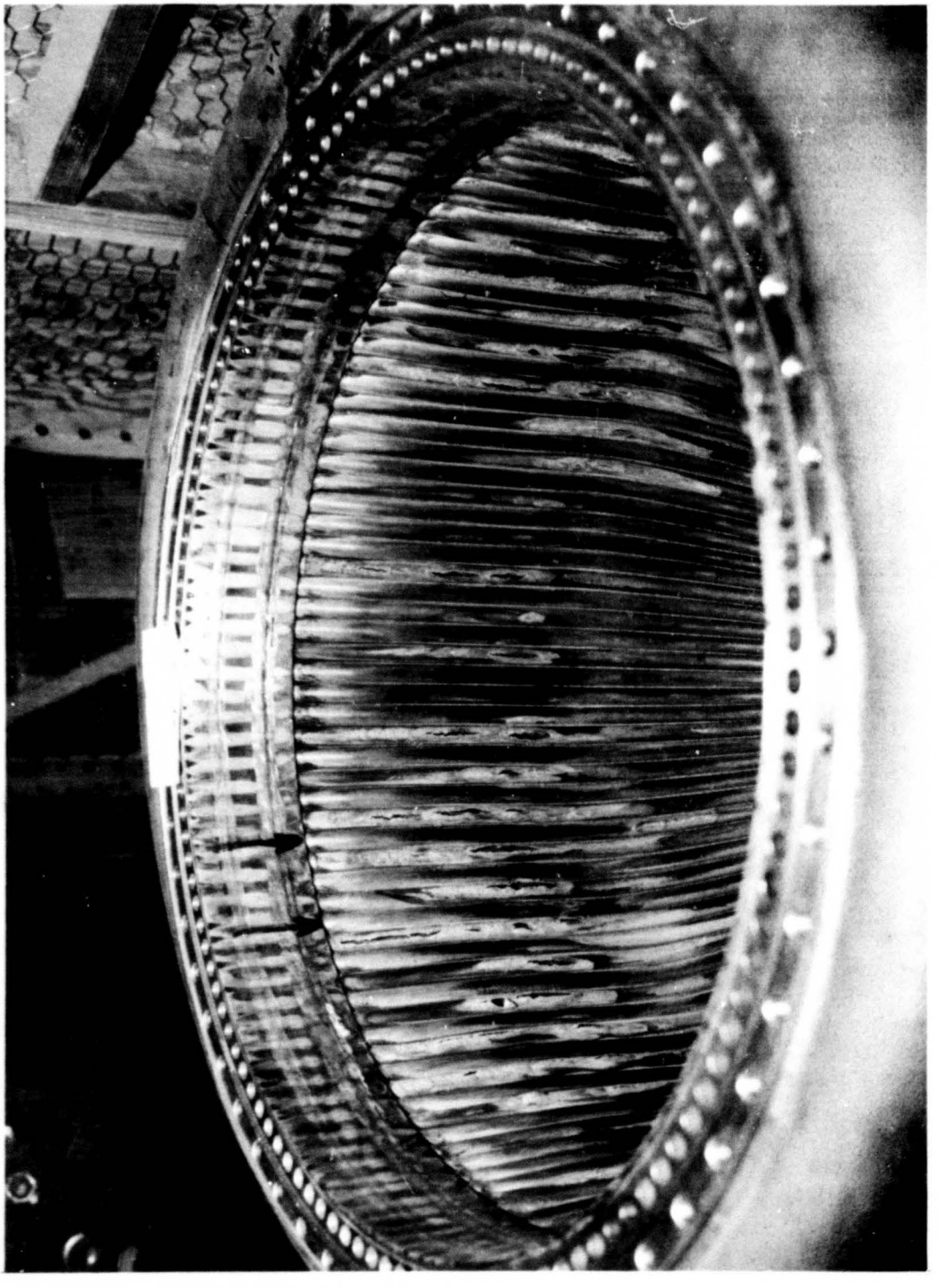

Figure 46 -- Chamber S/N 001 Posttest No. 3051-D01-1C-001

5, Testing (cont.)

5.3 TCA DEVELOPMENT TESTING

Two series of development tests were conducted during the period September 1966 through March 1967. Test Series 3051-D04-1J, conducted on Test Stand C-1, was intended primarily to obtain the baseline sea level performance of the AJ-11 injector and secondarily its compatibility with the redesigned combustion chamber both at nominal operating conditions and at extremes of mixture ratio and chamber pressure. Test series 3051-D01-1M was conducted on Test Stand C-2 at simulated altitude conditions, using a diffuser to create a partial vacuum. An ablative skirt was installed on the chamber for five tests to obtain altitude performance data. Tests on both stands were conducted with servo flow control systems.

Four combustion chambers were employed for the development tests -- Serial numbers 002, 004, 005 and 013, the latter having six Hastelloy cooling tubes. The areas of primary concern were:

a. Structural integrity, particularly in the strength of the flanges, the ability of the reinforcing shell to support the throat, and the adequacy of the braze to prevent leaks in the hydraulic circuit and to contain the chamber gases.

b. Cooling capacity as demonstrated by maintaining the burnout heat flux ratio below 0.82 under extremes of operating conditions.

c. Compatibility with the AJ-11 injector and the 15:1 ablative skirt.

By testing with four chambers built to the same design the effect of manufacturing tolerances would also be evaluated.

5.3, TCA Development Testing (cont.)

The four chambers were tested 33 times for a total duration of 1641 seconds. All four chambers were in good condition. The only unusual circumstances during the testing are noted below:

Test Series 3051-D04-1J, Test Stand C-1

Test No. 010

Slight roughness was noted on some tubes near the throat.

Test No. 015

There was slight additional roughness.

Test No. 014

The chamber was tested in conjunction with an injector supplying only 10 percent film cooling. There was no damage to the chamber. However, the test duration was only 6 seconds because of an invalid shutdown caused by the test stand controls.

Test No. 015

Approximately a dozen tubes were noted as discolored after this test (60 seconds duration). The discolored tubes were all in the vicinity of the baffles. The heat rejection rate was approximately 12 percent higher than with the previous injector used; both had the same matrix pattern, but the film cooling was less on this test.

5.3, TCA Development Testing (cont.)

Test No. 021

Postfire inspection revealed a spot of erosion on the mounting flange. The erosion was below baffle No. 2 and was 1/4 inch long by 1/8 inch wide and was approximately 0.80 inch deep.

Test No. 025

This test was conducted with propellants conditioned to 90°F. There was no hardware damage.

Test No. 026

A slight roughness on the mounting flange was noted after this test.

Test Series 3051-D01-1M, Test Stand C-2

Test No. 007

The injector mounting flange suffered erosion below baffle Nos. 3, 5, and 7. Two coolant tubes were discovered leaking beneath a V-band. Weld repair was made and there was not recurrence of leakage.

Test No. 008

The chamber film cooling supplied by the injector was reduced to 10 percent; nevertheless there was no damage to the chamber.

5.4 ENGINE DEVELOPMENT TESTS

The redesigned 6:1 area ratio combustion chamber was further evaluated during four series of engine development tests, in accordance with SSD-CR-65-8180-140, System Test Development Plan. The principal test objectives were:

(a) To evaluate the performance and mutual compatibility of the redesigned engine components, including the combustion chamber.

(b) To provide engine system data for use by other contractors, for generating specifications and other systems data, and for preparing operating procedures and the design of ground equipment.

(c) To provide feedback to component design.

5.4.1 Sea Level Systems Tests (Series A)

A series of 28 sea level tests were conducted utilizing Subassembly 2 of engine S/N RD-12. Tests were conducted at both nominal and extreme operating conditions. For the combustion chamber the principal objectives were to evaluate performance and compatibility with the engine system. Additionally, data were obtained on engine side loads, heat transfer, and performance of the chamber-ablative skirt combination. Detailed data for each test are tabulated in Table 12, Section 4.2. The first seven tests were conducted with AJ-9 injectors.

Test No. 3051-D01-001

Combustion chamber S/N 002 was instrumented with strain gages for determining transverse starting loads and bending stresses on the chamber. After assembly of the TCA, it was noted that the outer Raco seal protruded into the injector-to-chamber bolt holes. The bolt holes were filled with TRV-731 to provide backing to the seal. The postfire inspection indicated that the chamber was in excellent condition with no heat marked tubes, erosion or epon cracking.

5.4, Engine Development Tests (cont.)

Test No. 3051-D01-1A-002

Test hardware included an ablative skirt. The rupture of a fuel line caused a stand fire and the test was shut down after 15.45 seconds. There were no changes noted from the last postfire inspection of the chamber. Heat transfer and strain patch data were obtained.

Test No. 3051-D01-1A-003

This was a full duration test at nominal operating conditions utilizing the same hardware as used on test -002. The chamber tubes were in very good condition as were the "V" bands. A crack approximately 0.050-in. wide and 6-in. long in the chamber epoxy over the wire wrap below the throat was noted during the postfire inspection. This exceeded the production specification but further testing was authorized.

Test No. 3051-D01-1A-004

This was a 30-second balance test at nominal operating conditions. Chamber S/N 002 was again utilized on conjunction with injector S/N 249, which was approximately 12% fuel film cooling. The chamber was completely unmarked with the exception of the mounting flange which had minor erosion (1/4 in. x 1 in.) (Figure 47). The wire wrap crack did not propagate during this test.

Test No. 3051-D01-1A-005

Test -005 was conducted utilizing injector S/N 249 (AJ-9 with 16 percent film cooling) and an ablative skirt at the most adverse heat transfer conditions for the skirt. Posttest inspection of chamber S/N 002 after engine Test No. 3051-D01-1A-005 revealed that one chamber tube was heat marked in the divergent section from approximately 18 inches below the throat to the aft end of the tube. Figures 48 and 49 show the location relative to the chamber. Penetrating erosion had occurred in two places (Figure 7, supra). All other chamber tubes were in satisfactory condition.

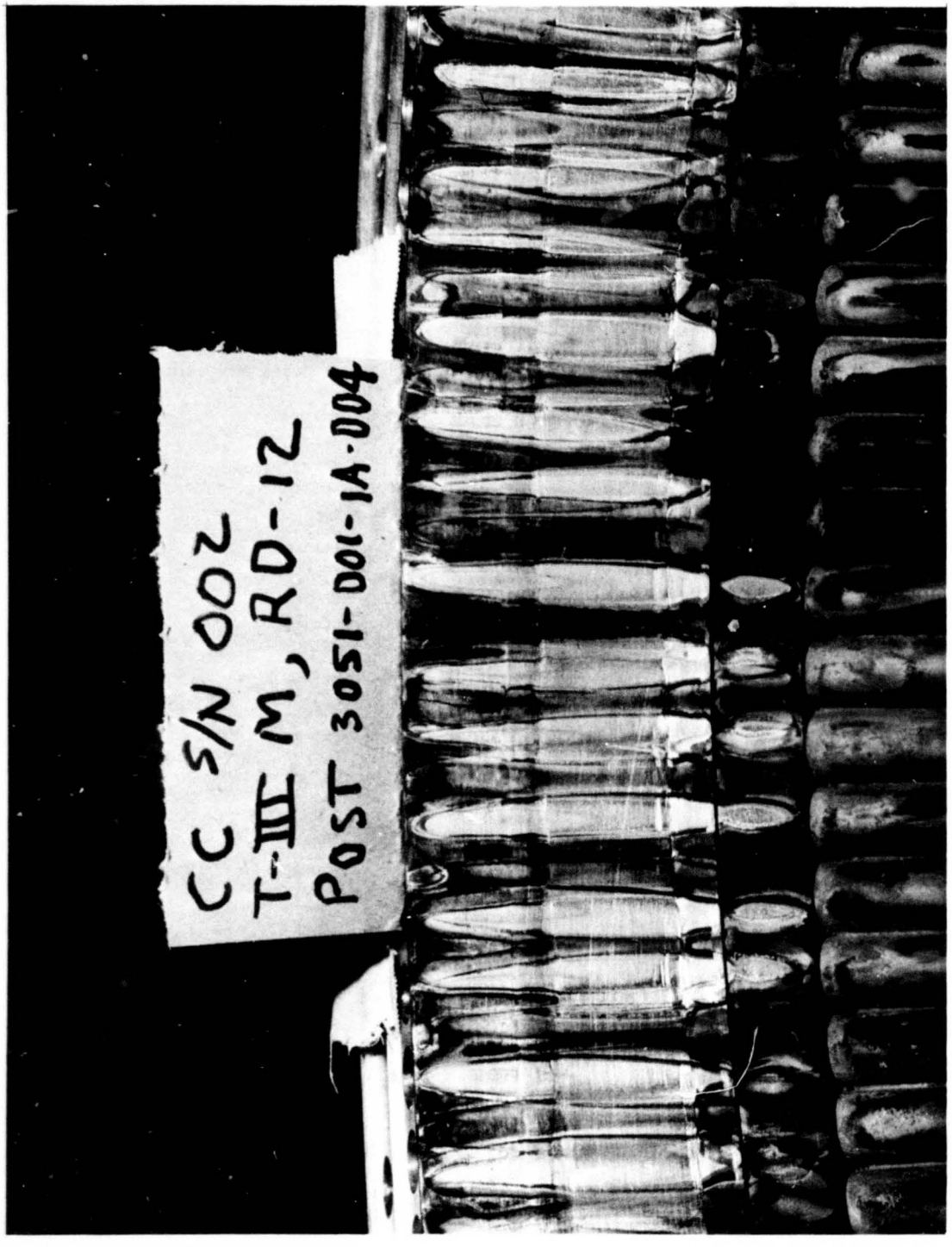

Figure 47 -- Chamber S/N 002, Showing Minor Erosion to Flange

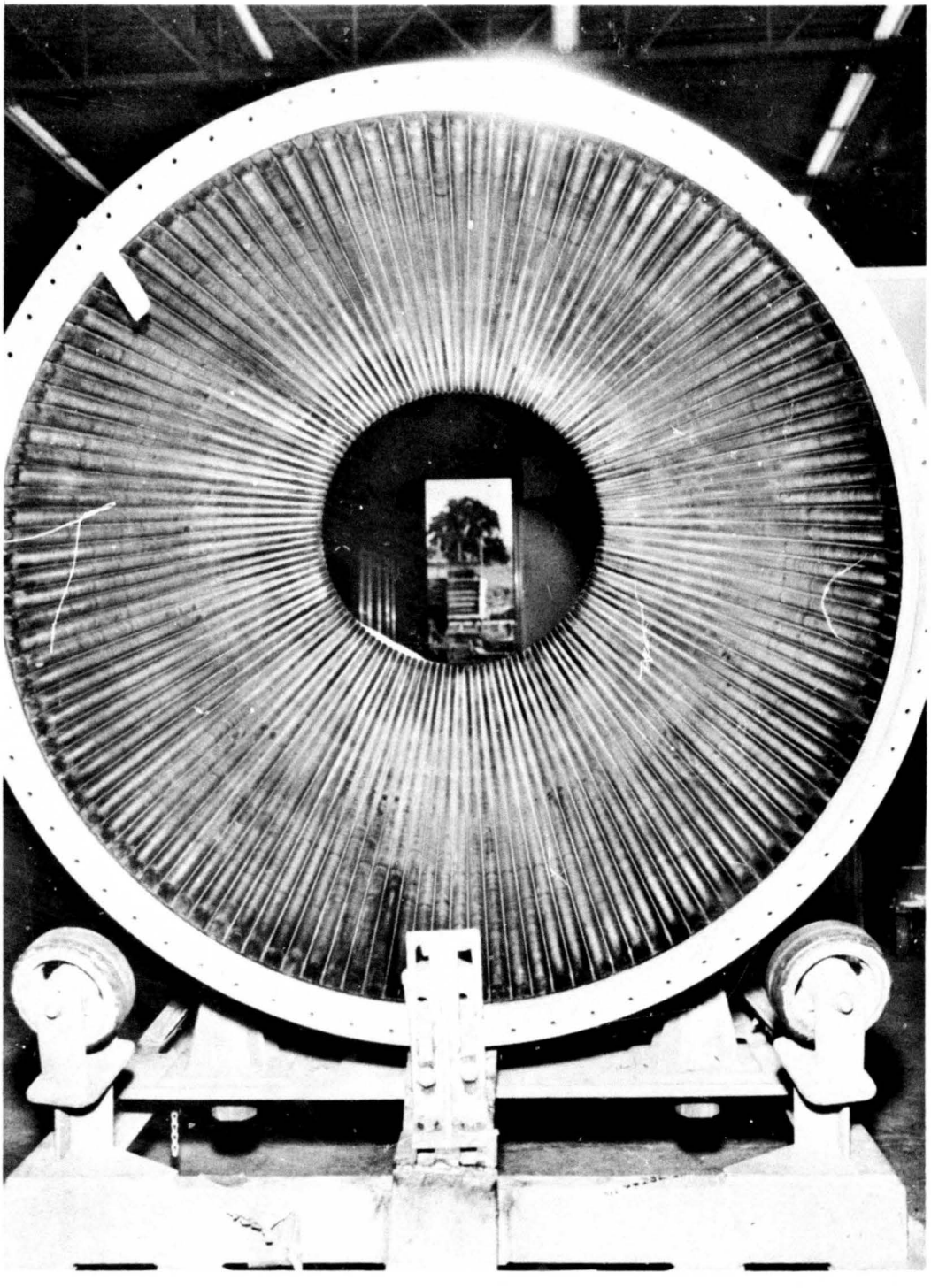

Figure 48 -- Combustion Chamber after Test No. 3051-D01-1A-005

Figure 49 -- Chamber Flange Showing Heat-Marked Tube

5.4, Engine Development Tests (cont.)

Test No. 3051-D01-1A-006

Test -006 was conducted with chamber S/N 003 and injector S/N 214 (Standard 2BIE-38) at the worst heat transfer conditions for the chamber, which are:

Planned Test Conditions		Actual Test Conditions
$MR_{(TCA)}$	= 2.13	2.13
P_c	= 794	787
$T_{P(TCA)}$	= 107°F	112°F

The posttest inspection revealed that the hardware was in excellent condition.

Test No. 3051-D01-1A-007

Test No. -007 was conducted utilizing chamber S/N 002 and injector S/N 214 (2BIE-38) and scheduled for the worst flight conditions for chamber heat transfer. Prior to retesting the split tube was repaired by cutting out a section and replacing it with an undamaged portion of a new tube. Inspection after Test No. -007 indicated no heat transfer problem.

Test No. 3051-D01-1A-008

Test -008 was conducted with chamber S/N 003 and injector S/N 657 (300 lb/element). This test was scheduled for the nominal Titan IIIM conditions. The posttest inspection revealed several failed tack welds on the chamber shell and "V" bands. (Figure 50). Review of the records indicated chamber pressure oscillations commenced at FS_1 + 1.3 seconds during the secondary Pc rise and continued during the entire run.

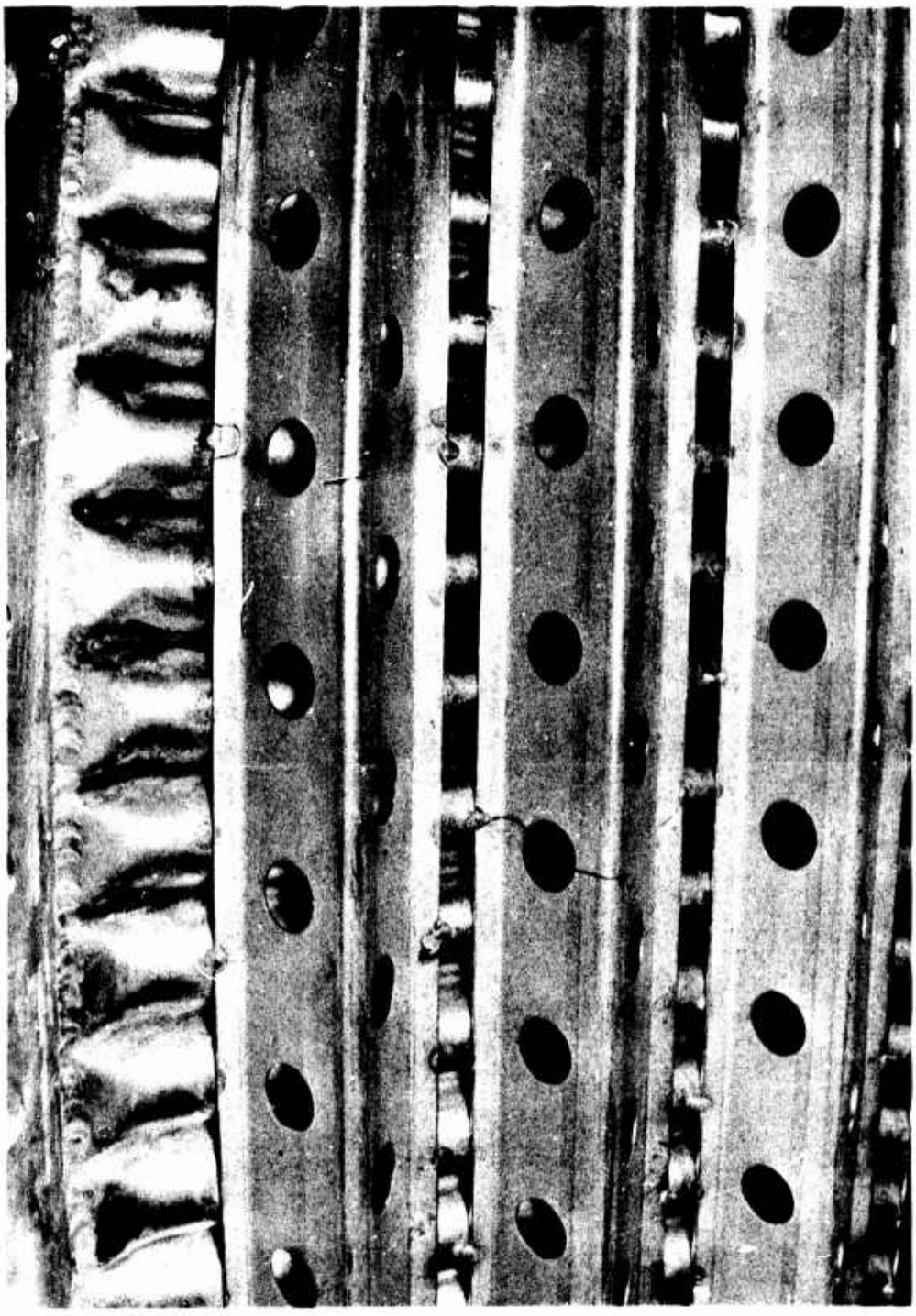

Figure 50 -- V-Band Tack Weld Failure -- Chamber S/N 003

5.4, Engine Development Tests (cont.)

Test No. 3051-D01-1A-009

This test was conducted with injector, S/N 651, which had a 12% chamber film cooling pattern; it had not been tested subsequent to its conversion to the latest injector pattern (P/N 1130465). The combustion chamber, S/N 004, had no previous testing. The test was terminated at FS_1 + 63.169 seconds because of a leak in the chamber inlet torus. Postfire inspection, Figure 51, of the combustion chamber revealed a 4-in. long crack in the weld joint between the torus and the injector mounting flange. No additional damage was sustained by the combustion chamber.

Test No. 3051-D01-1A-010

This test was conducted with injector S/N 251, chamber S/N 005, and an ablative skirt. The injector had not been tested since being upgraded to the latest injector pattern (P/N 1129527). The chamber had no prior testing and had been instrumented with braze patches (Figure 28 supra). The braze patches on the chamber indicated approximately the same temperatures as recorded on Test No. 006 with chamber S/N 003. The maximum temperature measured at the throat in Test No. 010 was between 1570-1670°F. No appreciable difference was noted between baffled and unbaffled locations. Postfire inspection revealed a spot of erosion of the injector mounting flange of the chamber below baffle No. 3, shown earlier in Figure 13. It was decided to repeat the test without repair.

Test No. 3051-D01-1A-011

The injector was a 7-pie, 450 lb/element quadlet with 12% film coolant. The same chamber and skirt were again utilized as in Test No. -010. Postfire inspection revealed no new chamber damage. The TCA was left assembled for the next engine subassembly test. Studies of the braze patch data indicated no noticeable increase in wall temperature from the previous test.

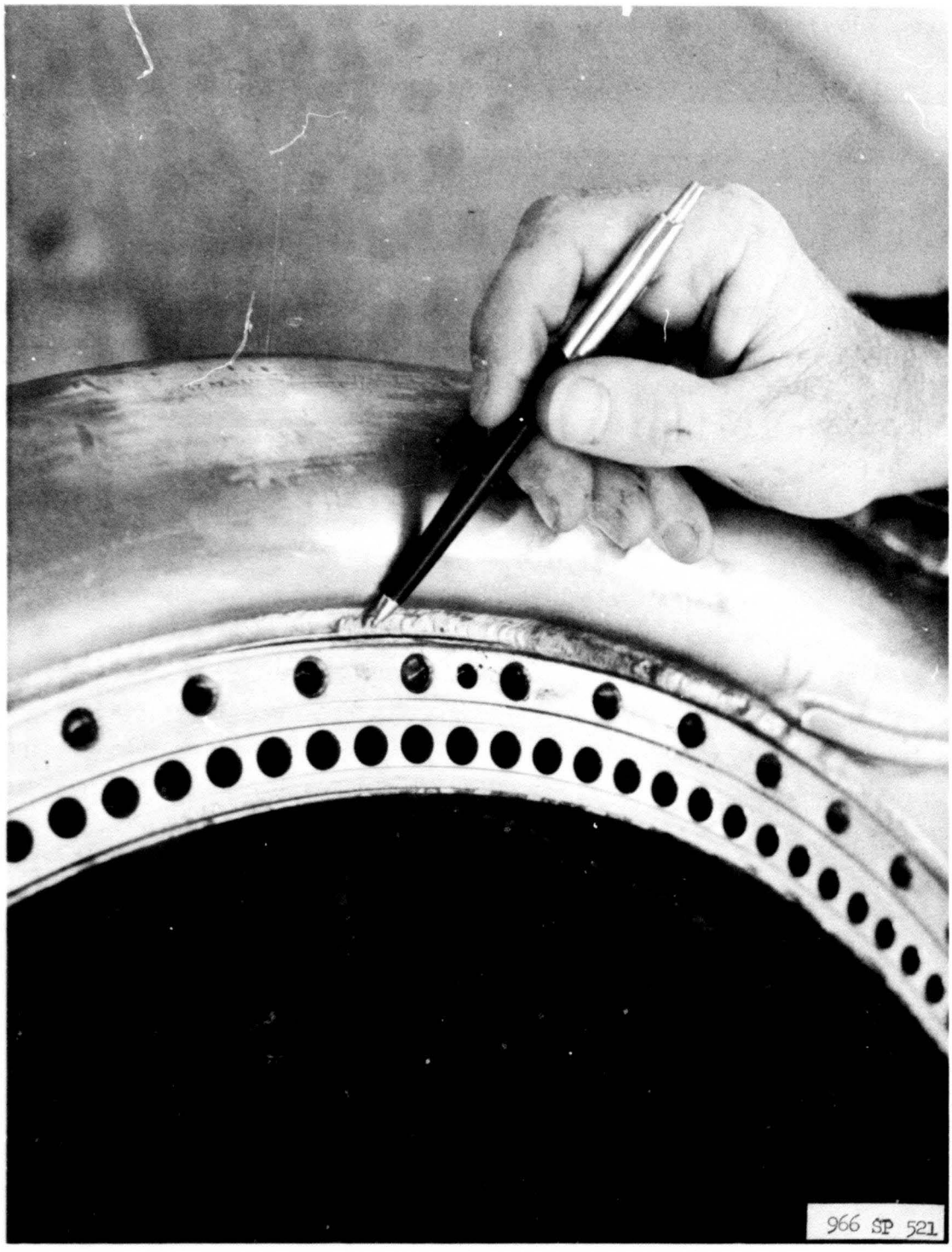

Figure 51 -- Combustion Chamber S/N 004, Showing Torus Crack

5.4, Engine Development Tests (cont.)

Test No. 3051-D01-1A-012

The engine subassembly was programmed to operate at the "worst flight" conditions for the skirt. The test was terminated at FS_1 + 186.6 seconds because of an indication of a discrepancy in the operation of the turbopump system. Postfire inspection of the chamber revealed another spot of erosion on the injector mounting flange similar to that incurred in Test No. -010. The new erosion spot on the chamber coincided with a minor spot of erosion on the injector in the 17th channel ring. This new erosion was located in a similar position relative to baffle location as the old erosion. The chamber injector mounting flange was rough in an area near baffle No. 3 indicating a possible consistency in the occurrence of the erosion.

Test No. 3051-D01-1A-013

The primary objective of the test was to continue the investigation of the 1000 cps combustion oscillations and to evaluate the chamber "worst flight" conditions. The injector had 12.6 percent film cooling. Chamber S/N 005 had been fired three times previously to this test.

Pressure oscillations were recorded similar to those recorded on Test No. -012. There was no hardware damage.

Test No. 3051-D01-1A-014

The primary objective was to continue the system dynamics investigation and component evaluation. The injector configuration consisted of 400-lb-thrust quadlet elements with 12.6% chamber fuel film cooling. The test was terminated after 73.8 seconds by the combustion stability monitor. No additional injector or chamber damage was noted.

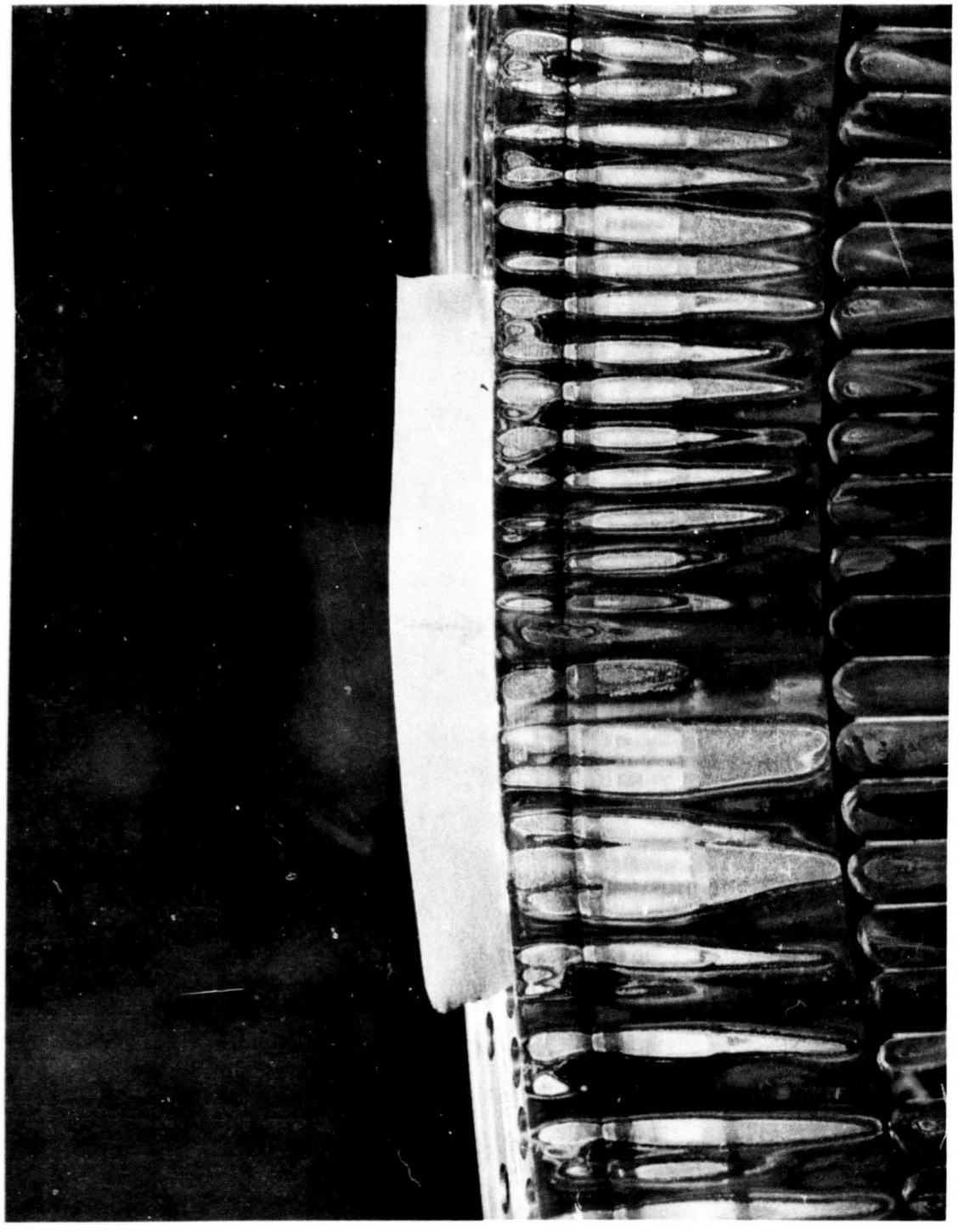

Figure 52 -- Combustion Chamber S/N 007 -- Mounting Flange Erosion

5.4, Engine Development Tests (cont.)

Test No. 3051-D01-1A-015

The objective of the test was to evaluate the seven acoustic dams in the 17th fuel channel of the injector. The injector had a 300-lb thrust-per-element quadlet pattern with 12.6% chamber fuel film cooling. The test was terminated by the combustion stability monitor after 5.4 seconds operation. There was no damage.

Test No. 3051-D01-1A-016

The injector configuration was the same as used previously during the Test No. -013. This was the first test with chamber S/N 007. Due to low gas generator c* operation the engine system did not operate properly and was shutdown after approximately 37 seconds firing.

Test No. 3051-D01-1A-017

The objectives of this test were further stability analysis and skirt durability evaluation. The test was conducted for the full duration. There was slight erosion of the mounting flange as shown in Figure 52.

Test No. 3051-D01-1A-018

Chamber S/N 004 had an acoustic dam in the torus (Figure 53) in an effort to reduce the magnitude of the feed system pressure amplitudes. The test was terminated after approximately 5 sec by the combustion stability monitor.

Test No. 3051-D01-1A-019

The primary objectives of the test were to continue the system dynamics investigation and component evaluation at the "worst flight, skirt" conditions. The injector had a 450-lb thrust/element quadlet pattern with

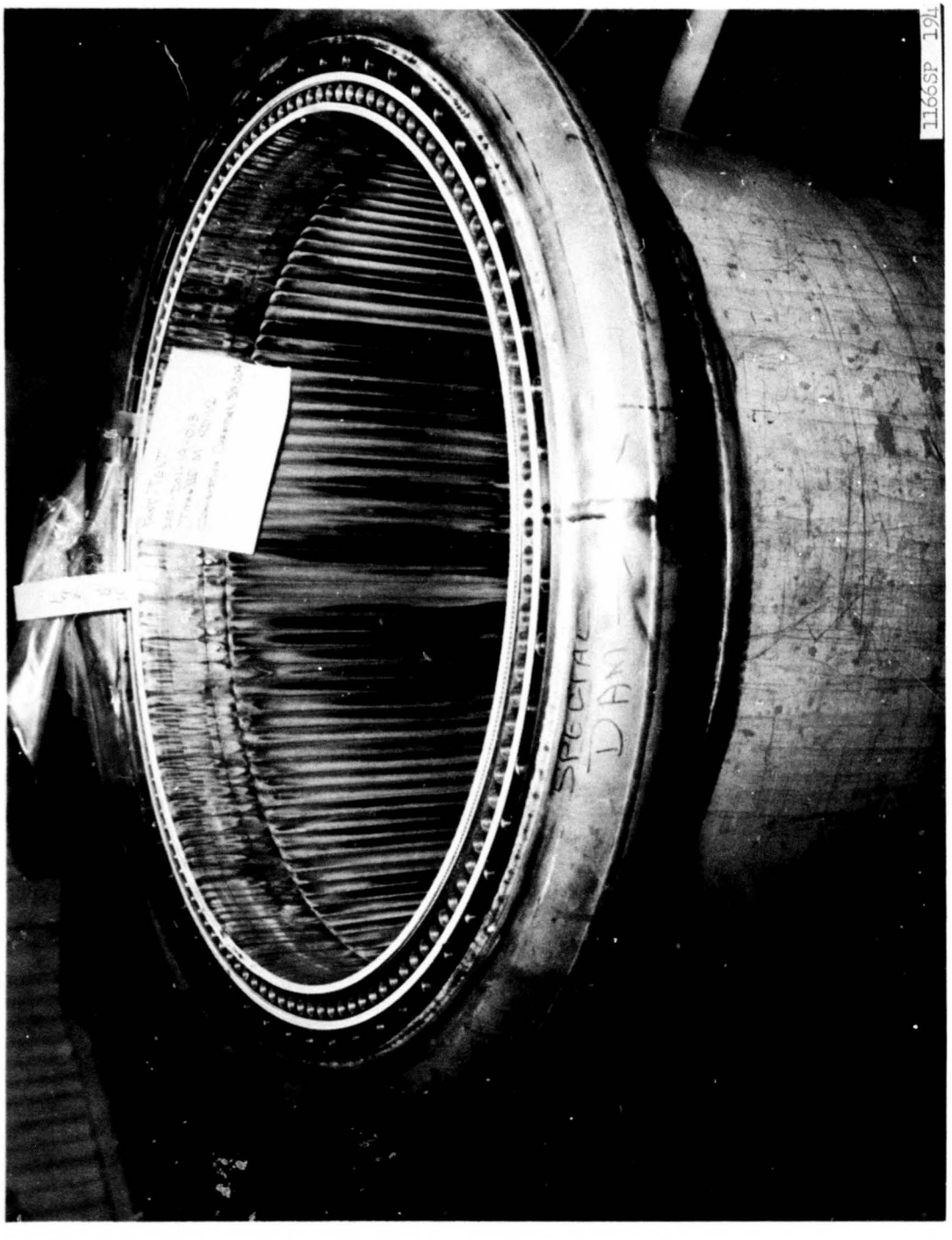

Figure 53 -- Acoustic Dam in Chamber Torus

5.4, Engine Development Tests (cont.)

12.6 percent film cooling. Combustion chamber S/N 007 had been fired twice previously to this test. Further erosion to the mounting flange on the chamber was noted after this test.

Test No. 3051-D01-1A-020

Strain gages were mounted on the chamber prior to this test to obtain data on chamber flexure during start and shutdown. The primary objectives of the tests were to continue the system dynamics investigation. No injector or chamber damage was noted after this test.

Test No. 3051-D01-1A-021

This test was conducted with chamber S/N 006. The injector had a 450-lb thrust/element quadlet pattern with 9.4 percent chamber fuel film cooling. This was the first test on the injector and the chamber. The chamber was instrumented with strain gages and braze patches. No injector, chamber or skirt damage was noted after this 200.8-second test.

Test No. 3051-D01-1A-022

This test was conducted with chamber S/N 008. The injector had a 400-lb thrust-per-element quadlet pattern with 12.6 percent chamber film cooling. The test was terminated at FS_1 + 5.2 sec by the CSM without any hardware damage.

Test No. 3051-D01-1A-023

The primary objective of the test was to continue the system dynamics investigation. The combustion chamber was S/N 008. The injector had 10.3% chamber fuel film cooling. TCA hardware damage was very minor and confined to the injector.

5.4, Engine Development Testing (cont.)

Test No. 3051-D01-1A-024

The primary objective of the test was to continue the system dynamics investigation. The injector had 10.3% chamber fuel film cooling. There was no damage.

Test No. 3051-D01-1A-025

The primary test objective was to continue the investigation of system dynamics. The injector had 12.6 percent film cooling. There was no hardware damage.

Test No. 3051-D01-1A-026

The combustion chamber was S/N 006. Failure of an engine line resulting in a fire caused secondary damage to the thrust chamber assembly. Erosion approximately 0.020 in. deep was noted on the chamber mounting flange below baffle No. 7. However, the chamber was suitable for further testing.

Test No. 3051-D01-1A-027

Chamber S/N 008 was used for this test. No erosion was noted but post fire checks revealed that a tack weld had pulled loose at the aft wire lock band attachment to the chamber tubes causing an external leak. A simple weld repair eliminated the leak. Internal leakage was also found at the joint of the cooling tubes to the forward flange. The investigation of this discrepancy is reported in Section 4.4.

Test No. 3051-D01-1A-028

This 60-second test completed the test series. There was no hardware damage.

5.4, Engine Development Testing (cont.)

5.4.2 Engine Baseline Tests, Test Series 3051-D02-1A.

A series of 10 tests was conducted to establish the operating baseline for the LR87-AJ-11 engine in accordance with SSD-CR-65-8180-140, System Test Implementation Plan. The series consisted of five tests with each of two sets of thrust chamber assembly components.

The combustion chambers tested were S/N 009 and S/N 012, which had not previously been fired. Tests were nominally of 200 seconds duration. Test conditions included propellants conditioned at the high and low specification limits with the engine balanced at the high and low margins of thrust and mixture ratio. Gimballing was performed during the tests conducted with ablative skirts.

Test No. 3051-D02-1A-101

This test was conducted at nominal operating conditions. There was no hardware damage.

Test No. 3051-D02-1A-102

This test was conducted at the extreme of flight operating conditions most adverse to the chamber with respect to heat transfer -- low thrust, high mixture ratio with propellants conditioned to 90°F. There was no erosion, discoloration of the tubes, leakage, or other damage to the chamber.

Test No. 3051-D02-1A-103

Test No. -103 was conducted at the most adverse flight conditions for the ablative skirt. Gimballing was conducted in each plane for a period in excess of 40 seconds. Postfire inspection showed no damage to the chamber or other abnormal effects.

5.4, Engine Development Testing (cont.)

Test No. 3051-D02-1A-104

This test was conducted at the high thrust, low mixture ratio condition. An ablative skirt was installed and gimballing was conducted for 40 seconds. Postfire examination disclosed a hot gas leak between the chamber tubes and beneath the wire wrap amounting to 20 cc per minute. It was judged that this leakage was too small to warrant interrupting testing for repair.

Test No. 3051-D02-1A-105

The last test with combustion chamber S/N 009 was at nominal engine inlet conditions. There was no increase in the chamber leakage that was reported after Test No. -104 and no other damage to the chamber.

Test Nos. 3051-D02-1A-106 through -110

The same series of tests was conducted using combustion chamber S/N 012. Following Test No. -106 a 0.040-inch diameter hole was found piercing the mounting flange into the inner seal groove. The hole occurred approximately 1/4 inch from the edge of baffle No. 2. The cause of the hole is undetermined. The area was repaired with weld metal.

Two areas on the mounting flange showed slight indications of erosion also after Test No. -106 -- one below the aforementioned hole and the other near baffle No. 7. These spots were only 0.010 inch to 0.015 inch deep and were not repaired. There was no extension of the erosion at baffle No. 7 on subsequent tests; the spot near baffle No. 2 increased to a depth of 0.040 inch which is not much after 1000 seconds firing duration.

Over the five tests the gap between the injector and chamber mating flanges increased to 0.040 inch. The investigation is reported in Section 4.1 and the corrective design action is discussed in Section 2.6.3.

There were no other abnormalities.

5.4, Engine Development Testing (cont.)

5.4.3 Engine Pulse Testing

A series of six engine pulse tests (Test Series 3051-D03-1A) was conducted utilizing the 6:1 area ratio combustion chamber and the AJ-11 baffled injector. The objective of these tests was to demonstrate the dynamic stability of the engine system. Nondirected pulse charges were detonated immediately after the ignition spike and during the transition to steady state.

No instabilities were in evidence during the testing. It was concluded that the natural damping inherent in the combustion chamber supplemented by the baffles in the injector was sufficient to assure stable operation despite external disturbances.

5.4.4 Engine Altitude Testing

A series of six tests (Test Series 3051-D05-1A) was conducted with an engine subassembly at altitude conditions. One of the test objectives was to measure the side loads occurring during the start transient; the other objectives did not relate to the combustion chamber. Chambers S/N 009, S/N 012 and S/N 015 were utilized for this test series.

The test series demonstrated that the side forces were less than the Titan IIIM specification values for which the combustion chamber was designed. There was no damage to the combustion chamber or other abnormalities.

5.5 TCA VERIFICATION TESTS

The design of the 6:1 area ratio combustion chamber was confirmed by a series of verification tests, Series 3051-D02-1M, which consisted of eight tests on each of three different thrust chamber assemblies to establish performance, compatibility, and hardware durability of the new design. Combustion chambers S/N 011, S/N 014, and S/N 015 were the three chambers employed for verification. Each of these units went through the complete test cycle.

5.5. TCA Verification Tests (cont.)

Chamber S/N 016 had been originally scheduled for verification testing, but it was destroyed on the first test by a test stand malfunction. As an additional test objective, chamber S/N 013 was tested once to determine the burnout margins of CRES and of Hastelloy-X tubes.

The eight-test cycles consisted of three sea level and three altitude tests with propellants conditioned at 35°F, 60°F, and 90°F during which chamber pressure and mixture ratio excursions of ± 7 percent and ± 3.6 percent were conducted. The sea level excursion tests were conducted at Test Position C-1 and the altitude excursion at Position C-2, utilizing a diffuser to stimulate vacuum conditions. In each cycle one sea level test was conducted at Position C-2 in order to relate the thrust calibrations of the two test positions and thus diminish instrumentation differences. The eighth test in each cycle was reserved for contingencies or for obtaining additional experimental data.

During the verification test series the 6:1 area ratio combustion chamber met all contract specification requirements. Most tests were routine. The following summaries include only abnormalities.

Test No. -001

A spot of erosion approximately 0.025 inch deep was noted on the mounting flange of chamber S/N 014 in the proximity of baffle No. 7. It did not increase during the remainder of the sea level tests.

Test No. -005

The tubes of combustion chamber S/N 016 were severely damaged by an out-of-specification mixture ratio excursion caused by the malfunction of a test stand propellant control valve. Chamber S/N 016 was removed from service and replaced with chamber S/N 011.

5.5, TCA Verification Tests (cont.)

Test No. -011

The inner Raco seal between chamber S/N 011 and the injector leaked, causing a loss in performance of 1.2 seconds. The steps taken to correct the Raco seal problem are described in Section 2.6.4.

Test No. -017

Postfire inspection of chamber S/N 011 revealed a slight hot gas leak and a half-inch long crack in the weld of the cover band to the forward flange. There were also two pinhole leaks in the welded area. A metallographic analysis was conducted as described in Section 4.4 and the design of the coverband was modified as described in Section 2.6.3.

A slight hot gas leak in the vicinity of the torus was also detected. It was traced to the same brazing problem that had earlier been noted with chamber S/N 008 (See Section 4.4) and which was corrected for the demonstration and later chambers.

Test No. -018

A pinhole leak was discovered in the cover band weld in chamber S/N 014. The occurrences were similar to the experience with chamber S/N 011 after Test No. -017.

Test No. -019

A slight hot gas leak, too small to measure, was found between the tubes in the cylindrical section of chamber S/N 014.

Test No. -020

Postfire inspection of chamber S/N 015 revealed erosion of the flange in the vicinity of baffle No. 7. There was also a pinhole leak in Tube No. 60. No repairs were made at this time.

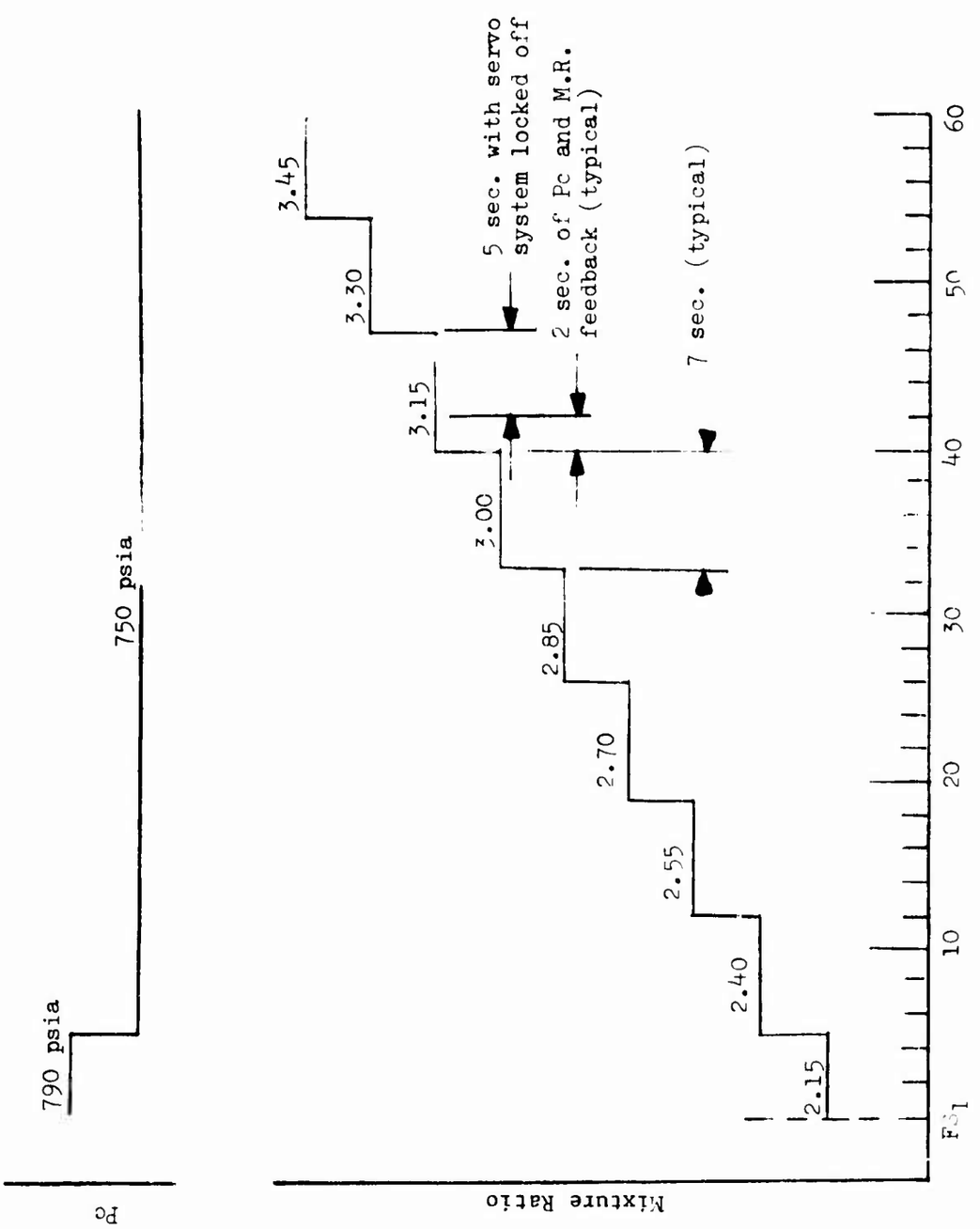

Figure 54--M.R. and Pc Profile--Chamber S/N 013

5.5, TCA Verification Tests (cont.)

Test No. -021

The erosion previously noted in chamber S/N 015 progressed into the inner Raco seal groove. A similar erosion occurred near baffle No. 2. Both spots of erosion and the leak in tube No. 60 were repaired.

Test No. -023

Four minuscule leaks were detected in chamber S/N 015 at the joint of the tubes to the forward flange. The leakage resulted from inadequate braze coverage as described in Section 4.4.

Test No. -024

A fifth leak was detected at the tube to forward flange joint.

Test No. -026

This test was conducted with chamber S/N 013 to determine the margin before burnout of a Titan IIIM Stage I combustion chamber comparing CRES with Hastelloy-X tube material. The test was conducted on Test Stand C-1 with the servo control system utilized to vary the chamber pressure (Pc) and mixture ratio (M_R) levels during the test. Figure 54 is a layout of the Pc and MR profile. The test was terminated manually at FS_1 + 45.0 sec because of a shift in the noise level generated by the firing. The test engineer interpreted the noise level shift as an indication of hardware damage and elected to stop the test.

Examination of the chamber revealed a split in one tube upstream of the throat. The split tube (No. 101) is a down-tube and is located about 30 degrees from the torus inlet, which is a known region of low coolant flow. Hydrolab tests have shown that variations down to 93% of nominal flow are possible in this region. The Hastelloy tubes were practically untouched.

5.5, TCA Verification Tests (cont.)

Test No. -102

The erosion on the flange of chamber S/N 014 after Test No. -001 increased to approximately 0.090 inch deep. There was no further erosion during the test series with chamber S/N 014.

Test No. -105

This test was shut down prematurely because of an out-of-specification chamber pressure excursion which activated a command shutdown device. This was one of the optional tests conducted with chamber S/N 014 to obtain ablative skirt data, and therefore it was not necessary to repeat the test.

Test No. -108

An injector-to-chamber (S/N 015) gap of 0.035 inch was measured following this test. The investigation of this problem is discussed in Section 4.1 and the corrective action that was taken is described in Section 2.6.3.

Test No. -110

This test with chamber S/N 011 was conducted with a solid-spring Raco seal as a possible correction for the leakage noted after Test No. -011. Post-fire inspection revealed that a positive seal was effected throughout the test.

A series of four tests (3051-D06-1J-001 through -004) was conducted to establish the performance baseline for the injectors intended for use with demonstration engine S/N 14. Combustion chamber S/N 015 was utilized for these tests. There was no damage or other abnormality.

5.6 ENGINE DEMONSTRATION TESTS

A series of 30 engine demonstration tests was conducted extending from December 1967 through November 1968. The objective of these tests was to

Table 18 -- Engine Demonstratio

AGC Test Number	Test Plan No.	Date	Test Stand	Duration Sched	Duration Act.	Start Mode	Ablat. Skirt SN	Gimbal	F K lb
-201	1	12-20-67	G-2	20	19.657	N2	No	No	260
-202	2	12-29-67	G-2	200	200.825	Solid	No	No	260±3%
-203	4	1-10-68	G-2	200	200.585	Solid	No	No	260±3%
-204	3	3-11-68	G-2	200	115.438	Solid	25&37	Yes	260±3%
-205	5	4-4-68	G-2	20	20.851	N2	No	No	260±3%
-206	6	4-10-68	G-2	200	200.925	Solid	25&37	Yes	260±3%
-207	7	4-29-68	G-2	200	200.599	Solid	No	No	260±3%
-208	8	5-4-68	G-2	20	21.215	N2	No	No	260±3%
-209	14	7-1-68	G-1	20	20.575	N2	No	No	260-4%
-210	15	7-5-68	G-1	200	200.315	Solid	No	No	260-4%
-211	10	7-10-68	G-1	20	20.744	N2	No	No	260+3%
-212	11	7-12-68	G-1	200	201.006	Solid	No	No	260+2%
-213	12	7-16-68	G-1	20	20.762	N2	No	No	260-3%
-214	13	7-22-68	G-1	200	201.013	Solid	003 & 005	No	260-3%
-215	9	8-27-68	G-2	200	200.458	Solid	32&33	Yes	260+4%

Engine Demonstration Test Summary, Engine S/N 14

t. t	Gimbal	F K lb.	MRE	Prop. Temp. °F	Post psia	Pfst psia	Objectives/Remarks
	No	260	1.91	60±5	82±10	32±10	Adjustment Test. Gas Cooler Accelerometers Satisfactory Test.
	No	260±3%	1.91±2%	60±5	82±10	32±10	Performance Evaluation Test. Hot Gas Cooler Accelerometers. Satisfactory Test.
	No	260±3%	1.91±2%	60±5	82±10	32±10	Performance Evaluation Test. Hot Gas Cooler Accelerometers. Satisfactory Test. SA 2 CC replaced post test.
7	Yes	260±3%	1.91±2%	60±5	82±10	32±10	Performance Evaluation, Refrasil Insulation Gas Cooler Accelerometers. Premature Shut-down caused by SA 2 turbine rotor failure. Replaced SA 2 TPA.
	No	260±3%	1.91±2%	60±5	82±10	32±10	Adjustment Test. First Test 83-blade rotors. Interface Panel Accelerometers. Satisfactory Test.
7	Yes	260±3%	1.91±2%	60±5	82±10	32±10	Performance Evaluation Test. Refrasil Insulation. Interface Panel Accelerometers. Satisfactory Test.
	No	260±3%	1.91±2%	60±5	---	---	NPSH Evaluation Test. Oxidizer (44') and Fuel (43') at minimum. Oxidizer at 35'. Interface Panel Accelerometers. Satisfactory Test.
	No	260±3%	1.91±2%	60±5	82±10	32±10	Adjustment Test. Satisfactory Test.
	No	260-4%	1.91-4.3%	35-40	82±10	32±10	Adjustment Test. Satisfactory Test.
	No	260-4%	1.91-4.3%	35-40	82±10	32±10	Peripheral Evaluation Test. POGO Fuel Accumulators. Flight Instrumentation (TOS, TFS, TfPOI, DC Conv., Pc5). Satisfactory Test.
	No	260+3%	1.91-2%	60±5	82±10	32±10	Adjustment Test. Flight Instrumentation (TOS, TFS, ToPOI, DC Conv.). Satisfactory Test.
	No	260+2%	1.91-7%	85-90	67±5	37±5	Peripheral Evaluation Test. POGO Fuel Accumulators. Flight Instrumentation (TOS, DC Converter, Pc5). Satisfactory Test.
	No	260-3%	1.91+2%	60±5	82±10	32±5	Adjustment Test. Flight Instrumentation (TOS). Satisfactory Test.
&	No	260-3%	1.91+6%	85-90	110±5	26±5	Peripheral Evaluation Test. Flight Instrumentation (TFS, ToPOI, TfPOI), 12:1 Ablative Skirts, MMB 10 in.-sq. Gimbal Actuators. Modified Refrasil Insulation. Satisfactory Test.
3	Yes	260+4%	1.91+6%	35-40	110±5	26±5	Peripheral Evaluation Test, Flight Instrumentation (TFS, ToPOI), POGO Fuel Accumulators, SA 2 Fuel Cavitation Suppression, Refrasil Insulation. Low P Fuel GGCKV. Satisfactory Test.

Table 18 -- Engine Demonstration Test Summary,

AGC Test Number	Test Plan No.	Date	Test Stand	Duration Sched	Duration Act.	Start Mode	Ablat. Skirt SN	Gimbal	F K lb.	MRE	Pr Te o
-301	1	6-3-68	G-2	20	20.669	N2	No	No	260	1.91	6
-302	2	6-6-68	G-2	200	201.008	Solid	No	No	260+3%	1.91±2%	6
-303	4	6-14-68	G-2	200	200.341	Solid	No	No	260±3%	1.91±2%	6
-304	5	6-18-68	G-2	200	200.843	Solid	No	No	260±3%	1.91±2%	6
-305	3	6-24-68	G-2	200	200.645	Solid	35&38	Yes	260±3%	1.91±2%	6
-306	6	7-26-68	G-2	200	200.746	Solid	No	No	260±3%	1.91±2%	6
-307	7	8-1-68	G-2	200	200.470	Solid	14&21	Yes	260±3%	1.91±2%	6
-308	10	8-14-68	G-2	20	20.977	N2	No	No	260±3%	1.91-2%	6
-309	11	8-15-68	G-2	200	2.569	Solid	No	No	260±2%	1.91-7%	8
-310	11	8-16-68	G-2	200	200.361	Solid	No	No	260+2%	1.91-7%	8
-311	12	9-17-68	G-2	20	21.340	N2	No	No	260-3%	1.91+2%	6
-312	13	9-19-68	G-2	200	201.114	Solid	No	No	260-3%	1.91+6%	8
-313	14	9-28-68	G-2	20	20.845	N2	No	No	260-4%	1.91-4.3%	3
-314	15	10-1-68	G-2	200	200.908	Solid	No	No	260-4%	1.91-4.3%	3
-315	8	10-3-68	G-2	20	21.095	N2	No	No	260+3%	1.91+2%	6
-316	9	10-17-68	G-2	200	200.809	Solid	39&40	Yes	260+4%	1.91+6%	3

-- Engine Demonstration Test Summary, Engine S/N 15

Blat. Skirt SN	Gimbal	F K	F lb.	MRE	Prop. Temp. °F	Post psia	Pfst psia	Objectives/Remarks
o	No	260		1.91	60±5	82±10	32±10	Adjustment Test. Satisfactory Test.
o	No	260±3%		1.91±2%	60±5	82±10	32±10	Performance Evaluation. Satisfactory Test.
o	No	260±3%		1.91±2%	60±5	82±10	32±10	Performance Evaluation. Satisfactory Test.
o	No	260±3%		1.91±2%	60±5	82±10	32±10	Performance Evaluation. Satisfactory Test.
5&38	Yes	260±3%		1.91±2%	60±5	82±10	32±10	Performance Evaluation, Refrasil Insulation. Satisfactory Test.
o	No	260±3%		1.91±2%	60±5	82±10	32±10	Performance Evaluation. Satisfactory Test.
4&21	Yes	260±3%		1.91±2%	60±5	---	---	NPSH Evaluation - Oxidizer (44') and Fuel (43') at minimum. Oxidizer at 35' Piggyback-closure covers SN 006 and 005. Refrasil Insulation. Satisfactory Test.
o	No	260±3%		1.91-2%	60±5	82±10	32±10	Adjustment Test, Experimental RACL Seals. Flight Instrumentation (Pld & PgGB). Martin Fuel Prevalves. Satisfactory Test.
o	No	260±2%		1.91-7%	85-90	67±5	37±5	Peripheral Test - Experimental RACO Seals, Flight Instrumentation (Ped and PgGB), Martin Fuel Prevalves, POGO Fuel Accumulators SN 101 and 130. Invalid Test, SA 1 PSVOR Failure.
o	No	260±2%		1.91-7%	85-90	67±5	37±5	Repeat of Test -309. Satisfactory Test.
o	No	260-3%		1.91±2%	60±5	82±10	32±10	Adjustment Test - Flight Instrumentation (Pld and PgGB) Martin Fuel Prevalves. Satisfactory Test.
o	No	260-3%		1.91+6%	85-90	110±5	26±5	Peripheral Test - Flight Instrumentation (Pld and PgGB), Martin Fuel Prevalves, POGO Fuel Accumulators. Satisfactory Test.
o	No	260-4%		1.91-4.3%	35-40	82±10	32±10	Adjustment Test - Martin Fuel Prevalves. Special POGO Instrumentation. Satisfactory Test.
o	No	260-4%		1.91-4.3%	35-40	82±5	32±5	Peripheral Test - Martin Fuel Prevalves and POGO Fuel Accumulators, Special POGO Instrumentation. Satisfactory Test.
o	No	260±3%		1.91±2%	60±5	82±10		Adjustment Test - Martin Fuel Prevalves (Pld and PgGB). Satisfactory Test.
9&40	Yes	260±4%		1.91+6%	35-40	110±5	26±5	Peripheral Test - Martin Fuel Prevalves, and POGO Fuel Accumulators, Refrasil Insulation, Flight Instrumentation (Pld and PgGB), Exit Closure Covers. Satisfactory Test.

5.6, Engine Demonstration Tests (cont.)

demonstrate the performance and system compatibility over the range of specification operating conditions of the Stage I engine and the redesigned components. With reference to the combustion chamber the criteria were minimum specific impulse in conjunction with the baffled injector, adequate cooling over the full range of operating conditions including the most adverse flight conditions for the chamber and for the ablative skirt, and structural integrity as evidenced by containing the combustion gases and by supporting the ablative skirt under the extreme loads applied during the starting transient and during gimballing.

Combustion chamber Serial Numbers 017, 019, 020, 021, 022, and 092 were used for the demonstration. They had not been previously fired. Chambers S/N 021 and S/N 022 went through the full cycle of 15 tests. A summary of the test conditions and results is presented in Table 18. The total firing duration was 1856 seconds for engine S/N 14 and 2113 seconds for engine S/N 15. Included in the tests were 15 full duration firings and five occasions when gimballing was performed. On the basis of the test results it was concluded that the 6:1 area ratio combustion chamber had met the specification criteria adequately.

The following summary lists the abnormalities that were encountered. The discussion is by individual chamber rather than by test sequence for ease in following the discussion.

Chamber S/N 017

This unit had undergone considerable rework during fabrication; most notably, repair of the forward flange cover band which resulted in distortion to the flange that made remachining necessary. This chamber had therefore been withdrawn from the demonstration program but was substituted for chamber S/N 020 after Test No. -203.

Following Test No. -211, erosion was noted on the forward flange 2-in. above the joint with tube No. 64. The erosion was within the limits

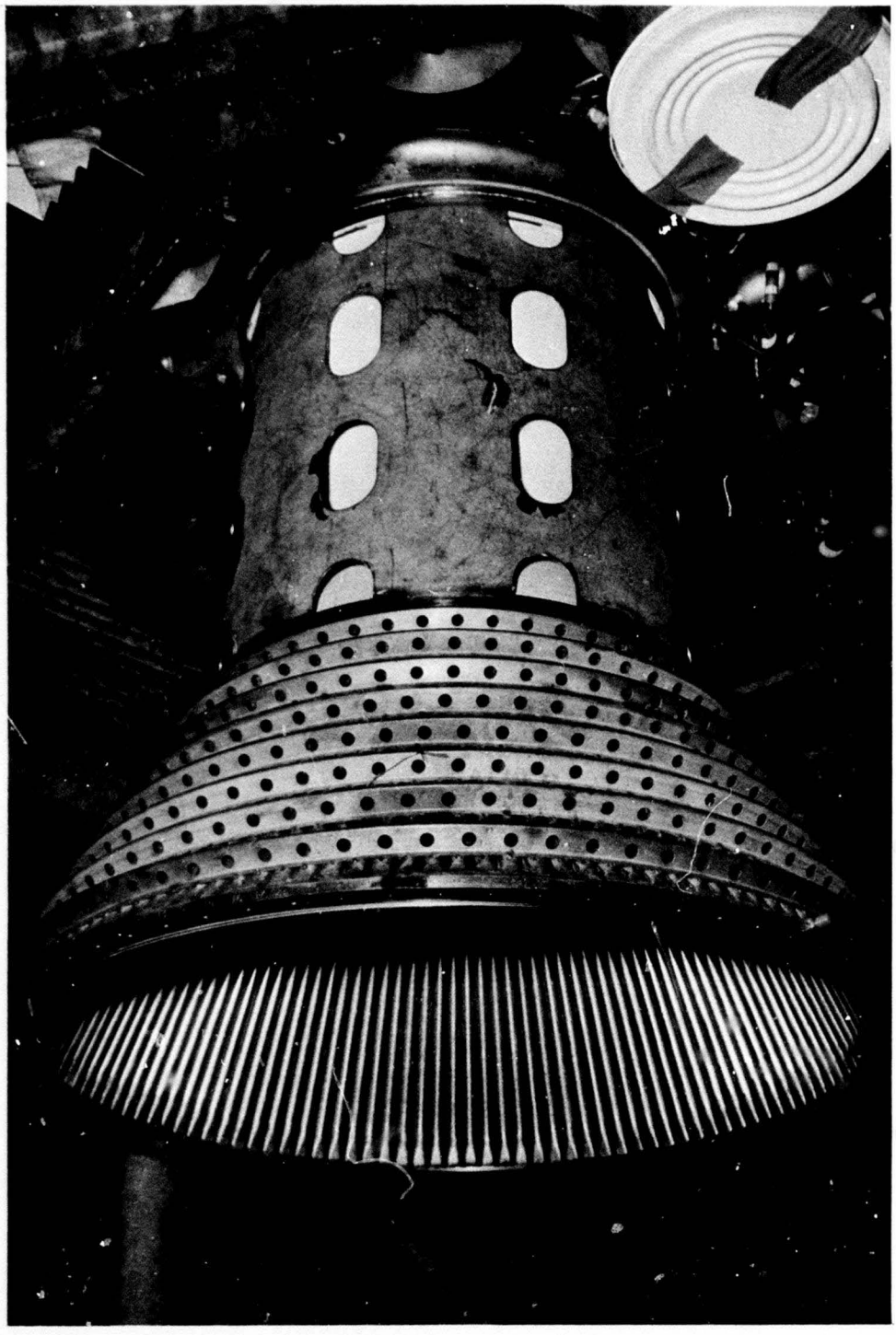

Figure 55 -- Chamber S/N 019 Prior to Start of Engine Demonstration

5.6, Engine Demonstration Tests (cont.)

defined by specification as acceptable for refiring and did not increase during the rest of the test series.

Seepage was detected from a crack in the crown of tube No. 64 following Test No. -212. The crack was attributed to the flow of metal from the aforementioned erosion. A slight increase in the seepage was noted following Test No. -214.

Chamber S/N 019 (Figure 55)

Seepage was noted from the joint between the tubes and the forward flange after Test No. -207. No repair was made prior to the next test. The chamber was removed from demonstration following Test No. -208 because the leakage had increased to a total of 24 cc/min.

Chamber S/N 020

Cracks were noted in the Epon covering of the wire wrapping and there was also looseness in the wire, as described previously and shown in Figure 6. The chamber was accepted for refiring because the following test was to be conducted without an ablative skirt and the extra loads imposed thereby. The looseness of the wire was judged not sufficient to jeopardize a test conducted without a skirt.

Following Test No. -204 two cracks were found in the forward flange in line with tube No. 44 and tube No. 108. The cracks were located approximately 1/2 inch from the base of the flange and extended 1/2 inch forward. A crack 1-3/4 inch long, starting 1 inch below the flange, was also noted in tube No. 64.

The chamber was removed from demonstration testing and an investigation was made of the abnormalities. The results of the investigation are given in Section 2.6.

5.6, Engine Demonstration Tests (cont.)

Chamber S/N 021

Leakage too small to measure was noted between tubes No. 117 and No. 118 and the forward flange after Test No. -305. The leakage did not increase until after Test No. -310, when the leakage had grown to 2 cc/min and additional leakage appeared adjacent to tube No. 119. No repairs were made at that time but the leakage was monitored thereafter. After two more tests the total leakage had increased to 6 cc/min, and tubes No. 114 and No. 116 had begun to leak. Following Test No. -313 several other tubes were found to be leaking and the total leakage amounted to 20 cc/min. There was no further change in the leakage during the three remaining tests.

Five cracks were noted in the weld joint between the shell and the aft wire lock ring following Test No. -315. They were repaired prior to Test No. -316.

Chamber S/N 022

Erosion was noted on the mounting flange 3/4 inch above tube No. 6 following Test No. -302. The erosion was within the limits of acceptibility given by the specification and no repairs were made. There was no recurrence of erosion.

Seepage similar to that reported for chamber S/N 021, and likewise too small to measure, was discovered at the joints of four tubes to the forward flange following Test No. -305. The leakage, as in the case with chamber S/N 021, did not increase to a measurable quantity until after Test No. -310, though it was noted that there was seepage at other tube joints. Following Test No. -311 the seepage was detected at many additional tube joints and the total seeping measured 10 cc/min. No repairs were made; during the remainder of the series no new tube joints were affected, but the total leakage had grown to 95 cc/min.

5.6, Engine Demonstration Tests (cont.)

A hair-line crack was noted in the crown of tube No. 25 following Test No. -310, but the leakage was too small to measure. The leakage did not increase. The crack was repaired after Test No. -313 and it did not reappear.

Following Test No. -315 an external leak was found at the tack weld (Figure 56) of tube No. 123 to the V-band. The leak was repaired as shown in Figure 57 prior to test No. -316.

A crack in the weld joint at the shell to the aft wire lock ring was detected after Test No. -315 and was repaired.

After testing was complete a 13-inch long crack was discovered in the weld joining the two shell halves. It is assumed that the crack resulted from the last test, but the crack had not been noticed previously, and it is entirely speculative as to when it occurred.

Chamber S/N 092

This chamber was withdrawn from the production lot to replace chamber S/N 019 after Test No. -208. It was subjected to seven tests for a total duration of 862 seconds. There were no incidents of leakage or other discrepancies except a 3-inch long crack in the joint of the shell to the aft wire lock ring which was noted after the testing had been completed.

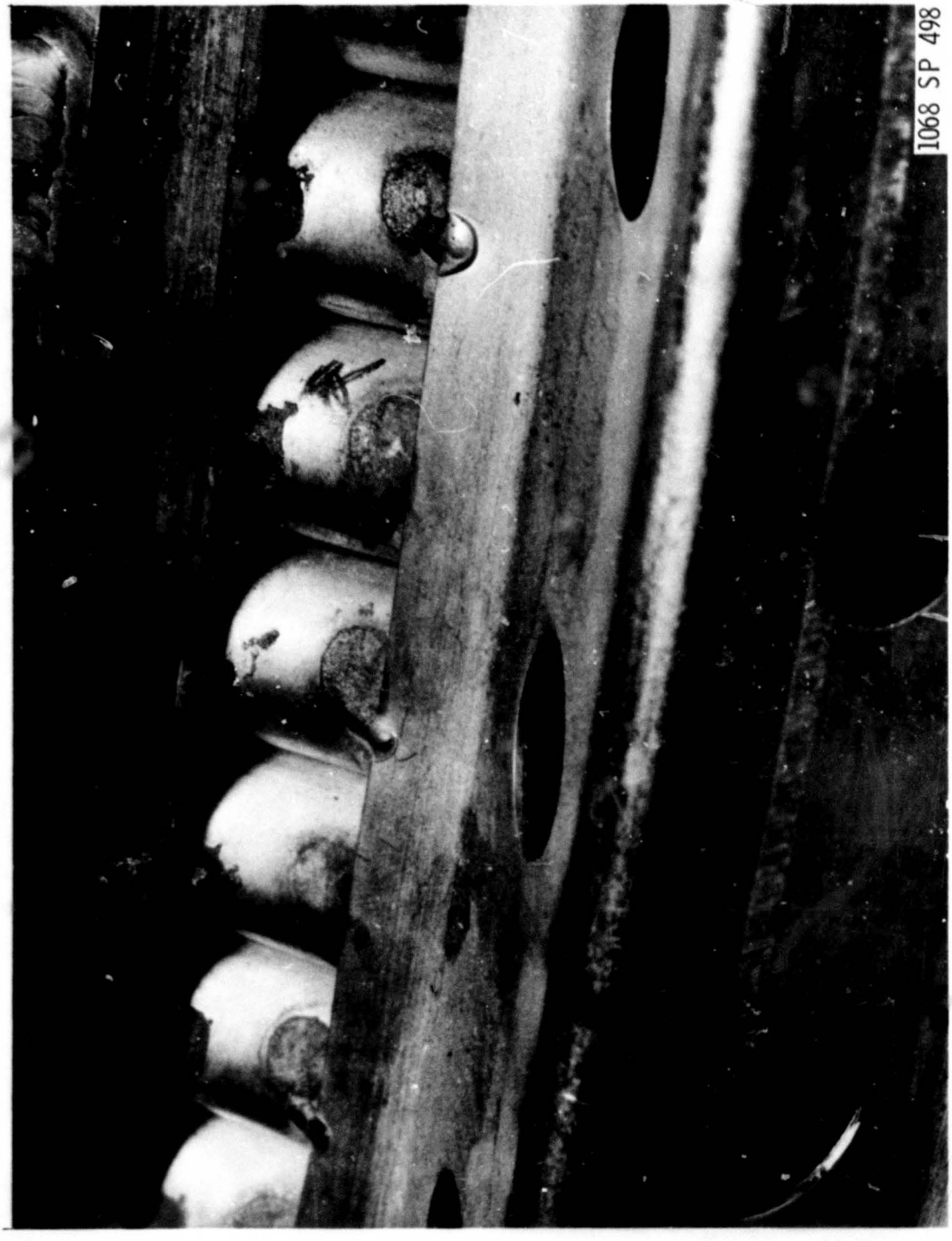

Figure 56 -- Weld Cracks -- Chamber S/N 022

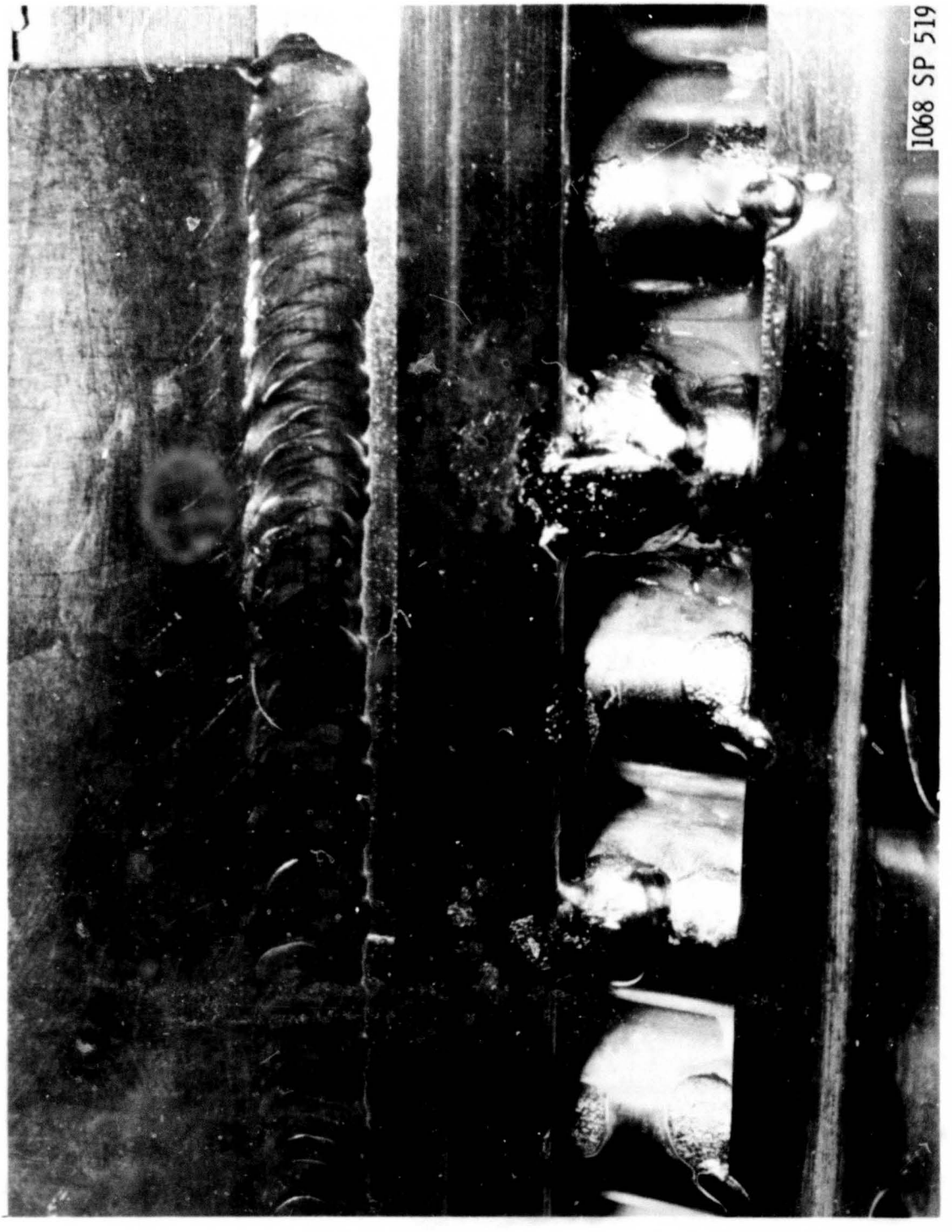

Figure 57 -- Repair of Weld Cracks -- Chamber S/N 002

Report 9180-941-DR-3

Section VI Hastelloy 6 Combustion Chamber

6. HASTELLOY-X COMBUSTION CHAMBER

Hastelloy-X had originally been considered as a canditate material for the combustion chamber. However, within the original schedule limits for development of the Stage I engine, it was felt that there was not sufficient time to overcome the fabrication problems associated with Hastelloy. As back-up, in the event that heat flux intensities should prove beyond the capacity to be handled with CRES 347, one chamber was assigned to be fabricated from Hasteiloy-X. As early testing indicated that the backup was unnecessary, the plan was modified to fabricating one chamber, mostly of CRES 347 but with some Hastelloy-X materials for comparison testing.

Combustion chamber S/N 013 was selected for the experiment. It differed from other developmental chambers only in that six of the tubes were made from Hastelloy. The tubes were of the same external configuration and wall thickness as the stainless steel tubes.

6.1 HASTELLOY MATERIAL STUDIES

A preliminary brazeability check of Hastelloy-X to 347 stainless steel tubing, using Coast Metals 62 (AGC 44080B) brazing alloy, resulted in the formation of inferior braze joints at lower brazing temperatures. Two specimen composed of three Hastelloy-X tubes and three 347 stainless steel tubes were brazed at the high temperature end (1990 $\pm$ 10^{o}F) and the low temperature end (1910 $\pm$ 10^{o}F) of the brazing temperature range allowed in the applicable thrust chamber brazing specification. Examination of the 1910^{o}F brazed joints under a low-power microscope (5-20X) revealed poor wetting of the Hastelloy-X to Hastelloy-X joints while the Hastelloy-X to 347 stainless steel and the 347 stainless steel to 347 stainless steel joints appeared sound. The 1990^{o}F brazed joints all appeared sound. A Hastelloy-X to Hastelloy-X sample in which the tube surfaces were mechanically polished was then brazed at 1950^{o}F and the braze joint displayed adequate wetting and appeared quite sound. Attempts to break or tear the tube-to-tube joints by

6.1, Hastelloy Material Studies (cont.)

twisting and pulling the tubes apart resulted in failure of the tube walls in all cases. No braze joints were fractured. The aluminum content of the Hastelloy-X tubing was established as 0.2 percent.

Because of the high aluminum residue (0.27% - 0.43%), present in current shipments of wrought Hastelloy-X, problems in brazing Hastelloy-X to Hastelloy-X using Coast 62, alloy B were anticipated. However, successful brazing was accomplished on samples taken from material used to fabricate the tubes. A spectroscopic analysis of the material showed an aluminum content of 0.12 percent. This finding relieved most of the concern with this problem. Close scrutiny of cleaning and assembly techniques was maintained by engineering and metallurgical personnel during buildup and brazing to ensure adequate braze results.

Tensile data were obtained from butt-brazed sheet specimens made from actual chamber tubing. The specimen were brazed for five minutes with AGC 44080B braze alloy in a dry hydrogen atmosphere at 1950^{o}F, hand polished to remove excess braze, and subjected to tensile testing at room temperature. Six specimens were used, two with zero joint clearance, two with 0.0015-in. clearance, and two with 0.003-in. clearance. Results ranged from 65,000 to 80,000 psi, with the larger clearances displaying the lower strengths. This strength level is normally greater than the yield strength of the parent material. The Hastelloy-X aluminum content was 0.014 percent.

In order to determine the effects of multiple furnace cycling upon oxide formation and thus the brazeability of the Hastelloy-X material, three 1/4-in. dia. tube specimen were exposed for five minutes to each of three normal brazing cycles of 1950^{o}F. On the first cycle braze alloy (AGC 44080B) was applied to Specimen No. I, on the second cycle braze alloy was applied to Specimen No. II, and on the third cycle braze alloy was applied to Specimen No. III. Examination of the joints revealed equivalent good braze joints on all three specimen. The Hastelloy-X aluminum content was 0.18 percent.

6, Hastelloy-X Combustion Chamber (cont.)

6.2 FABRICATION OF HASTELLOY-X CHAMBER

Figure 58 shows the location of Hastelloy-X tubes in the chamber relative to the injector mounting flange tooling hole.

Brazing of combustion chamber S/N 013, which contained six Hastelloy-X tubes in the tube bundle, was accomplished during December 1966. The chamber was brazed in two cycles using AGC 44080A braze alloy. The first cycle was performed with the aft end down, to braze the tube-to-tube joints from the throat area aft, at approximately 2010°F. The second cycle was performed with the forward flange down, to braze the combustion zone tube-to-tube joints and the tube-to-fuel torus joints, at approximately 2000°F. All tube-to-tube joints appeared sound although braze alloy progression through the joint to the "back-side" on both of the Hastelloy-X-to-Hastelloy-X joints was less than that noted on the 347-to-347 joints. An area of base metal dissolution (erosion) was noted on five of the six Hastelloy X tubes at the point of tangency between the tube crowns and aft edge of the forward flange as shown in Figure 59.

This erosion occurred subsequently to the second braze cycle. Wax impressions were made of the eroded areas, bisected, and measured using an optical comparator. The depth of the erosion varied from tube to tube over a range of 0.005 in. to 0.020 in.

The eroded condition is attributed to the concentration of braze alloy which had been replaced in this area prior to the second braze cycle, coupled with the highest brazing temperature employed for the "A" revision braze alloy and the long duration of the braze cycle (30 minutes). The manganese-nickel binary equilibrium diagram shows a solid solution type diagram with a liquid phase occurring at 1840°F and 58 percent manganese. The reaction between the liquid manganese-base braze alloy with the nickel-base tube material at the brazing temperature resulted in the tube dissolution. The sixth tube did not erode because a tack weld joining the tube crown to the flange occupied this area.

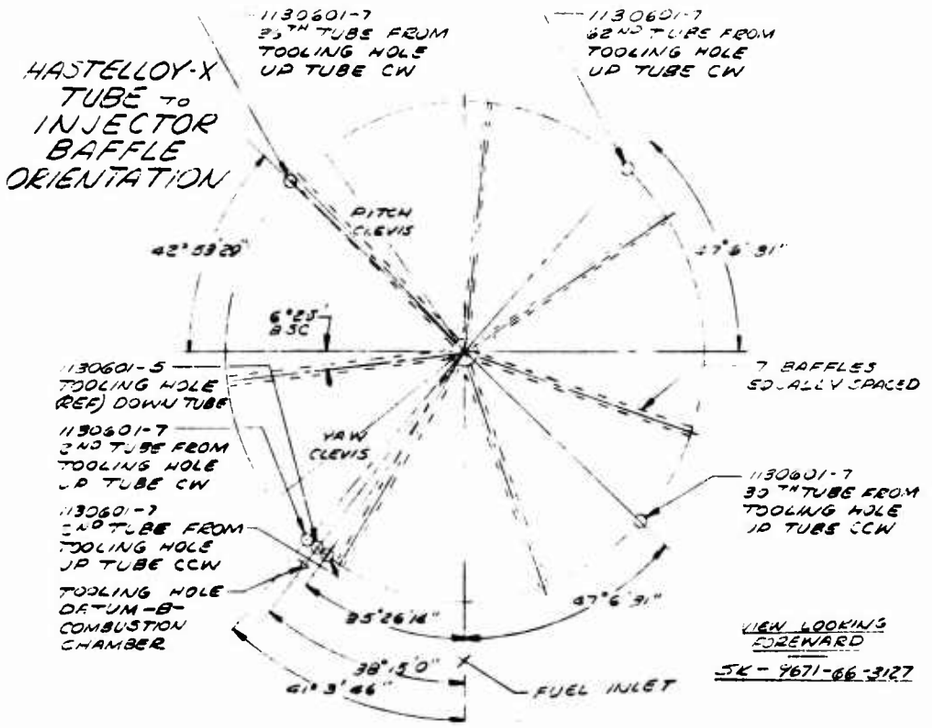

Figure 58 -- Location of Hastelloy Tubes in Chamber S/N 013

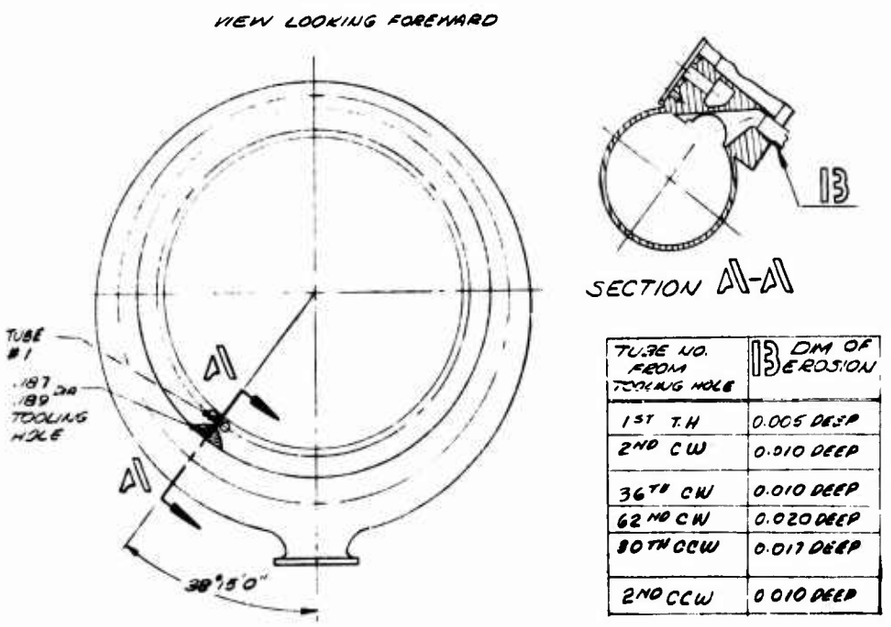

TUBE NO. FROM TOOLING HOLE	13 DIM OF EROSION
1ST T.H	0.005 DEEP
2ND CW	0.010 DEEP
36TH CW	0.010 DEEP
62 ND CW	0.020 DEEP
80TH CCW	0.017 DEEP
2ND CCW	0.010 DEEP

Figure 59 -- Erosion of Hastelloy Tubes

6.2, Fabrication of Hastelloy-X Chamber (cont.)

The areas of dissolution were repaired by applying Nioro (82 Au=18 Ni) braze alloy to the discrepant areas by the manual TIG method.

6.3 HASTELLOY CHAMBER TESTING

Chamber S/N 013 was used for five development tests, the results of which are reported in Section 5. Of primary interest here is a test conducted in October 1967 to compare the burnout heat flux of Hastelloy-X with that of CRES 347.

The test was conducted on Test Stand C-1 with the servo control system utilized to very the chamber pressure (P_c) and mixture ratio (MR) levels during the test. The chamber pressure and mixture ratio profile were shown earlier in Figure 54. The test was terminated manually at FS_1 + 45.0 sec by decision of the test engineer.

Examination of the chamber revealed a split in one CRES 347 tube upstream of the throat. The split tube (No. 101) is a down-tube and is located about 30 degrees from the torus inlet, which is a known low coolant flow region. There was no damage to the Hastelloy tubes. The calculated R_{BO} on this test was 0.84 maximum.

APPENDIX

Combustion Chamber Test Log

STAGE I THRUST CHAMBER ASSEMBLY TESTS

Test No.	Date	Test Stand	Duration	Injector S/N	Chamber S/N	Remarks
	Test Series 3051-D01-1C (2 BIE-38 Injectors)					
001	5-13-66	C-1	31.1	149	001	No damage
002	5-16-66	C-1	60.9	149	001	Wire wrap failure on chamber
101	7-19-66	C-2	10.4	248	001	Split and erode tubes in throat
102	7-23-66	C-2	60.7	1110	310	No damage
	Test Series 3051-D04-1J* (Second Generation Injector Evaluation)					
007	9-7-66	C-1	10.7	657	002	No change in erosion
008	9-9-66	C-1	60.2	657	002	No change in TCA
009	9-13-66	C-1	60.1	650	002	No damage
010	9-21-66	C-1	60.4	651	002	No injector damage. Rough tubes in throat
011	9-28-66	C-1	20.9	251	002	Injector mounting flange eroded
014	11-29-66	C-1	6.3	653	002	Invalid shut down; no damage
015	11-30-66	C-1	60.7	653	002	No damage. C.C. has some rough tubes in throat
016	12-1-66	C-1	60.9	655	004	Perf. evaluation of injector with shortened baffles. Satisfactory test - no hardware damage
017	12-7-66	C-1	60.6	655	002	Performance evaluation (Servo control excursion test with 90° propellants). Satisfactory test - no hardware damage

*Missing test numbers conducted with AJ-9 chambers

Stage I Thrust Chamber Assembly Tests (cont.)

Test No.	Date	Test Stand	Duration	Injector S/N	Chamber S/N	Remarks
	Test Series 3051-D04-1J (cont.)					
018	12-10-66	C-1	60.9	662	004	Performance evaluation (Servo control excursion test). Satisfactory test - no hardware damage
019	12-10-66	C-1	60.4	662	004	Performance evaluation (Servo control excursion test). Satisfactory test. Slight injector face erosion.
020	12-13-66	C-1	60.7	661	004	Performance evaluation (Servo control excursion test). Satisfactory test - no hardware damage.
021	12-13-66	C-2	52.4	661	004	Performance evaluation (Servo control excurion). Satisfactory test - no hardware damage.
022	12-21-66	C-1	60.9	650	002	Performance evaluation (Servo control excursion). Satisfactory test - no hardware damage.
023	12-21-66	C-1	60.7	650	002	Performance evaluation (Servo control excursion). Satisfactory test - no hardware damage.
024	2-14-67	C-1	60.4	662M	013	Clean. No damage except a rough spot on flange adjacent to Baffle No. 1.
025	2-15-67	C-1	60.4	662M	013	90^{o} propellant. MR excursion. No damage.

Stage I Thrust Chamber Assembly Tests (cont.)

Test No.	Date	Test Stand	Duration	Injector S/N	Chamber S/N	Remarks
	Test Series 3051-D04-1J (cont.)					
026	3-9-67	C-1	60.7	665	013	Injector performance with servo control system. Satisfactory test. Slight surface roughness on CC flange (0.010 in.).
027	3-10-67	C-1	60.7	665	013	Injector performance with servo control. Satisfactory test - no hardware damage.
028	12-22-66	C-2	60.2	661	004	Performance evaluation. Satisfactory test - no hardware damage

Test No.	Date	Duration	Injector S/N	Chamber S/N	Skirt S/N	Remarks
	Test Series 3051-D01-1M - Test Stand C-2					
001	10-4-66	40.7	251	002	---	No increase in damage
002	10-6-66	40.2	251	002	006	No inspection
003	10-7-66	21.6	251	002	006	No damage
004	10-12-66	60.2	650	002	006	No inspection
005	10-12-66	60.1	650	002	---	No damage
006	11-16-66	20.2	651	005	006	No damage
007	11-17-66	33.7	651	005	006	Severe oxidizer leak on stand

Stage I Thrust Chamber Assembly Tests (cont.)

Test No.	Date	Duration	Injector S/N	Chamber S/N	Skirt S/N	Remarks
	Test Series 3051-D01-1M (cont.)					
008	11-18-66	30.7	653	005	006	Manual shutdown due to stand problems. Diffuser came loose, jumped track. No TCA damage.
009	12-17-66	60.4	1110	002	---	Performance evaluation and checkout of Test Stand C-2. Satisfactory test - no hardware damage.
010	12-20-66	60.6	653	004	006	Performance evaluation (Servo control excursion). Satisfactory test - no damage.
011	12-21-66	60.5	653	004	006	Performance evaluation (Servo control excursion). Satisfactory test - no damage.
	Test Series 3051-D01-0X - Test Stand C-1 Servo Control Evaluation					
001	9-3-66	60.4	1110	310		No damage
002	1-11-67	2.0	1110	002		No damage
003	1-12-67	60.5	1110	002		No damage

Stage I Thrust Chamber Assembly Tests (cont.)

Test No.	Date	Duration	Injector S/N	Chamber S/N	Skirt S/N	Remarks
	Test Series 3269-D01-1M - 12:1 (Skirt Evaluation)					
001	6-25-68	3.7	782	014	---	Stand checkout. Premature shutdown because of chamber pressure control transducer (TPS).
002	6-26-68	61.0	782	014	---	6:1 baseline performance with servo control system. Satisfactory test.
003	6-28-68	60.5	782	014	002	12:1 baseline performance with servo control system and 35°F propellants. Satisfactory test.
004	7-1-68	60.6	782	014	002	12:1 performance evaluation with servo control system and nominal propellant temperature. Satisfactory test.
005	7-5-68	60.3	782	014	002	12:1 performance evaluation with servo control system and 90°F propellants. Satisfactory test.
006	8-7-68	60.6	661M	158	---	6:1 performance evaluation with servo control system and nominal propellant temperature. Satisfactory test.
007	8-8-68	60.6	661M	158	006	12:1 performance evaluation with servo control system and 35°F propellant temperature. Satisfactory test.

Stage I Thrust Chamber Assembly Tests (cont.)

Test No.	Date	Duration	Injector S/N	Chamber S/N	Skirt S/N	Remarks
	Test Series 3269-D01-1M (cont.)					
008	8-9-68	60.8	661M	158	006	12:1 performance evaluation with servo control system and 60°F propellant temperature. Satisfactory test.
009	8-10-68	60.7	661M	158	006	12:1 performance evaluation with servo control system and 90°F propellant temperature. Satisfactory test.

STAGE I THRUST CHAMBER VERIFICATION TESTS

Test No.	Date	Duration	Injector S/N	Chamber S/N	Skirt S/N	Remarks
	Test Series 3051-D02-1M					
001	3-17-67	60.6	665	014	---	TCA verification with servo control system - 35° propellants. Satisfactory test. Slight chamber flange erosion (.015") at baffle #7 location.
002	3-21-67	60.2	665	014	---	TCA verification with servo control system - 60° propellants. Satisfactory test. Slight increase (.005") in chamber flange erosion.
003	3-22-67	60.1	665	014	---	TCA verification with servo control system - 90° propellants. Satisfactory test.
004	4-5-67	60.3	665	014	---	TCA verification - 60° propellants. Satisfactory test - no damage.
005	4-20-67	6.8	664	016	---	TCA verification - 90° propellants. Premature shutdown - Test Stand malfunction. Injector all right. Combustion chamber tubes badly eroded.
006	5-2-67	60.4	664	015	---	TCA verification - 35° propellants. Satisfactory test.
007	5-2-67	60.3	664	015	---	TCA verification - 60° propellants. Satisfactory test.
008	5-3-67	60.2	664	015	---	TCA verification - 90° propellants. Satisfactory test.
009	5-18-67	60.6	663	011	---	TCA verification - 90° propellants. Satisfactory test.

Stage I Thrust Chamber Verification Tests (cont.)

Test No.	Date	Duration	Injector S/N	Chamber S/N	Skirt S/N	Remarks
	Test Series 3051-D02-1M (cont.)					
010	5-19-67	60.8	663	011	---	TCA verification - 60° propellants. Satisfactory test - no hardware damage.
011	5-23-67	60.7	663	011	---	TCA verification - 35° propellants. Satisfactory test - no hardware damage.
012	5-29-67	60.8	664	015	---	TCA verification - 60° propellants. Satisfactory test - no hardware damage.
013	6-1-67	60.3	663	011	---	TCA verification - 35° propellants. Satisfactory test - no hardware damage.
014	6-8-67	60.4	664	015	---	TCA verification - 60° propellants. Satisfactory test - no hardware damage.
015	6-23-67	3.1	663	015	---	TCA verification - terminated prematurely because of servo control system malfunction. No hardware damage.
016	6-23-67	60.4	663	015	---	TCA verification - 62° propellants. Satisfactory test - no hardware damage.
017	8-3-67 C-1	60.613	663	011	---	TCA verification. Satisfactory test - slight CC hot gas leak near torus.
018	8-10-67 C-1	60.475	663	014	---	TCA verification. Satisfactory test. No injector damage. CC had pin hole and cracked in weld area.

Stage I Thrust Chamber Verification Tests (cont.)

Test No.	Date	Duration	Injector S/N	Chamber S/N	Skirt S/N	Remarks
	Test Series 3051-D02-1M (cont.)					
019	8-12-67 C-1	60.358	663	014	---	TCA verification. 1/2 vaned oxidizer elbow. No significant changes in performance.
020	8-17-67 C-1	60.410	661	015	---	TCA verification.
021	8-22-67 C-1	60.259	661	015	---	Tests -020 and -021 established current performance level of S/N 661. Combustion chamber flange erosion on both tests. Injector will be modified and retested.
022	9-15-67	60.7	661M	015	---	Injector modification evaluation. Satisfactory test - no hardware damage.
023	9-16-67	6.2	661M	015	013	C-1 checkout with ablative skirt. Satisfactory test - no hardware damage.
024	9-19-67	7.2	661M	015	015	Premature shutdown - Test Stand malfunction. No hardware damage.
025	9-21-67	60.6	661M	015	015	Injector modification evaluation with ablative skirt. Satisfactory test - no hardware damage.
026	10-10-67	45.1	661M	013	015	R_{BO} evaluation per Action Item F-116 (C.C. has six Hastelloy tubes.) Slight C.C. (CRES) tube damage. No injector damage.
101	4-17-67	60.4	665	014	015	TCA verification - 35° propellants. Altitude test. Satisfactory test.

Stage I Thrust Chamber Verification Tests (cont.)

Test No.	Date	Duration	Injector S/N	Chamber S/N	Skirt S/N	Remarks
	Test Series 3051-D02-1M (cont.)					
102	4-25-67	62.6	665	014	015	TCA verification - 60° propellants. Altitude test. Satisfactory test - slight combustion chamber flange erosion.
103	4-28-67	61.7	665	014	015	TCA verification - 90° propellants. Altitude test.
104	5-9-67	61.8	665	014	014	TCA verification - 60° propellants. Altitude test. Satisfactory test.
105	5-17-67	23.9	665	014	011	TCA verification - 60° propellants. Altitude test. Shutdown prematurely because of high Pc. Slight tip strip erosion of injector baffle #5.
106	6-1-67	61.7	664	015	016	TCA verification - 35° propellants. Altitude test. Satisfactory test - no hardware damage.
107	6-14-67	61.5	664	015	016	TCA verification - 60° propellants. Altitude test - no hardware damage.
108	6-20-67	61.3	664	015	016	TCA verification - 42° propellants. Altitude test - no hardware damage.
109	7-3-67	61.5	663	011	017	TCA verification - 90° propellants. Altitude test. Satisfactory test - no hardware damage.
110	7-15-67	61.6	663	011	017	Performance verification - oxidizer elbow S/N 002.
111	7-20-67	61.5	663	011	017	Performance verification - oxidizer elbow S/N WHB.

Stage I Thrust Chamber Verification Tests (cont.)

Test No.	Date	Duration	Injector S/N	Chamber S/N	Skirt S/N	Remarks
	Test Series 3051-D06-1J - Test Stand C-1					
001	9-11-67	60.4	696	015	---	TCA verification. Establish performance level of DEMO injector. Satisfactory - no damage.
002	9-13-67	60.6	696	015	---	Same as Test No. -001.
003	9-25-67	60.5	697	015	---	Same as Test No. -001. Second DEMO injector.
004	9-27-67	60.6	697	015	---	TCA verification. Establish performance level with ablative skirt. Satisfactory - no hardware damage.

LABORATORY TESTS

Test No.	Pressure, psia	Velocity, ft/sec	Temperature, °F	Burnout Heat Flux, Btu/in.^{2}-sec
	AeroZINE 50 Heated Tube Test Program			
HT-5-102	1050	89.1	135	11.7
HT-5-104	1130	123.3	151.4	19.6
HT-5-105	1127	149.1	158.6	20.4
HT-5-106	1160	177.9	163.8	24.4
HT-5-107	1150	120.4	200.3	16.9
HT-5-109	1124	145.3	209.7	21.1
HT-5-110	1144	170.44	199.1	24.5
HT-5-111	1127	93.8	106.9	13.15
HT-5-112	1130	91.9	146.5	12.1
HT-5-113	1128	122.5	103.8	17.4
HT-5-114	1136	163.5	110.3	26.6
HT-5-115	1137	180.7	107.2	28.2
HT-5-116	1213	145.5	63.6	22.4
HT-5-117	841	152.1	171.3	22.8
HT-5-118	1475	152.7	158	23.6
HT-5-119	Duration Test, No Burnout			
HT-5-121	1115	8.9	140	3.96
HT-5-122	877	180.8	202.3	25.2
HT-5-126B	1166	98.4	69	15.67

ENGINE SUBASSEMBLY TESTS

Test No.	Date	Duration	Injector S/N	CC S/N	Skirt S/N	TPA S/N	Test Objective
	Test Series 3051-D01-1A Test Stand G-2						
001	6-3-66	30.450	1110	002	---	285	Engine Balance. Test met objectives.
002	6-8-66	15.450	1110	002	001	285	CC/Skirt Evaluation. Test met objectives. Blowback from turbine exhaust carry-off duct caused premature shutdown and minor damage. Ablative skirt capable of further firing.
003	6-14-66	200.89	1110	002	001	285	CC/Skirt Evaluation. Test met objectives. Side loads were not of expected magnitude at start. Ablative skirt and CC in good condition.
004	6-21-66	30.548	249	002	---	284	CC with 12% Film Cooling. Test met objectives - CC tube ruptured in 2 places near exit probably due to temporary flow restriction.
005	7-1-66	200.713	249	002	002	284	CC/Skirt Evaluation. Test met objectives. CC tube ruptured in 2 places near exit probably due to temporary flow restriction.
006	7-25-66	196.285	214	003	---	284	Worst Flight CC Evaluation. Test met objectives. Early shutdown due to test facility problems. No damage.

Engine Subassembly Tests (cont.)

Test No.	Date	Duration	Injector S/N	CC S/N	Skirt S/N	TPA S/N	Test Objectives
			Test Series 3051-D01-1A (cont.)				
007	7-29-66	200.873	214	002	---	284	Worst Flight CC Evaluation. Test met objectives - First with reverse-opening TCOV. No damage.
008	8-22-66	60.895	657	003	---	284	7 pie/7 blade 300 QM Baffled Injector Checkout. Test met objectives. 1000 cps at an amplitude of 105 psi in P_c. Minor reparable damage to injector and CC.
009	9-8-66	53.169	651	004	---	285	Baffled Injector Checkout (7 pie/7 blade 400 QM). Objectives met. Fire caused by cracked weld in CC fuel torus necessitated an early shutdown. Oscillation in P_c at 980 cps and 96 psi amplitude.
010	9-17-66	40.850	251	005	003	285	Baffled Injector Checkout (4 pie/7 blade 400 QM). Met objectives - Unique "soft" start due to unintentional FS_2 nitrogen purges being on at startup. Oscillations in P_c were 1000 cps at 40 psi amplitude.
011	9-20-66	20.773	650	005	003	285	Baffled Injector Checkout (7 pie/7 blade, 450 QM). Met objectives - Same purge - start as #-010. P_c oscillations intermittent 1200 cps at 25 psi amplitude.

Engine Subassembly Tests (cont.)

Test No.	Date	Duration	Injector S/N	CC S/N	Skirt S/N	TPA S/N	Test Objective
			Test Series 3051-D01-1A (cont.)				
012	9-26-66	187.103	650	005	004	285	"Worst Flight" - CC/Inj/Skirt (Same Inj as -011). Met objectives. Early FS_2 due to turbine seal failure (Fabrication error in gearbox) P_c oscillations were 1500 cps at 30 psi amplitude
013	10-4-66	200.701	650	005	---	284	CC tube burnout ratio test (Same Inj as -011). Met objectives - P_c oscillations were 960 cps at 20 psi amplitude. No hardware damage.
014	10-10-66	73.826	651	005	003	284	Skirt durability (7 pie/7 blade 400 QM Inj). Met objectives. Terminated early due to P_c oscillations reaching 123 psi amplitude at 990 cps. No damage.
015	10-13-66	5.365	657	005	---	284	Injector evaluatio[illegible] pie/ 7 blade 300 QM). Me[illegible]bjectives. Automatic shutdown due to P_c oscillations of 1000 cps at 119 psi amplitude.

Engine Subassembly Tests (cont.)

Test No.	Date	Duration	Injector S/N	CC S/N	Skirt S/N	TPA S/N	Test Objective
	Test Series 3051-D01-1A (cont.)						
016	10-17-66	36.714	650	007	003	284	"Worst Flight" Skirt Durability (Same Injector as -013). Did not meet objectives. Low GGA performance - probably due to contaminated propellant. Oscillations in P_c = 1000 cps at 12 to 15 psi amplitude.
017	10-20-66	207.410	650	007	003	284	Same as -016 (Same Inj. as -016). Met objectives. Performance at start was similar to -016, but climbed into steady state. P_c oscillations were 1000 cps at 27 psi amplitude.
018	10-31-66	5.313	657	004	---	284	Evaluate CC and Injector with dams (7 pie/7 blade Injector, 300 QM). Met objectives. Oscillations in P_c reached 221 psi amplitude at 1000 cps. No hardware problems.
019	11-12-66	140.149	650	007	005	284	"Worst Flight" Skirt Evaluation with Gimballing (Same Inj as -017). Met objectives. Shut-down early due to erroneous indication of a lube oil problem. P_c oscillations were 1000 cps at 74 psi amplitude.

Engine Subassembly Tests (cont.)

Test No.	Date	Duration	Injector S/N	CC S/N	Skirt S/N	TPA S/N	Test Objective
			Test Series 3051-D01-1A (cont.)				
020	11-16-66	20.677	655	008	---	284	Injector Evaluation (Low Baffle, 400 QM, 12.6 FFC). Met objectives. Low performer. Oscillations were 1000 cps at 25 psi amplitude.
021	11-18-66	200.818	653	006	005	284	Injector Evaluation (7 pie/ 7 blade, 450 QM 9.4% CFC). Met objectives. No damage. Oscillations in P_c were 1000 to 1500 cps at a maximum of 34 psi amplitude.
022	11-22-66	5.198	651	008	---	284	Injector Evaluation (7 pie/ 7 blade, Low fuel pies, 400 QM). Met objectives. Minor baffle tip erosion. P_c oscillations were 975 cps at 180 psi maximum amplitude.
023	12-15-66	60.5	662	008	010	284	Injector Evaluation (7 pie/ 7 blade, 450 QM, 10.3% CFC, high fuel ΔP). Met objectives. Slight erosion. No other engine damage. P_c oscillations were 1000 cps at 58 psi amplitude.
024	12-16-66	61.2	653	006	---	284	Injector Evaluation (7 pie/ 7 short blade/9.7% CFC, 450 QM). Met objectives. P_c oscillations were 1000 cps at 40 psi amplitude.

Engine Subassembly Tests (cont.)

Test No.	Date	Duration	Injector S/N	CC S/N	Skirt S/N	TPA S/N	Test Objective
			Test Series 3051-D01-1A (cont.)				
025	12-17-66	20.5	651	008	---	284	Injector Evaluation (7 low pie/ 7 short blade/400 QM). Met objectives. Very rough with 1000 cps at 35 psi amplitude.
026	12-20-66	60.7	661	006	010	284	Injector Evaluation (sister to injector on Test -023). Met objectives. P_c oscillations were random frequency at maximum of 47 psi amplitude. Oxidizer discharge line ruptured at FS_2.
027	12-30-66	60.442	662	008	010	285	Injector Evaluation (repeat of -023). Met objectives. P_c oscillations were 1550 cps at 40 psi amplitude.
028	2-8-67	60.6	662M	013	009	284	No hardware damage. "Quick look" indicated 1300 to 1500 P_c oscillation mainly at 50 to 60 psi with maximum near 80 psi. Performance slightly lower than -027.

Engine Subassembly Tests (cont.)

Test No.	Date	Duration	Injector S/N	CC S/N	Skirt S/N	TPA S/N	Test Objective
	Test Series 3051-D02-1A (Series B) Test Stand G-2						
101	1-25-67	200.9	665	009	---	284	Injector Evaluation. Met objectives. P_c oscillations were 1550 cps with maximum 65 psi amplitude.
102	2-16-67	200.8	665	009	007	284	P_c B oscillations steady between 1300 and 1500 cps, maximum amplitude 65 psi. No damage.
103	2-21-67	200.5	665	009	008	284	Satisfactory
104	2-23-67	200.5	665	009	009	284	Satisfactory
105	2-27-67	201.4	665	009	---	284	Satisfactory
106	3-2-67	201.2	661	012	---	285	Verification of second baffled injector at nominal engine inlet conditions. First baseline test on this injector. Satisfactory test. Baffle top strip erosion on baffle #7.
107	3-10-67	201.4	661	012	007	285	Verification test of following components at worst flight combustion chamber conditions: 1. Second oxidizer elbow. 2. Stiff link with skirt and prototype frame. 3. Second baffled injector at WFCC. 4. Injector clevis and stiff link. 5. Second combustion chamber at WFCC. Satisfactory test. Injector S/N 661 had numerous baffle root weld cracks and is being reworked.

Engine Subassembly Tests (cont.)

Test No.	Date	Duration	Injector S/N	CC S/N	Skirt S/N	TPA S/N	Test Objective
	Test Series 3051-D02-1A (cont.)						
108	3-23-67	201.9	661	012	011	285	Verification test of the second combustion chamber under gimballing condition with skirt. No posttest leaks allowed. WFSKT - high M.R. engine inlet conditions. Satisfactory test no hardware damage.
109	3-28-67	201.2	661	012	013	285	Verification test of the second prototype TCA under worst flight skirt low M.R. engine inlet conditions. Satisfactory test - no hardware damage.
110	3-31-67	201.0	661	012	---	285	Verification of baseline with second prototype TCA under nominal conditions. Satisfactory test.
	Test Series 3051-D03-1A (Series C, Pulse Tests) Test Stand E-5						
121	6-29-67	3.2	661	012	---	284	Engine plus. 40-gr ND pulse at FS-1 + 1.5 sec. Satisfactory test - no hardware damage. Pulse 250 psi. Damping time 0.010.
122	6-30-67	3.3	661	012	---	284	40-gr ND pulse at FS-1 + 0.9 sec.
123	7-3-67	3.3	661	012	---		Engine pulse. 40 gr ND pulse did not hit P_c step. No additional hardware damage.

Engine Subassembly Tests (cont.)

Test No.	Date	Duration	Injector S/N	CC S/N	Skirt S/N	TPA S/N	Test Objective
	Test Series 3051-D03-1A (cont.)						
124	7-6-67	3.5	661	012	---		Engine pulse. 40 gr ND pulse. hit P_c step at FS-1 + 0.028 sec. No additional hardware damage.
125	9-20-67	4.4	665	012	---		40 grain pulse charge. Check stability of injector 665 during start transient. Valid pulse - satisfactory test.
126	9-21-67	3.0	665	012	---		40 grain pulse charge. Check stability of injector 665 during start transient. Valid pulse - satisfactory test.
131	4-26-67	20.5	661	011	009	284	Test stand checkout and engine balance test. Satisfactory test.
132	4-28-67	300.7	661	011	012	284	Sea level demonstration of 200 second duration capability of engine and ablative skirt.
	Test Series 3051-D05-1A (Altitude Start Tests)						
141	9-5-67	3.3	665	009	011	284	Altitude start transient characteristics and side loads.
142	9-13-67	3.2	665	009	011	284	Altitude start transient characteristics and side loads. Test satisfactory. Secondary objective: verified capability of oxidizer lead to stage exit closure.

Engine Subassembly Tests (cont.)

Test No.	Date	Duration	Injector S/N	CC S/N	Skirt S/N	TPA S/N	Test Objective
	Test Series 3051-D05-1A (cont.)						
143	9-15-67	3.3	665	009	011	284	Altitude start transient characteristics and side loads. Test satisfactory. Secondary objective: verified capability of oxidizer lead to stage exit closure.
144	9-23-67	3.3	665	012	011	284	Altitude start transient characteristics and side loads. Forty grain ND pulse charge during step. Valid pulse, satisfactory test.
145*	1-14-68	3.7	661	015	019	284	Altitude start in conjunction with closure expulsion. Satisfactory test.
146*	1-19-68	3.5	661	015	019	284	Altitude start in conjunction with closure expulsion. Satisfactory test.

Test No.	Date	Duration	Injector S/N**	CC S/N**	Skirt S/N**	Test Objective and Results
	Test Series 3051-D05-1A (Test Stand G-2 Checkout)					Engine S/N RD-12
151	11-14-67 G-2	20.6	665/ 661M	015/ 009	015/ 023	G-2 checkout - complete engine. Satisfactory test.
152	11-20-67 G-2	201.0	661M	015	023	Engine performance - Subassembly Number 2 firing only. Satisfactory test.

*Also see Section L, Miscellaneous Tests, Exit Closure.
**SA No. 1/SA No. 2.

Engine Subassembly Tests (cont.)

Test No.	Date	Duration	Injector S/N	CC S/N	Skirt S/N	TPA S/N	Test Objective
	Test Series 3051-D07-1A						
161	5-27-68	3.0	661	015	004	019	Exit closure expulsion.
162	6-11-68	3.4	661	015	004	019	Exit closure expulsion.
163	11-6-68	3.1	782	159	019	080	Design verification of exit closure staging at altitude. Piggyback High Frequency Instrumentation Study of P_c Semi-step. Exit closure S/N 009.
164	11-11-68	3.0	782	159	019	080	Design verification of exit closure staging at altitude. Piggyback High Frequency Instrumentation Study of P_c Semi-step. Exit closure S/N 010. Satisfactory test.
165	11-14-68	3.1	782	159	019	080	Design verification of exit closure staging at altitude. Piggyback High Frequency Instrumentation Study of P_c Semi-step. Exit closure S/N 011. Satisfactory test.
	Test Series 3051-A01-1V						
001	11-22-68	300.5	782	159	041	080	Qualification of AGC-fabricated 15:1 ablative skirt. Skirt intact at end of test. No hardware damage.

Engine Subassembly Tests (cont.)

Test No.	Date	Duration	Injector S/N	CC S/N	Skirt S/N	TPA S/N	Test Objective
	Test Series 3269-D01-1A						
001	7-29-68	300.4	782	159	004	080	12:1 ablative skirt and Martin 10 sq. in. actuator evaluation. No failures.
002	1-30-69	321.0	853	158	007	010	Design verification of 12:1 ablative skirt. Worst flight conditions (ablative skirt). Gimballing. Satisfactory test.
	Test Series 3269-D04-1A, Test Stand G-2, Engine S/N RD-12						
001	1-18-69	201.0	853/ 782	158/ 159	008/ 009	010/ 080	Design verification of 12:1 ablative skirt. Gimballing. Worst ablative skirt flight conditions. Satisfactory test.

STAGE I ENGINE DEMONSTRATION TESTS

Test No.	Date	Duration	Injector S/N	CC S/N	Skirt S/N	TPA S/N	Remarks
	Test Series 3051-D07-1A						Engine S/N 14
201	12-20-67	19.6	696/ 697	019/ 020	--- ---	008/ 010	Balance test. Satisfactory test - no hardware damage.
202	12-29-67	200.9	696/ 697	019/ 020	--- ---	008/ 010	Full duration, 6;1 performance evaluation. Satisfactory test.
203	1-10-68	200.7	696/ 697	019/ 020	--- ---	008/ 010	Full duration, 6:1 performance evaluation. Satisfactory test.
204	3-11-68	115.4	696/ 697	019/ 017	025/ 037	008/ 010	Full duration performance evaluation with ablative skirts. Tests terminated prematurely due to TPA S/N 010 failure.
205	4-3-68	20.9	697/ 696	019/ 017	--- ---	008/ 006	Balance test. Satisfactory test.
206	4-10-68	201.9	697/ 696	019/ 017	025/ 037	008/ 006	Full duration performance evaluation with ablative skirts. Satisfactory test.
207	4-29-68	201.0	697/ 696	019/ 017	--- ---	008/ 006	Full duration oxidizer NPSH excursion test. Satisfactory test.
208	5-4-68	21.2	697/ 696	019/ 017	--- ---	008/ 006	Balance test.
209	7-1-68	20.6	697/ 696	017/ 092	--- ---	008/ 006	Rebalance to modified test plan. Satisfactory test.
210	7-5-68	200.4	697/ 696	017/ 092	--- ---	008/ 006	Satisfactory full duration peripheral evaluation with POGO accumulators installed.
211	7-10-68	20.8	697/ 696	017/ 092	--- ---	008/ 006	Satisfactory adjustment test.

Stage I Engine Demonstration Tests (cont.)

Test No.	Date	Duration	Injector S/N	CC S/N	Skirt S/N	TPA S/N	Remarks
	Test Series 3051-D07-1A (cont.)						Engine S/N 14 (cont.)
212	7-12-68	201.0	697/ 696	017/ 092	--- ---	008/ 006	Satisfactory full duration peripheral and POGO evaluation.
213	7-16-68	20.8	697/ 696	017/ 092	--- ---	008/ 006	Satisfactory peripheral adjustment test.
214	7-22-68	201.1	697/ 696	017/ 092	003/ 005	008/ 006	Satisfactory full duration peripheral test with 12:1 ablative skirts and 10-sq in. Martin actuators.
215	8-27-68	200.6	697/ 696	017/ 092	032/ 033	008/ 006	Peripheral test. Piggyback POGO (fuel prevalves and accumulators).
							Engine S/N 15
301	6-3-68	20.7	697/ 699	021/ 022	--- ---	009/ 011	Satisfactory adjustment test.
302	6-6-68	201.1	698/ 699	021/ 022	--- ---	009/ 011	Satisfactory full duration performance evaluation.
303	6-14-68	200.4	698/ 699	021/ 022	--- ---	009/ 011	Satisfactory full duration performance evaluation.
304	6-18-68	200.8	698/ 699	021/ 022	--- ---	009/ 011	Satisfactory full duration performance evaluation.
305	6-24-68	200.6	698/ 699	021/ 022	035/ 038	009/ 011	Satisfactory full duration performance evaluation with ablative skirt and Martin TCA insulation.
306	7-26-68	200.8	699/ 698	021/ 022	--- ---	009/ 011	Satisfactory full duration performance evaluation.

Stage I Engine Demonstration Tests (cont.)

Test No.	Date	Duration	Injector S/N	CC S/N	Skirt S/N	TPA S/N	Remarks
	Test Series 3051-D07-1A (cont.)						Engine S/N 15 (cont.)
307	8-1-68	200.6	699/ 698	021/ 022	014/ 021	009/ 011	NPSH evaluation. Gimballed. Exit closures 006 and 005 piggyback. Successful test.
308	8-14-68	21.0	699/ 698	021/ 022	--- ---	009/ 011	Peripheral adjustment test. Satisfactory test.
309	8-15-68	2.5	699/ 698	021/ 022	--- ---	009/ 011	Peripheral test with +2% - 7% MR. Subassembly 1 thrust chamber valve failed to open caused by discrepant PSV override.
310	8-16-68	200.4	699/ 698	021/ 022	--- ---	009/ 011	Peripheral test. Piggyback POGO (fuel prevalves and accumulators).
311	9-17-68	21.3	699/ 698	021/ 022	--- ---	009/ 011	Adjustment test. Targets -3% thrust, +2% MR. Satisfactory test.
312	9-19-68	201.2	699/ 698	021/ 022	--- ---	009/ 011	Peripheral test at worst flight conditions for combustion chamber. POGO accumulators on fuel pumps. Satisfactory test.
313	9-28-68	20.9	699/ 698	021/ 022	--- ---	009/ 011	Adjustment test. Targets -4% thrust, -4.3% MR. 35°F propellants. Extra high frequency POGO instrumentation. Satisfactory test.

Stage I Engine Demonstration Tests (cont.)

Test No.	Date	Duration	Injector S/N	CC S/N	Skirt S/N	TPA S/N	Remarks
	Test Series 3051-D07-1A (cont.)						Engine S/N 15 (cont.)
314	10-1-68	201.0	699/ 698	021/ 022	--- ---	009/ 011	Peripheral test at low thrust, low mixture ratio flight conditions. POGO accumulators on both fuel pumps. Secondary objective: evaluation of high frequency effects of POGO hardware.
315	10-3-68	21.1	699/ 698	021/ 022	--- ---	009/ 011	Adjustment test. N_2 start. +3% thrust, +2% MR. Sub-assembly 2 cavitation suppressing orifice installed in fuel bootstrap line.
316	10-17-68	200.9	699/ 698	021/ 022	034/ 036	009/ 011	Solid Start. Gimballed. +4% thrust, +6% MR. 35°F propellant Post 110, P_{fst} 26. POGO fuel accumulators and exit closures 007/008, S/A No. 2 cavitation suppressing orifice installed in fuel bootstrap line. Satisfactory test. All objectives met based on preliminary data.